Prion Protein Biochemistry in Creutzfeldt-Jakob Disease.

Submitted for the degree of Doctor of Philosophy in the department of Pathology, Faculty of Medicine.

Tristan Bunn BSc, MSc.
Department of Pathology
University of Edinburgh

Supervisors: Professor James W. Ironside
and Dr Mark W. Head

The work in this thesis is all my own

Contents

Figure scheme

Chapter 6

Chapter 7

Abstract

Properties of prion protein (PrP) conformational variation can be obtained by analysis of PrP^{Sc} by Western blotting. PrP^{Sc} is closely associated with infectivity and pathology in transmissible spongiform encephalopathies (TSE), such as Creutzfeldt-Jakob disease (CJD) and Bovine spongiform encephalopathy (BSE). PrP^{Sc} is notably insoluble and treatment with proteinase K produces a truncated protease resistant core; this form of the protein is termed PrP^{res}. It has been hypothesised that distinctive conformations and glycoform ratio properties (relative levels of the three possible glycoforms) of PrP^{res} are 'markers' or a diagnostic indicator of TSE strains. These banding patterns can be classified according to the molecular weight of the unglycosylated form of PrP^{res}, the relative glycoform ratio and correlated with the aetiology (sporadic, variant, iatrogenic and familial), codon 129 genotype, neuropathological features and clinical signs. A large scale study of PrP^{res} isotypes present in the cerebral cortex of suspected or confirmed human prion disease patients was carried out to investigate the consistency of these isotypes between different genotypic/aetiological subgroups, to determine the potentially distinguishing nature of PrP^{res} strain patterns.

Cases from different subgroups have been investigated to identify any anatomically specific features of PrP^{res} or strain consistency. The results show that all possible PrP isotype/codon 129 genotype combinations are represented in sporadic CJD (sCJD), albeit at differing frequencies. The consistency between and within genotypic/aetiological subgroups is, however, at odds with the findings of regional PrP^{res} isotype heterogeneity within the brains of some sCJD and iatrogenic CJD (iCJD) cases. In contrast the PrP^{res} isotype associated with variant CJD (vCJD) appears stereotyped both between cases and within the brains of individual cases. These results are consistent with the differing aetiologies associated with these diseases: one possibly involving stochastic events (sCJD) the other resulting from the infection of susceptible individuals by a single strain of agent (vCJD). The molecular strain hypothesis was further tested by the analysis of transmitted TSE samples (including mice and a marmoset) and a case each of BSE, natural scrapie and Feline Spongiform Encephalopathy (FSE).

The candidate confirms that the work submitted is his own and that appropriate credit has been given where reference has been made to the work of others.

Acknowledgements

This study would not have been possible without the benevolence of the patients relatives whose permission to retain tissues and use them for research was provided. I would like to thank them especially and dedicate this thesis to them

The PrP immunohistochemistry and haemotoxylin and eosin (H&E) information that was used to draw correlation's was the work of a large number of individuals, primarily, Kovacs Gabor, Suzanne Lowrie, Mary Moore, Margaret LeGrice, Debbie Aurus, Diana Best and Linda McCardle. Their help is greatly appreciated in providing some of this information as well as assisting in the maintenance of the tissue bank and procurement of consumables.

I would like to thank Matthew Bishop and Kathy Estebiero for genetic information.

The murine transmission tissues were kindly provided by Moira Bruce of the NPU.

Familial CJD tissue was kindly supplied by Randal Nixon.

I would also like to thank Vicky McLoughlin for her technical help, Anne MacKenzie for software assistance and encouragement, Neil McLennan, for informed discussion Jan McKenzie, for the wealth of database information, Bill Nailon for computer assistance and everyone else based at the unit who were all of great assistance and are too numerous to mention.

Thanks go to Nigel Hooper for being understanding and patient while writing up the thesis.

I would like to express my gratitude to my supervisors James and Mark, for their patience, advice, understanding and constructive criticism at all stages of the Ph.D.

Finally my parents and girlfriend, who have supported me and made my life far less stressful and far more enjoyable during the last few years.

Abbreviations

γ-aminobutyric acid (GABA)
4-(2-Aminoethyl)-benzenesulfonyl flouride hydrochloride (Pefabloc SC)
A Disintegrin And Metalloprotease (ADAM)
Alkaline phosphatase (AP)
Amino (NH_3)
Amino Acid (a.a.)
Ammonium persulfate (APS)
Amygdala (A)
Anterior thalamus (AT)
Antibody (Ab)
Area Under the Curve (AUC)
Asparagine (Asn or N)
Aspartic acid or Aspartate (D)
Basal Ganglia (BG)
Base pair (bp)
Bovine spongiform encephalopathy (BSE)
Carboxyl (COOH)
Central Nervous System (CNS)
Cerebellar cortex (CC)
Cerebellar vermis (CV)
Cerebellum (CB)
Cerebrospinal fluid (CSF)
Chronic wasting disease (CWD)
Circular dichromism (CD)
Creutzfeldt-Jakob disease (CJD)
Cysteine (Cys)
Cytosine (C)
Deionised water (dH_2O)
Deoxyribonucleic acid (DNA)
Diglycosylated (Di)
Dihydrofolate reductase (DHFR)
Doppel (Dpl)
Doppel gene (*PRND*)
Dots per inch (dpi)
Drowsy (DY)
Electroencephalogram (EEG)
Endoplasmic Reticulum (ER)
Enhanced chemiluminescence (ECL)
Entorhinal cortex (EC)
Ethylene-diamine-tetraacetic acid (EDTA)
Familial CJD (fCJD)
Fatal Familial Insomnia (FFI)
Fourier-transform infrared (FTIR)
Frontal cortex (FC)
Gastrointestinal (GI)
Gerstmann-Sträussler-Scheinker syndrome (GSS)
Glial fibrillary acidic protein (GFAP)
Glutamic acid (E)
Glycosylphosphatidylinositol (GPI)
Growth hormone therapy (GHT)
Guanine (G)

Grams (g)
Gravitational force (*g*)
Haemotoxylin and Eosin (H&E)
Hippocampus (H)
Horseradish peroxidase (HRP)
Human growth hormone (HGH)
Hyperactive (HY)
Iatrogenic CJD (iCJD)
Intermediate (INT)
Inhibitory postsynaptic currents (IPSC)
Long term potentiation (LTP)
Lymphoreticular System (LRS)
Lysine (K)
Magnetic Resonance Imaging (MRI)
Mark W. Head (MWH)
Meat and bone meal (MBM)
Mesencephalon (MC)
Messenger ribonucleic acid (mRNA)
Methanol (MeOH)
Methionine (M)
Micro (μ)
Milligram (mg)
Molar (M)
Monoglycosylated (Mono)
Mutant (mt)
Nitric oxide (NO)
Nonglycosylated (Non)
Nuclear Magnetic Resonance (NMR)
Occipital cortex (OC)
Oligosaccharyltransferase (OST)
Open Reading Frame (ORF)
Optical Density (OD)
Parietal cortex (PC)
Peptide–N^4-(acetyl-β-glucosaminyl)asparagine amidase (PNGaseF)
Peripheral Nervous System (PNS)
Phosphate buffered saline (PBS)
Phosphatidylinositol-specific phospholipase C (PIPLC)
Plasma Membrane (PM)
Poly (L-proline) II (PPII)
Polyacrylamide gel electrophoresis (PAGE)
Polymerase Chain Reaction (PCR)
Polyvinyl diflouride (PVDF)
Positron-emission tomography (PET)
Posterior thalamus (PT)
Prion protein (PrP)
Professor James Ironside (JWI)
Professor Jeanne Bell (JB)
Protease resistant PrP (PrP^{res})
Protein Misfolding Cyclical Amplification (PMCA)
Proteinase K (PK)
PrP cellular (PrP^{c})
PrP gene (*PRNP*)
PrP scrapie (PrP^{sc})

Recombinant PrP (recPrP)
Relative Mobility (M_r)
Restriction Fragment Length Polymorphism (RFLP)
Sample size (n)
Serine (Ser)
Severe combined immunodeficient (SCID)
Sodium-dodecyl-sulphate (SDS)
Spongiform encephalopathy (SE)
Sporadic CJD (sCJD)
Sporadic Fatal Insomnia (sFI)
Standard Deviation (SD)
Standard Error of the Mean (SE)
Subfrontal cortex (sFC)
Suboccipital cortex (sOC)
Subparietal cortex (sPC)
Subtemporal cortex (sTC)
Superoxide dismutase (SOD)
Temporal cortex (TC)
Threonine (Thr)
Transmissible mink encephalopathy (TME)
Transmissible spongiform encephalopathies (TSEs)
Tris (trishydroxymethylamine) buffered saline (TBS)
Valine (V)
Variant CJD (vCJD)
Volume / Volume (v/v)
Weight / Volume (w/v)
Wild type (wt)

Introduction

CHAPTER 1

1.1 Background

Transmissible spongiform encephalopathies (TSEs) are rare fatal neurodegenerative disorders. They can be both genetic and transmissible, which distinguishes them from other diseases (Aguzzi and Weissmann, 1996). They also have long incubation periods (Liberski and Gajdusek, 1997) and are known to afflict both humans and animals (Prusiner, 1991, Weissmann, 1994, Prusiner, 1995, 1998). They include Creutzfeldt-Jakob disease (CJD), Kuru, bovine spongiform encephalopathy (BSE) and scrapie.

The term spongiform encephalopathy (SE) derives from the characteristic neuropathology of vacuoles seen in the brains of affected individuals, which may be accompanied by neuronal loss, astrocytic gliosis and protein plaques (Budka *et al*, 1995, Jeffrey *et al*, 1995, Ironside and Bell, 1997, Ironside, 1998). Spongiform change is a result of focal dilation of neuronal processes and cell bodies by intracellular vacuoles in the grey matter which arise from the cisternae of neuronal smooth endoplasmic reticulum (Clinton *et al*, 1993, Levine *et al*, 1996). The transmissible nature of these diseases was demonstrated by the intraocular inoculation of scrapie infected spinal cord into a ewe by Cuille and Chellé in 1936, hence the term TSE. The TSEs are often referred to as prion diseases. Stanley Prusiner coined the term prion, which stands for *pro*teinaceous *in*fectious particle. The prion protein (PrP) forms the basis of the protein only hypothesis, proposed to explain the molecular mechanism involved in the pathology of the TSEs (Prusiner, 1982). The infective agent, termed a prion, is largely if not exclusively composed of PrP^{sc} (PrP scrapie), an abnormal isoform of the normal prion protein found in all mammals, termed PrP^{c} (PrP cellular). The findings to date support the protein only hypothesis and thus the role of the prion protein as the causative agent of the TSEs (Aguzzi and Weissmann, 1997). Despite this, in disease pathogenesis the precise molecular mechanisms involved in prion replication or PrP conversion are still to be determined.

1732 First documented case of scrapie (M'Gowan, 1914).
1920s Creutzfeldt and Jakob described neurological disease akin to TSEs.
1922 Spielmeyer "status spongiosis" CJD (this term is not specific to prion diseases).
1936 Gerstmann, Sträussler and Scheinker describe a familial human TSE.
1936 Cuille and Chellé demonstrated the first transmission of scrapie.
1957 Gadjusek and Zigas reported kuru in the Fore tribe of Papua New Guinea.
1959 Hadlow reported the similarities between scrapie, Kuru and CJD.
1961 Chandler reported scrapie transmission to mice.
1966 Gadjusek *et al*, first transmission of human TSE (kuru) to primate (chimp).
1968 Gibbs *et al*, reported transmission of CJD to a chimpanzee.
1974 Duffy *et al*, first report of iCJD (due to corneal transplant).
1983 Masters *et al*, first transmission of GSS. Thus infective-genetic paradox.
1985 Chromosomal gene cloned from amino acid sequencing of $PrP^{27\text{-}30}$.
1986 Lugaresi *et al*, first report of fatal familial insomnia (FFI).
1986 *PRNP* sequenced.
1987 Wells *et al*, identified Bovine Spongiform Encephalopathy (BSE).
1989 Hsiao *et al*, GSS genetic abnormality identified.
1990 CJD surveillance was re-instated in the UK.
1990 First case of FSE reported in a domestic siamese cat in the UK.
1992 FFI genetic abnormality identified.
1993 PrP structures determined.
1995 Tateishi *et al* and Collinge *et al*, transmitted FFI to rodents.
1996 Will *et al*, A new variant of CJD (nvCJD) was reported.
2001 Saborio *et al*, developed high yield PrP^{sc} amplification method.

A brief history of CJD and TSEs

1.2 The role of PrP

1.2.1 The transmissible agent

The agent responsible for TSEs is smaller than conventional pathogens (Prusiner, 1982). It can withstand treatments that inactivate more commonly encountered pathogens such as parasites, bacteria and fungi, including ionising and ultraviolet radiation which damage or destroy nucleic acids (Prusiner, 1982). However, infectivity is reduced by procedures which denature protein (Brown *et al*, 1986b). It is postulated that there is no requirement for nucleic acids in TSE infections, based on the infective resistance of the causative agent i.e. the ability of the causative agent to withstand treatments that would inactivate any other known transmissible pathogens. Protein as the agent responsible for TSEs was first postulated in 1967 (Alper *et al*, 1967) and the protein only hypothesis was outlined by Griffith (Griffith, 1967). Since that time the theory has been modified, most famously by Stanley Prusiner, to give the prion hypothesis (Prusiner, 1982). Other modifications have been made to the theory to take into account new findings, such as seeding/template assistance, nucleation polymerisation and physiological dimer models (Warwicker, 1997, Kelly, 1998). Other causative agents have been proposed from acetinobacter (Tiwana *et al*, 1999) to slow viruses (Gajdusek, 1977, Manuelidis *et al*, 1995). However, the evidence for other agents are lacking and there is very persuasive evidence against the presence of any of these agents. There is also evidence that there is another mechanism operating. This involves the 27-30 kDa protein (PrP^{sc}) which remains after limited Proteinase K (Raymond *et al*, 2000) digestion of infected brain homogenates (aka protease resistant PrP; PrP^{res}) and associates with infectivity (Aguzzi and Weissmann, 1997).

1.2.2 Structural properties of PrP

The transmissible properties of prions have become well recognised (Brown *et al*, 1994b), however it was the discovery that the prion protein was host encoded that opened up a whole new field of research. Using partial sequences of PrP and complementary DNA (cDNA) it was possible to clone the gene responsible (Oesch *et al*, 1985, Prusiner, 1991). Using this cDNA as a probe it was discovered that it corresponded to a host gene. *PRNP* is highly conserved and found on the short arm of chromosome 20 in humans and codes for the PrP^c protein. The same gene is found on chromosome 2 in mice and is termed *prn-p* (Sparkes *et al*, 1986). *PRNP* structure consists of a promoter, a single uninterrupted open reading frame (ORF) and two additional exons (Puckett *et al*, 1991, Lee *et al*, 1998). The human form of PrP contains 253 residues (Silvestrini *et al*, 1997), that is subsequently post-translationally amino (NH_3) and carboxyl (COOH) terminally truncated to 209 residues (figure 1) (Shyng *et al*, 1993, Kelly, 1998). It has two asparginine (Asn/N)-linked oligosaccharide chains (Haraguchi *et al*, 1989) potentially forming at least 30 different glycoforms (Stimson *et al*, 1999), a glycosylphosphatidylinositol (GPI) anchor and a single disulphide bridge (Stahl *et al*, 1987, Caughey and Raymond, 1991). Divalent cations (Zn^{2+}, Mn^{2+} and Ni^{2+}) particularly copper (Cu^{2+}) are capable of binding histidines, residing in the octapeptide repeat region (Hornshaw *et al*, 1995, Brown *et al*, 1997b) and a possible second upstream site found before the structured regions, with high affinity (dissociation constants of 10^{-13} to 10^{-14} M) (Manolakou *et al*, 2001). Several polymorphisms have been identified in *PRNP* the most extensively investigated of which is at codon 129 where the presence of methionine (M) or valine (V) maybe homozygotic or heterozygotic. In familial cases there is generally a wild type (wt) and a mutated copy (mt).

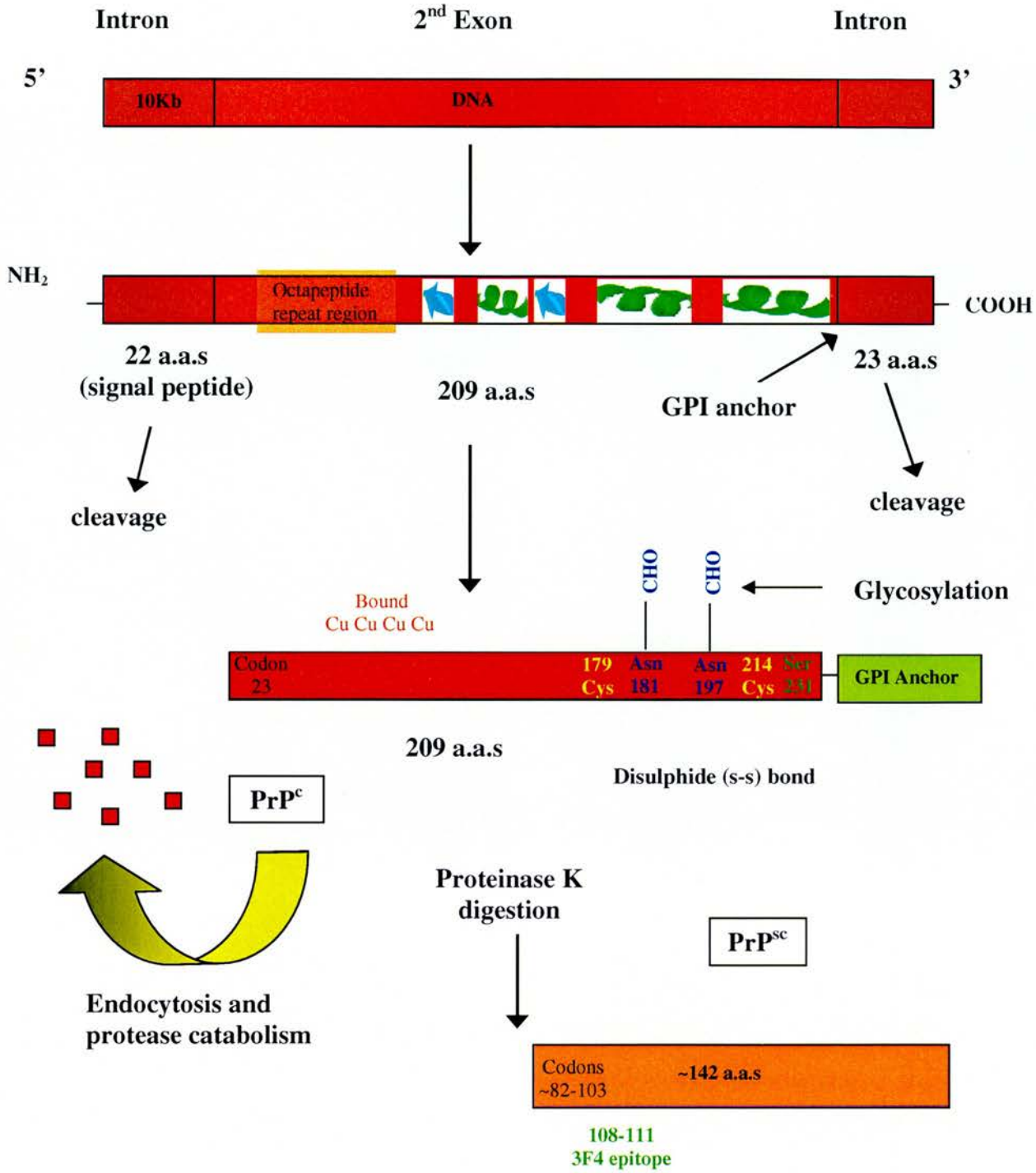

Figure 1. The life and death of PrP.

PrP^c and PrP^{sc} differ in their structural conformation, not their primary amino acid sequences, thus making them isomers or conformers of the same protein (Stahl *et al*, 1993). PrP^{sc} which displays resistance to the relatively non-specific protease, Proteinase K, has a different structure to PrP^c. Partial and complete structures of the C-terminal globular domain have been determined from Nuclear Magnetic Resonance (NMR) studies of recombinant mouse, hamster, bovine and human PrP (Riek *et al*, 1996, Korth *et al*, 1997, Liu *et al*, 1999, Calzolai *et al*, 2000, Zahn *et al*, 2000). This region corresponds to the infectious fragment (Prusiner *et al*, 1993, Nguyen *et al*, 1995) and contains the majority of ordered secondary structure and modifications. The results are supported by Fourier-transformation infrared (FTIR) spectroscopy and circular dichromism (CD) studies of purified hamster PrP^c and PrP^{sc} (Pan *et al*, 1993).

The structures of bovine and human PrP^c have been reported to be almost identical (Lopez Garcia *et al*, 2000). PrP^c is largely α-helical, approximately 42% (3 α helices comprising residues 144-154, 173-194 and 200-228), and contains only approximately 3% β-pleated sheet (a short anti-parallel β-sheet either side of the first helix, residues 128-131 and 161-164). In contrast, the PrP^{sc} β-sheet content is predicted to be approximately 40% and the α-helical content approximately 30% (2 β-pleated sheets and 2 α-helices) (Riek *et al*, 1996). The organised structural portions of PrP^c (α-helices and β-pleated sheet) are found at the carboxy-terminal end. The amino-terminal is composed of a random coil of amino acids in PrP^c, that take on an ordered structure only in the presence of copper (Brown *et al*, 1997b) when hydroxylation forms a poly(L-proline) II (PPII) helix (Gill *et al*, 2000). PrP^c is 30-35 kDa while the 27-30 kDa fraction is the protease resistant part of PrP^{sc} and corresponds to the helical regions of PrP^c (residues 90-228). It is postulated that the amino-terminal region and the conserved hydrophobic domain between codons 113 and 126, take on a β-sheet structure in the conversion from PrP^c to PrP^{sc}. This region does not contain the α-helical motifs, but the formation of the β-sheets results in an unstructured loop in place of the first hydrophilic α-helix (Morrissey and Shakhnovich, 1999). It is this β-sheet conformation that makes PrP^{sc} very stable and resistant to protease digestion (Pan *et al*, 1993, Peretz *et al*, 1997, Jackson *et al*, 1999a, Jackson *et al*, 1999b). This protein can therefore adopt 2 quite different conformations, both of which are very stable (Korth *et al*, 1997) (figure 2).

Prion Protein	Properties
Number of *PRNP* copies	2
Promoter	Guanine (G) cytosine (C) rich promoter.
Conserved sequence	5 tandem repeats of 8 or 9 amino acids near the NH_3 terminal.
Metal ion binding	Copper binding sites in the octapeptide repeat region.
Polymorphisms	Methionine or valine at codon 129, glutamic acid or lysine at codon 219.
Length	209 amino acid residues.
Disulphide bridge	A disulphide bond between two cysteine (Cys) residues at codons 179 and 214.
Glycosylation	2 asparagine (Asn) glycosylation sites (residues 181 and 197), N-linked with heterogeneous oligosaccharides.
GPI anchor	A GPI membrane anchor linked to the C terminal region via serine 231.

Table 1. Features of Human PrP^c.

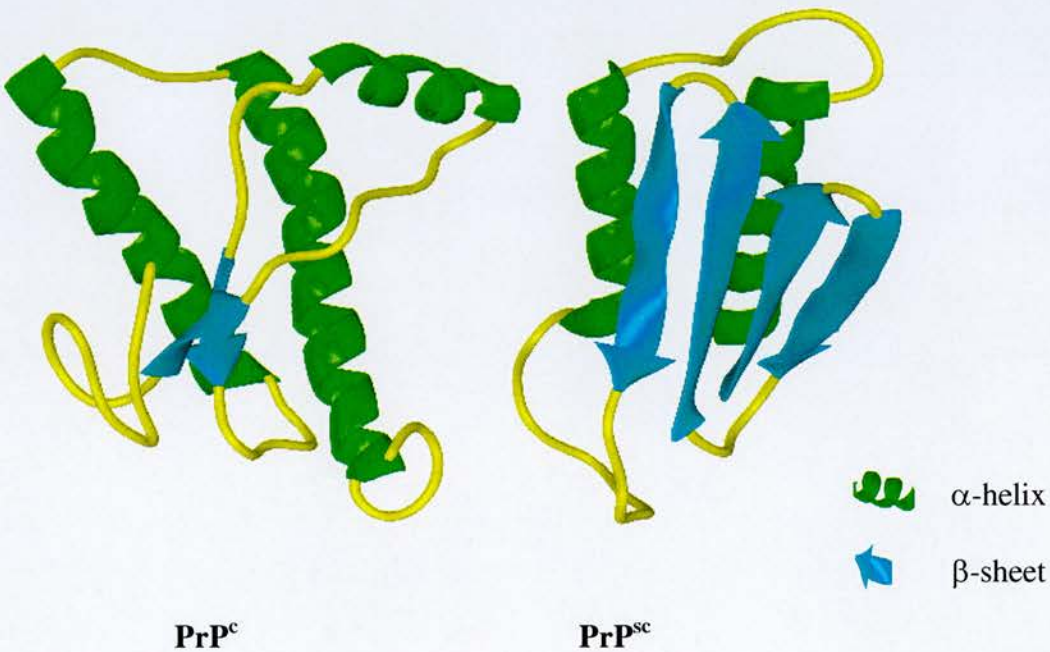

Figure 2. Predicted conformations of PrP^c and PrP^{sc}.

Adapted from http:\\www.cspharm

The conversion of PrP^{c} to PrP^{sc} may occur if *PRNP* is mutated or if PrP^{c} comes into contact with PrP^{sc}. Wild type and mutated PrP have been reported to be insoluble in fCJD carrying the E200K (Gabizon *et al*, 1996) though other studies have found only the mutant PrP to be insoluble and resistant to PK digestion in A117V patients (Tagliavini *et al*, 1995) or cell culture expressing mutant PrP (Lehmann *et al*, 1997). Both copies (wt and mt) in D178N CJD are found to be both insoluble and protease resistant (Chen *et al*, 1997). It is assumed that a two step process occurs; mutant PrP conversion to PrP^{sc} and subsequent conversion and accumulation of both mt and wt alleles.

The pH of the surrounding mileu and reduction of the disulphide bond reversibly alters the α-helical and β-sheet structure of recombinant PrP (Swietnicki *et al*, 1997, Jackson *et al*, 1999a, Jackson *et al*, 1999b). Binding of the NH_3-terminal to vesicle membranes has also been reported at acidic pH (Morillas *et al*, 1999). The conversion process occurs via a rapid unfolding and refolding process (Post *et al*, 1998) which at acidic pH (such as the internal mileu of lysosomes) features an intermediate conformational state. CD spectroscopy of recPrP91-231 indicates that the intermediate structure is predominantly β-sheet, prone to fibril aggregation and possesses a degree of PK resistance, however lack of the disulphide bond and suitable redox potential is required to induce these properties in PrP (Jackson *et al*, 1999a).

Synthetic PrP peptides in β-sheet conformation can impose a β-sheet structure on helical PrP peptides (Kaneko *et al*, 1995, Kaneko *et al*, 1997a). Implying this is a conversion process, not a replication process. PrP^{sc} molecules link together to form stable protease resistant chains or rods, PrP^{sc} then accumulate intracerebrally in cytoplasmic vesicles (Caughey *et al*, 1991, McKinley *et al*, 1991, Arnold *et al*, 1995). This accumulation of protein may compromise cell function. Findings suggest that acquisition of protease resistance, detergent insolubility or β-sheet structure and fibril formation by PrP *in vitro* is insufficient for propagation of infectivity (Hill *et al*, 1999a). Conversely, the entire PrP molecule is not required to support prion propagation, the $PrP^{27\text{-}30}$ fragment is infectious and cell based studies have found that lack of the GPI anchor and oligosaccharide chains does not prevent formation of PrP^{res} (Lehmann and Harris, 1997). Transgenic mice carrying deletions of large portions of PrP, including the unstructured NH_3-terminal (residues 23-88), the second β-sheet as well as the first α-helix and part of the second (residues 141-176) (Muramoto *et al*, 1997, Supattapone *et al*, 1999, Baskakov *et al*, 2000) can be infected

and subsequently transmit disease. It is also not required to induce neurotoxicity in cell culture with the 106-126 portion alone capable of forming β-sheets, amyloid structure (Rymer and Good, 2000) and inducing cell death (Brown, 1999, Rymer and Good, 2000).

1.2.3 PrP^c expression

PrP mRNA levels are unchanged in normal and scrapie-infected tissue (Sakaguchi *et al*, 1995). However, PrP^{sc} accumulates from one hundred to one thousand times the PrP^c levels (Prusiner, 1982) measured by sarkosyl purification of scrapie infected and uninfected mouse brain. PrP^c is expressed in numerous tissues including nervous, lymphoid, immune, haematological (lymphocytes, monocytes, but predominantly platelets) (Bendheim *et al*, 1992, Perini *et al*, 1996, Mabbott *et al*, 1997, Jimenez-Huete *et al*, 1998, Brown, 1999), epithelial (Pammer *et al*, 1999) and even germ line cells (Shaked *et al*, 1999b). PrP^c is constitutively expressed in the brain of adults, particularly the olfactory bulb. Developmental specific expression is seen during synaptogenesis (Sales *et al*, 1998). In the nervous system expression is found in astrocytes and in neurons, particularly at the synaptic membranes (Brown, 1999, Herms *et al*, 1999).

Nascent PrP^c is translocated into the lumen of the ER where the GPI anchor and glycan chains containing a high proportion of mannose are attached (Caughey, 1991). As the PrP^c is transported through the Golgi apparatus the sugar chains are trimmed (Caughey *et al*, 1989). PrP^c is primarily anchored in the plasma membrane via the GPI anchor, though a variety of topological forms have been described (Hegde *et al*, 1998) and there is evidence some is released as a secretory form (Borchelt *et al*, 1993). PrP^{sc} in contrast to PrP^c is not released from the plasma membrane (PM) by cleavage of the GPI anchor with phosphatidylinositol-specific phospholipase C (PIPLC) or trypsin (Borchelt *et al*, 1990, Stahl *et al*, 1990a, Stahl *et al*, 1990b). On the membrane PrP^c has been localised to caveolae-like domains (Vey *et al*, 1996). The membrane bound form is routinely taken back up into the cell either in association with these domains or by clathrin-coated pits (Pauly and Harris, 1998), though most of it returns from the ER to the surface (Shyng *et al*, 1993). PrP^c is degraded in endolysosomes and lysosomes (Caughey *et al*, 1991), where acidic conditions may alter the conformation of PrP^c and protease activity prior to digestion of the mid region (Shyng *et al*, 1993). PrP^c is cleaved between residues 110/111 and

112 in the toxic 106-126 domain, possibly by the protease ADAM10 (a disintegrin and metalloprotease) (Silvestrini *et al*, 1997) releasing a fragment termed N1 which may have neuroprotective properties and leaving a longer carboxyl-terminal fragment termed C2 (Chen *et al*, 1995). PrP^{sc} is found intracellularly (late-endosome-like organelles or lysosomes) (Taraboulos *et al*, 1990b, Borchelt *et al*, 1992, Arnold *et al*, 1995) extracellularly (Jeffrey *et al*, 1994) and at the cell surface (DeArmond *et al*, 1997a), dependant upon the cell under investigation, which implies that the processing of this isoform is different.

1.2.4 PrP^c function and pathology

The physiological function of PrP^c is currently unknown and attempts to elucidate the role it plays have been hampered by the relatively healthy phenotype of transgenic *PRNP* null mice. Developmental compensation for this loss of function has been proposed to account for the lack of an overt pathological phenotype. The function has been postulated, based on the loss of function phenotype of *PRNP* null mice in some studies (altered circadian activity rhythms, sleep patterns, motor co-ordination and long term potentiation [LTP]) (Collinge *et al*, 1994, Sakaguchi *et al*, 1996, Tobler *et al*, 1996, Katamine *et al*, 1998). Brain pathology and infectivity have been detected in the presence of low levels of PrP^{res} (Budka *et al*, 1997, Lasmezas *et al*, 1997) suggesting a loss of function as opposed to an accumulation of misfunctioning PrP^c. A gain of function has also been postulated in transgenic mice carrying truncated *PRNP* genes (display ataxia and neuronal loss in the cerebellum) (Shmerling *et al*, 1998) suggesting competition with a PrP^c ligand. Cellular studies (Pauly and Harris, 1998, Caughey *et al*, 1999) indicate a role as a receptor for an extracellular ligand possibly involving internalisation. The potential interaction of PrP^c with Bcl-2, Hsp60 (Edenhofer *et al*, 1996), Hsp70 (Kenward *et al*, 1996) Hsp104, GroEL (DebBurman *et al*, 1997), the laminin receptor (Rieger *et al*, 1997) and plasminogen (Fischer *et al*, 2000), has been observed and may be a result of non-specific binding or may hold a clue to the normal function of PrP^c (Prusiner *et al*, 1998). Of particular interest either as a binding partner or even a functionally comparable protein is the homologous downstream protein Doppel (Dpl) encoded by *PRND* (Lu *et al*, 2000). Dpl is a GPI anchored, N-glycosylated protein of 179 residues with ~20% homology to PrP (Silverman *et al*, 2000). Developmental studies of PrP^c expression, neural localisation, synaptic activity and neuropathological

degeneration studies indicate a role in embryogenesis, synaptogenesis or synaptic function (Manson *et al*, 1992, Clinton *et al*, 1993, Sales *et al*, 1998, Herms *et al*, 1999). Expression of PrP^c has been reported to coincide with a time in early development when synaptic contacts form and the neural tissue required for LTP in the hippocampus is generated (Sales *et al*, 1998) prior to any possible loss of function in the adult. However, PrP^c has been found in limbic-associated structures and in the striato-nigral complex (Sales *et al*, 1998). Loss of functional ability in these regions may explain reported γ-aminobutyric acid ($GABA_A$) deficiency (Collinge *et al*, 1994) as well as thalamic (FFI neuropathology and PET scans and CJD MRI), putamen and hippocampal (memory impairment and dementia) involvement in the pathology. Cu^{2+} binding and the oxidation of methionine residues (Wong *et al*, 1999) indicate antioxidant properties (Levine *et al*, 1996) and there is evidence for superoxide dismutase (SOD) activity (Brown *et al*, 1999a) which maybe related to the synaptic localisation. A function as a copper transporter and role in metal ion homeostasis is suggested by overall levels of metal ions in the brains of null mice, sCJD patients (Brown *et al*, 1997b, Wong *et al*, 2001a, Wong *et al*, 2001b, Wong *et al*, 2001c) and intracellular Ca^{2+} (Kristensson *et al*, 1993, Wong *et al*, 1996, Brown *et al*, 1997a, Herms *et al*, 2000, Kawahara *et al*, 2000). Dpl does not have the octapeptide repeat copper binding region of PrP^c and is thus unlikely to compensate for PrP^c in this respect. Defining the function of PrP^c is of great importance in understanding how TSE pathology arises, as conversion to PrP^{sc} may result in a loss of normal function or gain of pathological function.

The central nervous system is the primary site of pathological changes in prion diseases (Bell and Ironside, 1993b). There are no indications of inflammation in the brain, though immune responses have been detected. Inflamatory mediators such as cytokines (Williams *et al*, 1994b), microglial involvement (Barcikowska *et al*, 1993, Ironside *et al*, 1993a) and activation detected by their expression of MHC class II molecules (Williams *et al*, 1994a, Gray *et al*, 1999) as well as T-lymphocyte recruitment in lab mediated scrapie have been reported (Betmouni *et al*, 1996). PrP^c is expressed in many periphal tissues and is required for transport of PrP^{sc} from the periphery to the CNS (Blattler *et al*, 1997, Brown *et al*, 1999b). PrP^{sc} and PrP^{res} have been detected in many non-nervous system tissues, yet do not seem to generally cause pathological changes *in situ* (Groschup *et al*, 1996, Hill *et al*, 1997c, Hilton *et al*, 1998). There is growing evidence of peripheral nervous system involvement in the

TSEs (Groschup *et al*, 1999, Hainfellner and Budka, 1999, McBride and Beekes, 1999). This raises the question of the mechanism of tissue suceptibility to TSEs.

The pathological process involved is also poorly understood and incompletely resolved. It could be a result of loss of function of PrP^{c}, however this is unlikely based on experiments with PrP null mice which have some deficiencies; altered circadian rhythms (Tobler *et al*, 1996), synaptic degeneration (Clinton *et al*, 1993) involving inhibitory postsynaptic currents (IPSC) (Collinge *et al*, 1994) and slow after-hyperpolarisations (Herms *et al*, 1999), impaired long term potentiation, defective $GABA_A$ receptor-mediated fast inhibition (Collinge *et al*, 1994), impaired motor co-ordination and loss of cerebellar purkinje cells (Sakaguchi *et al*, 1996, Katamine *et al*, 1998). Yet they show none of the symptoms or neuropathology of scrapie infected mice and develop normally (Bueler *et al*, 1992).

Or it could be due to a toxic gain of function e.g. aggregative properties. Directly toxic effects as a result of build up of large PrP^{sc} aggregates are the most plausible explanation, however amyloid PrP deposits are not always detected in TSEs. Cleavage of the NH_3-terminal at the cell surface to yield an extracellular neurotoxic peptide is feasible, based on the toxic effects of PrP peptide fragments observed in cell culture studies (Brown *et al*, 1996), which need only stretch from codon 106 to 126 (Rymer and Good, 2000). However, in grafting experiments with PrP null mice and over expressing PrP^{c} tissue, intracellular toxicity as a result of PrP^{sc} build up seems more likely, due to the survival of the surrounding 'null' tissue. Triggering of signalling pathways such as the apoptotic pathway (Kuwahara *et al*, 1999) could initiate cell death and this may involve release of cytokines, nitric oxide (NO) or production of oxygen free radicals by microglia (Ironside *et al*, 1992a, Ironside *et al*, 1992b, Ironside *et al*, 1993a, Williams *et al*, 1994a, Williams *et al*, 1994b, Brown *et al*, 1996, Brown *et al*, 1997c, Choi *et al*, 1998) while glutamate or copper mediated pathways may be activated (Gray *et al*, 1999). High levels of ubiquitination in response to PrP^{sc} accumulation (Ironside *et al*, 1993b) may occur, while ion transport, homeostasis (Ca^{2+}, Cu^{2+} and Zn^{2+}) and membrane fluidity (Wong *et al*, 1995, Wong *et al*, 1996) may be disrupted. The CNS is not the only human tissue shown to display prion deposits. The use of tonsil tissue to aid in the diagnosis of vCJD has been undertaken (Hill *et al*, 1997c) with PrP localisation to germinal centres and PrP immunoreactivity has been detected in follicular dendritic cells of the appendix (Hilton *et al*, 1998). Oral and supposed meat and bone meal (MBM) exposure infection of primates presents evidence of PrP^{sc} in the gut, lymph tissue, tonsil and

spleen (Baker *et al*, 1993, Beekes *et al*, 1995, Bons *et al*, 1999) suggesting a route of infection. These findings have not been replicated in sporadic or familial CJD cases (Kawashima *et al*, 1997). The spread of prions possibly follows neuroanatomical pathways in the CNS (Taraboulos *et al*, 1994, Betmouni *et al*, 1996). Peripheral transport appears to involve the immune system including B cells (Klein *et al*, 1997), follicular dendritic cells (FDCs) and the spleen, according to severe combined immunodeficient (SCID) mouse resistance to peripheral prion infection, grafting and surgical studies (pronounced incubation period in mice peripherally infected after splenectomy). PrP^c is found on the surface of platelets (Ghetti *et al*, 1996) which presents a possible transfusion route of infection based on the transferal of GPI anchored proteins from the PM of one cell to another (Ilangumaran *et al*, 1996) and likewise peyers patches in the gastrointestinal (GI) and afferent nerves could provide vectors for prion neuroinvasion into the spinal cord.

1.3 Glycosylation

There are two forms of glycan adddition in the ER, N-linked and O-linked. Transfer of an N-acetylglucosamine, mannose, glucose chain to the NH_2 group of asparagine residues is termed N-linked glycosylation reviewed in (Sears and Wong, 1998). The preformed oligosaccharide chain (consisting of 2 N-acetylglucosmines, 9 mannose and 3 glucose residues) is transferred from the membrane bound lipid dolichol to asparagines in the sequence Asn-X-Ser or Asn-X-Thr (X representing any amino acid except proline). This is carried out in a single step catalysed by oligosaccharyltransferase (OST) as proteins are translocated into the lumen of the ER. While still in the ER the glucose residues and one mannose are removed. High-mannose oligosaccharides receive little additional modification, usually just removal of further mannose residues. Trimming of chains is carried out by specific glycosidases. Complex oligosaccharide chains, after trimming, are extended by addition of monosaccharides (galactose, sialic acid and fucose) in the *trans* Golgi, catalysed by glycosyltransferases using specific sugar-nucleotide donors. Once the core oligosaccharide chain is formed, prior to elongation, the bond between the N-acetylglucosamines becomes resistant to the highly specific endoglycosidase, *Endo H*, and is often used as a marker of complex oligosaccharides in the Golgi.

O-linked glycosylation occurs in the Golgi apparatus and involves the transfer of oligosaccharide chains to the COOH group of serine, threonine or hydroxylysine

residues. This form of modification is less common than N-linked glycosylation. The core glycan xylose is added to the serine residue and subsequently large glycosaminoglycan polymer chains can be added to yield a proteoglycan.

Glycosylation of proteins can alter their properties in a variety of ways including physical properties such as stability and solubility, as well as folding (Imperiali and Rickert, 1995), activity and cellular localisation. Of significance in relation to PrP is the ability for glycosylation to confer resistance to proteolysis and direct protein folding into more compact conformations. Influencing the correct glycosylation of proteins are a wide range of factors including; regulation of glycosyltransferases, substrate availabilty in the Golgi, competition between glycan processing enzymes as well as epigenetic and environmental factors (Dennis *et al*, 1999). The glycosyltransferases require divalent cations to function, usually Mn^{2+} and the correct pH, which must be maintained as a gradient across the Golgi. The protein itself can also influence glycosylation through local structure at the glycan addition sites.

1.4 The prion hypothesis

The prion hypothesis is based on a protein only theory (Prusiner, 1982) that purports there is no nucleic acid portion to the causative infectious agent and that the conversion of PrP^{c} secondary structure arises by direct homodimerisation with PrP^{sc} to bring about the observed pathology. The evidence from studies on the nature of the infective agent, co-purification of PrP^{res} and infectivity, transmission of familial TSEs, linkage of *PRNP* sequence and TSE disease, and *in vitro* conversion of PrP^{c} to PrP^{sc}, support a protein only hypothesis, however no definitive experiment has yet been carried out (see table 2). This thesis is following a line of investigation that is in accordance with the prion hypothesis.

The prion hypothesis centres on the prion protein or PrP^{sc} (Prion Protein scrapie) which is also referred to as the infectious particle and is defined as a modified form of PrP^{c} that readily forms protease-resistant aggregates after treatment with detergent. PrP^{sc} may convert PrP^{c} or a PrP^{c} precursor via post-translational, chemical or conformational modification to PrP^{sc}. It is thought that once PrP^{c} is converted into PrP^{sc} there is an autocatalytic propagation which results in the build up of PrP^{sc} as a consequence of resistance to endogenous protease mediated catabolic breakdown down by the normal protein recycling mechanisms of neurons.

1.4.1 Template assistance model

The template assistance model involves extremely slow conversion in the absence of PrP^{sc}. The template molecule directs the refolding and confers its own properties on the PrP^{c} (Aguzzi and Brandner, 1999). It may therefore require a third party known as protein X, which has been suggested might be a chaperone (Telling *et al*, 1996c). Binding of protein X appears to occur in the carboxyl-terminal α-helical region, to a discontinuous epitope formed with residues 214, 218 (in the helix) and residues 167 and 171 (Kaneko *et al*, 1997b) based on transgenic substitution experiments. The conversion step may occur on a membrane through direct contact between the two forms of the protein, to bring about the conversion of endogenous protein from one conformation to another. Transgenic, human molecular genetic and *in vitro* conversion studies support direct interaction between PrP^{c} and PrP^{sc} and an autocatalytic process which is most efficient when the proteins are of identical primary structure (Prusiner *et al*, 1990, Telling *et al*, 1994).

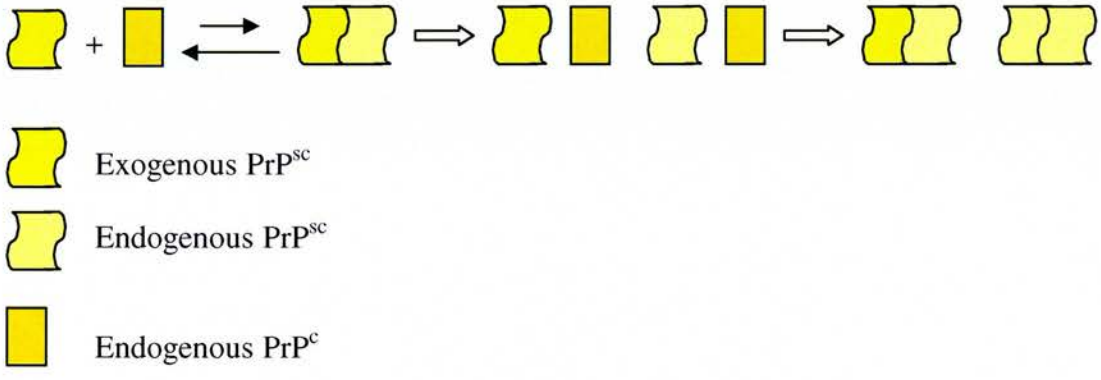

1.4.2 Nuclear polymerisation model

The conversion step on its own may not be sufficient and PrP aggregates may be required for infectivity (Shaked *et al*, 1999a). There is most probably more than one step in the conversion process (Prusiner *et al*, 1998, Shaked *et al*, 1999a). The nucleation polymerisation model hypothesises that a 'seed' of aggregated PrP^{sc} is required to facilitate conversion (Raeber *et al*, 1992). In this model the conversion of PrP^{c} to PrP^{sc} is relatively fast in the presence of a large aggregate of PrP^{sc}. However, in the absence of a PrP^{sc} aggregate the PrP^{c} conformation is favoured.

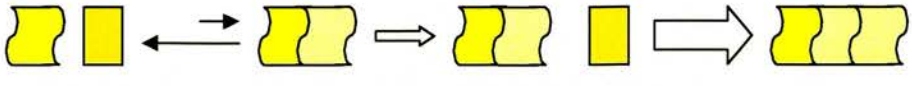

	Investigation
1.	Linkage of scrapie incubation times to the PrP gene (Carlson *et al*, 1986).
2.	Infective resistance to procedures which would 'neutralise or inactivate' conventional pathogens (Prusiner, 1991).
3.	Co-purification of PrP 27-30 and scrapie infectivity by biochemical and immunoaffinity chromatography (Prusiner, 1991).
4.	Neutralisation of infectivity by α-PrP antisera (Prusiner, 1991).
5.	NMR structure studies predict different conformations in the form of a greater level of β-pleated sheet in PrP^{sc} (Korth *et al*, 1997).
6.	Synthetic PrP peptides can induce PrP^{c} to fold into β-pleated sheets, develop PK resistance and aggregate into amyloid fibrils (Kaneko *et al*, 1995, Kaneko *et al*, 1997a, Pillot *et al*, 1997).
7.	Mixing of the two isoforms can bring about *in vitro* conversion of PrP^{c} to PrP^{sc} (Kocisko *et al*, 1994, Bessen *et al*, 1995, Kocisko *et al*, 1995, Raymond *et al*, 1997, Caughey, 1999, Saborio *et al*, 2001).
8.	Transgenic studies involving genetically engineered mice with point mutations that spontaneously develop TSEs (Hsiao and Prusiner, 1990, Palmer *et al*, 1991, Hsiao *et al*, 1994, Telling *et al*, 1996a).
9.	Resistance of PrP-knockout mice to transmission of TSEs (Bueler *et al*, 1993, Brandner *et al*, 1996a, Brandner *et al*, 1996b, Blattler *et al*, 1997).
10.	Susceptibility of PrP^{c} expressing grafts in PrP null mice (Brandner *et al*, 1996a, Brown *et al*, 1999b).
11.	Genetic linkage of human PrP gene mutations and development of familial TSEs (Hsiao *et al*, 1989, Goldfarb *et al*, 1991, Medori *et al*, 1992).
12.	Transmission of familial TSEs to experimental animals (Brown *et al*, 1994b, Collinge *et al*, 1995, Tateishi *et al*, 1995, Tateishi *et al*, 1996).

Table 2. Evidence for the protein only hypothesis.

The discovery of PrP^{c} and the host gene *PRNP*, which encodes the protein, made it possible to propose a mechanism of infection. However until the structure of PrP^{c} was determined a molecular explanation could not be suggested, though self propagating transcription (Griffith, 1967) and alternatively spliced mRNA had been postulated. Despite these breakthroughs, the molecular mechanism of conversion (possibly involving some or all of the following; unfolding, refolding, dimerisation, oligomer formation, non-covalent interactions, associated protein interactions and membrane interactions) remains undetermined.

Post-translational modification suggests that conversion of PrP^c occurs at some point during protein processing in the ER, while present on the surface of the cell or following endocytosis. The post-translational modifications of PrP^c and PrP^{sc} are the same (Pan *et al*, 1993) and the disulphide bond remains intact following conversion (Muramoto *et al*, 1997). Glycosylation affects the rate of the conversion process and increased glycosylation may confer protective effects (Caughey, 1999) which may have implications for the spectrum of glycoform ratios observed throughout the human prion diseases (see page 23). The conversion step is thus a conformational change that could be a result of a dysfunctional transport step or folding process prior to cell surface expression or a deficiency in the proteolytic machinery required to degrade or metabolise PrP^c. However, this does not allow for interaction between the two different isoforms and it has been shown that PrP^{sc} is not formed when PrP^c migration to the cell surface is inhibited. It is thus more likely the conversion would occur at either the cell surface, where dimerisation of the two different isoforms may be more feasible because of exposure to extracellular PrP^{sc} and orientation of the two isoforms in the membrane could facilitate protein interaction, or following endocytosis (Caughey *et al*, 1991, Arnold *et al*, 1995).

Spontaneous conversion is unlikely (Swietnicki *et al*, 1998). PrP^{sc} is more stable than PrP^c but conversion is kinetically unfavourable (Prusiner *et al*, 1998) and intermediate conformations do not constitute significant amounts with rapid folding and unfolding (Wildegger *et al*, 1999). Therefore conversion may require extensive unfolding and refolding of PrP^c under the direction of PrP^{sc}. This could possibly be mediated by another protein (protein X), but would require a source of energy to drive the conversion process. If so, this would explain why conversion *in vitro* can only be achieved in mixing experiments with large amounts of PrP^{sc} (Raymond *et al*, 1997). However, a method has been described recently that yields significant quantities of PrP^{res} from small amounts of PrP^{sc} template via a sonication induced protein-misfolding cyclical amplification (PMCA) method (Saborio *et al*, 2001). Familial mutations of *PRNP* occur in or close to regions of ordered secondary structure and may destabilise the PrP^c structure (Prusiner, 1998). The conformation of both PrP^c and PrP^{sc} is also dependent on Cu^{2+} binding (Brown *et al*, 1997b, McKenzie *et al*, 1998) and the levels of metal ions may alter the conversion process, storage or proteolytic breakdown.

Properties	PrP^c	PrP^{sc}
Concentration in normal Syrian hamster brain.	~1 to 5 μg	0
Concentration in scrapie infected Syrian hamster brain.	~1 to 5 μg	~5 to 10 μg
Protease resistance.	-	+ or partial
Presence after purification and protease treatment.	-	+
Formation of amyloid rods after purification and protease treatment.	-	+
Subcellular localisation in cultured cells.	Cell surface	Primarily in cytoplasmic vesicles
Membrane association after PIPLC treatment	-	+
Solubility in non-denaturing detergents.	+	-
Secondary structure	Predominantly α-helical	α-helical and β-sheet

Table 3. The differences between PrP^c and PrP^{sc}.
Adapted from Prusiner, 1991.

1.5 TSE Strains

Only pathogens containing nucleic acid display the characteristics of multiple strains (Bruce and Dickinson, 1987). If this were true, then the pathogen responsible for TSEs could not solely consist of protein, reviewed in (Ridley and Baker, 1997).

One apparent flaw in the prion hypothesis seems to be the existence of strains (Farquhar *et al*, 1998). Strains of scrapie have been isolated which produce different clinicopathological patterns in the same host and retain their strain characteristics between hosts upon passage, even after transmission into intermediate species with different PrP primary structure and reisolation (Fraser *et al*, 1994). Strain characteristics are demonstrated with isolates of scrapie infected brain that can be passaged in an inbred panel of mice with consistent incubation times (Westaway *et al*, 1987) and neuropathological features (Bruce *et al*, 1989, Hecker *et al*, 1992, DeArmond *et al*, 1993). They can even be passaged from different regions of brain tissue (Carp *et al*, 1997). Thus they are not the result of differences in PrP primary sequence. Numerous different strains have been isolated from distinct cases of scrapie (Fraser *et al*, 1994) and multiple strains can even be isolated from the same source of natural scrapie (Kimberlin and Walker, 1978). The 2 different strain types in transmissible mink encephalopathy (TME), termed hyper (HY) and drowsy (DY) on the basis of the clinical symptoms, correlate with different PrP^{res} banding patterns,

when analysed by Western blotting following PK treatment (Bessen and Marsh, 1994). The HY strain has a short incubation period featuring hyperexcitability, tremors, inco-ordination and cerebellar ataxia and accumulates PrP^{res} with a nonglycosylated band of 21 kDa, in contrast the DY strain produces progressive lethargy with a longer incubation period and accumulates a nonglycosylated PrP^{res} band of 19 kDa. Therefore the source of this strain variation may be differences in the protein conformation (Telling *et al*, 1996b). These confomers might then alter the binding or conversion kinetics and hence the time course of the disease, or the cell specificities, which may result in different symptoms and brain pathology. Differences in conformation need to be conferred (i.e. heritable) onto the host PrP to retain the strain properties of the agent. As well as conformation the degree of protease resistance has been shown to differ between different strains (Buschmann *et al*, 1998). Mutation of glycosylation sites affects the expression of PrP^{c} and the neuropathological profiles of PrP^{sc} deposition in transgenic mice (DeArmond *et al*, 1997b). Glycosylation is not required for PrP^{res} formation in transgenic mice (DeArmond, 1999), cell culture (Taraboulos *et al*, 1990a) or cell-free conversion assays (Kocisko *et al*, 1994).

1.6 The species barrier

Another hurdle for the prion hypothesis has been the existence of the species barrier. When transmissions are carried out from one species to another there is often a lack of success or increased incubation times, which decrease as the number of passages in the new species are carried out (Kimberlin and Walker, 1978, Fraser *et al*, 1994). It appears that the greater the similarity between the 1° structure of PrP^{sc} and PrP^{c}, the more likely it is that the new host will acquire the disease (Bartz *et al*, 1994). Transgenic mice with both their own and a Syrian hamster PrP gene, when inoculated with PrP^{sc} from either other mice or Syrian hamsters, specifically accumulated PrP^{sc} of the same species (Prusiner *et al*, 1990).

1.7 CJD

CJD is a fatal neurodegenerative TSE disorder that affects humans. It can be subdivided into a number of classes, depending on the aetiology (idiopathic, inherited or acquired) and the resultant clinical and pathological features. It is a rare disease

with the incidence being approximately 0.7 case per million per annum worldwide (Will *et al*, 1998).

Sporadic CJD (sCJD) is the most common form of CJD and makes up approximately 87% of cases (Will *et al*, 1998). The cause of sCJD is not currently known, but is assumed to be due to somatic *PRNP* mutation or spontaneous conversion of PrP^{c} to PrP^{sc} as a rare stochastic event rather than environmental exposure to prions.

Familial CJD (fCJD) (along with other inherited prion diseases such as Gerstmann-Sträussler-Scheinker syndrome [GSS] and fatal familial insomnia [FFI]) are linked to autosomal dominantly inherited mutations in the PrP gene and account for approximately 8% of the human prion diseases (Will *et al*, 1998).

Iatrogenic CJD (iCJD) occurs only in those individuals who have been exposed to contaminated tissues, tissue products or surgical instruments and only accounts for 5% of CJD cases (Will *et al*, 1998). The time and route of infection in iatrogenic CJD can de defined and indicates that the route of infection influences both the incubation period and spread of the disease (Turner and Ironside, 1998).

Variant CJD (vCJD) is thought to result from the consumption of BSE contaminated meat products, based on epidemiological, clinical and neuropathological findings (see section 1.8), transmission studies and molecular strain typing with Western blotting (Collinge *et al*, 1996, Bruce *et al*, 1997, Hill *et al*, 1997a).

1.7.1 Clinical features of CJD

The symptoms of prion diseases generally involve neurological dysfunction that corresponds to global CNS impairment i.e. cerebellar, pyramidal and extrapyramidal signs. Abnormalities arising from damage to other organs and tissues outwith the central nervous system (CNS) have not been noted.

Sporadic CJD has characteristic clinical features; it generally affects older individuals with a mean age at onset of 65 years and has a rapidly progressive prodrome (duration of approximately 2-6 months) and profound presenile dementia which presents with either loss of memory, behavioural changes or 'higher cortical functioning deficits' e.g. dysphasia or dyslexia (Ironside, 1998). Deterioration to a demented state occurs along with visual disturbances, a lack of co-ordination, rigidity and involuntary movements e.g. myoclonic jerks, ataxia. This progresses to a terminal rigid state, featuring cortical blindness, akinetic mutism and dysphagia, with death often resulting from inhalation pneumonia. The disturbance noted in the

putamen on magnetic resonance imaging (MRI) may relate to obstruction of procedural actions involving movement. Electroencephalogram (Lemstra *et al*, 2000) triphasic sharp wave spike complexes occur in conjunction with these clinical features (Brown, 1996).

The age at onset and duration of disease due to iCJD exposure is dependent upon the route of infection (Allan and Tuft, 1997). Peripheral infection such as growth hormone therapy (GHT) can take ~15 years from adolescent treatment to present (Huillard *et al*, 1999), but cranial surgery or corneal transplants may be carried out on a wide age range and presents quickly (~18 months). The symptoms of iCJD are variable depending on the route of transmission. There is primarily progressive cerebellar ataxia and myoclonus in cases of peripheral infection, whereas dementia occurs in central inoculation. The presence of dementia in both centrally infected iCJD and sCJD patients suggests that sCJD arises in the brain and not from contact with an exogenous source. In iatrogenic disease the route of infection influences the development of pathology as demonstrated by the clinical symptoms reviewed in (Brown *et al*, 1992).

One of the most distinguishing initial features of vCJD was the occurrence in young individuals (Will *et al*, 1996) mean age 26. Variant CJD has certain clinical features that distinguish it from other forms of CJD. The presenting symptoms are usually psychiatric and sensory (Will *et al*, 1996, Zeidler *et al*, 1997a). Patients generally develop ataxia early in the course of the disease. All patients suffer from progressive dementia, but in only a few is memory impairment part of the initial clinical presentation. Some develop myoclonus, though often late in the course of the disease. A slower progression occurs with the mean duration being 13 months (range 6 to 39) in comparison to 2-6 months for sCJD, a lack of classical triphasic short wave complexes seen on EEG (Ironside, 1998). The similar symptoms of ataxia in peripheral iCJD, vCJD and kuru may relate to the peripheral route of infection, while sensory symptoms may relate to thalamic involvement (Zeidler *et al*, 1997a).

Phenotypic feature	Sporadic CJD	Variant CJD
Mean age at onset (range)	65 (14-90)	26 (12-74)
Duration of illness	<6 months	13 months
Symptoms	Progressive dementia Myoclonus Visual or cerebellar disturbance Pyramidal or extrapyramidal dysfunction Akinetic mutism	Psychiatric (depression) Sensory (hallucinations, pains) Neurological (ataxia, cognitive impairment, myoclonus) Sleep disorders
Codon 129 genotype	MM, MV, VV	MM
PrP^{sc} molecular typing	1 or 2A	2B
MRI	Signal change in basal ganglia, putamen, posterior thalamus.	High signals in posterior thalamus in some cases.
EEG	Triphasic sharp wave complexes (66%)	Abnormal but not characteristic of CJD.
PrP plaques	Present in MV	Present in all cases
Tissue distribution	CNS	CNS, PNS, LRS

Table 4. Differential features of sporadic and variant CJD.

1.7.2 Diagnostic criteria (from www.cjd.ed.ac.uk):

CLASSIFICATION

Suspect cases are classified according to the criteria below by a neurologist from the CJDSU. This is an on-going process, being constantly up-dated as more information is ascertained. The date of any change of classification and the reason for that change is recorded. In addition, the classification is recorded at the following key stages:

At notification;

When the suspect case was first seen in life by a neurologist from the CJDSU; The highest classification on the basis of clinical information alone (ie. not including neuropathological information); **and** when review by the CJDSU is complete (ie. when the case-file is 'closed').

CLASSIFICATION CRITERIA:

SPORADIC CJD (Rotterdam 1998)

I Rapidly progressive dementia

II A Myoclonus

B Visual or cerebellar problems

C Pyramidal or extrapyramidal features

D Akinetic mutism

III Typical EEG

DEFINITE SPORADIC CJD

Neuropathological/immunocytochemical confirmation.

PROBABLE SPORADIC CJD

I, 2 symptoms of II and III OR possible sCJD and positive 14-3-3.

POSSIBLE SPORADIC CJD

I, 2 symptoms of II and duration < 2 years.

IATROGENIC CJD

Progressive cerebellar syndrome in a pituitary hormone recipient **OR** sporadic CJD with a recognised exposure risk, eg. dura mater transplant.

FAMILIAL CJD

Definite or probable CJD plus definite or probable CJD in a first degree relative **OR** neuropsychiatric disorder plus disease-specific *PRNP* mutation.

VARIANT CJD (UK, 2000)

I A Progressive neuropsychiatric disorder.

B Duration of illness > 6 months.

C Routine investigations do not suggest an alternative diagnosis.

D No history of potential iatrogenic exposure.

II A Early psychiatric symptoms*

B Persistent painful sensory symptoms**

C Ataxia.

D Myoclonus or chorea or dystonia.

E Dementia.

III A EEG does not show the typical appearance of classical CJD (after review by CJDSU staff)***

OR no EEG performed.

B Posterior thalamic high signal on MRI scan (after review by CJDSU staff).

IV A Positive tonsil biopsy.

DEFINITE VARIANT CJD

IA and neuropathological confirmation of vCJD****

PROBABLE VARIANT CJD

I and 4 or 5 symptoms of II and IIIA and B OR

PROBABLE VARIANT CJD

I and IVA

POSSIBLE VARIANT CJD

I and 4 or 5 symptoms of II and IIIA

* depression, anxiety, apathy, withdrawal, delusions.2

** including both frank pain and/ or unpleasant dysaesthesia.

*** generalised triphasic periodic complexes at approximately one per second.

**** spongiform change and extensive PrP deposition with florid plaques, throughout the cerebrum and cerebellum.

In addition, there are three additional sub-categories for those referrals that do not meet the criteria of possible CJD, which are:

Diagnosis unclear- when the diagnostic criteria for possible, probable or definite CJD are not met nor is there a reasonable alternative diagnosis and, therefore, CJD remains a possibility;

CJD thought unlikely- when information indicates that a clinical diagnosis of CJD is very unlikely because of atypical disease features, and/or an atypical course, and/or atypical clinical investigation results, and/or a reasonable alternative diagnosis is made, but is not confirmed. This category includes cases which improve clinically without another firm diagnosis being made; and

Definitely not CJD- when information indicates that CJD is not the diagnosis and there is another definite diagnosis proven by clinical examination, clinical investigations or pathology.

1.7.3 Neuropathology of CJD

The neuropathology observed in the brain of sporadic, iatrogenic and familial CJD patients consists of spongiform change in one or all of the following grey matter regions of the brain, cerebrum, cerebellar cortex and subcortical, detected by conventional haemotoxylin and eosin (H&E) staining (Bell and Ironside, 1993b). Neuronal loss occurs as a result of apoptosis (Dorandeu *et al*, 1998, Gray *et al*, 1999), along with astrocytic and microglial proliferation and activation (Williams *et al*, 1994a, Betmouni *et al*, 1996). This is accompanied by PrP^{sc} accumulation as plaques in the neuropil, a diffuse synaptic PrP^{sc} pattern of perivascular PrP accumulation as detected by PrP immunocytochemistry (Bell and Ironside, 1993b), recrudescence of synaptic contacts (Clinton *et al*, 1993) and axonal damage (Gray *et al*, 1999). These features display considerable variation between cases and between brain regions in individuals (Ironside *et al*, 1996).

The spongiform change and amyloid plaque formation is largely dependent on *PRNP* genotype in sCJD. Individuals homozygous for methionine at codon 129 of *PRNP* show cerebral cortical spongiform change and synaptic or perivacuolar PrP^{res} accumulation, however, individuals homozygous for valine show corpus striatum and cerebellum spongiform change but PrP^{res} plaque-like structures in the cerebellum, thalamus and basal ganglia. MV genotypes have a varied neuropathology that can resemble either of the homozygote patterns (Parchi *et al*, 1995a, Ironside, 1998, Parchi *et al*, 1998b) and the PrP^{res} isotype determines the formation of plaques (type 1 patients) or kuru type plaques (type 2). Amyloid plaques also occur in familial prion diseases, particularly in GSS where multi-centric cerebellar plaques are characteristic. Variant CJD has a distinct neuropathology. Multiple "florid" amyloid plaques have been seen in the cerebrum and cerebellum as well as typical plaques and deposits (Ironside and Bell, 1997). Florid plaques are seen very rarely, most commonly in cases of kuru and experimental Icelandic scrapie, aside from vCJD. Florid plaques are fibrillary PrP^{res} plaques surrounded by a halo of spongiform vacuoles. They are also seen in the brain stem and spinal cord. Overall, PrP^{res} staining in the form of clusters of multiple small plaques and amorphous deposits around neurones and blood vessels is most intense in the cerebellar cortex molecular and granular layers and occipital lobe. Punctate PrP^{res} staining is seen in the pontine nuclei. The basal ganglia shows perineuronal and linear periaxonal deposits. Spongiform change is seen in the basal ganglia and there is a marked thalamic gliosis and neuronal loss

involving dorsomedial and posterior nuclei (Ironside, 1998) but no confluent spongiform change or status spongiosis.

1.8 Kuru

Kuru was first reported in 1957 by Gadjusek and Zigas, in the Fore tribe residing in the Eastern Highlands of Papua New Guinea. The suggestion that it was a TSE akin to scrapie and CJD was made in 1960 by Hadlow and in 1966 the first transmission of a human TSE to a primate was reported by Gadjusek *et al.* The disease is thought to be transmitted by cannibalistic funerary practices and since the cessation of these events the incidence of the disease has diminished (Liberski and Gajdusek, 1997).

The presumed oral route of infection has provided a comparative model of human TSE infection with vCJD. Kuru patients homozygous for methionine at codon 129 display a earlier age at onset and shorter disease duration (Cervenakova *et al*, 1999). The clinical signs of kuru (the native termed used to describe the pronounced tremors) involve progressive cerebellar ataxia. Comparison of kuru and vCJD neuropathology have found spongiform change in the putamen, caudate nucleus and thalamus as well as involvement of both the granular and molecular cerebellum cell layer with gliosis and PrP^{sc} deposition (McLean *et al*, 1998). Prion plaque formation in kuru is seen in reasonably well preserved regions and forms proper plaques that in some cases are multicentric. The neuropathology of kuru cases show PrP^{res} plaques, only in individuals with at least one allele carrying methionine at codon 129, thus the MM vCJD cases noted to date may not be representative of all individuals exposed to BSE (Cervenakova *et al*, 1999). However, this has been contradicted in a number of other studies (Hainfellner *et al*, 1997, Lantos *et al*, 1997, McLean *et al*, 1998). The levels of PrP in vCJD brain are far higher and overall the pathology of these two diseases differs, suggesting that the strain of agent plays a greater role than the route of infection in determining the clinico-pathological phenotype (McLean *et al*, 1998).

1.9 Genetics

There is continued identification of variant *PRNP* genotypes in humans and animals and the influence they have on both the spontaneous development of inherited TSEs and the susceptibility to developing TSEs on exposure to PrP^{sc} (Hsiao and

Prusiner, 1990, Goldfarb *et al*, 1994, Ikeda *et al*, 1995, Pickering-Brown *et al*, 1995, Goldmann *et al*, 1998, Lee *et al*, 1998, Wopfner *et al*, 1999, Gilch *et al*, 2000). Familial forms of human spongiform encephalopathies are tightly linked to certain mutations in *PRNP*. The familial forms are passed on in an autosomal-dominant fashion (Baker *et al*, 1985, Collinge *et al*, 1992). Families carrying these mutations are sometimes related to certain ethnic groups such as Libyan or Sephardic Jews or Slovakians carrying the E200K mutation (Lee *et al*, 1999). Carriers of the E200K mutation may be heterozygous or rarely homozygous for the mutation, with the latter presenting a little earlier and having a longer disease duration, but otherwise a similar clinical phenotype (Simon *et al*, 2000). The influence of other host factors in the development of human TSE disease is most clearly demonstrated by a large pedigree containing 47 affected members carrying a 144 base pair insertion of six octapeptide repeats in the octapeptide motif (Collinge *et al*, 1992).

There are over 20 different non-conservative substitution and insertion mutations in the human *PRNP* gene which can bring about inherited prion diseases (Goldfarb *et al*, 1991, Bosque *et al*, 1992, Medori *et al*, 1992, Gabizon *et al*, 1994, Campbell *et al*, 1996, Windl *et al*, 1996, Lee *et al*, 1999, Collins *et al*, 2000, Nixon *et al*, 2000, Peoc *et al*, 2000) and are associated with the familial forms of human TSE. All of the known substitutions occur in the 4 putative α-helices of PrP^c or at their borders (Riek *et al*, 1996). At least 13 different mutations are present in fCJD and GSS, including point mutations and insertions of various lengths, which are found around the octapeptide repeat-coding region (Silvestrini *et al*, 1997). These mutations may result in inappropriate amino acids at critical sites in the PrP required for three dimensional conformational stability which may be lost and destabilise the α-helix conformation therefore increasing the likelihood of β-sheet refolding. Thus mutation may facilitate or enhance the rate of PrP^c conversion, whether it is PrP^{sc} or spontaneously driven. The phenotype of the disease varies according to the specific mutation. It is possible that some of the mutations in familial forms of human TSE result in pathology through mechanisms not involving PrP conversion or accumulation, such as protein processing problems. This could explain a lack of PrP plaques or spongiform degeneration and the uncharacteristic banding patterns in forms of GSS (Collinge *et al*, 1990, Piccardo *et al*, 1998) and possibly FFI. This would be consistent with a protein only hypothesis.

1.10 Effects of polymorphisms

In addition to inherited cases, there are sporadic cases and acquired cases of CJD. Genetic factors that predispose, protect or alter the outcome of infection or exposure to infected tissues have been studied. Thus far the most important variations appear to be the polymorphisms at codon 129 of *PRNP*. The incubation period of iCJD and kuru can be influenced by the *PRNP* codon 129 genotype, with heterozygotes in some studies presenting later and at a much lower incidence than homozygotes for either amino acid (Deslys *et al*, 1998, Shibuya *et al*, 1998, Cervenakova *et al*, 1999). Furthermore, the susceptibility to sCJD, iCJD and kuru appears to be influenced by this polymorphism (Palmer *et al*, 1991, Deslys *et al*, 1998). Homozygosity for either methionine or valine at codon 129 is present in approximately 49% of the normal population (Palmer *et al*, 1991). In contrast individuals with sCJD or iCJD are found to be homozygous in approximately 71% (Windl *et al*, 1996, Will *et al*, 1998, Alperovitch *et al*, 1999) and 80% of cases respectively (Brown *et al*, 2000). The age at onset in patients with sCJD is influenced by the codon 129 genotype with greater numbers of methionine homozygotes over 49 years of age than under, while greater numbers of the valine homozygotes were under 50 years of age than over (Alperovitch *et al*, 1999). In iCJD acquired from growth hormone treatments, valine homozygotes are more common (Bendheim *et al*, 1992, Alperovitch *et al*, 1999). This polymorphic effect could be influenced by the potential oxidation of methionine in PrP (Wong *et al*, 1999) or the propensity for β-sheet conformation of valine (Jackson *et al*, 1999b). The possibility that this polymorphism influences dimer formation and aggregation due to allelic homology is unlikely because PrP^{sc} aggregates are found to contain both the methionine and valine alleles (Chen *et al*, 1997).

The homozygosity at codon 129 predisposes to sCJD and so far all cases of vCJD have been homozygous for methionine. This would imply that a similar mechanism is in operation in these two subtypes of CJD. However, the differences in Western blotting banding patterns of PrP^{res} imply a different 'strain' of TSE is causing the appearance of the new CJD subtype. In the initial report of vCJD the PrP genotypes for 8 cases were analysed and all were methionine homozygotes at codon 129 of *PRNP* (Will *et al*, 1996). Variant CJD occurring in an individual with a valine allele is yet to be reported among the 132 cases of definite or probable vCJD as of the 3rd of March 2003 (http://www.cjd.ed.ac.uk/figures.htm).

There is also an inherited susceptibility to CJD in human carriers of the D178N mutation, dependent on M or V at codon 129 (129M linked to FFI, 129V linked to fCJD). While the D178N mutation induces development of the TSE, the codon 129 genotype affects the form of the disease (Parchi *et al*, 1995a, Parchi *et al*, 1995b, Parchi *et al*, 1998b, Parchi *et al*, 1998c). The clinical and pathological features of these two diseases differ markedly. FFI features a prominent insomnia and thalamic atrophy, but fCJD displays prominent spongiform degeneration of the cerebral cortex. When FFI patients with differing codon 129 polymorphisms on the unmutated allele are compared, significant differences in disease duration are noticed, the MM cases were found to have a mean duration of 9.1 months and the MV cases 30.8 months (Montagna *et al*, 1998). The 144 base pair (bp) insertion in one kindred, co-segregating with M, has different age at death depending on M or V on the normal allele. The latter, displaying later age at death (Baker *et al*, 1991). The P102L mutation as well as four or five repeat inserts can cosegregate with methionine or valine, resulting in different neuropathology and clinical signs (Baker *et al*, 1991, Young *et al*, 1997). This difference in disease duration presumably arises due to differential allelic homology and is proposed to account for the differences in neuropathology and clinical signs. Cases of fCJD with the E200K mutation are usually in conjunction with methionine at codon 129 and homozygous for methionine. This is due in part to the large Libyan Jewish kindred that is primarily MM (Rosenmann *et al*, 1997).

1.11 Evidence that vCJD is a result of BSE exposure

BSE was first reported in 1987 in the UK (Wells *et al*, 1987). From November 1986 to May 1995 there were 150,00 reported cases (Anderson *et al*, 1996). As little as 1 gram of BSE infected bovine brain tissue is transmissible to a wide range of animals by peripheral injection and oral infection (Collee, 1996). It is postulated to represent a distinct strain and has been reported to be consistent among, BSE, vCJD, zoo animals (Kirkwood *et al*, 1993), macaques, marmosets (Baker *et al*, 1993), FSE in domestic cats (Aldhous, 1990, Pearson *et al*, 1991, Pearson *et al*, 1992, Wells and Wilesmith, 1997) and captive wild cats (Willoughby *et al*, 1992, Baron *et al*, 1997). The neuropathology is concordant with other TSEs as well as being reproducible on transmission to cattle, primates (Baker *et al*, 1993, Lasmezas *et al*, 1996b) mice (Bruce *et al*, 1994, Lasmezas *et al*, 1996a, Bruce *et al*, 1997, Hill *et al*,

1997a, Raymond *et al*, 1997, Ironside, 1998) cheviot sheep, goats and pigs (Foster *et al*, 1993, Foster *et al*, 1996, Ryder *et al*, 2000). Suspected cases arising from BSE such as feline spongiform encephalopathy (FSE) or BSE in greater kudu, nyala have also been transmitted to mice (Bruce *et al*, 1994, Fraser *et al*, 1994). BSE was initially identified in 3 domestic cats with FSE (Aldhous, 1990, Leggett *et al*, 1990, Wyatt *et al*, 1990, Pearson *et al*, 1991, Wyatt *et al*, 1991, Pearson *et al*, 1992), a prion disease which appeared in 1990 in the UK. Since then numerous captive and domestic (85) cases (Wells and Wilesmith, 1997) have been reported.

The source of the epidemic was traced to food supplements including the MBM from dead sheep and cows. This has been given to cows since the 1920s but the important solvent extraction step in the processing of sheep carcasses was excluded in the early 1980s and the temperature of the procedure was changed. PrP^{sc} is solvent sensitive, therefore it has been proposed scrapie PrP^{sc} was deactivated in this step and without it the PrP^{sc} remained infectious (Prusiner, 1997). BSE may represent a cattle adapted strain of scrapie or a propogated case of either familial or sporadic BSE, the original cause as in kuru is unknown. The identification of a single strain would support the potential for de novo initiation of a new strain. The epidemic was amplified by recycling of infected cattle that commenced in 1984, and led to a marked increase in incidence of BSE in 1989.

Variant CJD is a subtype of CJD unidentified previous to 1996 (Will *et al*, 1996). It has a number of characteristics that distinguish it from other forms of CJD. A very distinctive neuropathology and atypical clinical symptoms, along with the very noticeable incidence of the disease in young people, in comparison to sCJD, which generally afflicts individuals between the ages of 50 and 70. The occurrence of these cases following the BSE epidemic and the distinctive features provide circumstantial evidence of a link. While transmission studies (Bruce *et al*, 1997, Hill *et al*, 1997a, Raymond *et al*, 1997, Ironside, 1998, Bruce *et al*, 1999) provide experimental results to back up the association between the two outbreaks. The most important evidence with relevence to this study is the consistent identification by Western blotting of a distinctive PrP^{res} banding pattern (Collinge *et al*, 1996, Parchi *et al*, 1997).

1.12 PrP^{sc} biochemistry

Studies on PrP^{sc} biochemistry include *in vitro* mixing experiments (Raymond *et al*, 1997), the production of synthetic peptides (Kaneko *et al*, 1995), structural

studies (Riek *et al*, 1996, Korth *et al*, 1997) and electrophoresis studies (Brown *et al*, 1986a, Bessen and Marsh, 1992, 1994, Collinge *et al*, 1996, Parchi *et al*, 1996, Castellani *et al*, 1997, Hill *et al*, 1998). Electrophoresis studies have included investigations into the protease resistance, relative molecular mass, glycosylation profiles, tissue distributions and the investigation of the biochemical basis of strain variation of PrP^{res} (Prusiner *et al*, 1983, Bockman *et al*, 1985, Hope *et al*, 1986, Brown *et al*, 1995, Telling *et al*, 1996b). Protease resistance of the pathological isoform of PrP was observed in 1985 by Oesch *et al* (Oesch *et al*, 1985) and by Meyer *et al* in 1986 (Meyer *et al*, 1986). The purification of PrP can be carried out by detergent extractions, enzymatic digestions, differential centrifugations (separating out membrane fractions) and discontinuous sucrose gradient sedimentation as used by Prusiner *et al*, in 1983 (Prusiner *et al*, 1983). PrP^{c} migrates to 33-35 kDa, but PrP^{res} is found at 27-30 kDa (Beekes *et al*, 1995) due to NH_3-terminal proteolytic cleavage (Hope *et al*, 1986). The first indication of molecular weight differences in CJD derived PrP^{res} were made in 1985 (Bockman *et al*, 1985) and in the same year differences in the relative amounts of SAF immunoreactive bands, dependent upon host and scrapie strains, were observed (Bode *et al*, 1985). The SAFs were found to be composed of a low molecular weight glycosylated protein in the same year (Multhaup *et al*, 1985). PrP was then found to co-purify and appear at a similar molecular weight to the SAF protein (Hope *et al*, 1986). The heterogeneity in the molecular weights of the banding pattern observed is a result of N-linked glycosylation (Somerville and Ritchie, 1990). Electrophoresis studies are proving increasingly important for strain typing and diagnosis. The molecular analysis of human TSEs may allow the identification of distinct strains of prion disease, based on PrP^{res} conformation differences elucidated through partial Proteinase K digestion (Bessen and Marsh, 1992, 1994). The incubation period or clinical signs may be related to different protease sensitivity. At present distinct banding pattern types are being equated with strains in human SEs, however there is little data on the repeated passage of these 'strains' in mice (Bartz *et al*, 1994, Bartz *et al*, 1998) and on passage in humans (el Hachimi *et al*, 1997). Pattison isolated brain from two separate groups of goats with scrapie (Pattison, 1966). The passage of these extracts into Chandler mice resulted in different symptoms, one made animals drowsy (DY), the other hyperactive (HY). Transmissible mink encephalopathy (TME) likewise has two strains which produce excitable and drowsy symptoms, as stated previously, (Bessen and Marsh, 1992). Similarly the banding patterns observed in human TSEs may

represent phenotypic strain differences. The isoform differences are represented by different PrP^{res} fragments after PK digestion and degrees of glycosylation. There are a number of problems in investigating and diagnosing CJD. One of these has been the need to carry out post mortem investigations to accurately diagnose the disease. PrP^{sc} biochemistry may allow prenecropsy and preclinical tests to be carried out by brain or tonsil biopsy (Castellani *et al*, 1996, Castellani *et al*, 1997, Hill *et al*, 1997c).

1.13 Interpretation of banding patterns

Cases of CJD can be readily distinguished upon Proteinase K treatment. Only the abnormal form of PrP is partially resistant to this protease and non-TSE diseases do not display the characteristic banding pattern. Western blots of PrP^{res} from CJD cases results in 3 bands, 2 glycosylated bands which correspond to a greater molecular mass and 1 nonglycosylated band which is of lower molecular mass (figure 3). The relative molecular weights and glycosylation ratios vary and the classification systems employed differ between two groups, Collinge *et al* and Parchi *et al*.

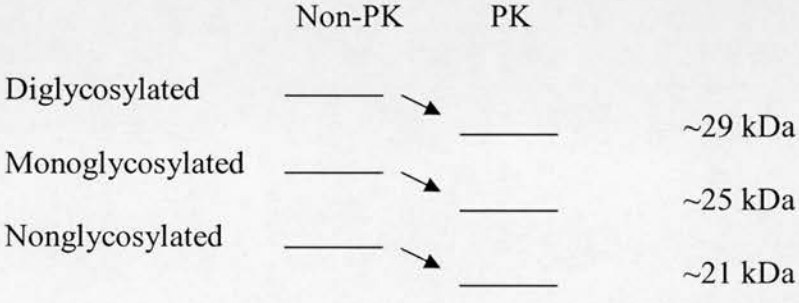

Figure 3. Schematic diagram of the PrP Western analysis of TSE samples.

The distinct mobilities are due to different degrees of PK cleavage of the amino-terminal portion of PrP^{sc}, possibly due to different conformations of PrP^{res} (Bessen and Marsh, 1994). Individual fragments (bands) may correlate to the mutated allele, spongiform changes or multi-centric amyloid plaques (Parchi *et al*, 1998a). The size of cleavage fragments are retained after transmission of fCJD and FFI (Telling *et al*, 1996b) and it is postulated that this is a strain specific characteristic (Bessen and Marsh, 1992).

1.13.1 Collinge *et al*, 1996

The banding patterns observed by Collinge *et al*, (Collinge *et al*, 1996) in sCJD case are termed type 1 and type 2. Type 1 forms the majority of cases with the codon 129 genotype always being methionine homozygous (MM) and the deglycosylated PrP^{res} band being found at approximately 21 kDa. The type 2 nonglycosylated PrP^{res} band is found at approximately 20 kDa in a few MM genotype individuals, heterozygote (MV) and valine homozygote (VV) individuals. A type 3 banding pattern has been described, with a decreased apparent molecular weight of 2-3 kDa in comaprison to type 2, in MV and VV cases of sCJD and pituitary derived iCJD (Collinge *et al*, 1996, Wadsworth *et al*, 1999b, Jackson and Collinge, 2001). There appears to be some degree of variation in the glycoform ratios of sCJD, this was first indicated by a slight difference between types 1 and 2. Type 1 and 2 have different clinicopathological phenotypes in the sCJD. Type 2 has a greater middle band intensity than type 1. When type 3 was compared with either type 1 or type 2 the intensity of the bands and their ratios were not significantly different (Collinge *et al*, 1996). Some MM iCJD cases have the type 1 or 2 pattern, growth hormone derived in the former and dura mater derived in the latter. Type 3 iCJD (peripheral/intramuscular injection of human cadaveric hormones) presents with a distinct clinicopathological phenotype (cerebellar ataxia and psychiatric disturbance) to iCJD resulting from CNS exposure (dura mater grafting) and resembles classical sporadic CJD. All of these banding patterns, after Proteinase K treatment, have similar but not identical glycoform ratios. They are differentiated on the basis of their fragment size (Hill *et al*, 1997a).

All patients with vCJD are MM and have banding patterns significantly different to types 1,2 and 3 in terms of high-relative molecular mass, proteolytic cleavage site and glycosylation ratio. The banding patterns seen in cases of vCJD are different to types 1 and 2. The mobility of the bands are the same as that seen in type 2 or 3 cases, however the glycoform ratios differ from that seen in sporadic cases of CJD. Deglycosylation with PNGase F gave a single band that may be consistent with a single proteolytic cleavage site. The glycoform with the higher relative molecular mass is the most abundant judging by band intensity while there is relatively little of the mono and nonglycosylated bands which implies that unlike types 1, 2 and 3, type 4 is a distinct CJD subtype (Collinge *et al*, 1996). Variant CJD has a glycoform signature similar to transmitted BSE; experimental murine (wt FVB mice and C57BL

mice) BSE (Bruce *et al*, 1997), naturally transmitted domestic cat BSE and experimental macaque BSE (Lasmezas *et al*, 1996a) which supports the proposition that vCJD has occurred as a result of infected material from BSE afflicted cattle entering the human food chain.

The consistency of molecular strain typing was supported by the fact that CJD transmission to wt FVB mice resulted in banding patterns that resembled the inoculum (Collinge *et al*, 1996). The murine PrP^{res} apparent mobility and glycoforms were the same as those seen in humans. However, transgenic mice (homozygous for human *PRNP* codon 129 valine, null for murine *PRNP*) inoculated with type 1 sCJD produced type 2 PrP^{res}, and transmission of vCJD to the same strains of mice lead to production of a type 5 pattern (PrP^{res} with a type 2 relative mobility and prominent diglycosylation).

PrP^{res} has only been detected in the CNS in cases of sCJD (Hill *et al*, 1999b). In tissues outside the nervous system it has been reported that there is a different glycosylation pattern to that reported in the CNS of the same host. The banding pattern observed in tonsil tissue taken from patients with vCJD has shown a far greater proportion of the diglycosylated band than in the brain and this has been designated 4t (Hill *et al*, 1997c). Types 6 and 7 have also been reported, characterised by prominence of the nonglycosylated band and higher molecular weight than type 1 respectively (Collinge *et al*, 1996, Hill, 1998).

1.13.2 Parchi *et al*

In contrast to Collinge's findings Parchi *et al*, 1996 and 1997, report that immunoblot analysis of SDS-PAGE PrP^{res} shows only two mobility variants. Type 1 has a M_r of approximately 21 kDa, which corresponds to types 1 and 2 of Collinge *et al*, yet type 2 has a M_r of approximately 19 kDa (Parchi *et al*, 1997) and corresponds to types 3 and 4 of Collinge *et al*. The study included a case of kuru and it was found that the vCJD, kuru, one case of iCJD (VV homozygous at codon 129) and the 88 cases of sCJD were type 2. The type 1 pattern was composed primarily of sCJD cases and iCJD (MM homozygous at codon 129), though Tranchant *et al*, have reported MV cases in this group (Tranchant *et al*, 1999). Type 1 and 2 have different clinicopathological phenotypes in the sCJD cases (Parchi *et al*, 1996). There is further classification of banding types by Parchi *et al*, based on glycosylation patterns, though vCJD was still found to be highly diglycosylated and designated type 2B.

However there was reported variability of the type 1 M_r and only one kuru and one vCJD case were investigated.

The banding pattern as well as clinical symptoms and neuropathology are affected by the codon 129 genotype, with fCJD D178N-129VV showing type 1 mobility while FFI D178N-129 MM or MV showing type 2 mobility (Monari *et al*, 1994, Parchi *et al*, 1998c). The glycoform ratios of fCJD D178N and FFI differ, however within each group they do not differ in relation to the unmutated allele (Monari *et al*, 1994). Iatrogenic CJD displays different mobilities according to route of infection yet like sCJD it shows the opposite effect of the codon 129 polymorphism, with valine predisposing to generation of type 2 PrP^{res}. The formation of particular PrP^{res} banding patterns is constrained by host *PRNP* codon 129 genotype. This finding is supported by conversion of type 1 to type 2 when passaged into transgenic mice with the human PrP gene (Telling *et al*, 1996b). When material was transmitted from FFI patients to mice the 19 kDa fragment was retained yet when material from fCJD or sCJD was used the PrP^{res} migrated to 21 kDa (Telling *et al*, 1996b) implying strain dominance over host genotype. Cell free conversion reactions have also provided evidence for the maintenance of strain specific conformations as defined by PK cleavage (Bessen *et al*, 1995).

A high proportion of the diglycosylated banding has been reported in familial cases, (GSS P102L and E200K) that have type 1 migration patterns (Parchi *et al*, 1998a, Cardone *et al*, 1999), while FFI displays type 2 mobility (Gambetti *et al*, 1995, Parchi *et al*, 1995b, Parchi *et al*, 1998c, Rossi *et al*, 1998) and on transmission of Chronic Wasting Disease (CWD) to ferrets (Bartz *et al*, 1998) and TME to hamsters (Bessen and Marsh, 1992). Thus the characteristic glycoform feature of vCJD is not unique. Though vCJD, GSS P102L and FFI cases with this feature are almost completely restricted to the methionine carrying population, aside from fCJD E200K valine homozygotes. However, it may be a feature of first passage with crossing of the species barrier selecting for the diglycosylated form of PrP^{c}.

The banding patterns of other human prion diseases (kuru, fCJD V210I and GSS) have been investigated and they also migrate to 21 or 19 kDas in some cases, though there are many more fragments of PrP^{res} after PK treatment. A 37 kDa band was observed prior to PK treatment in patients with insertional mutations that corresponds to the extended mutant allele (Capellari *et al*, 1997). The production of small molecular weight fragments and their subsequent detection is dependent upon the accesibility PK has to cleavage sites and the presence of the respective epitope to

allow binding of antibody to the fragments. Cases of FFI have type 2 mobility, while cases of GSS show 7-8, 11 and 21 kDa fragments (Tagliavini *et al*, 1991, Parchi *et al*, 1998a). As well as having a more varied production of fragments the relative proportions of the different glycoforms can be more extreme and may correlate to spongiosis (Piccardo *et al*, 1998). Fragments have also been detected in sCJD designated C1 and C2 (Chen *et al*, 1995). The identification of sporadic cases of fatal insomnia (sFI) based on spongiform changes, reactive astrogliosis and PrP^{sc} deposition (Mastrianni *et al*, 1999), with type 2 mobility, as in FFI suggests that the conformation of the PrP^{sc} affects the clinicopathological phenotype (Piccardo *et al*, 1998).

Investigators Diagnosis / Codon 129	Parchi and Gambetti *et al*	Collinge and Hill *et al*
Sporadic CJD MM	1	1, 2, 7
Sporadic CJD VV	1	2
Sporadic CJD MV	1	2, 6
Variant CJD MM	2B	4
Iatrogenic CJD DM MM	-	2
Iatrogenic CJD GHT MV VV	-	3
Iatrogenic CJD GHT MM	-	1
Familial CJD E200K M<	1	-
Familial CJD E200K VV<	2	-
Familial CJD D178N VV	1	-
FFI D178N MM/MV	2	-
Sporadic FI MM	2	-
GSS P102L	1, ± 8 kDa	-
GSS F198S D202N	2, ±8 kDa	-
GSS Q217R	-	27-29 kDa
Kuru	2A	2, 3

Table 5. Comparative isotype classification.

1.14 Investigative frontiers

The main problem facing researchers in this area is the still disputed nature of the causative agent. There is a reasonable amount of agreement that the infectious agent is a protein even though the prion hypothesis is still unproven, however at present this does not help in the management or treatment of TSEs. They are fatal diseases with no cure as yet. The risks from TSEs are limited by the banning of offal, meat on the bone and cattle over 30 months for consumption as well as blood transfusions or organ donations by infected individuals or affected families. Prion replication in spleen and other lymphoreticular tissues makes it possible to detect the PrP^{sc} 27-30 molecular marker for prion infection in tonsil or lymph node biopsy in scrapie (Roels *et al*, 1999) and vCJD. However, the risks of transmission from lymphoid and haematological tissues remains undetermined (Turner and Ironside, 1998). The transmission of BSE to humans was thought to be unlikely due to the species barrier, however, the host range of a TSE agent can broaden upon passage (Bartz *et al*, 1998). It is possible that a large proportion of the population are incubating vCJD, which might be transmitted iatrogenically (Hill *et al*, 1999b, Hill *et al*, 2000) (secondary transmission). Thus continued surveillance is necessary to manage the wider health care implications (recommendations of the Southwood Committee). The possible transmission of vCJD by blood transfusion and use of preclinical tonsil biopsy tests for vCJD, represent some of issues that need to be discussed by groups other than scientists and clinicians. Similar issues concern those families who have offspring born to mothers with vCJD, a group of people who may well increase as more cases of vCJD arise.

The possible routes and spread of infection need to be determined to allow proper risk assessments of primary and secondary transmission of BSE, which might be further elucidated by the detection of PrP^{sc} immunoreactivity and molecular markers of vCJD in peripheral tissues. The risks of oral transmission in terms of doses also need to be better determined for an increased sensitivity in determining the risks to humans of eating food products such as meat on the bone. This will most likely be resolved through transmission studies involving transgenic mice. Studies with scrapie suggest the lymphoreticular system (LRS) is involved. Exactly how genetics affect the outcome of TSE exposure is important and may play a significant role in determining the likely size of the epidemic.

PrP^{res} typing is important for epidemiological studies, especially if BSE transmission to different genotypic, age or ethnic groups has occurred that does not present itself in a similar manner to vCJD. Investigating unusual cases of sCJD is prudent to establish the range of pheontypic presentation and identifying vCJD cases found to be MV or VV at codon 129 could help to identify more closely the relationship between the disease phenotype, genotype and PrP^{res} banding patterns (Zeidler *et al*, 1997b). Investigations of peripheral iCJD infection will help establish the pathological mechanisms of peripheral TSE infection. Typing of various animals may also prove useful considering the possibility of BSE having infected sheep. Identification of BSE in sheep, which may seem to be affected by "scrapie" is important and would pose a significant hindrance to eradication of the disease (Foster *et al*, 1993, Raymond *et al*, 1997, Hill *et al*, 1998, Baron *et al*, 1999, Hope *et al*, 1999, Baron and Biacabe, 2001).

1.15 Hypothesis

The current dogma regarding the different PrP^{res} banding patterns observed in TSEs is that differences in molecular weight correspond to differences in conformation and these differences in conformation represent a molecular marker of prion strains (i.e. strain characteristics are enciphered by protein conformation). Furthermore, this molecular marker can be used reliably and consistently to determine TSE aetiology and differentiate between CJD subgroups. To test this hypothesis two approaches will be adopted:

1. The comparison of a large cohort of CJD cases and analysis of multiple brain regions, to determine the consistency of PrP^{res} banding patterns. These banding patterns can be compared with clinical, genetic and neuropathological data to determine if the clinico-pathological phenotype correlates to a molecular strain of agent. Comparison of neuropathological data and PrP^{res} will allow a greater understanding of the relationship between the pathological process and the prion protein.

2. The use of Western blotting as a tool for differential diagnosis of CJD subgroups and aetiologies will also be examined. This study will focus on CJD for two main reasons; CJD is the most common form of human spongiform encephalopathy and presents with a variety of different phenotypes. Also the differential diagnosis of sCJD and vCJD may be possible based on the unique

Western blotting isotype but this needs to be confirmed and analysis extended to a larger cohort of patients. Being based at the UK National CJD Surveillance Unit provides an unparalleled resource of tissues obtained by biopsy and at autopsy from CJD patients. This will allow analysis of the PrP^{res} presentation of CJD cases in the UK and identification of epidemiological or chronological changes. It will also allow future studies to be carried out in relation to PrP^{res} isotype subgroups.

Materials and Methods

CHAPTER 2

2.1 Collection of material in the National CJD Surveillance Unit

Tissues were obtained with consent from cases referred to the Unit, with no preselection. Referral bias cannot therefore be excluded and the cases were initially examined "blind" to the clinical and pathological data. Investigations were approved by the Lothian Regional Ethics Committee. Cases were assigned a laboratory identification number (RU#year/case) to maintain confidentiality and will be referred to where individual cases are discussed. The Unit has an impressive record on autopsy achievement rates, with 70% of clinically suspected cases examined, which is in contrast to the typical rate of 10% in UK hospitals (Ironside *et al*, 1998).

To carry out SDS-PAGE, frozen material was required. Samples that were frozen at -70°C shortly after autopsy provided the most suitable tissue preparations for recovering and detecting proteins by Western blotting. The autopsy protocol for frozen tissue sampling is included in the appendix. Limitations in terms of local facilities available for tissue handling and storage may influence studies on protease resistant PrP deposition in different brain regions (Bell and Ironside, 1993b, a, 1997). The tissues available range from small portions of undefined brain tissue or spinal cord, to complete half hemispheres frozen as a whole. A range of cases were available for Western blot diagnosis;

Diagnosis	Cases
sCJD	135
vCJD	50
iCJD	18
fCJD	6
GSS	3
FFI	1
Non-human	34
TOTAL	247

Table 6. Cases investigated.

There were also a small number of tissues obtained from outside the UK. Tissues from Alzheimer's disease, lewy body dementia and non-CNS disease patients were analysed as controls. In addition, animal tissues have been investigated; mice inoculated with vCJD, natural scrapie in a sheep, BSE in a cow, FSE in a domestic cat (presumed to be of BSE aetiology) and a marmoset experimentally infected with BSE.

2.2 Sample storage and handling

The frozen tissues were stored at -80°C in a level 3* containment facility. After tissue sampling and homogenisation, samples were stored at -20°C in safe-lock eppendorf tubes. The handling of material, decontamination and safety procedures were carried out in accordance with the Advisory Committee on Dangerous Pathogens, Spongiform Encephalopathy Advisory Committee, "Transmissible Spongiform Encephalopathy Agents: Safe Working and the Prevention of Infection." guide 1999. All work with frozen material not denatured in SDS, was carried out in a Class 1 bio-safety containment hood. Exposure of wrapped nitrocellulose or polyvinyl diflouride (PVDF) membranes and enhanced chemiluminescence (ECL) reagents to Hyperfilm was carried out in a level 2 containment dark room.

2.3 Brain sampling

The frozen tissues were transported from the brain store to neuropathology laboratory using a designated box as secondary containment. Samples were taken observing the full safety procedures for category hazard 3* laboratories. Tissues were sampled in a class 1 bio-safety hood. Work was carried out in pairs as a 'clean/dirty team'. Dissection instruments were provided and notes taken by the 'clean' individual. The 'dirty' individual carried out tissue dissection. Both participants wore chain-mail gloves between two pairs of surgical gloves to safeguard against accidents with disposable scalpels. Dissection was carried out on a cut resistant surface to minimise contamination of the dissection area. Approximately 100 mg pieces of CNS material enriched for grey matter were excised for each sample. Frontal cortex material was routinely analysed whenever possible. Samples taken when a frozen half brain was available for detailed neuroanatomical investigation are detailed in table 7.

When samples were taken from a half brain stored at -70°C, it was left to

warm to approximately -20°C before sampling. This allowed better identification of anatomical features and easier excision. The samples were transferred to 2 ml safe-lock Eppendorf tubes, pre-weighed, labelled and held in a -20°C freeze block in a dedicated transport box (IsoTherm-system 3880, Eppendorf). This secondary containment was then used to transfer samples to the protein laboratory.

Brain Region	Abbreviation
Frontal cortex	FC
Subfrontal cortex	sFC
Parietal cortex	PC
Subparietal cortex	sPC
Temporal cortex	TC
Subtemporal cortex	sTC
Occipital cortex	OC
Suboccipital cortex	sOC
Entorhinal cortex	EC
Hippocampus	H
Amygdala	A
Basal ganglia	BG
Anterior thalamus	AT
Posterior thalamus	PT
Mesencephalon	MC
Cerebellar cortex	CC
Cerebellar vermis	CV

Table 7. Brain regions sampled.

2.4 Western blotting

PrP was analysed by Western blotting as described by Collinge *et al*, (Collinge *et al*, 1996), with modifications as follows.

2.4.1 Western blot sample preparation

2.4.1.1 Homogenisation

Tissues were weighed and homogenised in NPD buffer (Tris buffered saline [TBS] pH 7.6 containing 0.5% Nonidet P40 [NP-40] and 0.5% sodium deoxycholate) to give a 10% w/v (weight/volume) brain homogenate. Homogenisation was carried out in a safe locked Eppendorf tube using a disposable micro-pestle and cleared by centrifugation. Samples were centrifuged at 2000 rpm (420 *g*) at 4°C for 5 minutes (Centrifuge 5417C/R, Eppendorf). The cell debris pellet was retained and the postnuclear supernatant removed to a separate Eppendorf. Loading and unloading of the centrifuge rotor was carried out in the hood and an opening tool used on the Eppendorf tubes to limit the risk of spillage and minimise contact with samples.

2.4.1.2 Metal ion chelation and addition

EDTA (500 mM) was added to the NPD buffer of various samples prior to standard PK treatment (outlined below) to chelate metal ions. These samples were not included in routine analysis and their isotyping is discussed in Chapter 6. Control postnuclear supernatant samples (Alzheimer's disease and Lewy body dementia) were incubated overnight at 4°C, 20°C and 37°C with excess MnCl (100 mM) in NPD buffer prior to standard PK treatment. This was carried out to assess the ability of manganese to induce PrP^{res} formation.

2.4.1.3 Experimental proteolytic degradation

Aliquots of the cleared 10% brain homogenates were subjected to limited proteolysis by digestion with Proteinase K (BDH, UK) at a final concentration of 50 μg/ml for 1 hour at 37°C in a heat block (QBT1 block heater, Grant Instruments [Cambridge] Ltd). Proteinase K is a widely used relatively non-specific protease

classified as a serine endopeptidase and isolated from the filtrate of the fungus *Tritirachium album limber*. It cleaves peptide bonds adjacent to the carboxylic group of aliphatic, aromatic or hydrophobic amino acids. The reaction was terminated by addition of Pefabloc SC (4-[2-Aminoethyl]-benzenesulfonyl flouride hydrochloride) to a final concentration of 1 mM. Pefabloc SC (Boehringer Mannheim/Roche, Germany) is an irreversible inhibitor of serine proteases.

2.4.1.4 Centrifugal concentration of PrP^{res}

Increased yields of PrP^{res} was obtained with the following method; 100 µl of PK digested supernatant and an equal volume of MeOH was spun in a safe lock Eppendorf tube at 14,000 rpm (21,000 *g*) (Centrifuge 5417C/R, Eppendorf) for 1 hour at 4°C. The supernatant was then aspirated and discarded. The remaining pellet was dissolved in 20 µl 2X SDS-PAGE dissociation buffer (outlined below 2.4.2) by vortexing and heating to 100°C for 10 minutes.

2.4.1.5 Enzymatic deglycosylation

PrP^{res} was deglycosylated using PNGaseF (peptide–N^4-[acetyl-β-glucosaminyl] asparagine amidase) Peptide N-glycosidase (New England Biolabs) purified from *Flavobacterium meningosepticum*, under the manufacturers' recommended conditions. It catalyses the following reaction:

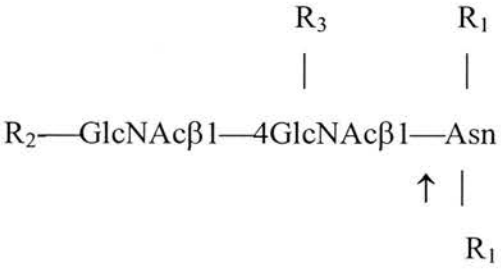

R_1 = N and C substitution

R_2 = H or the rest of the oligosaccharide

R_3 = α1-6 fucose

Denaturation solution (10X, supplied in conjunction with PNGaseF, containing 5% SDS and 10% 2-Mercaptoethanol) was mixed with 12 fold aliquots of PK treated sample and heated at 100°C for 10 minutes in a heat block to denature and

reduce the samples. Deionised H_2O was added at 10% and buffered with 10X G7 buffer (0.5 M sodium phosphate, pH 7.5, supplied with PNGaseF) at 10%, supplemented with 1% NP-40 (supplied with PNGaseF) and a final concentration of 500 U/µl of PNGaseF made and incubated at 37°C for 2 hours in a heat block. The proteins were precipitated by addition of 4 volumes ice cold methanol (MeOH) (160 µl) and centrifugation at 14,000 rpm for 10 minutes at 4°C. 25 µl of homogenisation buffer was added and dissolved by boiling for less than 10 minutes.

This removes, intact, the oligosaccharide chains attached to PrP at the two consensus sequence sites at Asn codons 181 and 197. The asparagine residue is deaminated to aspartic acid. This removes heterogeneity and allows easier resolution of types. It enables the mobility of unglycosylated PrP to be established and helps confirm that the top two bands seen are glycosylated forms of PrP.

2.4.2 Denaturation.

Treatment of the samples in preparation for SDS-PAGE involves boiling samples in Laemlli sample buffer i.e. Dissociation/denaturation buffer (2X) an aqueous solution containing, 125 mM Tris (BDH/Merck), 5% SDS (BDH/Merck), 0.02% bromophenol blue (BDH/Merck) and 20% glycerol (BDH/Merck) in a heat block at 100°C for 10 minutes. Dissociation buffer was added at equal volume to samples and markers.

2.4.3 Electrophoresis

Routine analysis

Mini-PROTEAN® II Dual cell gel (Bio-Rad Laboratories) system was used according to the manufacturers' instructions;

SDS gels were hand-cast at a thickness of 0.75 mm with a 10 well comb. Denatured samples were spun at 2,000 rpm for 5 minutes. Initial screening involved loading 14 µl of denatured samples, as this was found to give a well-resolved signal after X-ray film exposure of between 30 seconds and 3 minutes. Samples were equalised in their loading by addition of homogenisation buffer and dissociation buffer was added to unoccupied wells to prevent distortion of the bands. The buffers

used were based on Laemmlis' method (Laemmli, 1970). Approximately 300 ml of SDS-PAGE running buffer was added to the upper and lower tanks and air bubbles flushed from below the resolving gel with a pasteur pipette. The bromophenol dye front was run close to the bottom of the gel to enhance separation but not run off to minimise contamination of the lower tank. Re-usable components in contact with sample, such as glass plates and spacers, were decontaminated in 2 M NaOH for 1 hour.

Mini-gels reduce electrophoretic run time and reagent usage, thus minimising decontamination. The gel was cast between glass plates separated by spacers, held in a casting assembly. A 12%T (final total monomer concentration) (1%C) (crosslinking monomer concentration) acrylamide SDS-PAGE mini-gel was routinely run (see appendices). Hand-cast gels were overlayed with dH_2O and left to polymerise overnight. The stacking gel (3%T) was overlayed onto the first gel the following day. Electrophoresis was carried out with a Bio-Rad PowerPac 300. Electrophoresis was run on a 0.75 mm 12%T gel at a constant 200 volts for 45 minutes.

Alternative Conditions

Gel thickness was determined by spacers. Gel thickness as well as acrylamide concentration affects the electrophoretic run time and transfer conditions required (see below), the electrophoresis run time was longer with thicker gels. 1.5 mm thick gels allowed the addition of more sample to the wells and produced sharper resolution. 16%T gels were made by altering the constituents according to the formula (see appendices). 16%T gel was run for 1 hour and a 12%T 1.5 mm gel for 40 minutes. The electrophoretic run time must be increased to 1 hour for 16% T gels. Combs forming 12 or 15 well gels were also used.

Bio-Rad precast mini-protean II gels; Tris-Tricine 8 cm x 10 cm (WxH) 1 mm thick with 10-20%T acrylamide, based on Schagger & von Jagow formulation (Schagger and von Jagow, 1987) were used to aid identification of mobility in chelated PrP^{res} samples. Proprietary dissociation buffer (containing 1 M Tris-HCL, pH 6.8, glycerol, 10% SDS, β-mercaptoethanol, 0.5% coomasie G-250) and run buffer (Tris, Tricine, SDS) were used in conjunction with Tris-Tricine precast gels. The electrophoresis was run at 100 volts constant current (approximately 65 mA) for 100 minutes according to manufacturers' instructions. The transfer conditions were the same as hand-cast gels.

Criterion Cell Precast system (Bio-Rad Laboratories) was used as instructed by the manufacturers. A range of different resolving gels including 12%T, 15%T and 8-16% gradient gels, utilising an SDS-free Tris-HCl system were employed. The electrophoretic run time was 55 minutes at a constant 200 volts. Transfer times were altered to account for the larger size of the gels (13.5 by 8.5 cm) from 18 to 25 minutes at 192 mA/gel. The increased size requires longer to run (as outlined in the appendix, A3) and involves diposal of more contaminated waste but it allows a greater number of samples to be loaded (12 as opposed to 10 lanes).

2.4.4 Markers

The molecular weight of PrP^{res} was estimated by reference to biotinylated enhanced chemiluminescence (ECL) (Amersham Pharmacia Biotech) molecular weight markers (1 µl per lane). ECL markers were visualised by the inclusion of streptavidin peroxidase (Amersham Pharmacia Biotech) at a dilution of 1:1500 in the secondary incubation. These markers contain Phosphorylase b (97,400 Da), Bovine serum albumin (68,000 Da), Ovalbumin (46,000 Da), Carbonic anhydrase (31,000 Da), Trypsin inhibitor (20,100 Da) and Lysozyme (14,400 Da) to produce a molecular weight ladder. Benchmark™ prestained protein ladder (Gibco BRL Life Technologies or Bio-Rad Laboratories) (7 µl per lane) and Kaleidoscope markers (Bio-Rad Laboratories) (7 µl per lane) were used to monitor the electrophoretic run and transfer steps. These markers were mixed with dissociation buffer prior to loading on the gel. They contained either one or a range of coloured markers allowing easy identification. BFAV (federal research centre for virus diseases of animals) markers were kindly supplied by Dr Martin Groschup. These markers were dihydrofolate reductase (DHFR) constructs ranging in molecular weight from 16.2-21 kDa 6xHis and mab P4 tagged and use the QIAexpress detection system (Qiagen).

2.4.5 Semi-dry transfer

Proteins were routinely transferred to Hybond-P PVDF membranes (Amersham Parmacia Biotech). Transfer was carried out using a semi-dry transfer apparatus (Sammy-Dry, Schleicher and Schuell) following the method outlined by Towbin *et al*, (Towbin *et al*, 1979) using a Pharmacia EPS 600 power supply. Twenty pieces of blotting paper (3MM) and two pieces of PVDF were required (5.5

by 9 cm). The PVDF was first wet in MeOH, then equilibrated in dH_2O for 15 minutes followed by transfer buffer (192 mM Glycine, 50 mM Tris in dH_2O) for 15 minutes. The SDS page gel was equilibrated in transfer buffer for 5 minutes. The transfer apparatus was setup with 5 sheets of blotting paper laid on the anode with a membrane on top followed by the gel and then another 5 sheets of blotting paper. Air bubbles were expelled by rolling a Universal relatively firmly over the upper layer of blotting sheets before the lid was placed on top. Transfer occurs downwards from the cathode to the anode (graphite electrodes) at 140 mA per gel, 18 minutes for 0.75 mm or 25 minutes for 1.5 mm and 25 minutes for 16%T gels (calculations are outlined in the appendix). After transfer the blotting sheets and gels were disposed of in 2 M NaOH and the transfer assembly was wiped down with paper towels also disposed of in 2 M NaOH. The size of molecules and gel thickness determine the rate of sample migration out of the gels onto the membrane, thus affecting quantitation.

2.4.6 Wet transfer

Novex Xcell II™ blot module (Novex) was used according to the manufacturers' instructions with precast Tris-Tricine gels (Novex) based on Schagger & von Jagow, (Schagger and von Jagow, 1987) formulation. Transfer was carried out at a constant 25 volts (~100 mA) for 1-2 hours.

2.4.7 Gel and Membrane staining

Proteins were visualised nonspecifically on PVDF membranes with Ponceau S or in polyacrylamide gels with Coomassie Blue dye to confirm complete transfer of proteins from the gel to the membrane. Ponceau S staining was carried out with 0.5% Ponceau S in 1% acetic acid incubated for 5-10 minutes with agitation before washing in dH_2O for 2 minutes. Coomassie staining was carried out with 0.1% Coomassie Blue R-250 in an aqueous solution of 7% volume/volume (v/v) acetic acid and 50% v/v MeOH and incubated for 15 minutes. The destaining was carried out in two consecutive 10 minute washes with 7% v/v acetic acid and 50% v/v MeOH.

2.4.8 Western blotting

Western blotting was used for specific identification of PrP^{res}. The use of specific antibody binding and secondary detection systems enabled semi-quantitative results to be obtained with a high degree of confidence in the identity of the protein.

After transfer to PVDF or nitrocellulose the membrane was first washed in TBS-T (20 mM Tris Buffered Saline 137 mM NaCl, 0.1% Tween-20 pH 7.6) for 2 x 5 minutes. The membrane was then washed in 20 ml blocking buffer (5% w/v dried skimmed milk [Safeway] in TBS-T) for 1 hour at room temperature with agitation or overnight at 4°C. The membrane was rinsed and washed in TBS-T (3 x 5 minutes). Then the membrane was incubated with primary antibody for 1 hour at room temperature with agitation or overnight at 4°C. The membrane was washed again in TBS-T (3 x 5 minutes) before being incubated in secondary horse radish peroxidase (HRP) conjugated sheep anti-mouse IgG antibody 1:1000 for 1 hour at room temperature with agitation (kindly provided by Diagnostics Scotland). Streptavidin peroxidase where ECL markers were used was added at 1:1500. A final wash in TBS-T was carried out (4 x 5 minutes).

Antibody concentrations required may differ depending on the source (1:1,000 Dako, 1:10,000 Senetek). The anti-PrP monoclonal antibody 3F4 (Senetek or Dako) was used at a final concentration of 100 ng/ml IgG for 1 hour on human samples. The antibody was supplied as purified IgG2a kappa of ascites diluted in 0.05 mol/L Tris/HCl, 15 mmol/L NaN_3, pH 7.2, 1% bovine serum albumin (BSA). The 3F4 antibody detects an epitope at amino acid residues 108-111 in humans and hamsters and was produced from immunisation with hamster scrapie strain 263K (Kascsak *et al*, 1987). Alternatively 6H4 (Prionics, Switzerland) was used at dilutions from 1 in 10-20,000 (which detects human amino acid residues 144-152, DYEDRYYRE), IgG1 mouse monoclonal with light chain κ subtype, stock 2 mg/ml), final concentration of 100-200 ng/ml. Some anti-PrP monoclonal antibodies such as KG9 do not work on Westerns, despite being of great use in immunohistochemistry (as stated earlier). Antibody cross reactivity with PK may occur and was seen on longer exposures of PrP^{res} negative samples at approximately 28 kDa just above the position that the diglycosylated band was found in on positive samples.

The incubation steps were routinely carried out using a Western processor (Bio-Rad laboratories) and occasionally by hand. The Western processor automatically washes with controlled incubation times and volumes. Reagents were

aspirated. This minimises the contact with potentially contaminated fluids and ensures a consistent treatment of all membranes. Rocking speeds were adjusted to medium (incubations) or fast (washes) settings (15 rpm or 30 rpm). The ISTAR program number 5 or custom PRP program was followed and matched the steps described above. A purge cycle was run with 2% bleach to cleanse tubing after each assay, then rinsed and dried.

2.4.9 PrP^{res} visualisation

PrP^{res} bands can be visualised by a number of different methods. Detection employed the ECL (Amersham Pharmacia biotech) or ECL Plus™ (Amersham Pharmacia biotech) reagents and Hyperfilm ECL (Amersham Pharmacia Biotech). The ECL reagent is converted by the HRP to hydrogen peroxide (H_2O_2) which in combination with the oxidation of luminol and the enhancer produces light. There was a final wash in TBS-T before the development reagents were added to the membrane. The ECL kit reagents were mixed in equal amounts (2 ml of reagent A and 2 ml of reagent B), spotted onto the membrane and incubated for 1 minute. ECL plus was mixed with 4 ml reagent A and 100 µl reagent B. The membranes were wrapped in cling film (Saran) and ECL Plus™ was left to incubate for 5 minutes before disposable of excess reagents. ECL Plus™ reagent Lumigen® PS-3 (2,6-diflourophenyl*N*-methylacridan-9-carboxylate) reacts with HRP and peroxide to produce acridinium ester intermediates that react with peroxide to produce light with a maximum emission at 430 nm (Akhavan-Tafti, 1995). A series of exposures were made with hyperfilm. The film was then developed using an X-Ray film Hyperprocessor (Amersham Pharmacia Biotech). Developing and fixative solutions were obtained from X-ograph imaging systems.

2.5 Prionics Kit

Animal samples were assessed by both standard procedures and the use of a commercially available kit designed for detection of disease specific prion protein in cattle and sheep. The Prionics kit procedure was similar; a 10% brain homogenate was produced, treated with PK, boiled in dissociation buffer and electrophoresed on a 12%T gel. Proteins were transferred to Hybond-P membranes, and the membranes were incubated with 6H4 and a secondary goat anti-mouse IgG alkaline phosphatase

(AP) conjugated antibody, before being detected with CDP-Star (1, 2-dioxetane), an alkaline phosphatase substrate in a proprietary buffer (Tropix buffer). AP dephosphorylates the substrate to yield an anion with a relatively long half life leading to light emission for hours to days. It is ideal in conjunction with PVDF and emits light at 461 nm. This kit has been validated for use in the diagnosis of BSE (Schaller *et al*, 1999).

2.6 Total protein concentration

A modified Lowry assay (Lowry *et al*, 1951) suitable for samples in buffer containing detergent was used following the manufacturers' instructions (DC Protein Assay, Bio-Rad Laboratories). The assay is compatible with Tris and NP-40.

A standard dilution curve was generated from stock BSA (1.4 mg/ml) to give the following concentrations; 0.2, 0.4, 0.8, 1.2, 1.4 mg/ml, in homogenisation buffer. A standard or sample volume of 37.5 µl was added to 187.5 µl of working reagent (20 µl of reagent S per ml reagent A [alkaline copper tartrate solution]) and vortexed. 1.5 ml reagent B (dilute Folin reagent) was then added and incubated for 15 minutes. The absorbance of samples in a disposable 1cm path length cuvette was read at 750 nm up to 1 hr later with an Ultrospec 3000 spectrophotometer (Pharmacia).

2.7 Isotype and glycotype analysis

The banding patterns were classified alongside standard samples according to mobility and relative glycoform ratios as stated in the introduction.

2.8 Densitometry

Glycoform analysis was performed using a GS-700 imaging densitometer and Quantity One 4.1 software (Bio-Rad Laboratories). X-ray films were chosen based on the quality of the exposures. Those with high background, distorted lanes, transfer bubbles, under or over exposed, or other assorted experimental artifacts such as smudges, specks or spots were eliminated. X-ray films were scanned into the densitometer and compared to a grey scale calibration template. A standard protocol was established and applied to all the results (detailed in the appendix A5).

2.9 Quantitation

With the use of a densitometer with sophisticated image manipulation software, strict control over image quality and analysis of multiple exposures, values within the linear range can often be obtained with confidence. Bands were defined manually as $1/3^{rd}$ of the width of a lane, background was removed and a base line intensity determined. The procedure is detailed in the appendix. The linear range was determined based on dilution curves of sCJD and vCJD cases. It corresponded to optical densities (OD) between 0.7 and 7 or 0.8 and 8 (see appendix A5). The variance that can arise due to repeat exposure times or repeated analysis of the same sample (intra-assay error) has been quantified (see appendix).

2.10 Storm™ ImageQuant Densitometry

PVDF membranes were incubated for 5 minutes with ECLPlus™, following Western blotting. The Storm 860 (Molecular Dynamics™) was set to detect chemiluminescence (Fluorescence mode Red [635 nm] / 650 LP 800 volts) and scans performed at normal and high sensitivity with a resolution of 50 dots per cm. A protocol of image manipulation is detailed in the appendix.

2.11 Statistics and presentation of the data

Glycoforms were determined by separation of the three bands, within the linear range (see appendix), as percentages. The mean percentages for each band were determined along with the standard deviation and standard error. Values are expressed as means ± standard error of the mean. Glycoforms were displayed as histograms. The glycoform ratio means for each patient were displayed on scattergraphs with the diglycosylated and monoglycosolated values input onto the x and y-axis respectively. This results in the nonglycosylated band being taken as the remaining percentage of 100 and emphasises the need to characterise the banding patterns as a total of 100% lane density. Statistical analysis was carried out with SPSS version 11. Independent two tailed *t* tests and one way ANOVA analysis was performed to compare the mean di, mono and nonglycosylated bands of cases. Paired two tailed *t* tests were performed on EDTA treated samples. One sample two tailed *t*

tests were carried out to compare the animal samples with vCJD cases. All significant results were within a 95% confidence interval.

2.12 Genetics

The results of genetic analysis of blood taken from the patients while alive was provided by CJD Surveillance Unit staff, including both codon 129 and mutational data. This invaluable resource enabled the subgrouping of the cases. Retrospective analysis of cases in which there was only frozen brain tissue (n=45) were analysed as follows:

2.12.1 DNA Extraction

DNA extraction was carried out primarily on frozen tissues, preferably tissues containing high levels of nuclei but low infectivity, i.e. liver as opposed to CNS, wherever possible. Extraction was carried out in a Category 3* laboratory in a Class 1 bio-safety containment hood. The QIAamp DNA mini kit was used (Qiagen) and the manufacturers' frozen tissue or paraffin embedded protocol followed where appropriate. Buffer reagents were prepared according to the manufacturers' instructions and the reagents were equilibrated to room temperature. Spins were carried out with an Eppendorf Centrifuge 5417C/R.

Samples were analysed alongside 1 co-processed negative per 5-6 samples. Tissues were weighed with the addition of 80µl phosphate buffered saline (PBS) per 25 mg, homogenisation, followed by addition of a detergent buffer (ATL). Proteinase K (20 mg/ml, final concentration 2 mg/ml) was added at 20 µl per 25 mg of tissue and the samples vortexed prior to overnight incubation at 56°C in a heat block. The PK was added in excess to remove protein contaminants. Proprietary wash buffer (AL) was added and vortexed for 15 seconds, incubated at 70°C for 10 minutes followed by a brief centrifugation. Ethanol (96-100%) was added at a volume of 200 µl per 25 mg of original tissue sample, vortexed for 15 seconds, followed by another brief centrifugation. Samples were transferred to QIAamp spin columns (with 2 ml collection Eppendorf) including any white precipitate. The spin columns were centrifuged at 6000 *g* (8000 rpm) for 1 minute. The filtrate collection tube and contents were discarded and the spin columns were placed in a fresh collection tube. Proprietary wash buffer (AW1) was added to the spin columns and centrifuged at

6000 *g* for 1 minute. The filtrate was discarded and AW2 buffer was added to the spin columns for a further wash and centrifuged at 20,000 *g* for 3 minutes. The filtrate was discarded and the spin columns placed in a clean-labelled 1.5 ml microcentrifuge tube. Proprietary elution buffer (AE) or distilled water was added and incubated at room temperature for 1 minute then centrifuged at 6000 *g* for 1 minute. The elution was carried out twice and the two eluates were combined and stored at -20°C.

2.12.2 Polymerase chain reaction

The first two steps were carried out in a class II hood using dedicated equipment and stored separately to other pipettes tubes and racks to prevent cross contamination of polymerase chain reaction (PCR) product. The Qiagen HotStarTaq™ PCR kit was used following the manufacturers' guidelines. Reagents in the stated volumes were added to each tube in the hood in the following order;

Qiagen PCR buffer (TrisHCl containing KCl, $[NH_4]_2SO_4$ and 15 mM $MgCl_2$, pH 8.7) 10 µl, Qiagen $MgCl_2$ (25 mM, final concentration 3 mM) 6µl, Promega dNTPs (10 mM) 2µl, primers A2/A3 (0.1-0.5 µM) 1µl, HotStarTaq (5 units/µl, 1 unit per reaction) 0.2 µl, dH_2O 78.8 µl. Taq is sensitive to agitation so was carefully mixed and briefly centrifuged, prior to aliquoting 98 µl per tube. Extracted DNA templates were thawed, mixed and pulsed down. 2 µl of extracted DNA was added to each tube with a positive displacement tip. 2 µl of dH_2O was added to the reagent negative in place of a template. A2 primer (forward) TGA TAC CAT TGC TAT GCA CTC ATT C, A3 primer (reverse) GAC ACC ACC ACT AAA AGG GCT GCA G. Samples were then incubated using the Peltier Thermal Cycler-200 DNA engine (MJ-Research), and run on program PrPA2A3, featuring the following cycles of denaturation (steps 2 and 6), step down annealing temperatures annealing (steps 3 and 7) and elongation (steps 4, 8 and 10) with an initial HotstarTaq DNA polymerase activation step.

1. 95°C 15 minutes
2. 94°C 1 minute
3. 65°C 1 minute (decrease 0.5°C per cycle)
4. 72°C 2 minutes
5. Repeat steps 2-4 10 times.
6. 94°C 45 seconds
7. 60°C 30 seconds
8. 72°C 1 minute
9. Repeat steps 6-8 30 times.
10. 72°C 15 minutes
11. 4°C forever
12. END

PCR products were then stored at 4°C.

2.12.3 *PRNP* codon 129 restriction digest assay

PCR products were cleaved with the restriction enzyme Nsp1 to generate DNA fragment lengths specific to the polymorphism at codon 129 (Zimmermann *et al*, 1999). Nsp1 from *Nostoc* species is cloned and expressed in *E. coli*. The Nsp1 restriction site cuts at the following sequence encoding methionine;

5'-Pu CATG↓ Py-3'
3'-Py ↑GTAC Pu-5'

The following reagents were mixed in the stated volumes, NEB buffer 2, 1 µl, BSA 100 µg/µl (NEB), 0.1 µl, Nsp1 5 U/µl (NEB) 0.2 µl and dH_2O 3.7µl and pulsed down. 5 µl of reagent mix and 5 µl of DNA (PCR product) was added to each tube and mixed well. Samples were once again run on the DNA Engine, program 37DEG1DIG (37°C, 5 hours).

2.12.4 Agarose gel electrophoresis

To give a 1.5% agarose gel 2.25 g of agarose (Merck) was mixed with 150 ml 1X 89 mM Tris-boric acid, 2 mM disodium EDTA, dihydrate pH 8.3 (TBE) and heated until the agarose melted and the solution was clear. Once cooled sufficiently to be handled, Ethidium Bromide (10 mg/ml) was added (to give 0.33 μg/ml) and gently mixed. The gel was then poured into a gel assembly and allowed to set for 30 minutes. TBE (1X) was added to the gel tank to equilibrate with the gel for 5 minutes. Bromophenol Blue loading dye was mixed with an equal volume of Nsp1 digested PCR product. A 100 bp ladder was added to the first lane and the samples added subsequently. Electrophoresis using a power pack at 75-100 Volts for approximately 1 hour, until there was migration of the dye front by ~5 cm to ensure good band separation. The gel was orientated so that the samples migrated to the anode. Gels were photographed under UV.

2.13 Histology

The PrP immunohistochemistry and haemotoxylin and eosin (H&E) information was obtained from autopsy reports and detailed investigative studies (Kovacs *et al*, 2000, Kovacs *et al*, 2002). The findings were described in terms of typical features of the disease, spongiform vacuolation, neuronal loss and amyloid deposits identifiable on H&E sections. Astrocytic gliosis was identified by glial fibrillary acidic protein (GFAP) immunostaining and PrP deposits identified by immunostaining with numerous anti-PrP antibodies, primarily 3F4 and KG9. The PrP immunoreactive staining was subclassified into four main patterns by Kovacs, G.; vacuolar, diffuse/synaptic, neuronal or granular deposits and plaques. Vacuolar deposits were found around areas of confluent spongiform vacuolation in a sparse granular pattern. Diffuse staining was a nondescript pattern found in the neuropil with small granular deposits. Neuronal staining was in either intracellular or pericellular punctate form with granular deposits surrounding an unstained region around the nucleus (the perikarya). Finally granular deposits were found in association with plaques forming a dense centre that was only detected on immunostaining.

The wide array of subjects and ancillary information enables a detailed definition of subgroups and correlations to be drawn between PrP^{res} and other

phenotypic features. Those involved in obtaining and providing the data are duly acknowledged.

2.14 Transmission procedure

The transmission procedure was as outlined in Nature (Bruce *et al*, 1997). Samples were taken from each of three vCJD patients in the category 3* diagnostic laboratory facilities of the National CJD Surveillance Unit. The sampling was from areas showing the maximum pathology, whenever possible and stored at -80°C before transport to the IAH Neuropathogenesis Unit (Edinburgh, Scotland). They were homogenised at 10% (w/v) concentration in sterile physiological saline and stored at -20°C. The samples were thawed and resuspended by being drawn repeatedly through a series of graded needles. Control samples consisted of saline passed through the homogeniser and glassware prior to infected samples, also frozen at -20°C. The samples were inoculated into mice under halothane anaesthesia by intracerebral (20 µl) and intraperitoneal (100 µl) injection. Three inbred mouse strains were used; C57BL and RIII (both of the $Sinc^{s7}$ or $Prn\text{-}p^{a}$ genotype) and VM ($Sinc^{p7}$ or $Prn\text{-}p^{b}$ genotype). Two controls per mouse strain were inoculated and each of the vCJD patients' samples was inoculated into two mice of each strain i.e. vCJD patient 1 inoculated into two C57BL mice. Mice were coded, examined daily throughout their lifespan, and formally scored for signs of neurological disease from 250 days after injection. Mice showing definite signs for two consecutive weeks were killed and incubation periods calculated as the interval between injection and this standard clinical endpoint. All other mice were maintained to full life span. Post-mortem, a lateral third of each mouse brain was dissected aseptically and frozen at -20°C. The samples were then transported to the CJD surveillance unit, handled in the same way as potential human TSE material was and stored at -20°C. They were thawed and homogenised in the category 3* facilities of the protein laboratory prior to Western blotting in exactly the same manner as for human CNS material, as stated above. Samples were obtained with a blind ID number from 1 to 32, 24 samples in all. The samples were then amalgamated into the protein lab sample records and assigned extract numbers 00.516 to 00.539 (year.chronological number). The samples were homogenised, PK treated and run on 12% SDS-polyacrylamide gels, followed by semi-dry transfer onto PVDF membrane and Western blotting with 6H4 primary monoclonal antibody. Detection was carried out with ECL Plus reagents. Storm

chemiluminescence analysis and X-ray film records were made where possible. The samples were run alongside previously classified human CNS CJD standards and consensually 'typed' according to our classification nomenclature (Ironside *et al*, 2000) when PrP^{res} could be detected.

Results

CHAPTER 3: PrP^{res} isotyping.

3.1 Classification

The study started as a retrospective analysis of definite CJD cases. A comprehensive group of cases were investigated, including a range of human TSE cases and a few pertinent animal TSEs. Along with these were cases of non-TSE neurodegenerative disease used as controls. This constitutes the largest study of the PrP biochemistry of prion disease cases conducted in the UK so far and the largest reported cohort of vCJD and iCJD cases. By increasing the sample size (n) of studies and attempting to correlate Western blotting banding patterns with genetic, clinical and histological data, a better understanding of the phenotypes of disease can be established, allowing anomalous cases to be further investigated. Continued surveillance of CJD cases, especially unusual cases e.g. those of long duration or in young people is essential to potentially identify vCJD *PRNP* codon 129 MV or VV genotypes which may or may not have recognisable neuropathology or banding patterns. Therefore, is there a relationship between the PrP^{res} banding pattern and either the aetiology, codon 129 polymorphism, age at onset, disease duration, neuropathology or clinical features?

Cases referred to the UK CJD surveillance unit were ordered into aetiological subgroups (sCJD, fCJD, iCJD, vCJD) according to final diagnosis. Further classification was then carried out to take into account codon 129 genotype (MM, MV, and VV) to determine the relative contribution of this well-defined host factor to the disease phenotype.

Western blot analysis of PrP from CJD frontal cortex (figure 4) shows three bands in the low molecular weight range. These correspond to di, mono and nonglycosylated PrP (Haraguchi *et al*, 1989, Bessen and Marsh, 1992). Deglycosylation of PrP with PNGaseF results in a single PrP glycoform with a M_r of around 20 kDa. Experimental PrP constructs and familial forms of CJD incapable of N-linked glycosylation (discussed in chapter 7) as well as treatment of PrP expressing cultured cells with tunicamycin (glycosylation inhibitor) have demonstrated the nature of this characteristic banding pattern. Treatment with the non-specific serine protease, Proteinase K (PK) is a standard test of TSE and results in NH_3-terminal

truncation of the three glycoforms and the appearance of three bands of increased M_r, termed PrP^{res} (Caughey *et al*, 1991). This isotyping study focussed on the use of the banding pattern as a molecular marker for diagnosing TSEs and investigated the scope of variation within this pattern.

3.2 Non-prion diseases

Non-prion CNS/neurodegenerative diseased tissues were tested. Neurological diseases, e.g. Alzheimer's, Lewy Body Dementia (LBD), corticobasal ganglionic degeneration and murine brain tissue from mice inoculated with saline were chosen as suitable negative control cases. PK (50 μg/ml) treatment of all these cases lead to a complete loss of PrP specific signal (figure 4). 10% brain tissue homogenates treated with PK were loaded at the same levels as PrP^{res} positive controls. Concentration of samples 15 fold as detailed in the Materials and Methods and over exposure of X-ray film failed to detect PrP^{res}. PK treated control samples have a lack of bands being indicative of susceptibility of host PrP to PK treatment and thus a lack of the disease associated PrP^{res}. The detection of PrP^{res} under the standard protocol in conjunction with clinical and neuropathological findings was therefore deemed sufficient to declare samples TSE negative. It should be noted that PK itself has a molecular weight of 28.9 kDa and can sometimes be observed as a sharp band due to cross-reactivity in concentrated samples and should not be misinterpreted as a PrP band (Jany and Mayer, 1985).

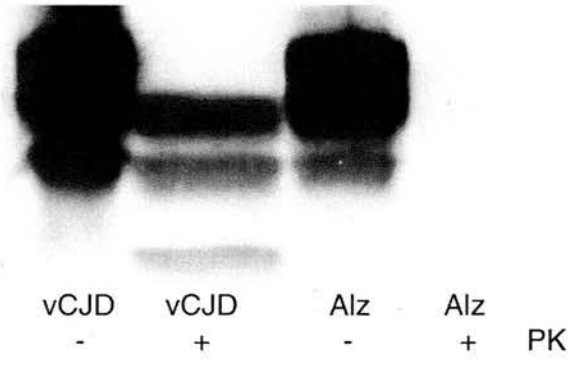

Figure 4. Proteinase K treatment of CJD and Alzheimer's. 10% w/v brain homogenates of variant CJD and Alzheimer's disease before (PK-) and after proteinase K digestion (PK+). Lane 1 and 2, vCJD postnuclear supernatant, lane 3 and 4, Alzheimer's postnuclear supernatant.

3.3 Prion disease classification

3.3.1 Standard isotyping

Samples were loaded at equivalent levels for primary screening (14 μl) as stated in the materials and methods. PrP^{res} was invariably detected when loaded at this level by X-ray exposures of 30 seconds to 3 minutes. The consistency of PrP^{res} levels in screened samples aided rapid positive identification of TSE disease. PrP^{res} banding intensity after PK treatment did not correlate to overall protein levels either prior to or after PK digestion e.g. if the banding intensity seen on X-ray film was high there was not necessarily a high overall protein content. Relative signals as compared to positive standards were a more useful guide than total protein content in assessing molecular weight and glycoform ratio.

The first stage of the study involved analysing a wide range of samples, blinded to diagnosis, codon 129 genotype and all other patient information (blind study 1 n = 59, blind study 2 n = 52) and comparing their banding patterns. The resultant molecular weights and glycoform patterns were compared with classifications of a limited number of samples analysed previously by Collinge *et al*, and the classification systems applied by Collinge *et al*, 1996 and Parchi *et al*, 1996. Two molecular weight groups of samples were identified in all but two cases and two glycoform patterns (figure 5). The molecular weights were termed types 1 and 2 as described by Parchi *et al*, 1996 with type 1 having a nonglycosylated band of 21 kDa and type 2 having a nonglycosylated band of 19 kDa. Consistent correlation with samples analysed by Collinge *et al*, 1996 could not be made. Glycoforms were classified A or B, with A representing a prominent monoglycosylated content and B representing a prominent diglycosylation. In no cases was prominent nonglycosylation seen, though some cases had nonglycosylated bands of similar intensity to the monoglycosylated band (discussed further in chapter 4). All subsequent investigations were classified according to these isotypes and in total 213 human TSE cases were investigated.

Figure 5. PrP^{res} isotypes. PK treated brain tissue from sporadic and variant CJD analysed on a 12% polyacrylamide gel with the anti-PrP monoclonal antibody 3F4, demonstrating types 1, 2A and 2B. Lane 1, sCJD MM type 1, lane 2, sCJD VV type 2A, lane 3, vCJD MM type 2B. Markers are indicated by horizontal bars and their molecular weights indicated in kDa.

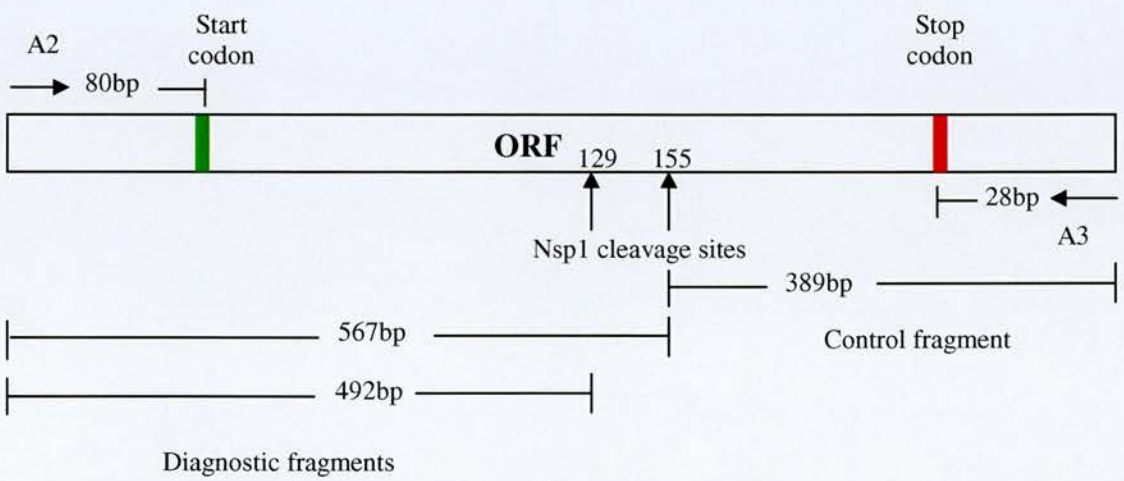

Figure 6. *PRNP* primer and restriction digest map.
A2 and A3 represent the corresponding primer sequences.

3.3.2 Codon 129 determination

Restriction fragment length polymorphic (RFLP) digestion of purified and amplified DNA with Nsp1, results in three *PRNP* fragments (figure 6). The three banding patterns seen on agarose gel electrophoresis resemble the three possible polymorphic subgroups MM, MV, VV (figure 7). This is a result of the different specificity for DNA cleavage of Nsp1 at codon 129 of *PRNP*. Nsp1 also cuts at codon 155 of the *PRNP* ORF but only cuts at codon 129 if a methionine is present (figure 6). The uncut DNA migrates at 956 bps and an internal control band of 389 bps is generated from cleavage at codon 155 in all samples. The distinguishing bands are at 567 bps (the valine encoding gene uncleaved by Nsp1) and at 492 bps (the cleaved methionine encoding gene), both of which can be seen in heterozygotes.

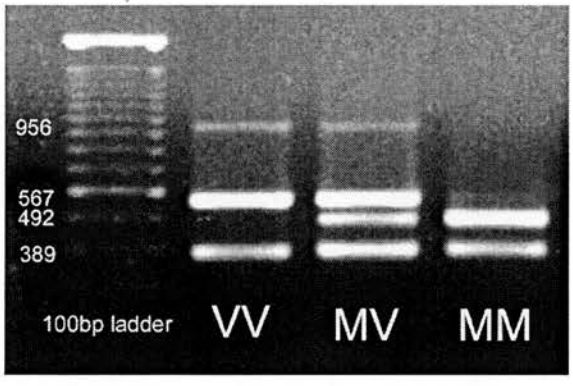

Figure 7. *PRNP* codon 129 analysis by agarose gel electrophoresis of RFLP digest fragments of PCR products. Lane 1, 100 bp DNA ladder, lane 2, VV patient, lane 3, MV patient, lane 4, MM patient.

3.3.3 Subgroup classification

The PrP isotype classification was considered in combination with the final diagnosis of sCJD, vCJD, iCJD, fCJD and the methionine/valine polymorphism at codon 129 of the *PRNP* gene e.g. sCJD MM 1.

Typical examples of the three isotypes (1 MM, 2A VV and 2B MM), shown in figure 5, were selected and used throughout the study as positive control standards against which the isotype of new samples were determined. Repeated sampling of brain tissue from these standard cases gave consistent mobility (vCJD n=25, sCJD MM 1 n=9, sCJD VV 2A n=17). Prior to proteinase K digestion, PrP in brain

homogenates showed no obvious difference in M_r (figure 4). Proteinase K digestion produces an increase in the mobility of each glycoform in all three samples, enhances the resolution of the bands and removes background protein staining/signal.

The foregoing classification of CJD cases was made on the basis of analysis of PrP^{res} found in the cortex, usually frontal cortex. Western blot analysis of CNS tissue from a total of 213 cases of CJD showed the presence of two predominant PrP^{res} conformations either 21 kDa (type 1) (n=84) or 19 kDa (type 2) (n=48) nonglycosylated PrP^{res}. There were a few cases of sCJD, iCJD (GHT) and 1 case of fCJD (GSS) that could not be classified as types 1 or 2 (table 8). The glycoform ratios were broadly of type A (predominantly monoglycosylated) or type B (predominantly diglycosylated), though once again there were exceptions to the rule and a range of glycoform ratios were detected. A non-quantitative approach to isotyping can be determined visually, however, a quantitative assessment will be covered in chapter 4. Cases with type 2 mobility in which the diglycosylated PrP^{res} glycoform predominates were termed type 2B (Parchi *et al*, 1997). So far this pattern is distinct and specific to vCJD.

3.3.4 Intermediates

A number of cases did not fit conveniently into the classification system adopted. A limited number of cases had nonglycosylated PrP^{res} with a mobility intermediate (INT) between type 1 and type 2. This was clearly seen in two cases of sCJD during the initial characterisation exercise, both of which were methionine homozygotes (RU#96/060 and RU#96/128) (figure 8). These two cases were 68 and 82 years old at onset of symptoms and their disease duration was 9 and 3 months respectively. These values are more akin to the sCJD MM 1 subgroup than the MM 2A subgroup. Repeated sampling gave a consistent mobility. Subsequently, one other case of sCJD (valine homozygote), three cases of iCJD GHT (two VV RU#92/019, RU#95/055 and one MV RU#97/013) and one GSS case (RU#94/007), failed to conform to the above classification system and displayed an intermediate mobility.

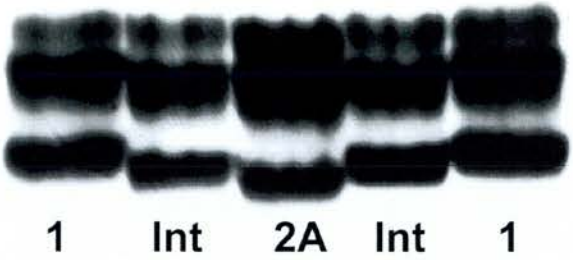

Figure 8. Intermediate mobility type in sCJD MM patients. Lane 1, sCJD MM type 1, lane 2, sCJD MM type INT, lane 3, sCJD VV type 2A, lane 4, sCJD MM type INT, lane 5, sCJD MM type 1.

The biochemical basis of this intermediate type mobility may represent type 1 PrP^{res} isolated in a metal-depleted form. This could represent the *in vivo* state of the PrP^{res}, isolated, as metal ion chelators are omitted from our extraction procedure or could be an experimental anomaly due to the removal of metal ions prior to PK cleavage (for results see chapter 6).

Diagnosis	129	Type 1 (%)	INT (%)	Type 2A (%)	Type 2B (%)	Total (%)
Sporadic CJD	MM	68 (81)	2 (66)	13 (27)♦	0	83 (61)
	MV	12 (14)	0	15 (31)♦	0	27 (20)
	VV	4 (5)•	1 (33)	20 (42)▪	0	25 (19)
Total		84	3	48	0	135
Variant CJD	MM	0	0	0	50 (100)	50
	MV	0	0	0	0	0
	VV	0	0	0	0	0
Total		0	0	0	50	50
Iatrogenic CJD	MM (DM)	2	0	0	0	2
	MV (GHT)	2	1	5▲	0	8
	VV (GHT)	1	2	5	0	8
Total		5	3	10	0	18
Familial CJD	MM	7	0	0	1	8
	MV	1	1	0	0	2
	VV	0	0	0	0	0
Total		8	1	0	1	10
Total		97	7	58	51	213

Table 8. Isotype/genotype classes in sCJD, vCJD, iCJD and fCJD.

• includes 1 case in which type 2 PrP^{res} was subsequently detected, ▪ includes 2 cases in which type 1 PrP^{res} was also detected. ♦ includes 3 cases in which type 1 PrP^{res} was subsequently detected. ▲ includes one case displaying predominantly type 2 PrP^{res} with some type 1. Values in brackets represent percentages of each codon 129 genotype in each isotype subgrouping.

3.4 Sporadic CJD

Sporadic CJD was found to be heterogeneous in terms of isotype and genotype. All six possible isotype / genotype combinations (MM 1, MM 2A, MV 1, MV 2A, VV 1, VV 2A) were represented but there was a clear difference in the number of cases in each subgroup (table 9). Overall type 1 (63.9%) was more frequently observed than type 2 (36.1%) and within the type 1 group, methionine homozygotes were most abundant (81%). Within the type 2 group the genotypes were more evenly represented but with a slight preponderance of valine carriers (72.3%). The over representation of MM individuals with sCJD (61.8%) in comparison to the general population ~40% (Palmer *et al*, 1991, Alperovitch *et al*, 1999) extends to isotyping. The distribution of codon 129 genotypes in isotyped cases (61.8% MM: 19.9% MV: 18.3%VV) reflects that seen for sCJD cases analysed at the CJD unit since 1990 (69% MM: 15% MV: 17% VV) (National UK CJD Surveillance Unit, 10th annual report, 2001). The greater numbers of type 1 individuals may be due to type 1 PrP^{res} being formed by MM patients or alternatively type 1 PrP^{res} may afflict MM individuals to a greater degree. Whether the codon 129 is a susceptibility or determining host factor is therefore not apparent based merely on the prevalence of MM 1 cases.

Codon 129	Isotype	Cases	Gender M/F %	Age at onset Years (range)	Disease duration Months (range)
MM	1	68	44 / 56	65.3 (42-86)	4.7 (1-21)
	2A	13	54 / 46	54 (37-72)	19.1 (8-38)
MV	1	12	55 / 45	60.3 (15-79)	12.2 (2-54)
	2A	15	36 / 64	64.5 (50-78)	18.3 (3-52)
VV	1	4	50 / 50	46.5 (25-78)	16.5 (8-29)
	2A	20	45 / 55	62.7 (46-79)	5.5 (2-11)
MM	2B	50	56 / 44	27 (12-53)	15.3 (7-39)

Table 9. Sporadic and Variant CJD subgroups. Gender, age at onset and duration.

The sCJD MM 1 subgroup constitutes the majority of sporadic cases (51.1%) with a mean age at onset of 65.3 years (range 42-86) and a mean disease duration of 4.7 months (range 1-21). This subgroup contains two cases with deletions of 24 bps, found in a small proportion of the population (Bosque *et al*, 1992) not shown to cause familial TSE and classified as sCJD. The sCJD MM 2A subgroup (9.8% of total cases) constitutes cases with a mean age at onset of 54 years (range 37-72) and mean disease duration of 19.1 months (range 8-38). The age at onset ($p < 0.000$, unpaired two tailed *t* test) and disease duration ($p < 0.000$, unpaired two tailed *t* test) is significantly different for these two subgroups. Sporadic CJD MM cases, as a whole, have a mean age at onset of 63.6 years and a disease duration of 6.9 months. The MM 2A subgroup has a younger age at onset and significantly longer duration than the MM 1 subgroup. These features, along with the same codon 129 genotype, are in common with some vCJD cases especially considering the occurrence of vCJD in older individuals. The separation of the MM 1 and MM 2A two codon 129 sCJD subgroups would not be possible without Western blotting analysis and suggests that there is a correlation between clinical features and PrP^{res} conformation. Chronological analysis of MM 2A cases shows the identification of only one case prior to 1996, in 1991. There are similarities between MM 2A cases and vCJD particularly in terms of the duration, though to some extent also the younger age at onset. However, this does not suggest that these cases classified as sCJD are a result of BSE exposure and their identification is most likely the result of improved ascertainment. This highlights the usefulness of the glycoform pattern in distinguishing the two aetiological groups. Importantly, these cases are still clinically and neuropathologically distinct from vCJD.

The sCJD MV 1 subgroup (9% of total cases) constitutes a minority of sporadic cases with a mean age at onset of 60.3 years (range 15-79) and a mean disease duration of 12.2 months (range 2-54). As seen with the MM 2A subgroup, chronological analysis only shows two cases prior to 1997, in 1991 and 1992, once again long disease duration may be a factor in this or the relative rarity of cases falling within this subgroup. The sCJD MV 2A subgroup (10.5% of total cases) constitutes cases with a mean age at onset of 64.5 years (range 50-78) and a mean disease duration of 18.3 months (range 3-52). The disease duration is not significantly different between the two MV subgroups ($p = 0.316$, unpaired two tailed *t* test). Most noticeable is the gender difference within this subgroup (36% male: 64% female). Interestingly the disease duration in the heterozygotes patients is not notably

prolonged in comparison to MM 2A or VV 1 patients and in the MV 1 group aside from one case with a very long 54 month duration (RU#97/292) is actually more in keeping with the MM 1 subgroup (4.25 months, excluding RU#97/292). The wide range of age and duration along with intermediate mean values, implies that individual cases may be atypical, but as a group heterozygosity tempers the extremes of codon 129 influence. This subgroup includes a case carrying a deletion suspected to be 24 bps in the octapeptide repeat region that will be discussed in more detail in the next chapter.

Cases making up the sCJD VV 1 subgroup (3% of total cases) are the rarest and have a young mean age at onset of 46.5 years (range 25-78) and prolonged mean disease duration of 16.5 months (range 8-29). The sCJD VV 2A subgroup is the second most prevalent subgroup (15% of total cases) constituting cases with a mean age at onset of 62.7 years (range 46-79) and a mean disease duration of 5.5 months (range 2-11). The age at onset ($p = 0.027$, unpaired two tailed *t* test) and disease duration is significantly different between these two subgroups ($p < 0.0001$, unpaired two tailed *t* test). A detailed analysis of 12 cases falling within the VV subgroup is detailed in Kovacs *et al*, 2000 (see appendix). Referred to as CJD1, CJD2 to CJD12, five of these cases (CJD2 RU#96/011, CJD4 RU#92/046, CJD7 RU#93/014, CJD10 RU#94/083, and CJD12 RU#94/136) isotyped from frozen frontal cortex material are from the VV 2A subgroup and their clinical and neuropathological features suggest all 12 cases would have type 2 PrP^{res}. The average age at death of 63.6 years (range 49-80) and duration of illness, 6 months (range 4-17) are in line with the VV 2A subgroup. The patients presented with unsteady gait and half suffered memory loss, they all became demented and exhibited myoclonus, before akinetic mutism and death. No CSF findings or EEG triphasic complexes indicated CJD. Neuropathological findings were obtained (with kind permission) from Kovacs *et al*, (Kovacs *et al*, 2000). The histopathology of these cases represents an in depth examination of VV sCJD cases and provides a good description of the VV 2A subgroup. Spongiosis is common as are PrP plaque-like structures in cortical, basal ganglia, parahippocampal gyrus, thalamus, hypothalamus and cerebellum, sometimes also present in the subcortical white matter and hippocampus and diffuse/synaptic PrP staining.

With all these cases the availability of frozen tissue implies further investigation was warranted and this may be due to either doubt over the diagnosis of possible CJD or similarity to vCJD. For this reason the age and duration data may be

more similar to vCJD than for sCJD subgroups as designated by codon 129 data alone. Differences in gender are marginally over represented by females in the larger sCJD cohorts (MM 1, MV 2A and VV 2A) (table 9).

3.5 Variant CJD

All cases (n=50) with a final diagnosis of vCJD appeared relatively homogeneous and quite distinct from sCJD. All cases showed a type 2B isotype and occurred in methionine homozygotes. In addition, the cases all had a prominent diglycosylated PrP^{res} band in stark contrast to all the sCJD cases that displayed predominant monoglycosylated or more rarely nonglycosylated PrP^{res}. This confirms earlier observations (Collinge *et al*, 1996, Hill *et al*, 1997a, Ironside *et al*, 2000, Parchi *et al*, 2000b, Head, 2001) and reaffirms this discriminating feature as a means of distinguishing between sporadic and variant CJD. Western blotting is thus a reliable ancillary diagnostic test for vCJD.

The vCJD cases continued to display a consistent isotype throughout the study, distinct from any sporadic cases, despite a changing range in age at onset since the first reported cohort in 1996, with a mean age at onset of 26.8 years and range (Will *et al*, 1996). Recent figures show a mean age at onset of 26 years but a range of 12 to 74 years and a mean disease duration of 13 months (range 6-39) (National UK CJD Surveillance Unit, 10th annual report, 2001). The total number of definite and probable vCJD cases in the UK up to 31st of January 2002 was 114, 53% male and 47% female (National UK CJD Surveillance Unit, 10th annual report, 2001). The cases investigated by Western blotting were representative of the cases as a whole with 56% male and 44% female, mean age at onset of 27 years (range 12-53) and mean disease duration of 15.5 months (range 7-39). This study is the largest analysis of vCJD cases, spanning 5 years and enables the establishment of a good baseline from which changes in the molecular phenotype can be identified. If this coincides with any other epidemiological, clinical or phenotypic changes in vCJD presentation an increased understanding of linkage to pathogenesis may be established.

3.6 Iatrogenic CJD

Between 1970 and the end of 2001, 45 cases of CJD in the UK have been related to surgical procedures or therapeutic treatments. Six cases were in individuals who received dura mater (DM) grafts, 38 received human-derived growth hormone and one received human gonadotrophin (National UK CJD Surveillance Unit, 10th

annual report, 2001). The 18 iCJD cases described here are the largest single cohort of cases so far reported. They are primarily divided into two major aetiological subgroups, those caused by dura mater transplants (n=2) and those treated with pituitary derived growth hormone/gonadotrophin (GHT) (n=16), prior to codon 129 classification. The iCJD GHT cases as a whole had a mean age at death of 29.5 years (range 20-45) while the dura mater cases were on average 43 years old at death (27 and 59) (National UK CJD Surveillance Unit, 10th annual report, 2001). The two DM cases with available frozen tissue were both MM type 1 (figure 9), but the age and disease duration figures were very different; 44 years old with a duration of 5 months and 24 years old with a duration 33 months. The GHT cases analysed were in individuals with MV or VV genotypes, 8 of each i.e. 50:50. The mean age at onset for the GHT cases analysed was 30.7 years (range 37-23) and mean disease duration is 11 months (range 5-18). The homozygous cases have a younger mean age at onset (28.8 years) and shorter disease duration (6.5 months) than heterozygotes, 31.9 years and 13.9 months respectively. The distribution of isotypes within the subgroups reflected that seen in sCJD with the presence of a valine allele; 56% (9/16) predisposing to generation of type 2A PrP^{res}. Equal numbers were diagnosed as type 1 or intermediate 18.8% (3/16) and at least one case had an anomalous finding (co-existence of types 1+2). As with sCJD, all mobilities were represented (1, 2A and INT) (table 8). In one case PrP^{res} was hard to detect, only spinal cord tissue was available in this case and appeared to have an intermediate mobility. The presence of PrP^{res} has been confirmed by immunocytochemistry in this case and reported in other peripheral iCJD infections (Goodbrand *et al*, 1995, Sutherland *et al*, 1996).

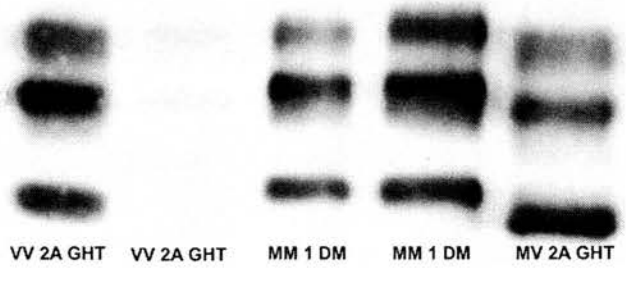

Figure 9. Iatrogenic CJD cases displaying the aetiological and isotype differences. Lane 1, GHT VV type 2A case, lane 2 GHT VV type 2A case with low PrP^{res} levels, lane 3, DM MM type 1, lane 4, DM MM type 1, lane 5, GHT MV type 2A.

Similar proportions of isotypes among the iCJD and sCJD codon 129 groups were obtained despite the route of infection being an additional factor in the

pathogenesis. This implies that the codon 129 polymorphism does not influence peripheral conversion or transport to the CNS. The small sample size makes it difficult to draw conclusions from the results of this study alone. Type 1 MM cases were restricted to DM infection, while GHT cases showed a preponderance of type 2 mobility and were either MV or VV.

3.7 Familial CJD, GSS, FFI

Familial CJD, GSS and FFI cases arise as a result of a number of different *PRNP* sequence mutations. They do not reflect any route of exposure or interactions between host and infecting strains, however their phenotypic characteristics are still of interest and a range of isotypes were identified.

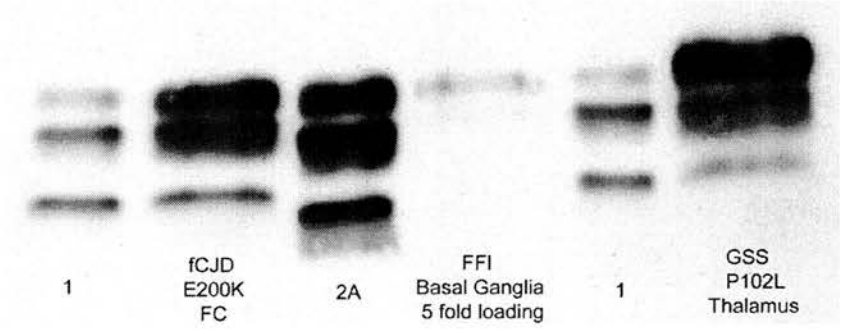

Figure 10. Comparison of sCJD standards and the three phenotypic familial prion diseases. The standards are from frontal cortex material and the tissues of the familial cases are indicated. Lane 1, sCJD MM type 1, lane 2, fCJD MM E200K type 1B, lane 3, sCJD VV type 2A, lane 4, FFI MM D178N, lane 5, sCJD MM type 1, lane 6, GSS MM P102L.

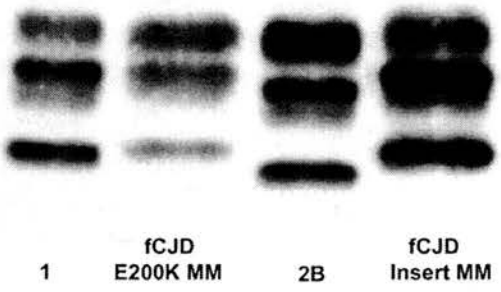

Figure 11. Comparison of isotype and glycoform differences between sCJD MM type 1 and vCJD MM 2B standards and fCJD MM patients. Lane 1, sCJD MM type 1, lane 2, fCJD MM E200K type 1B, lane 3, vCJD MM type 2B, lane 4, fCJD MM insert type 1.

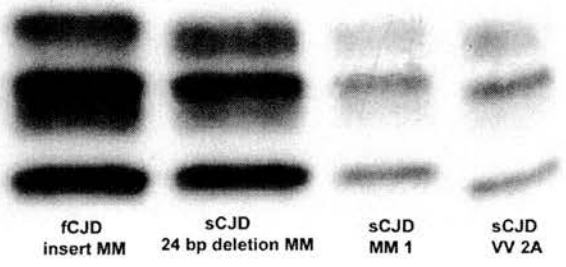

Figure 12. Comparison of familial CJD case carrying an insert with a case featuring an uncommon polymorphism classified as sCJD and sporadic CJD standards. Lane 1, fCJD 4 octapeptide repeat insert MM, lane 2, sCJD MM 24 bp deletion, lane 3, sCJD MM type 1, lane 4, sCJD VV type 2A.

Familial CJD, FFI and GSS cases were available (n = 6, 1 and 3 respectively). The fCJD cases included 3 cases carrying the E200K mutation (Lee *et al*, 1999), 2 with inserts (an undefined insert in one, figure 11, and 4 octapeptide repeats in the other, figure 12) and one with a rare V180I mutation (Nixon *et al*, 2000) (discussed further in chapter 7). The FFI case had a confirmed D178N mutation coupled with methionine homozygosity and age at onset of 67 years. The GSS cases were of the classical P102L variant, one was heterozygotic at codon 129 and displayed a different isotype (INT) to the two MM cases. The heterozygote patient was unrelated to the homozygous patients, one of whoms PrP^{res} is shown in figure 10 (Adam *et al*, 1982, Baker *et al*, 1985). Presence of a valine can lead to a greatly different clinical

presentation (Young *et al*, 1997). The isotype patterns were diverse and in many cases quite unlike sCJD and somewhat more similar to vCJD. Cases with a 1B pattern have been detected but are restricted to fCJD cases (figure 10). The 1B classification was adopted from Cardone *et al*, 1999, in line with our adoption of the B suffix denoting glycosylation status. This isotype was present in the cases carrying the E200K mutation (table 10). Figures 10 and 11 both show case RU#94/097. All the cases carrying deletion or insertion mutations were type 1 mobility without prominent diglycosylation. Not all CJD cases carrying deletions are classified as familial (figure 11 shows a CJD case with a 24 bp deletion RU#97/232, classified as sporadic). The ability to molecularly distinguish the deletion or insertion mutations was not seen after PK treatment, due to the removal of the NH_3-terminus. Analysis of samples without PK treatment may display a broader mobility due to the decrease or increase in molecular weight of the mutant PrP in conjunction with the presence of the wt PrP. The influence of the NH_3-terminus on the PK cleavage site will be discussed in chapter 6, and the ability of PrP mutated at the octapeptide repeats to bind metal ions may influence the PK cleavage, though the consistency of the mobility does not suggest that it plays any part in familial disease.

Diagnosis	129	Mutation	Type 1	Type INT	Type 2A	Type 2B	Total
Familial CJD	MM	Inserts	2	0	0	0	2
		E200K	2	0	0	0	2
		V180I	1	0	0	0	1
Total			5	0	0	0	5
Familial CJD	MV	E200K	1	0	0	0	1
Total			1	0	0	0	1
FFI	MM	D178N	0	0	0	1	1
Total			0	0	0	1	1
GSS	MM	P102L	2	0	0	0	2
	MV	P102L	0	1	0	0	1
Total			2	1	0	0	3
Total			8	1	0	1	10

Table 10. PrP^{res} isotyping patterns of patients carrying *PRNP* mutations.

Summary

- Cases diagnosed with aetiologies other than TSEs did not display PK resistant PrP.
- The majority of cases displayed nonglycosylated PrP^{res} bands with molecular weights of either 21 or 19 kDa and were termed type 1 and type 2 respectively.
- Two banding patterns were observed, either predominantly monoglycosylated or predominantly diglycosylated.
- A small number of cases displayed a nonglycosylated PrP^{res} band intermediate between types 1 and 2. Neither aetiology, codon 129 or phenotypic features distinguished these cases.
- Type 1 MM sCJD cases were the most prevalent.
- Type 2 sCJD cases were more frequently observed in conjunction with a valine allele at codon 129.
- All vCJD cases displayed a 2B isotype.
- DM iCJD cases were type 1 but the majority of GHT iCJD cases were type 2.
- Some familial cases displayed a 1B isotype and the FFI case displayed an isotype similar to vCJD.

The findings indicate that two major PrP^{res} conformations are formed that differ in their susceptibility to PK cleavage. Both these conformations are found in all of the TSE aetiologies. Therefore, the conformation of the PrP^{res} does not define the cause of the disease. The glycoforms were either of the type A or B, with the type A occurring in sCJD and iCJD, and the type B occurring in vCJD and familial prion disease. The accumulation of greater levels of diglycosylated PrP^{res} is distinctive of vCJD so long as the *PRNP* sequence is taken into account. Conversely, the type A pattern can occur in familial prion diseases and therefore does not correlate with the aetiology.

Among the sCJD cases the type 1 conformation was the most common, however, when the cases were ordered according to the codon 129 genotype it was seen that the type 2 conformation is more common among cases carrying a valine allele. The conformation was not restricted between codon 129 subgroups but implies that there is a relationship between the two factors. The phenotypic features of sCJD did not correlate with the PrP^{res} pattern, however, MM 1 and VV 2 cases displayed shorter disease durations and VV 1 cases had a younger age at onset. The restriction

of DM iCJD cases to type 1 is most likely due to the prevalence of MM individuals in the population. Likewise the prevalence of type 2 in the GHT cases probably arises due to the prevalence of the valine allele, that is more commonly associated with type 2 in sCJD. Therefore, the PrP^{res} may be a contributing factor in disease presentation that is modulated by the codon 129 polymorphism.

CHAPTER 4: PrP^{res} glycoform analysis.

The foregoing classification of CJD cases was made on the basis of analysis of PrP^{res} found in the cortex, usually frontal cortex. Repeated sampling from the same cortical region typically gave a consistent isotype. The only feature of PrP^{res} that allows vCJD to be distinguished from other forms of human TSE is the prominent diglycosylation. This feature is termed type 2B as discussed in the previous chapter, however the classification is by eye and requires quantitative testing. To establish the quantitative difference between vCJD and sCJD the percentage representation of the three glycoforms were measured. Densitometric analysis of the signal detected from the three glycoforms was repeated in an identical manner for all experiments (see appendix A5). Can more accurate quantitation of the PrP^{res} glycoforms identify subtle differences between the sCJD subgroups and is there any overlap with vCJD cases?

4.1 Quantitation

As in previous studies the 'linear range' (the range over which X-ray film has a linear response, generally taken as 1 log), of the samples was determined, within which densitometric readings of the three glycoforms represent their *in vivo* levels. The linear range was established by dilution curves of standard samples to determine the lower and upper levels of density within which the glycoforms were quantitatively relative to each other (see appendix). There are a few caveats to take into consideration when interpreting the values obtained in relation to *in vivo* levels of PrP^{res}.

Not all samples analysed were within a 1 log scale of relative levels i.e. if the diglycosylated levels comprised 80% of the total PrP^{res} density yet the nonglycosylated band comprised less than 8%. In such a situation the X-ray film results would become saturated with the diglycosylated band before the luminescent output of the nonglycosylated band reached a quantitative level. This limit of the experimental technique affected very few human samples, however it presupposes that all cases produce all three glycoforms of PrP^{res} with levels no greater than 10 times either of the other bands. The use of the STORM™ 860 phosphoimager to analyse chemiluminescent output of samples was able to increase the linearity limits to 2 logs (see appendix). This approach was available later in the study and was primarily used for murine transmission samples. Due to the restrictions in

interpreting three way ratios on a linear scale, equal levels of all three bands are easily misinterpreted as reaching saturation, as all three bands tend towards 33% at complete saturation. Theoretically this artificially excludes a proportion of cases, however, in very few cases were equal levels seen by eye and these appeared to represent high PrP^{res} levels. The analysis of all human cases involved the use of 3F4. Non-human tissues were analysed with 6H4 and the possibility that glycosylated PK resistant PrPII is measured cannot be discounted. The main aim is to establish a quantitative molecular differentiation assay for sporadic and variant CJD involving one standard antibody for ease of interpretation.

The consistency of the technique was assessed upon repeated runs of the same standard samples used to type the cases and between different samplings of those cases. Multiple experimental analyses were conducted in the majority of cases (detailed in the appendix). Statistical analysis was carried out on the standard cases to determine the degree of variability in glycoform ratio using the approach detailed in the appendix. Standard deviations were calculated for multiple linear exposures in each experiment and between each experiment for each case to identify any variability within individual cases.

Cases within each subgroup, cases between subgroups and sCJD and vCJD cases as a whole were compared. The glycoform ratios were established from frontal cortex material where possible. In some cases this was merely stated as being cortical on the autopsy report or unavailable, in which case other cortical regions were used. Rarely other CNS material was used, sometimes only certain regions contained significant quantities in non-cortical regions; such as FFI in which the use of thalamic tissue was required. The analysis of glycoform ratios in numerous brain regions will be covered in the following chapter.

4.2 Sporadic CJD

Glycoform ratios were obtained in the majority of sCJD cases (n=124) and further analysed. The glycoform ratios of sCJD cases of all genotype / isotype combinations are most easily displayed as histograms to express the relative levels of each band. Figure 14 displays the mean ratios for each sCJD subgroup with error bars representing standard errors of the mean (SE) between cases within the subgroup.

Figure 13. Composite image showing examples of the range of banding patterns observed. Lanes 1 and 2, 3 and 4, and 5 to 7 are from separate Western blots. All the images are from 12% gels detected with 3F4. Lane 1, sCJD MM 1, lane 2, sCJD VV 2A, lanes 3 and 4, sCJD MV 2A, lane 5, vCJD MM 2B, lane 6, sCJD VV 1, lane 7, Markers (from top 46 kDa, 31 kDa, 20 kDa).

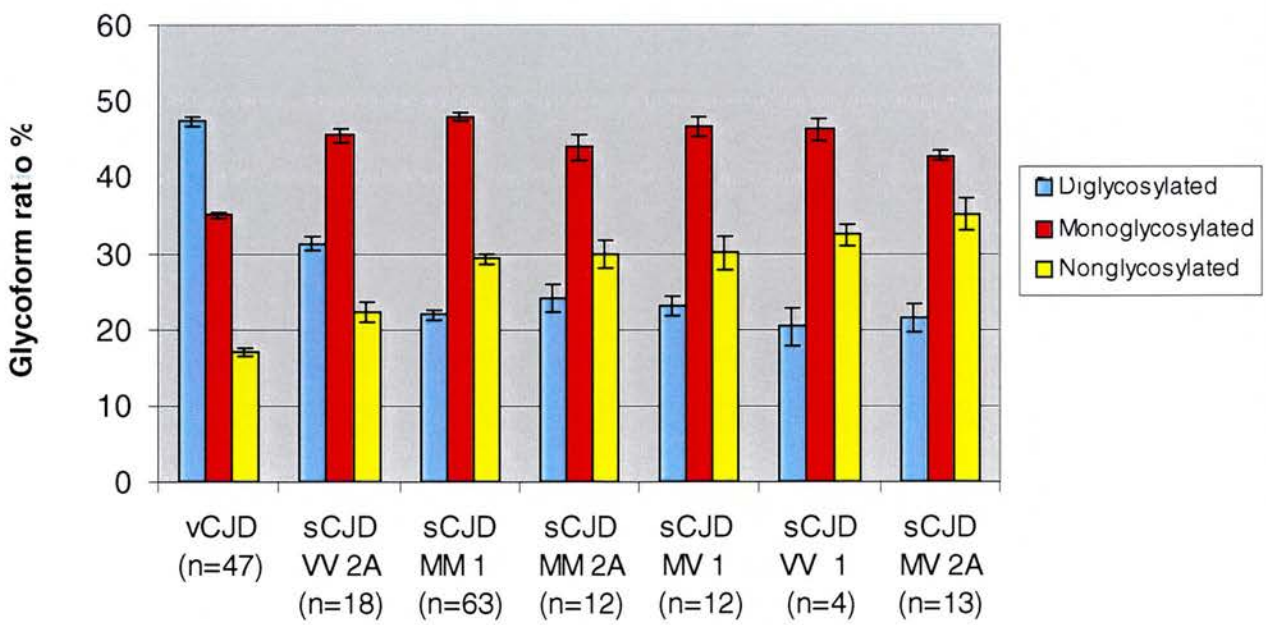

Figure 14. Histogram of sCJD and vCJD subgroup glycoform ratios. Error bars represent SEs.

The sCJD MM 1 subgroup is the most prevalent form of sCJD and displays a strikingly consistent glycoform ratio with prominently monoglycosylated PrP^{res} and a greater level of nonglycosylated PrP^{res} than diglycosylated (diglycosylated 21.9% ± 0.6: monoglycosylated 47.9% ± 0.6: nonglycosylated 29.3 % ± 0.6).

The sCJD MM 2A subgroup was the first to be closely investigated because the duration of the clinical signs, codon 129 polymorphism and PrP^{res} mobility could be taken to resemble vCJD. The small number of cases also allowed data to be gathered quickly. As with the MM 1 group a prominence of monoglycosylated PrP^{res} was detected, though the levels of nonglycosylated and diglycosylated PrP^{res} were similar. The prominence of monoglycosylated PrP^{res} is a consistent feature in sCJD (figure 14) and the ratios were therefore most easily distinguishable in terms of the relative levels of diglycosylated to nonglycosylated PrP^{res} (diglycosylated 24.1% ± 1.8: monoglycosylated 43.9% ± 1.7: nonglycosylated 29.9% ± 1.9).

A slight range of di to nonglycosylated ratios was observed from the MM 2A subgroup to the VV 1/MV 2A groups, with the monoglycosylated band always being the most abundant (figure 14); VV 1 cases (diglycosylated 20.4% ± 2.5: monoglycosylated 46.3% ± 1.4: nonglycosylated 32.4% ± 1.4), MV 1 cases (diglycosylated 22.9% ± 1.3: monoglycosylated 46.7% ± 1.3: nonglycosylated 30.1% ± 2.3) and MV 2A cases (diglycosylated 21.4% ± 1.9: monoglycosylated 42.8% ± 0.7: nonglycosylated 35.1% ± 2.2). There was no significant difference in glycoform ratios between these subgroups as assessed with unpaired two tailed *t* tests. Cases displaying the diametrical pattern of pronounced nonglycosylated PrP^{res} are less common but predominate in sCJD MV (both type 1 and 2) and sCJD VV type 1. The appearance of these banding patterns was noticeable in some cases as can be seen in figure 13. Cases with predominantly nonglycosylated PrP have previously been identified and termed type 6 (Hill, 1998). Though lane 3 of figure 13 appears to be a type 6 case, densitometry measurements within the linear range did not show greater levels of the nonglycosylated than the monoglycosylated band (figure 14). It was thus decided that this appearance is not a true representation of the proportions of the three bands present. As the type 6 classification does not denote an additional mobility type and the suffix A already indicates a majority of monoglycosylated PrP^{res}, this term was not adopted.

Only the VV 2A group has a significantly different glycosylation pattern, characterised by a greater proportion of the diglycosylated PrP^{res} band than the nonglycosylated PrP^{res} band (diglycosylated 31.3% ± 0.9: monoglycosylated 45.5% ±

0.9: nonglycosylated 22.3% ± 1.3). The proportion of the diglycosylated PrP^{res} band was not more than that of the monoglycosylated PrP^{res} band, or enough to be indistinguishable from the vCJD glycoform ratio. The limits of the analysis, as mentioned previously, did not pose a significant problem in assessing any of the sCJD subgroups as they all displayed all three glycoforms in sufficiently relative levels.

The quantitative results may also be expressed in the form of a scattergraph, allowing individual cases to be compared between subgroups and clustering of cases investigated (figure 15). The X:Y bisecting line represents the nonglycosylated axis, with cases containing higher levels of nonglycosylated PrP^{res} being found closer to the origin. As can be seen the sCJD subgroups cluster in the same general area.

The VV 2A subgroup stands out clearly due to higher levels of diglycosylated PrP^{res} (unpaired two tailed *t* test found a significant difference between the di and nonglycosylated bands of the MM 1 and VV 2A subgroups, $p < 0.000$, the monoglycosylated $p = 0.083$). The MV cases are more dispersed, which reflects the range of ages at onset and duration durations seen in these cases. The MV 2A subgroup is spread out predominantly in the direction of the origin. The level of monoglycosylated PrP^{res} found in these cases appears to remain fairly consistent. However, the relative diglycosylated levels vary, most likely due to higher levels of nonglycosylated PrP^{res} in some cases. This may be due to differences in levels of glycosylated PrP^{res} present or may be an experimental artifact. Identification of PrP^{res} species isolated is dependent on the antibodies employed and nonglycosylated PrP^{res} lacking the 3F4 epitope (PrPII) would not be identified. Some of the cases appear to be on the X:Y axis, primarily in the VV 2A subgroup, this may be explicable due to saturation of the di and monoglycosylated bands at the detection level of the nonglycosylated band.

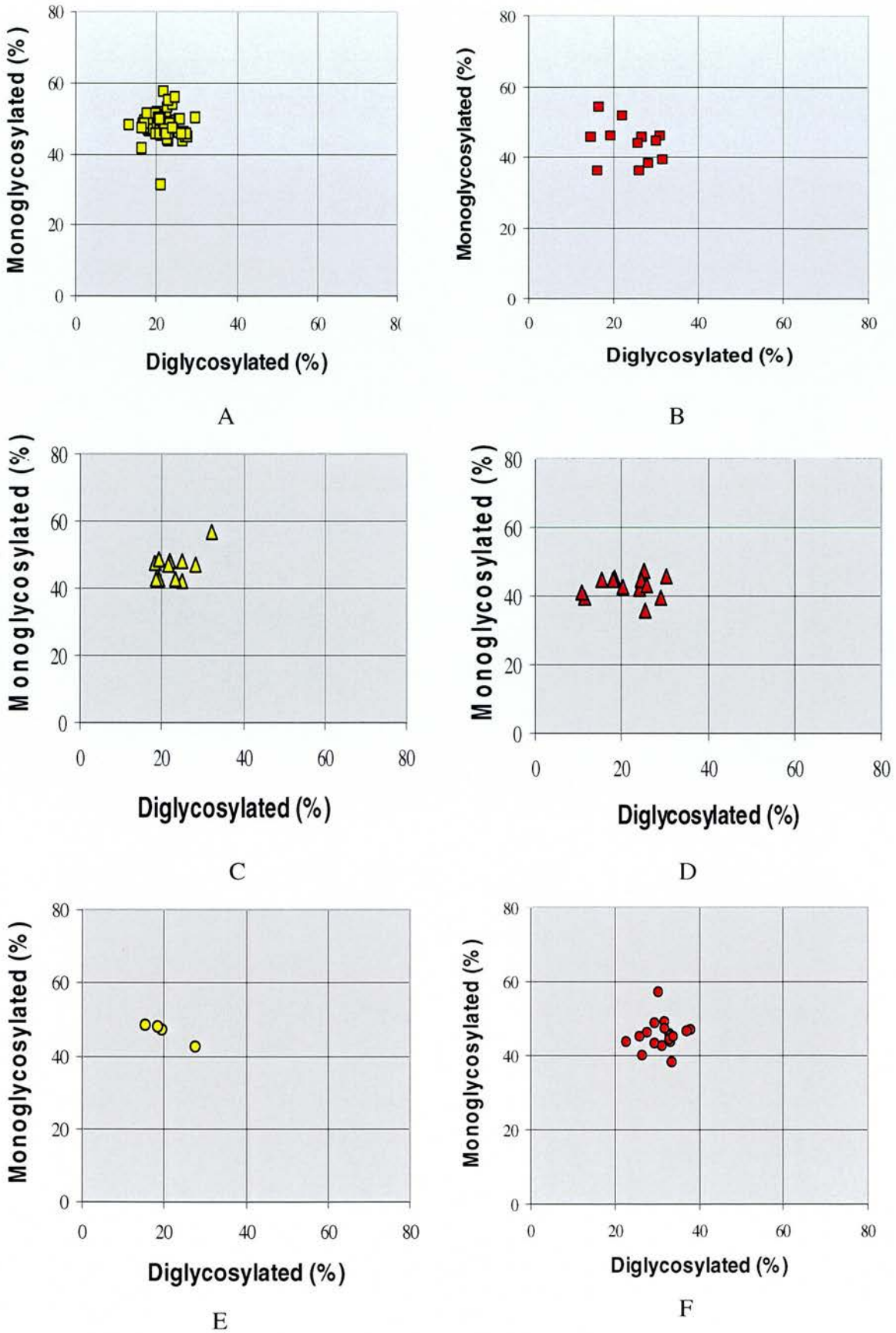

Figure 15. Scattergraphs of the mean glycoform ratios in sCJD cases according to codon 129/isotype subgroups. The standard deviation range of individuals within a group is stated in brackets, for the diglycosylated (di) and monoglycosylated (mono) bands. **A.** MM 1 (di 0-6.8, mono 0-7.5) **B.** MM 2A (di 0-5.7, mono 0-10.6) **C.** MV 1 (di 0-7.6, mono 0-3.9). **D.** MV 2A (di 0-3.4, mono 0-5.5). **E.** VV 1 (di 1.3-6.5, mono 3.8-6.5. **F.** VV 2A (di 0-5.7, mono 0-10.3).

The two sCJD cases displaying intermediate mobility were also quantitatively analysed and did not have glycoform ratios (diglycosylated 21.1% ± 0.2: monoglycosylated 46.8% ± 0.2: nonglycosylated 31.3% SD 0.02) that significantly distinguished them from type 1 (diglycosylated 22.4% ± 0.5: monoglycosylated 47.3% ± 0.5: nonglycosylated 29.5% ± 0.6) or type 2 (diglycosylated 26.3% ± 1.1: monoglycosylated 44.4% ± 0.6: nonglycosylated 28.1% ± 1.3) sCJD cases. The glycoform ratios of type 1 and type 2 were not significantly different and neither was the difference seen between the glycoform ratio of MM (diglycosylated 22.7% ± 0.6: monoglycosylated 46.9% ± 0.6: nonglycosylated 29.3% ± 0.6) and MV (diglycosylated 21.6% ± 0.6: monoglycosylated 44.9% ± 0.8: nonglycosylated 33.1% ± 1.6) cases. The di and nonglycosylated bands of VV patients (diglycosylated 29.3% ± 1.2: monoglycosylated 45.6% ± 0.8: nonglycosylated 24.1% ± 1.4) differed significantly from both MM and MV cases as a whole ($p < 0.000$).

One case (RU#97/257) diagnosed as sCJD and classified as MV 1 displayed a shift in the 452 bp DNA band after restriction enzyme digest, indicating a 'silent' (non-pathogenic) deletion (figure 17). However, there was no permission for research purposes to carry out full sequencing of the ORF to characterise the deletion in detail. This case stood out from the other cases in the MV 1 subgroup and displayed a greater degree of diglycosylation (figure 16), akin to that seen in sCJD VV 2A cases (figure 18). The atypical glycoform ratio (diglycosylated 32.3%: monoglycosylated 56.8%: nonglycosylated 10.6%) and long disease duration (14 months) implies that the deletion affects the phenotypic presentation. The presence of the deletion on the M allele (shown by the shift in the middle band) precludes the possibility that this is the result of intra-allelic interaction between the deletion and the valine present at codon 129. The two sCJD MM type 1 cases with 24 bp deletions of the octapeptide repeat region did not display glycoform ratios that set them apart from the sCJD MM 1 group as a whole (diglycosylated 25.3%: monoglycosylated 45.8%: nonglycosylated 28.6% and diglycosylated 22.6%: monoglycosylated 45.7%: nonglycosylated 31.9%). However, disease duration data was available for one of these cases (13 months) and is in stark contrast to the typically short duration observed in the MM 1 subgroup. Rare polymorphic deletions in the tandem repeat region of *PRNP* are carried in ~1% of the population (Bosque *et al*, 1992, Windl *et al*, 1996) and do not appear to affect the conformation due to metal ion binding as type 1 cases invariably have bound cations (see chapter 6).

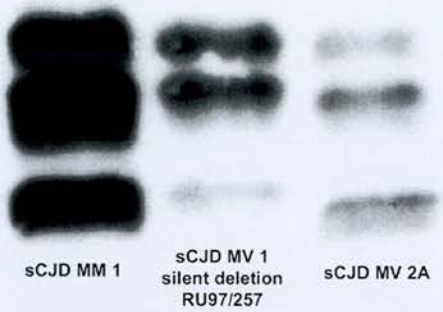

Figure 16. Western blot of sCJD case with rare polymorphism analysed with 3F4. Lane 1, sCJD MM 1, lane 2, sCJD MV 1 with a 24 bp deletion, lane 3, sCJD MV 2A.

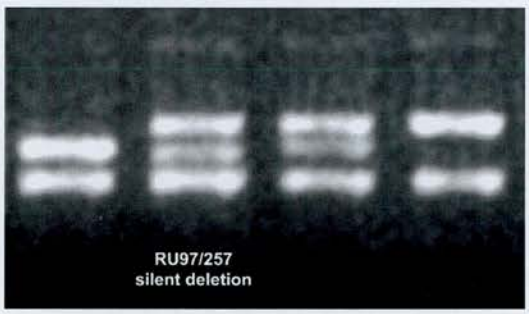

Figure 17. Agarose gel electrophoresis of *PRNP* after RFLP digest with Nsp 1. Lane 1, MM, lane 2, RU#97/257, lane 3, MV, lane 4, VV.

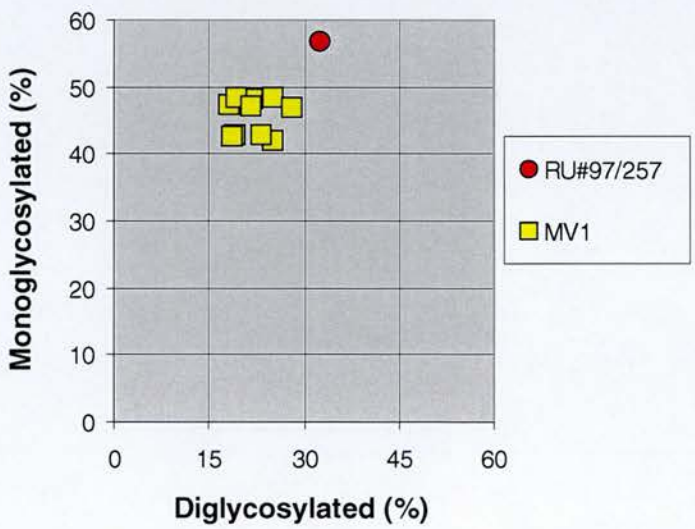

Figure 18. Scattergraph sCJD MV 1 cases *vs* MV 1 silent deletion.

4.3 Variant CJD

Variant CJD appeared homogeneous by visual inspection, quantitative analysis confirmed the discreet nature of this group from sCJD. Since the extent of glycosylation alone distinguishes PrP^{res} in vCJD from the MM type 2 class of sCJD, the glycosylation ratios of the first 12 vCJD cases were compared with those of the 12 MM type 2A sCJD cases (figure 19). The sCJD MM 2A subgroup acts as the differential genotypic/molecular diagnosis, thus the degree of quantitative separation between the two groups is important to establish. The glycoform ratios of all three bands were significantly different between the sCJD MM 2A cases and the first 12 vCJD cases ($p < 0.000$, unpaired two tailed *t* test). The analysis confirmed the discreet nature of these two groups and supports the diagnostic use of the 2B isotype.

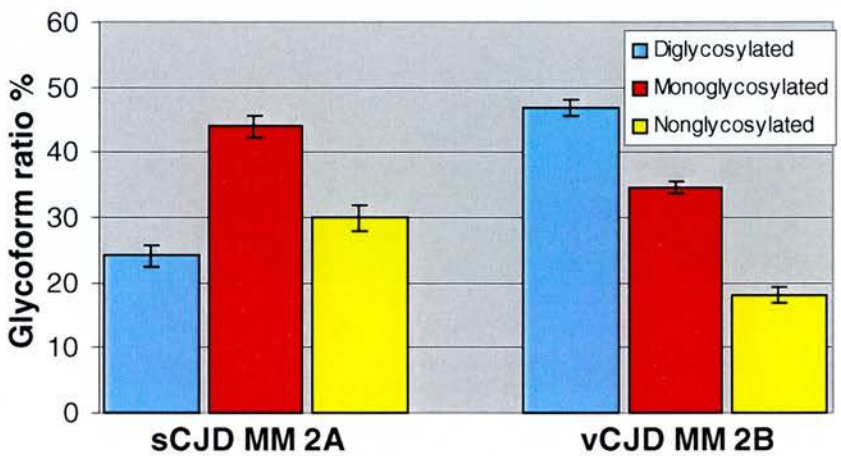

Figure 19. Histogram of mean glycoform ratios of 12 sCJD MM 2A cases and the first 12 vCJD cases with available frozen tissue. Error bars represent SEs.

In total 50 vCJD cases were analysed. This only represents half of the cases reported during the study and is due to ethical and consent considerations as well as frozen tissue availability. Glycoform ratios were obtained in 47 cases (diglycosylated 47.3% ± 0.7: monoglycosylated 35% ± 0.4: nonglycosylated 17.1% ± 0.5). There was a significant glycoform ratio difference between vCJD and all the sCJD cases in all three bands ($p < 0.000$, unpaired two tailed *t* test). The type 2 VV sCJD subgroup, represents the most similar glycoform pattern to vCJD. However, these cases are quite distinct from that of vCJD (unpaired two tailed t test found a significant difference between all three bands $p < 0.000$ for the di and monoglycosylated band

and $p < 0.001$ for the nonglycosylated band). When plotted on a scattergraph with the sCJD cases (figure 20), distinct clustering is observed without any overlap. The X:Y axis (X=Y line) separates the two aetiological groups and represents the difference between the 2B and 2A isotypes.

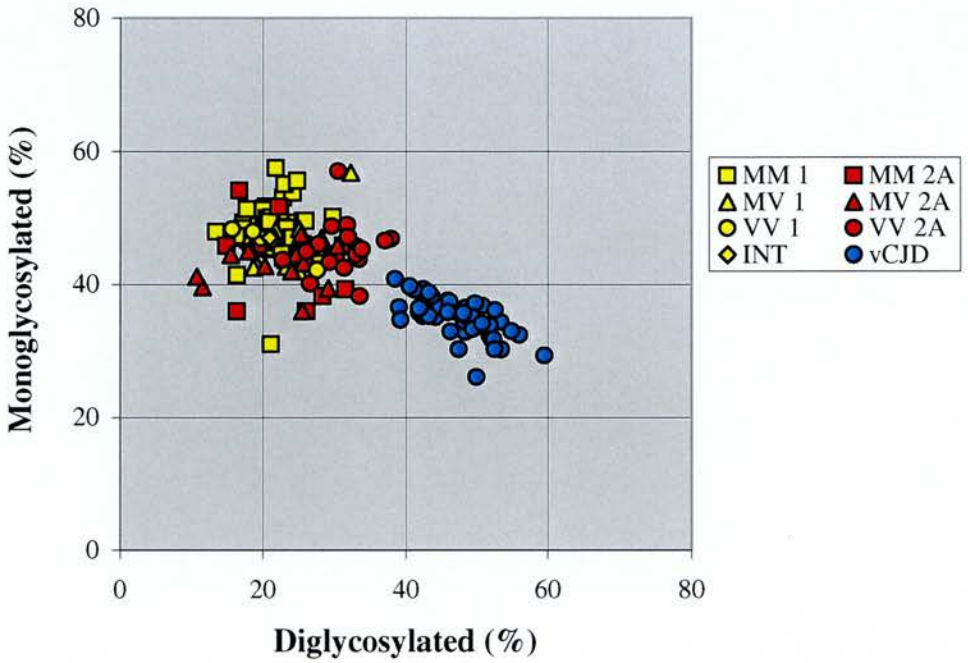

Figure 20. Scattergraph of mean glycoform ratios of sCJD and vCJD cases. Yellow squares represent sCJD MM 1, red squares represent sCJD MM 2A, yellow circles represent sCJD MV 1, red circles represent sCJD MV 2A, yellow triangles represent sCJD VV 1, red triangles represent sCJD VV 2A, yellow diamonds represent sCJD MM INT and blue circles represent vCJD.

4.4 Iatrogenic CJD

Comparison of DM cases and GHT cases showed a strict codon 129 segregation as discussed in the previous chapter, however in terms of glycoform ratio the two DM cases (figure 21B, white triangle and white diamond) are indistinct from any other iCJD case. Comparison of MV (circles) and VV (squares) GHT cases in figure 21, does not clearly divide the two groups though a slight preponderance of the nonglycosylated portion may be in evidence in the MV cases. Cases displaying the

diametrical pattern of pronounced nonglycosylated PrP^{res} were less common in sCJD, but predominate in iCJD MV cases (figure 21B). The bands were often harder to resolve and could thus constitute greater levels of PrP^{res} or possibly cases with multiple isotypes or ragged NH_3-terminals. The nature of this appearance thus needs greater biochemical investigation. As mentioned earlier this pattern was termed type 6 by Hill, 1998, however, a quantitative approach may be more enlightening. Comparison of the MV type 1 cases (green and yellow filled in circles) with type 2 MV or VV GHT cases also shows evidence of increased nonglycosylation in the two MV 1 cases. This may represent a similar effect of the VV genotype seen in sCJD that increases the level of diglycosylated PrP^{res}. A wide range of glycoform ratios were observed but none with a type 2B pattern. There was no statistically significant difference in glycoform ratio of PrP^{res} in DM or GHT derived infections. No apparent correlation of the route of entry or codon 129 genotype with glycoform ratio was seen.

4.5 Familial CJD, GSS and FFI

The glycoform ratios of the fCJD cases were predominantly classified as highly diglycosylated (B). However, not all cases were the same and as is well known with fCJD E200K, fCJD D178N and FFI it can be the mutation or the codon 129 that determines the molecular phenotype both in terms of glycoform ratio and isotype. The glycoform ratios should thus be considered in respect to the mutation and codon 129 status. The range of glycoform ratios can be seen in figure 21C. Some cases displayed very low levels of PrP^{res} and others had a low proportion of nonglycosylated PrP^{res} making linear range readings difficult. In such cases single readings or nearly linear readings were taken with estimates in some cases of the levels, i.e. if less than 5% nonglycosylated PrP^{res}.

A

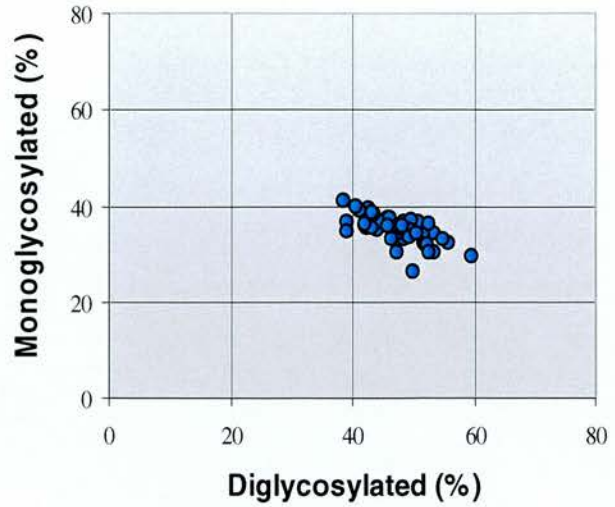

B

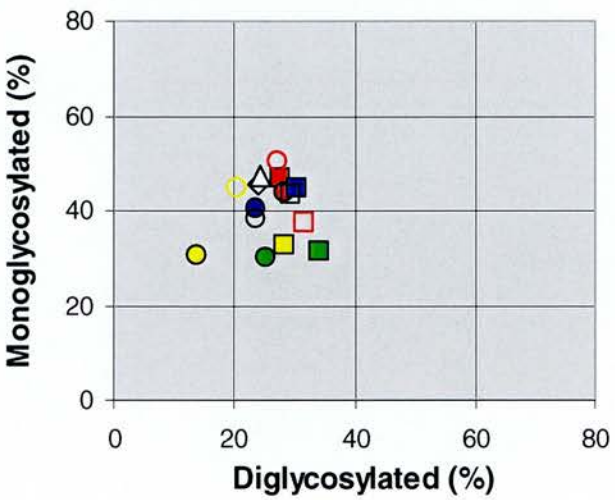

C

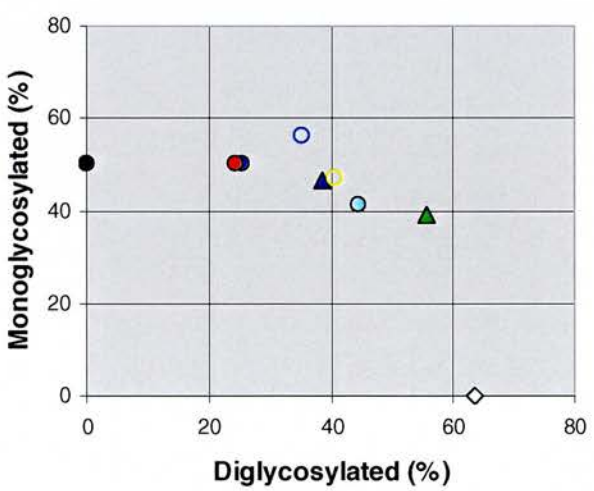

Figure 21 A. Scattergraphs of the mean glycoform ratios in vCJD, iCJD and familial prion diseases. The standard deviation range of individuals within a group is stated in brackets, for the diglycosylated (di) and monoglycosylated (mono) bands. **A.** Variant CJD cases, (di 0-9.7, mono 0-8.3). **B.** Iatrogenic CJD cases, DM cases are represented by white triangle and white diamond, GHT MV cases are represented by circles and GHT VV cases by squares, (di 0-10, mono 0-13.7). **C.** Familial prion disease. Familial CJD cases are represented by circles (V180I represented by the black circle), GSS cases are represented by triangles and the FFI case by the white diamond, (di 0-9.2, mono 0-6.4).

Summary

- All sCJD cases had a predominantly monoglycosylated glycoform ratio. In all but the VV 2A subgroup, the unglycosylated band was found in greater levels than the diglycosylated ban.
- Aside from sCJD VV 2A cases and a few MV 1 cases, sCJD subgroups could not be distinguished by their glycoform ratio.
- None of the sCJD glycoform ratios overlapped with vCJD.
- A sCJD MV 1 case carrying an octapeptide repeat deletion had a different glycoform ratio to the other sCJD MV 1 cases.
- Iatrogenic CJD cases did not have significantly different glycoform ratios from sCJD cases. The route of entry or codon 129 did not influence the glycoform ratio.
- Familial CJD cases displayed glycoform ratios in the range of vCJD, however, these two groups are distinguished by their isotype or *PRNP* genotype.

The quantitation of PrP^{res} glycoforms clearly distinguished the sCJD and vCJD cases. The glycoform ratios in sCJD established a greater level of monoglycosylated than diglycosylated PrP^{res} in all but the VV 2A subgroup. The sCJD subgroups could not be distinguished by their glycoform ratios. This limits the use of the glycoform ratio as a diagnostic marker to differentiating sCJD and vCJD. However, even then care needs to be taken in measuring glycoform ratios, to ensure that under exposed sCJD VV 2A cases are not misinterpreted as vCJD. The *PRNP* sequence must also be taken into account as familial cases can display a glycoform ratio similar to vCJD. The glycoform ratio should therefore be considered alongside the isotype, codon 129 polymorphism, *PRNP* genotype, neuropathology and clinical features in making a diagnosis.

CHAPTER 5: Regional studies.

5.1 Rationale

The aim of investigating the banding patterns within and between different tissues was to determine the reliability of basing molecular diagnosis on biopsies or a single autopsy sample. Detection of PrP^{res} by Western blotting has been demonstrated to be reliable in numerous host organisms and tissues in identifying and confirming TSE disease (Brown *et al*, 1994b, Moynagh *et al*, 1999, Oesch *et al*, 2000, Wadsworth *et al*, 2001). The consistency of intra-CNS and inter-tissue isotypes is essential for the results from one region to be used as representative of the patient *in toto*. It is also important to enable the role of PrP^{res} patterns in strain typing to be established and investigate the possibility of multiple strains (Ridley and Baker, 1997, Bartz *et al*, 2000). This study focuses on the CNS and in particular poses a number of questions. 1. Is an isotype constant throughout the CNS in a single individual? 2. Do isotypes correlate with their location in numerous individuals? 3. Do the brain region isotype patterns differ from those of the corresponding subgroup? The typing was blind to all host factors but codon 129 genotype. To identify any phenotypic features that may correlate with isotyping and factors that would preclude extrapolation of direct comparisons between cases a cursory comparison of gender, age at onset, disease duration and neuropathological features were examined where pertinent.

In order to directly test the uniformity of PrP isotype within individual cases, 17 neuroanatomical regions were sampled from six cases of sCJD (one each previously classified as MM 1, MM 2A, VV 1, VV 2A and two MV 2A cases), five cases of vCJD (MM2B), one iCJD case (MV 2A GHT) and two fCJD cases (E200K MM and MV). Multiple regions were analysed in a number of other cases where frozen tissue, but not a half hemisphere, was available. In total 276 regions were analysed, 238 from half hemispheres, five regions (frontal, temporal, parietal and occipital cortices as well as cerebellum) in an additional vCJD case (RU#98/148), paired biopsy autopsy tissue from one sCJD case (RU#98/153), 8 cerebellums paired with frontal cortex (5 sCJD, 3 vCJD), occipital cortex and parietal cortex from one sCJD case (RU#99/025), 6 regions (frontal cortex, temporal cortex, thalamus, basal ganglia, brain stem and cerebellum) from a case of FFI (RU#91/017), 3 regions (frontal, parietal and temporal cortices) in GSS case (RU#94/007) and 2 regions in GSS case (RU#94/098).

5.2 Regional Comparisons

The isotype/genotype/aetiological subgroup classification along with the glycoform ratios indicated a fairly consistent pattern within each subgroup. However while conducting this study a case of suspected vCJD with onset at 42 years and a final duration of 18 months was investigated that on cortical biopsy displayed type 1 PrP^{res} and was genotyped as VV at codon 129. This case also had a glycoform ratio (diglycosylated 17.2% ± 3.0: monoglycosylated 47.3% ± 1.3: nonglycosylated 33.2% ± 2.5) in keeping with the VV type 1 subgroup (diglycosylated 20.4% ± 2.5: monoglycosylated 46.3% ± 1.4: nonglycosylated 32.4% ± 1.4). Yet, when the subsequent autopsy sample from the contra-lateral frontal cortex was analysed the mobility was type 2 and the glycoform ratio was distinct from that of the biopsy sample (diglycosylated 45.2% ± 2.8: monoglycosylated 43.6% ± 2.4: nonglycosylated 9.3% ± 0.6) and closely resembling that of vCJD (figures 22 and 23). There was a significant difference between the proportions of the diglycosylated and nonglycosylated PrP^{res} in the biopsy and autopsy ($p < 0.000$, unpaired two tailed *t* test) but no significant difference between the monoglycosylated bands ($p = 0.324$, unpaired two tailed *t* test). Such differences might be attributed to regional variation or to changes associated with disease progression.

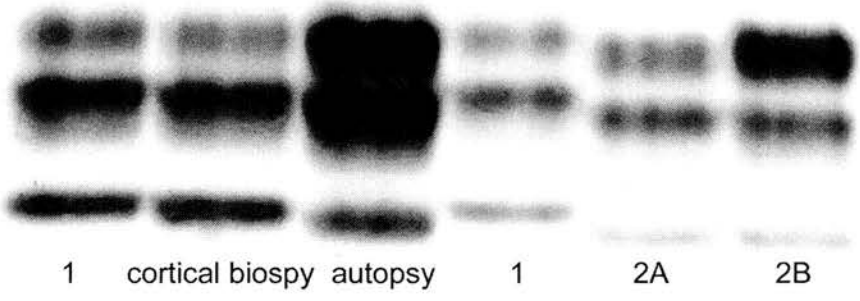

Figure 22. Lane 1, sCJD MM 1 standard, lane 2, cortical biopsy type 1, lane 3, autopsy type 2B, lane 4, sCJD MM type 1, lane 5, sCJD VV 2A standard, lane 6, vCJD standard 2B.

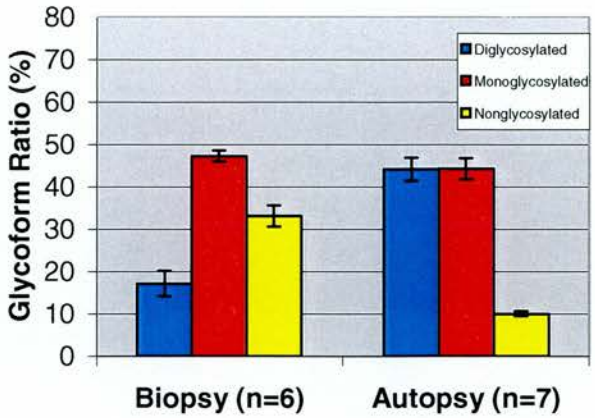

Figure 23. Histogram glycoform ratio analysis at biopsy and autopsy. n = number of experimental runs, error bars represent SEs.

This chance finding led to re-examination of the assumption that the molecular diagnosis based on restricted analysis of cortical material is definitive for the patient as a whole. The case was given a final diagnosis of sCJD, following careful assessment of clinical and neuropathological features. The significance of this diagnosis was important due to the similarities with vCJD cases and the epidemiology. At present, cases of vCJD occurring outside of the UK are restricted to France (Chazot *et al*, 1996, Deslys *et al*, 1997) and Ireland and since the patient resided in the Netherlands this would have expanded the epidemiological spread of vCJD to an otherwise unaffected country.

Glycoform ratio analysis of this sCJD case (VV) with the only other biopsy / autopsy paired tissues (from a case of vCJD RU#98/137) (MHW) suggested that change associated with disease progression is not a general rule (ethical guidelines require retrospective analysis of biopsy material once a diagnosis has already been made). The possibility of regional variation thus required further investigation into the fidelity of cortical isotype diagnosis.

In addition to this variability, multiple isotypes were detected in another sCJD case MM (RU#99/068) during another investigation (Kovacs *et al*, 2000) (figure 24). Type 1 was seen in the cerebellum (figure 25) in contrast to the classification of the case as type 2. This finding suggests that reliance on cerebellar material for isotype

diagnosis may result in misdiagnosis. Only 3 cases were diagnosed from cerebellar material in the sCJD MM 1 subgroup, one from 1992 and two from 1999. Only one of these cases had a long disease duration (10 months) in combination with a young age at onset (42 years) suggesting it is more comparable to MM type 2A cases.

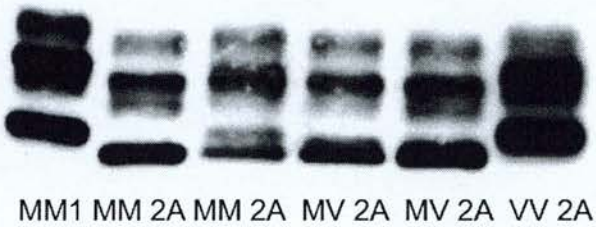

Figure 24. RU#99/068 showing two types. Sporadic CJD frontal cortex samples, lane 1, MM 1 standard, lane 2, MM 2A, lane 3, RU#99/068 MM 2A+1, lane 4, MV 2A, lane 5, MV 2A, lane 6, VV 1.

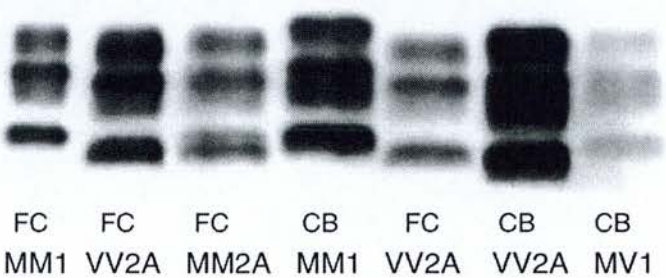

Figure 25. RU#99/068 showing type 1 in the cerebellum. Tissues are indicated frontal cortex (FC) and cerebellum (CB). Lane 1, MM 1 standard, lane 2, VV 2A standard, lane 3, RU#99/068 MM 2A, lane 4, Ru#99/068 MM 1, lane 5, VV 2A, lane 6, VV 2A, lane 7, MV 1.

Based on these findings a neuroanatomically wide spread investigation was initiated with comprehensive analysis of cortical, deep grey matter and cerebellum tissues to identify any regional variation (as detailed in the materials and methods).

5.3 Sporadic CJD

The number of cases that could feasibly be investigated in detail was limited, therefore one case from each isotype/genotype subgroup with an available frozen

hemisphere was chosen. At least one case from each subgroup was available aside from the MV 1 cases (table 11), due in part to the relative rarity of this subgroup. Among the sCJD cases PrP^{res} variation was found in three cases.

Diagnosis, Codon 129, Isotype	Age at onset (years)	Disease duration (months)	Gender (M/F)
Sporadic CJD MM 1	86	4	F
Sporadic CJD VV 1	41	11	M
Sporadic CJD VV 2A	75	4	F
Sporadic CJD MM 2A	61	11	M
Sporadic CJD MV 2A[1]	62	21	F
Sporadic CJD MV 2A[2]	61	8	F
Iatrogenic CJD MV 2A	37	9	M
Familial CJD MM 1B	57	-	M
Familial CJD MV 1B	61	-	M
Variant CJD MM 2B[3]	35	15	M
Variant CJD MM 2B[4]	21	29	F
Variant CJD MM 2B[5]	30	9	M
Variant CJD MM 2B[6]	17	18	F
Variant CJD MM 2B[7]	51	11	F
Variant CJD MM 2B[8]	19	11	M

Table 11. Age at onset, disease duration of regional studies patients.

[1] case RU#98/123, [2] case RU#96/153, [3] case RU#98/154, [4] case RU#98/156, [5] case RU#96/045, [6] case RU#00/025, [7] case RU#99/015, [8] case RU#98/148.

The sCJD MM 1 (RU#98/088) (figure 26A and B, figure 27A), VV 1 (RU#96/027) (figure 26C and D, figure 27B), and VV 2A (RU#94/083) (figure 26E and F, figure 27C) cases were consistent throughout the brain both in terms of isotype and glycoform ratio. Comparison of the glycoform ratios in brain regions of the sCJD MM 1 case found no significant differences. When the regions were compared with the sCJD MM 1 subgroup as a whole none had significant differences aside from the level of the diglycosylated band in the amygdala (29.2% $p = 0.016$, One way ANOVA) being slightly higher than in sCJD MM 1 cases. No significant difference in glycoform ratio between the brain regions of the VV 1 case or the VV 1 subgroup

was found. The glycoform ratios of the brain regions in the VV 2A case were only significant ($p = 0.001$, one wav ANOVA, dunnett *t* 2 sided post hoc test) in the diglycosylated band of the temporal cortex in comparison to the VV 2A subgroup as a whole. The amount of the diglycosylated band was lower (21.1%) in the temporal cortex than the VV 2A subgoup, as found in other sCJD cases. Comparison of the brain regions as a whole found only the temporal cortex diglycosylated band to differ from other brain regions ($p = 0.033$ parietal cortex, 0.035 hippocampus, 0.006 basal ganglia, one way ANOVA, bonferroni post hoc test). This consistency was surprising in that neither of the VV patients displayed variation similar to that seen in the Dutch case. It may seem unlikely that PrP^{res} of a certain conformation found at biopsy would be converted or cleared from the brain before the death of the patient, however a systematic analysis of regions by biopsy is uncalled for and thus precludes the testing of such a hypothesis. The VV 1 patient (RU#96/027) investigated had an age at onset of 41 and disease duration lasting 11 months, similar to that in the Dutch case (42 years, 18 months). The other two cases within the VV 1 subgroup analysed solely in the frontal cortex had age at onset and disease duration of 78 years and 8 months respectively and 25 years and 29 months emphasising the variable features for this subgroup. The wide range of onset and duration may be due to the small sample size, however cases in this group may be mistaken for vCJD. The VV 2A patient (RU#94/083) had an age at onset of 75 years and duration of 4 months. The MM 1 patient (RU#98/088) had an age at onset of 86 years and duration of 4 months similar to other cases of the subgroup.

There were roughly equivalent levels of PrP^{res} in all of the brain regions (figure 26A and B), of the sCJD MM 1 case (RU#98/088). The glycoform ratios were also similar in all the brain regions (figure 27A). The autopsy report (JWI or JB) indicated spongiform change in the cerebral cortex, primarily in the frontal, temporal and occipital lobes. The frontal cortex displayed marked astrocytosis and neuronal loss, which was also seen to some extent in the other cortical regions. Spongiform change, astrocytosis and neuronal loss are also seen in the basal ganglia, thalamus and molecular layer of the cerebellum. There were no amyloid plaques present and PrP immunostaining showed a synaptic pattern in the cerebral cortices and in some areas perivacuolar accumulation and occasional accumulations around pyramidal neurones.

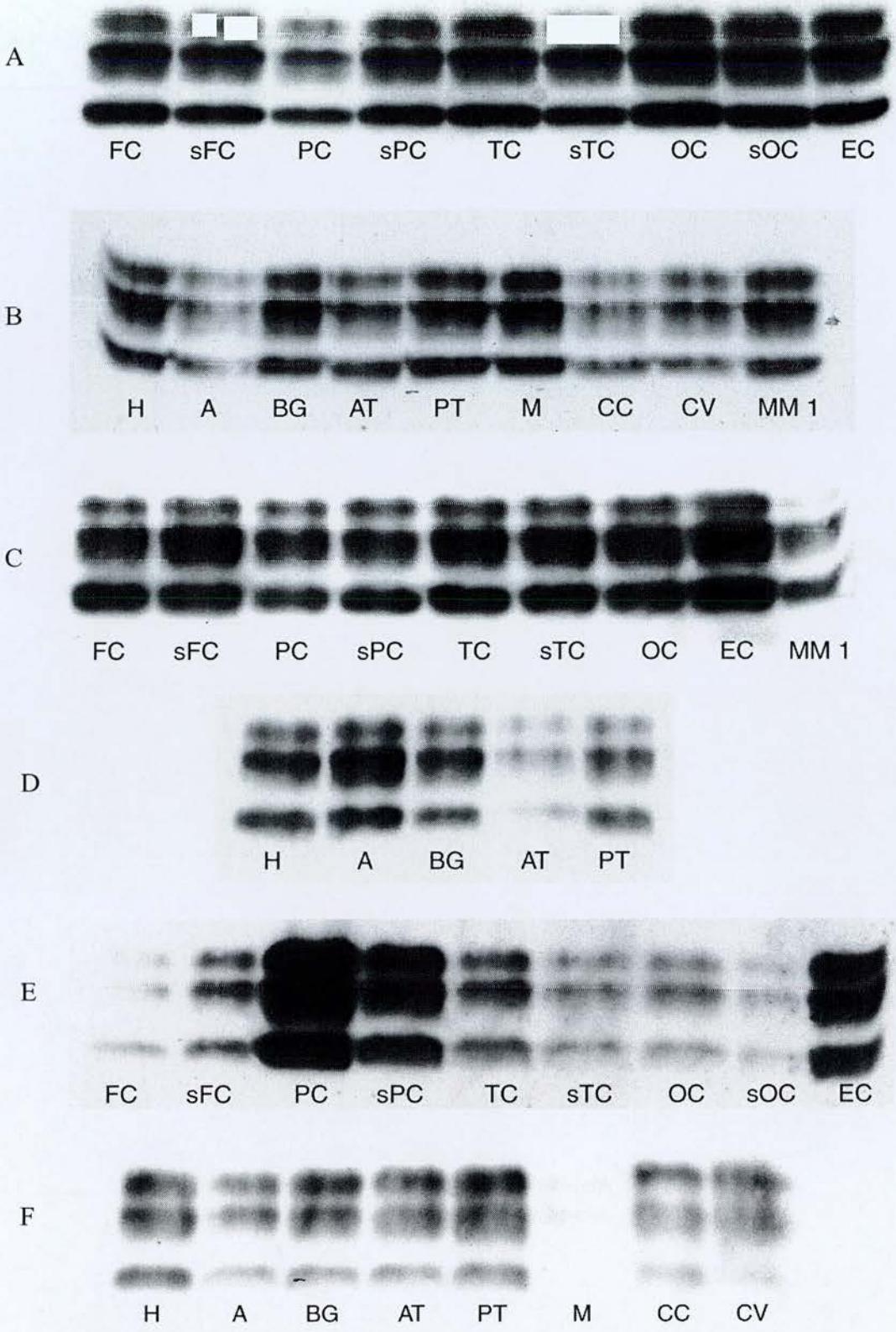

Figure 26. Sporadic CJD PrP^{res} in different brain regions. **A;** sCJD MM 1 RU#99/088 lanes 1 to 9, frontal cortex to entorhinal cortex. **B;** sCJD MM 1 RU#99/088 lanes 1 to 8, hippocampus to cerebellar vermis, lane 9, sCJD MM 1 standard. **C;** sCJD VV 1 RU#96/027 lanes 1 to 8, frontal cortex to entorhinal cortex, lane 9, sCJD MM 1 standard. **D:** sCJD VV 1 RU#96/027 lanes 1 to 5, hippocampus to posterior thalamus. **E;** sCJD VV 2A RU#94/083 lanes 1 to 9, frontal cortex to entorhinal cortex. **F;** sCJD VV 2A RU#94/083 lanes 1 to 9, hippocampus to cerebellar vermis.

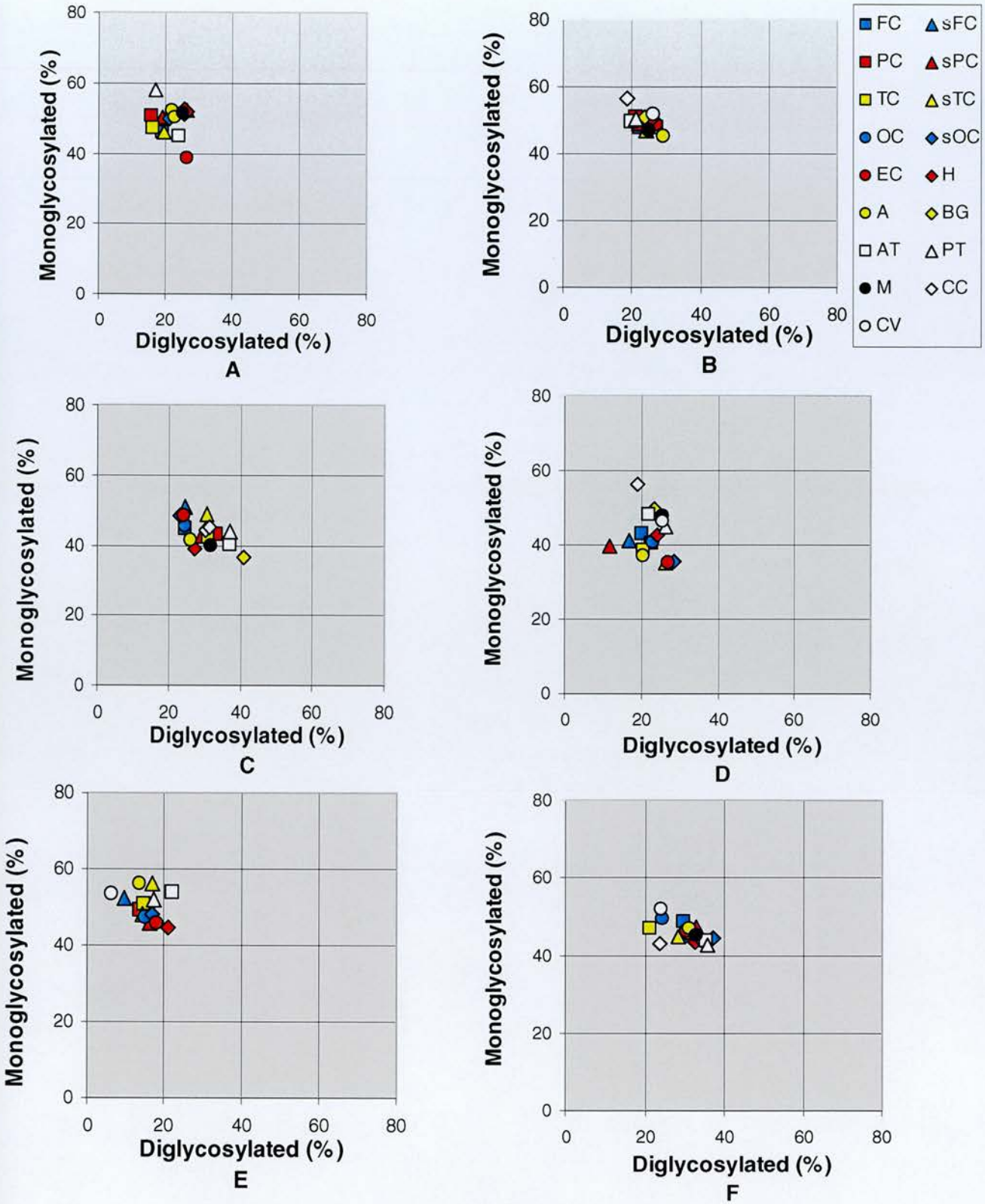

Figure 27. Sporadic CJD regional glycoform ratios. Scattergraphs of the mean glycoform ratios from different brain regions within an individual. The standard error range of brain regions is stated in brackets, for the diglycosylated (di) and monoglycosylated (mono) bands. **A.** MM 2 A (di 0.3-2.2, mono 0.5-1.7). **B.** MM 1 (di 0.7-6, mono 0.7-3.3). **C.** MV 2A case 1 (di 1.4-3.4, mono 1-2.6). **D.** MV 2A case 2 (di 2.1-2.9, mono 1.7-2.3). **E.** VV 1 (di 2.8-3.6, mono 3.3-4.3). **F.** VV 2A (di 2.8-3.1, mono 0.3-1.9).

The sCJD VV 1 (RU#96/027) case had no significant differences in glycoform ratios of any of the neuroanatomical regions (figure 27B). There was extensive neuronal loss and astrocytic proliferation within the cerebral cortex resulting in status spongiosis. Spongiform change was also noted in the basal ganglia along with less prominent neuronal loss and gliosis. The cerebellum displayed spongiform change most prominent in the vermis, but this region did not display detectable PrP^{res}. Non-PrP amyloid plaques were absent from the brain as a whole. The immunostaining displayed weak reactivity in the cerebral cortex, basal ganglia and molecular layer of the cerebellar cortex. There were no PrP reactive plaques in the brain. The cerebral cortical regions and deep grey matter regions all displayed PrP^{res} (figure 26C and D). The neuropathological findings were not dissimilar to the Dutch case with significant spongiform change, neuronal loss and diffuse or granular synaptic staining for PrP^{res}. However, small PrP positive plaque-like structures were noted in this case and may be an indicator of the type 2B PrP^{res} pattern, as they were not detected on biopsy.

The sCJD VV 2A patient (RU#94/083) also had spongiform change accompanied by gliosis and neuronal loss, though in this case despite the occipital cortex being spared, low levels of PrP^{res} were detected in both the occipital and suboccipital cortices relative to the other brain regions (figure 26E). Perineuronal deposits of PrP were detected in cerebral cortex with small diffuse deposits and the occasional PrP positive plaque-like deposits seen in the granular layer. The hippocampus, basal ganglia and thalamus also displayed spongiform change. The cerebellum had marked spongiform degeneration of the molecular layer leading to cortical atrophy. The neuropathological features do not appear to influence the PrP^{res} formation in different brain regions. The plaque-like formation is quite distinct from vCJD florid plaques, yet may be related to the proportion of diglycosylated PrP^{res}.

Neuropathological findings from a group of 12 sCJD VV cases were obtained (with kind permission) from Kovacs *et al*, (Kovacs *et al*, 2000) and from the autopsy reports. Five of these comprised of cases classified as part of the VV 2A subgroup described in chapter 3. PrP^{res} as detected by immunocytochemistry was classified as one of four types of deposit; vacuolar, diffuse/synaptic, neuronal or granular deposits and plaques (a more detailed description of these four patterns can be found in the appendix, A6). The neuropathological findings in these 12 patients included spongiform change and prion protein immunopositivity most apparent in the subcortical grey matter and cerebellum. Plaque-like deposits staining for PrP were evident in all brain regions with laminar PrP deposition in the cerebral cortex and the

hippocampus. Involvement of the hippocampus is rarely seen in sCJD. The neuropathological findings of this group of patients is similar to that of case RU#94/083. The uniform features of these patients as a whole along with the consistent PrP^{res} banding pattern and their distinction from other sCJD cases in terms of hippocampal involvement and the slight increase in diglycosylated PrP^{res} indicates that this subgroup has a distinct phenotypic spectrum that could be regarded as a 'strain'.

The investigation of a sCJD MM 2A patient (RU#99/014) was of particular significance in light of case RU#99/068 as already discussed. The age at onset and duration were 61 years and 11 months respectively, thus unexceptional for the subgroup as a whole. This case displayed both type 1 and 2 mobilities. The subfrontal cortex was found to be type 1 mobility on initial analysis (figure 28A). Closer examination of overlying frontal cortex sample clearly showed that although the majority of nonglycosylated PrP^{res} in the sample was type 2, there was also trace levels of type 1 PrP^{res} present (figure 28C) and some type 2 could be detected in subfrontal cortex (figure 28B). Twelve regions displayed type 2 PrP^{res}, but in addition to the frontal cortex and subfrontal cortex the basal ganglia and cerebellum samples showed some degree of type 1 PrP^{res}. The glycoform ratios in this case were fairly consistent though a slight decrease in the proportion of monoglycosylated PrP^{res} was observed in the frontal cortex relative to the subfrontal cortex possibly due to the extra band observed (figure 27D). This highlights the dependence of glycoform analysis on distinct and discrete PrP^{res} fragments for proportional comparisons. This case had widespread cerebral cortical spongiform encephalopathy, most severe in the occipital cortex where confluent spongiform change, severe neuronal loss and astrocytosis were observed. There is strong positivity to PrP in a synaptic and perivacuolar pattern, particularly in the occipital cortex. Spongiform change was observed in the basal ganglia, thalamus and cerebellum. In the thalamus this was patchy and the molecular layer of the cerebellum only displayed focal spongiform change. Both synaptic and perivacuolar PrP deposits were seen in the basal ganglia and thalamus, but in the cerebellum there was merely focal synaptic staining of the molecular and granular layers. This age at onset and neuropathological features suggest this case corresponds to the MM 2 cortical subgroup described by Parchi *et al.* All brain regions displayed roughly equivalent levels of PrP^{res} (figure 28).

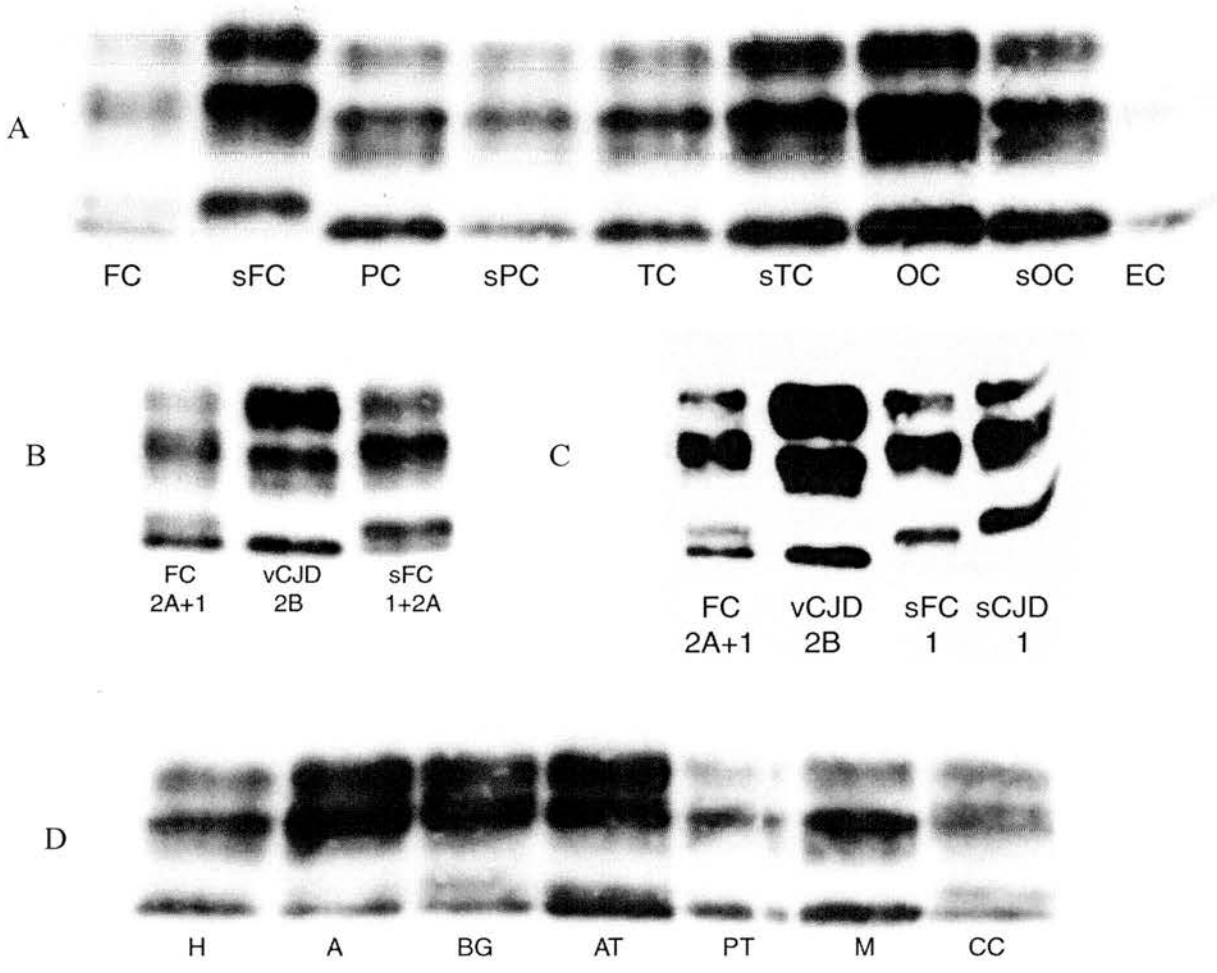

Figure 28. Sporadic CJD brain regions showing multiple isotypes in MM 2A case RU#99/014. **A;** Lane 1, frontal cortex, type 2A+1, lane 2, subfrontal cortex , type 1, lane 3 to 9, parietal cortex to entorhinal cortex, type 2A. **B;** Lane 1, RU#99/014 frontal cortex, type 2A+1, lane 2, vCJD frontal cortex, type 2B, lane 3, RU#99/014 subfrontal cortex, type 1+2A. **C;** Lane 1, RU#99/014 frontal cortex, type 2A+1, lane 2, vCJD type 2B standard, lane 3, subfrontal cortex, type 1, lane 4, sCJD MM 1 standard. **D;** Lane 1, hippocampus, type 2A, lane 2, amygdala, type 2A, lane 3, basal ganglia, type 2A+1, lane 4, anterior thalamus, type 2A+1, lane 5, posterior thalamus, type 2A, lane 6, mesencephalon, type 2A, lane 7, cerebellar cortex, type 2A + 1.

This case was the first to demonstrate both types of PrP^{res} in the same sample (i.e. the same brain region). Since the discovery of this co-occurrence phenomenon more cases have been identified through ongoing routine testing of new cases, retrospective analysis of iCJD cases and regional analysis. Co-occurrence has been observed in 5 sCJD cases (RU#99/014, RU#98/082, RU#00/008, RU#00/017, RU#97/008), and an iCJD case (RU#99/062), where both type 1 and 2 nonglycosylated bands can be seen in the same brain sample. Different isotypes have also been identified in separate brain regions of individuals in 3 sCJD cases (RU#98/153, RU#99/068, RU#96/153) and 2 fCJD cases (RU#92/070 and RU#94/097). Co-occurrence is not restricted to one region of the brain and cases of sCJD co-occurrence have been found carrying each of the codon 129 genotypes (table 12). The numbers of cases are small yet there is a preponderance of homozygotes. A majority of heterozygotes would be expected if there is allele preference for one conformation over the other, resulting in two isotypes. If the preference for the type 1 conformation of MM cases applied, as suggested by the findings in chapter 3, a dominant type 1 band with residual type 2 would be expected. The cases in which this phenomenon was identified were initially classified as type 2A, but were older and had shorter disease duration than the other MM type 2A cases. In the MM 2A group as a whole the mean age at onset was 54 years and disease duration was 19 months. The mean age at onset was 65.3 years and 10.3 months in the multiple isotype cases but single isotype cases were on average 50.2 years old at onset and had disease duration of 20.2 months. These cases had similar onset and duration to cases classified as MM type 1 and these may be more indicative of the PrP^{res} conformation. This strengthens the finding that the codon 129 alone does not determine PrP^{res} conformation.

Case	Codon 129	Number of cases
Sporadic CJD	MM	3
	MV	2
	VV	3
Iatrogenic CJD	MV	1
Familial CJD	MM	1
	MV	1

Table 12. Cases displaying two isotypes and their codon 129 breakdown.

The first MV 2A case (RU#98/123) investigated had a consistent mobility but displayed variation in glycoform ratio according to neuroanatomical region. This was most clearly seen in the comparison of three cortical regions with the basal ganglia and thalamus, which is more heavily glycosylated (figure 29). Comparison of the glycoform ratios of this case with the sCJD MV 2A subgroup found there to be significant differences in the glycoform ratios between the individual regions and the subgroup as a whole (diglycosylated $p < 0.000$, monoglycosylated $p = 0.005$, nonglycosylated $p < 0.000$, one way ANOVA). Thus analysis of the frontal cortex alone may not provide an indication of the glycoform ratio throughout the brain. The regions most significantly different from the MV 2A subgroup for the diglycosylated levels were the parietal cortex $p = 0.016$, basal ganglia, anterior thalamus, posterior thalamus $p < 0.000$ and cerebellar cortex $p = 0.048$, dunnett *t* 2 sided post hoc test). There was no significant difference between the levels of the monoglycosylated band, but the same regions were all significantly different in the nonglycosylated band as well as the subtemporal cortex (parietal cortex $p = 0.049$, subtemporal cortex $p = 0.003$, basal ganglia $p = 0.007$, anterior thalamus $p = 0.025$, posterior thalamus $p < 0.000$, cerebellar cortex $p = 0.003$). There was a significant difference between the levels of all three bands, when compared as a whole with the vCJD cases (diglycosylated $p<0.000$, monoglycosylated $p<0.000$, nonglycosylated $p<0.000$). However, there was no significant difference between the levels of nonglycosylated PrP in the subfrontal cortex, parietal cortex, temporal cortex, subtemporal cortex, basal ganglia, anterior thalamus, posterior thalamus, cerebellar cortex and vermis). Indicating that misclasssification from non-cortical tissue is possible, though unlikely provided all three bands are considered in conjunction, quantitation of the glycoform levels is carried out and the tissue being investigated is taken into account. The basal ganglia and thalamic regions of RU#98/123 did overlap with the glycoform ratios of some vCJD regions. The overlap of glycotype appearance or glycoform ratios with vCJD, based on single sampling of deep grey matter regions or cerebellum, raises the potential for misdiagnosis of sCJD cases if relying solely on the PrP^{res} banding pattern. It also raises the question of the contribution of an M allele to diglycosylated PrP^{res} formation in deep grey matter regions, particularly the thalamus as observed in FFI.

This glycoform variation was further investigated by resampling twice from each region and investigating another MV 2A case. Resampling did not show as

convincing a variation, though this may be due to the limited number of repetitions performed on the resampled tissue and the second case (RU#96/153) did not display similar anatomically specific variation in glycoform ratio (figure 27F). However analysis of the glycoform ratios in comparison with the sCJD MV 2A subgroup as a whole found the subtemporal, suboccipital and entorhinal cortical regions to have significantly different monoglycosylated bands ($p = 0.017, 0.034, 0.022$ respectively, one way ANOVA, dunnets *t* 2-sided post hoc). This case was significantly different to the vCJD cases. The variation of glycoforms may be specific for cortical neuroanatomical region. As with subgroups of cases, regional analysis can be quantitated and spatially compared for individuals with differing genotypes and aetiologies.

The second case (RU#96/153) also displayed both type 1 and 2 mobilities. Similarly to the MM 2A case a subcortical region, in this case subparietal cortex, displayed type 1 mobility, other regions had type 2 mobility though some contained small amounts of type 1 PrP^{res} particularly the amygdala and mesencephalon (figure 30).

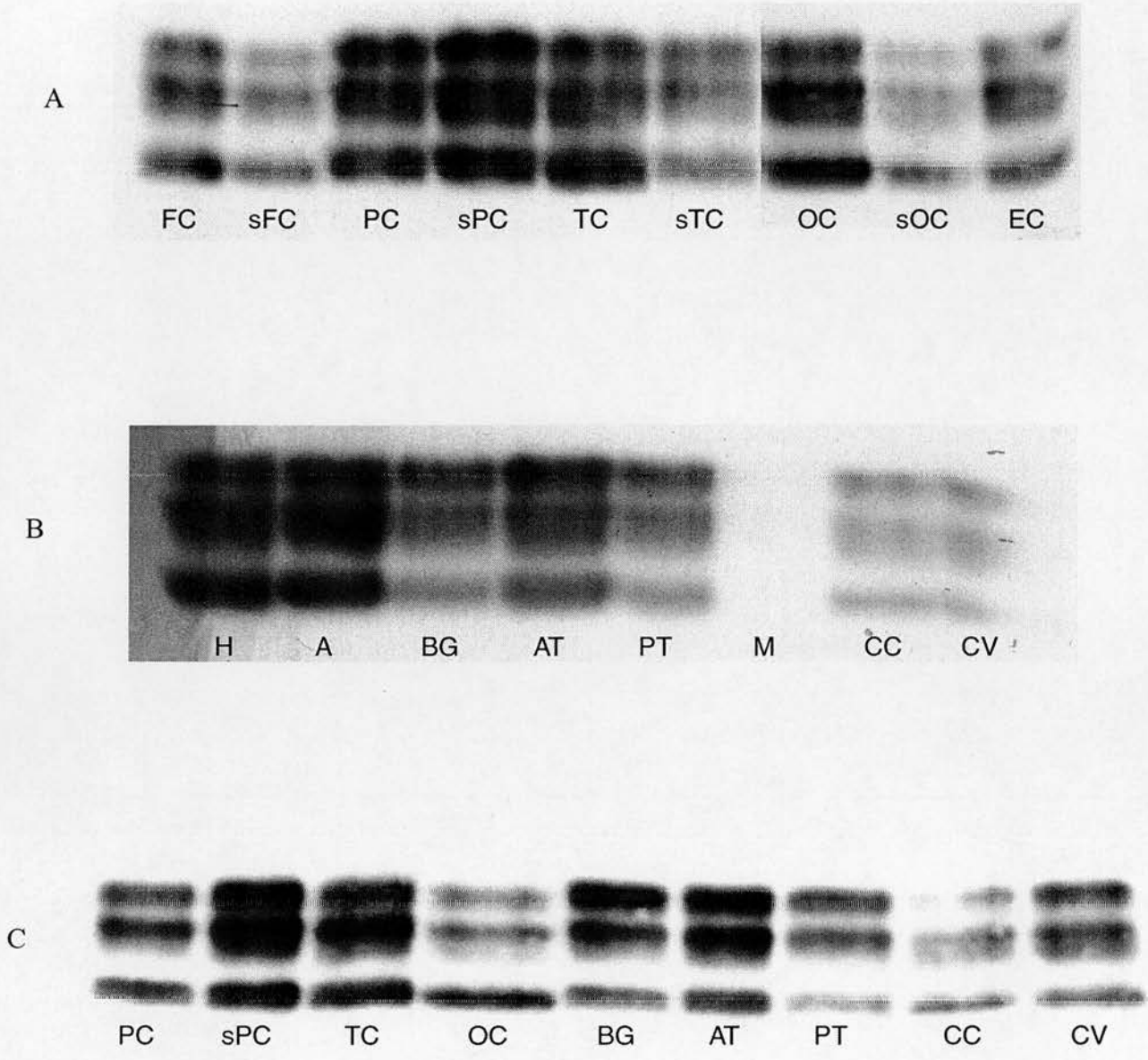

Figure 29. Brain regions in sCJD MV 2A case RU#98/123, showing similarity in relative mobility and differences in glycoform ratio. **A;** Differences in glycoform ratio, lane 1 to 6, frontal cortex to subtemporal cortex at 10 second exposure, lane 7 to 9, occipital cortex to entorhinal cortex from the same western blot at 30 second exposure. **B;** Difference in glycoform ratio, lane 1 to lane 9, hippocampus to cerebellar vermis. **C;** Most contrasting regions in terms of glycoform ratio, lane 1, parietal cortex, lane 2, subparietal cortex, lane 3, temporal cortex, lane 4, occipital cortex, lane 5, basal ganglia, lane 6, anterior thalamus, lane 7, posterior thalamus, lane 8, cerebellar cortex, lane 9, cerebellar vermis.

A

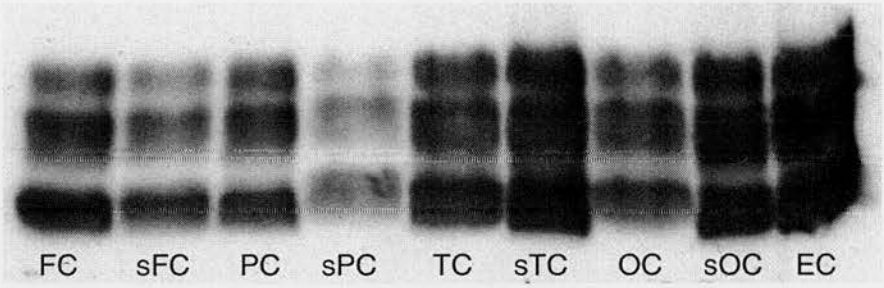

B

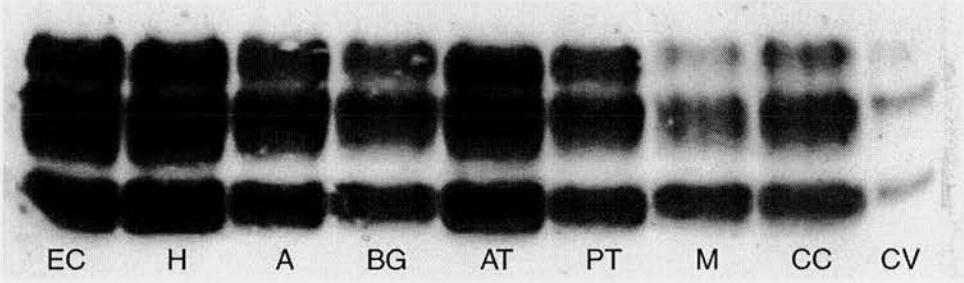

C

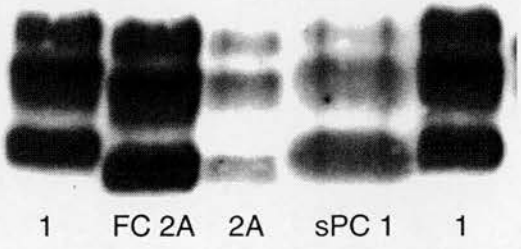

Figure 30. Brain regions in sCJD MV 2A case RU#96/153 showing differences in relative mobility. **A;** Lane 1 to 9, frontal cortex to entorhinal cortex, type 2A, lane 4, parietal cortex type 1. **B;** Lane 1 to 9, entorhinal cortex to cerebellar vermis, type 2A. **C;** Difference in relative mobility in comparison to standards. Lane 1, sCJD type 1 standard, lane 2, RU#96/153 frontal cortex, type 2A, lane 3, sCJD type 2A standard, lane 4, RU#96/153 subparietal cortex, type 1, lane 5, sCJD type 1 standard.

The first case (RU#98/123) investigated in the MV 2A subgroup had an age at onset of 62 years and duration of 21 months, but the second case, which had a very similar age at onset of 61 years, had disease duration of 8 months. The first case displayed widespread spongiform encephalopathy in the cerebral cortex and basal ganglia. This was most prominent in the parietal cortex were it was accompanied by neuronal loss and astrocytosis. Routine staining identified occasional small non-'florid' amyloid plaques. These plaques were also seen in the hippocampus. PrP immunostaining identified a strong synaptic pattern of staining. Perineuronal staining was seen in layer 5 with PrP plaques found in layers 1-4. The basal ganglia displayed widespread spongiform change, extensive gliosis and neuronal loss. The thalamus has less severe but widespread spongiform change. The basal ganglia and thalamus had synaptic PrP deposits but few plaques. The cerebellum suffered spongiform change in the molecular layer in conjunction with pale staining plaques also observed on PrP immunostaining and more prevalent in the granular layer. There was also synaptic staining around the dentate nucleus. The second case (RU#96/153) also displayed cerebral cortex and cerebellum spongiform change, most prominently in the frontal and temporal lobes, and cerebellar cortex. This was less apparent in the basal ganglia and thalamus. The neuronal loss and astrocytosis were most evident in the cerebral cortex, but non-PrP plaques were not observed. Immunostaining showed strong perivacuolar deposits with occasional small plaque-like deposits in the cerebral cortices, while in the cerebellum a more diffuse pattern with small dense plaques was seen in the granular layer.

There are no significant neuropathological differences between these two cases that correspond to the differences observed in mobility or glycoform ratio of PrP^{res}. The levels of PrP^{res} were fairly similar with only the subfrontal and suboccipital cortices displaying less PrP^{res}. In both cases neither of these lower levels corresponded to a greater degree of spongiform change, in fact the first case displayed greater levels of PrP^{res} in the parietal cortex where there was a high degree of spongiform change and neuronal loss.

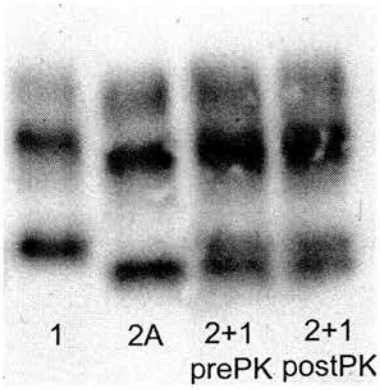

Figure 31. Comparison of standards with mixed standard samples. Criterion precast 8-16% gradient gel analysed with 3F4. Lane 1, sCJD MM 1 standard, lane 2, sCJD VV 2A standard, lane 3, type 1 and 2A standards mixed prior to PK treatment, lane 4, type 1 and 2A standards mixed after PK digestion.

Mixing of equal amounts of type 1 and 2 PrP^{res} to determine the appearance of potential sample cross contamination either before PK treatment (i.e. during sample handling) or after PK treatment (i.e. during sample loading) produced patterns similar to type 2 PrP^{res} with an additional type 1 unglycosylated band (figure 31). This suggests that type 2 PrP^{res} can potentially mask lower levels of type 1 PrP^{res}.

5.4 Iatrogenic CJD

To assess the possibility of codon 129 heterozygosity giving rise to glycoform ratio variability independent of aetiology an iatrogenic CJD MV 2A case (RU#99/111) was investigated. Analysis of a GHT iCJD case was also intended to establish the possibility of neuroanatomically specific host response presiding over the glycoform ratio of the infective strain i.e. can different glycoform ratios arise in the host from the discrete infectious glycoform ratio? Isotyping of cortical tissue from the iCJD cases revealed a GHT case containing both types 1 and 2 (figure 32) and an undefined high proportion of nonglycosylated PrP^{res} in other cases. However, glycoform ratio variability had not been established. The case available had displayed only type 2A PrP^{res} on analysis of the frontal cortex. The same isotype mobility was seen in all the brain regions (figure 33). Glycoform ratio data for repeated runs was established for the frontal and parietal cortices, the corresponding sub cortical regions, basal ganglia, thalamic regions and cerebellum. There was a similar increase in the level of diglycosylated PrP^{res} in the basal ganglia and thalamic regions (figure 35F). This similar spatial distribution of glycoform ratios to the sCJD MV 2A case suggests there is neuroanatomical specificity to PrP glycosylation.

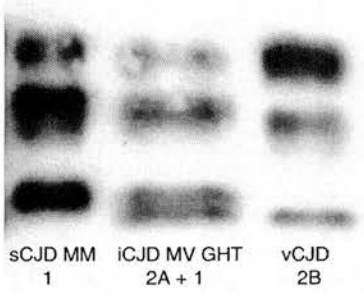

Figure 32. Multiple isotypes in iatrogenic CJD. Lane 1, sCJD MM 1 standard, lane 2, iCJD MV GHT types 1 and 2, lane 3, vCJD standard.

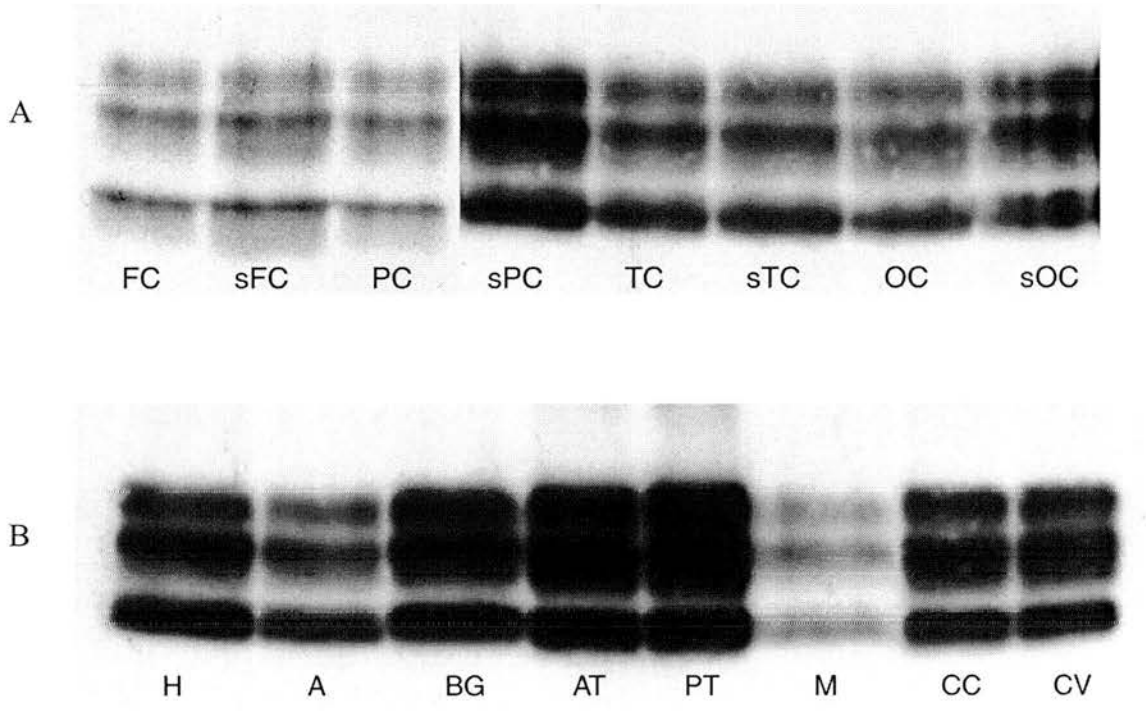

Figure 33. Brain regions in iCJD showing consistent isotype pattern. **A;** Composite image from different 12% SDS-PAGE western blots analysed with 3F4, to show similar PrP^{res} levels. Lane 1 to 3, frontal cortex to parietal cortex, 1 minute exposure, lane 3 to 8, subparietal cortex to suboccipital cortex, 3 minute exposure. **B;** Lane 1 to 8, hippocampus to cerebellar vermis.

5.5 Variant CJD

Four cases of vCJD were examined in the stated 17 regions (figure 34), one case in 15 regions and one case in 5 regions due to the availability of frozen tissues. In contrast to the sCJD, iCJD and fCJD cases (shown below) the vCJD cases examined showed a uniform type 2 mobility irrespective of the region tested and a consistent glycoform ratio (figure 35D). Initially one typical case with age at onset of 35 years and a duration of 15 months was examined (RU#98/154). The consistent isotype pattern in all regions prompted the investigation of cases with differing ages at onset and duration to establish if either parameter influenced the isotyping. One case with a long duration (29 months, age at onset 21 years) (RU#98/156), one with a short duration (9 months, age at onset 30 years) (RU#96/045) the 2B isotyping standard, one young case (age at onset 17 years, duration 18 months) (RU#00/025) and one older case (age at onset 51 years, duration 11 months) (RU#99/015). The final case was 19 years old at disease onset and had an 11 month duration (RU#98/148). All the vCJD cases were consistent in mobility and glycoform ratio (figure 34). The glycoform ratios were plotted on a scattergraph and did display some variability towards decreased diglycosylation and increased levels of nonglycosylated PrP^{res} (figure 35D), however the monoglycosylated levels remained very consistent. There was no statistically significant difference in glycoform ratios between the cases or among brain regions of individual cases. When plotted on a scattergraph the glycoform ratios did not overlap with sCJD, iCJD or the majority of fCJD regional glycoforms. A few samples from the fCJD E200K MV case did overlap with vCJD, primarily cerebellum and deeper grey matter regions.

The glycoform ratio values were in the region of equal levels of all three glycoforms for some of the samples i.e. 33% on both the monoglycosylated and diglycosylated scales (figure 35D). This phenomenon may be related to saturation of sample loading as the PrP^{res} levels were very high (1-2 µl of a 10% brain homogenate producing a comparable signal intensity to approximately 15-20 µl of a typical sCJD homogenate) and shorter X-ray exposures did not compensate. Further dilution of the samples would likely reduce the effect of high PrP^{res} levels as this was seen to produce a greater resolution and more pronounced ratio on general analysis. The levels of PrP^{res} were frequently highest in the basal ganglia and thalamus (figure 34B) where marked spongiform change, severe neuronal loss and marked gliosis were detected.

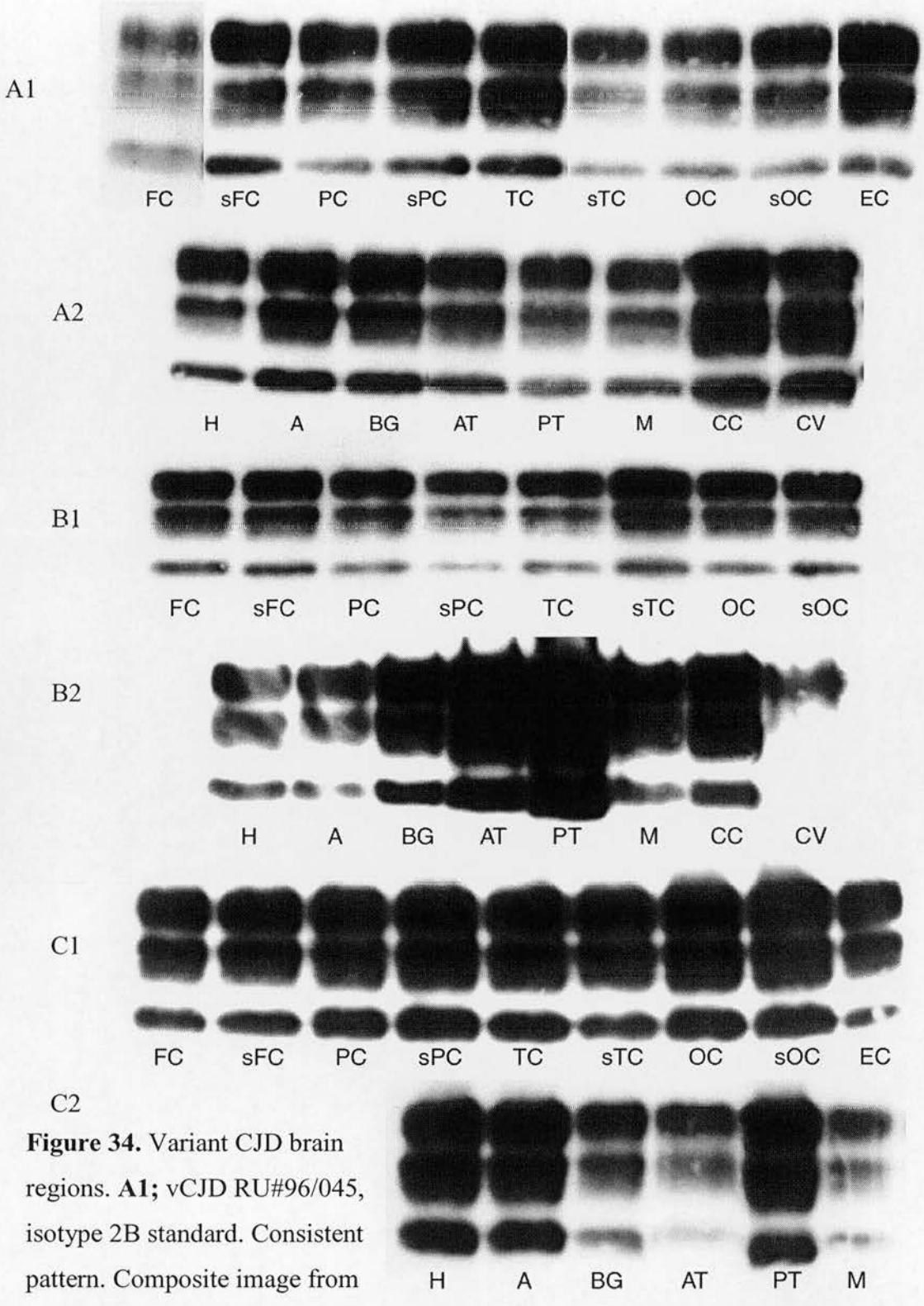

Figure 34. Variant CJD brain regions. **A1;** vCJD RU#96/045, isotype 2B standard. Consistent pattern. Composite image from 12% SDS-PAGE western blots analysed with 3F4 at different exposure periods to equalise appearance of PrP^{res}, Lane 1, FC 10 second exposure, lane 2 to lane 5, sFC to TC 3 minute exposure, lane 6, sTC to sOC 30 second exposure, lane 9, EC 3 minute exposure. **A2;** Lane 1 to lane 8, H to CV. **B1;** vCJD RU#98/154 with typical age at onset and disease duration. Lane 1 to lane 8, FC to sOC. **B2;** Lane 1 to lane 8, H to CV. **C1;** vCJD RU#98/156. Lane 1 to lane 9, FC to EC. **C2;** Lane 1 to lane 6, H to M.

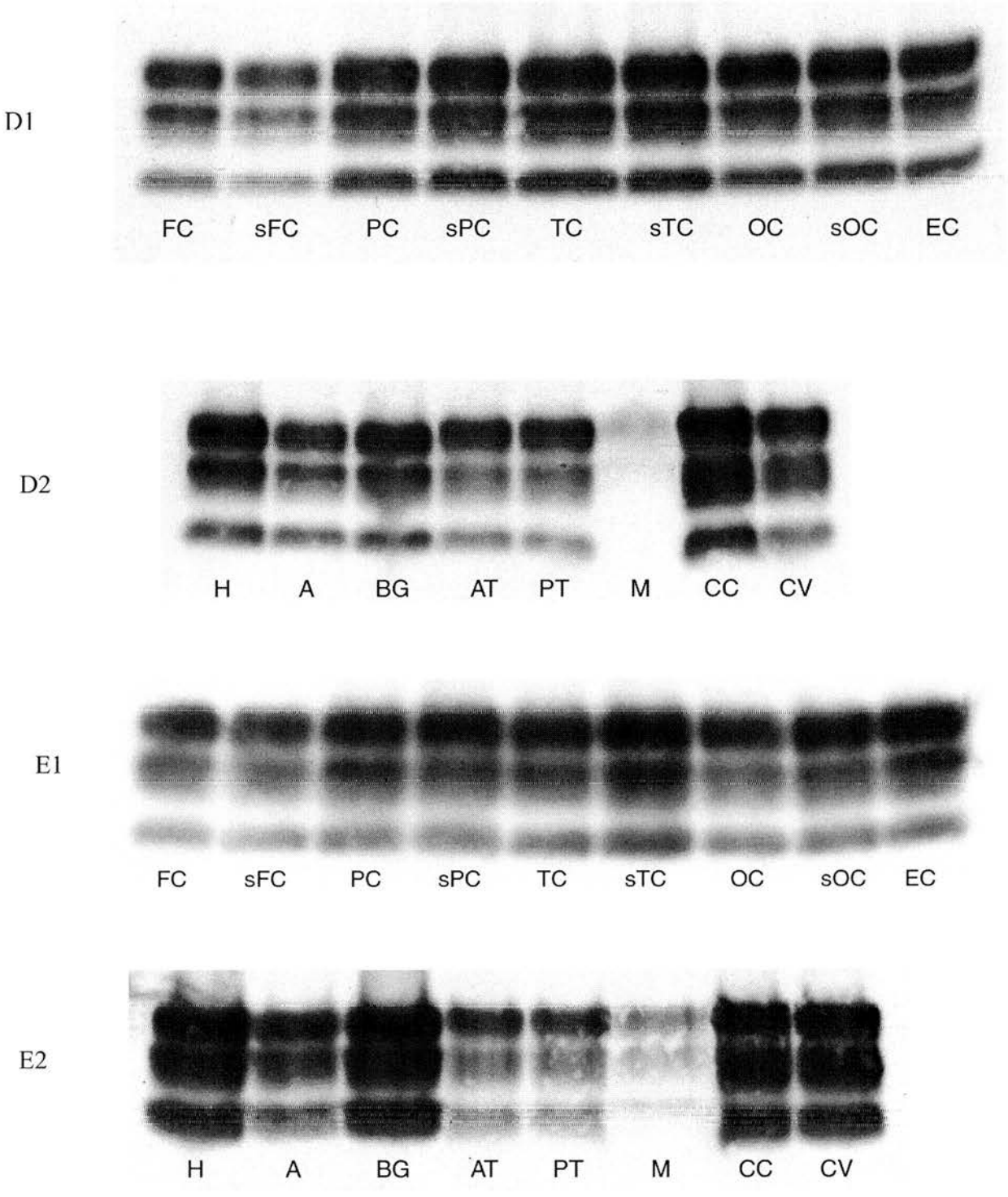

Figure 34 continued. D1; vCJD RU#99/015. Lane 1 to lane 9, frontal cortex to entorhinal cortex. **D2;** Lane 1 to 8, hippocampus to cerebellar vermis. **E1;** vCJD RU#00/025. Lane 1 to lane 9, frontal cortex to entorhinal cortex. **E2;** Lane 1 to lane 8, hippocampus to cerebellar vermis.

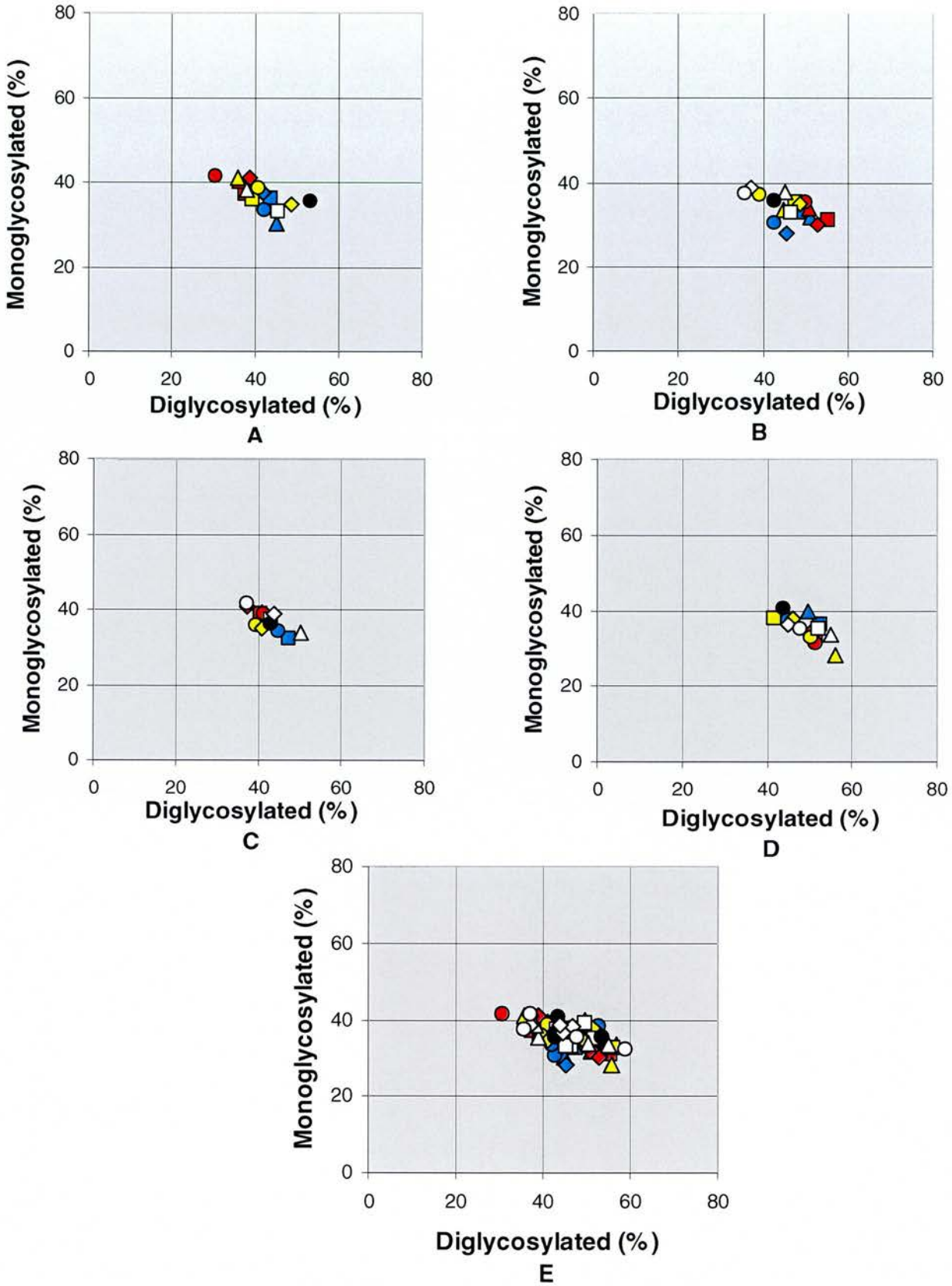

Figure 35. Variant CJD regional glycoform ratios. Scattergraphs of the mean glycoform ratios from different brain regions within an individual. The standard deviation range of brain regions is stated in brackets, for the diglycosylated (di) and monoglycosylated (mono) bands. **A.** vCJD long duration case (di 0.7-6, mono 0.7-3.3). **B.** vCJD short duration case (di 1.4-3.4, mono 1-2.6). **C.** Younger vCJD case (di 2.1-2.9, mono 1.7-2.3). **D.** Older vCJD case, (di 2.8-3.6, mono 3.3-4.3). **E.** All vCJD regionally analysed cases (di 2.8-3.1.).

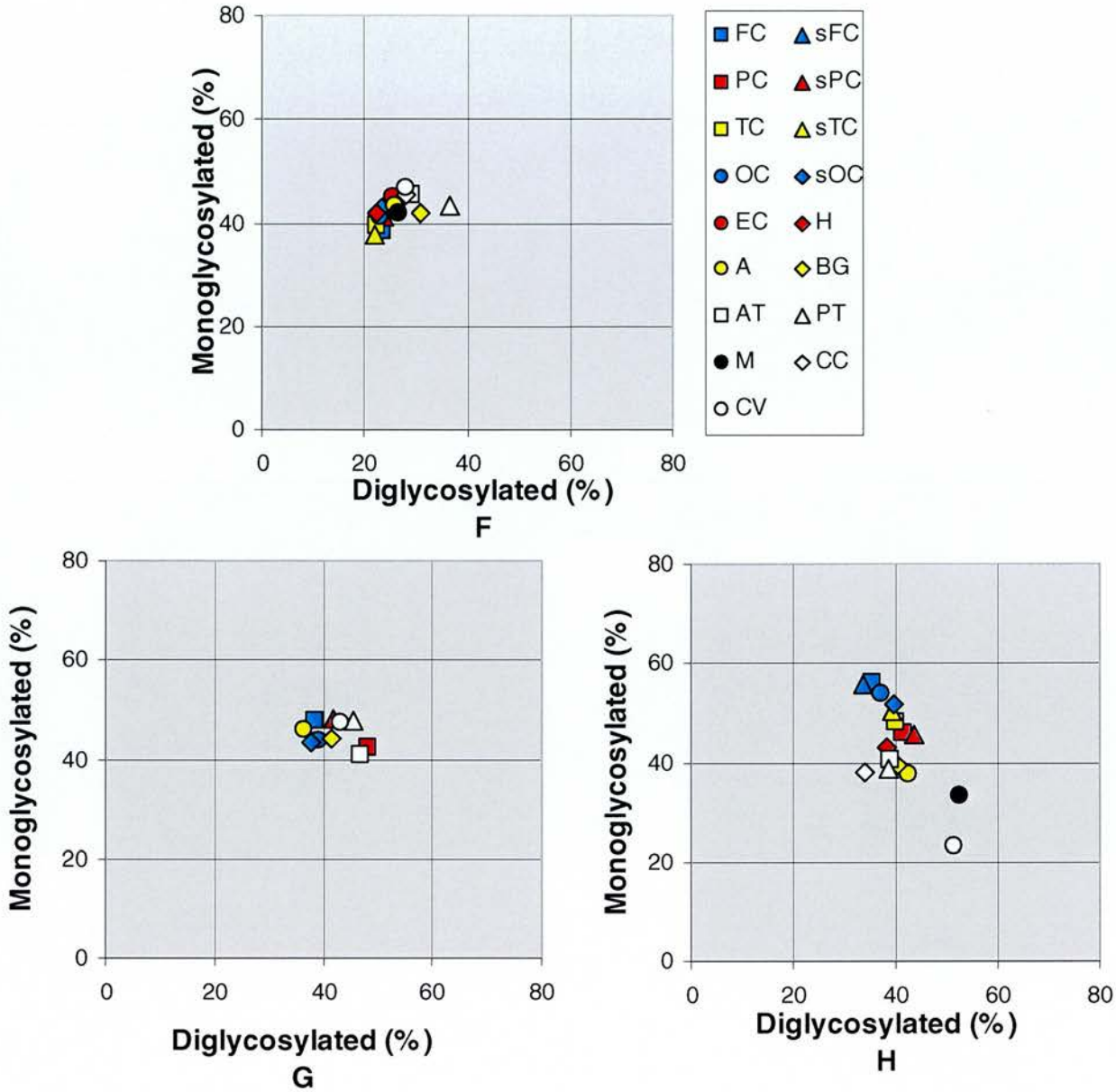

Figure 35 continued. Iatrogenic CJD and fCJD regional glycoform ratios. Scattergraphs of the mean glycoform ratios from different brain regions within an individual. The standard deviation range of brain regions is stated in brackets, for the diglycosylated (di) and monoglycosylated (mono) bands. **F.** iCJD MV 2A (di 0-4.55, mono 0-5.89) **G.** fCJD MM case(di 0-9.8, mono 0-7.5) **H.** fCJD MV case (di 0-9.26, mono 0-7.25).

Over the course of these investigations a partial difference in glycoform ratio was detected and seemed most apparent in the basal ganglia, thalamic regions and in particular the cerebellar cortex, where a slight increase in monoglycosylation could be detected but was devoid of significant variance (figure 35). Optimal resolution of the cerebellar samples identified a greater proportion of monoglycosylated PrP^{res}, characterised by the prominence of the lower region of the band (figure 36). This regional specific difference in the mobility of monoglycosylated PrP^{res} could be due to a degree of preferential occupancy of either the 181 or 197 asparagines by N-linked glycan chains. This was further investigated by the sampling of 26 vCJD cerebellums, most of which clearly demonstrated this feature of the more diffuse monoglycosylated band. The apparent decrease in diglycosylated PrP^{res} may actually be due to an increase in monoglycosylated PrP^{res} causing a relative shift in proportions of the three bands. This phenomenon emphasises the need for statistical analysis that can compare all three bands in conjunction so as not to misinterpret levels of the glycoforms in isolation. Densitometry and improved resolution can aid in quantitation of this phenomenon. In summary the isotype banding pattern in vCJD displayed a very minor variability between brain regions, the differences in PrP^{res} morphological deposits did not show any correlation with different banding patterns and the prominence of the monoglycosylated band in the cerebellum appears to be tissue specific as florid PrP plaques are found in the cerebral cortex. Surprisingly high levels of PrP^{res} deposition in the occipital cortex as observed by immunocytochemical techniques did not give rise to strong signals on Western blots and high PrP^{res} levels in fact correlated with spongiform change or astrocytosis.

Examination of sCJD and iCJD cerebellums displayed the same lower prominence phenomenon of the monoglycosylated band and an apparent greater relative proportion of monoglycosylated PrP^{res} (figure 37). Eleven sCJD cases were sampled in addition to the 6 regional cases and 1 iCJD case in additional to the regional case. In some cases only the cerebellum was available to provide isotyping data for the patient as a whole (4 of the sCJD cases and the iCJD case). Classification of patients on the basis of cerebellum material may be misleading due to potential co-occurrence of isotypes and glycoform analysis and may be atypical for the case as a whole, with a potential apparent increase in both monoglycosylated and nonglycosylated bands. This phenomenon along with cases RU#98/123 and RU#99/111 represents good evidence to support tissue specific PrP^{res} glycoform ratios.

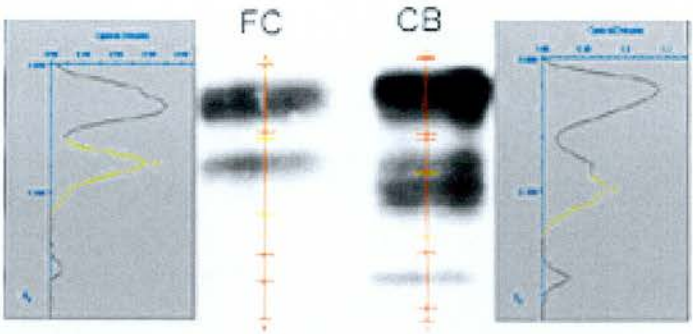

Figure 36. Variant CJD MM 2B standard frontal cortex (FC) *vs* cerebellum (CB) line density trace.

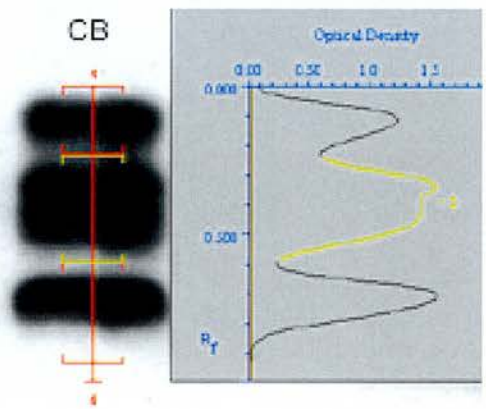

Figure 37. Sporadic CJD cerebellum (CB) line density trace.

5.6 Familial CJD

Two cases of fCJD carrying the E200K mutation were available for regional analysis, one case was MM the other MV. Their analysis was pertinent, owing to the similar glycoform ratio seen in frontal cortex (type 1B) and the occurrence of the disease in MM individuals. Establishing if any regions had the type 2 mobility and retained the predominant diglycosylation seen in vCJD was therefore important in terms of determining the exclusive nature of the 2B pattern. Two separate UK families have been described (Collinge *et al*, 1993) with average age at onset 55, rapidly progressive dementia, myoclonus, and pyramidal, cerebellar or extra-pyramidal signs, characteristic pseudoperiodoc EEG, histologically typical for CJD with PrP but no plaques. Establishing both isotype and glycoform ratio proved far

harder than previous cases due to a distinct lack of nonglycosylated PrP^{res}. Most regions had roughly equal levels of diglycosylated and monoglycosylated PrP^{res}. Establishing the mobility required PNGaseF treatment, which along with the high PrP^{res} levels often lead to intense broad signal, hampering resolution. Multiple mobility patterns were observed in both cases. In the MM case RU#94/097, who died at the age of 57 following a rapidly progressive dementia featuring myoclonus and had abnormal EEG readings, there was significant PrP^{res} accumulation throughout most of the brain (figure 38). Some regions were clearly shown to contain type 1 nonglycosylated PrP^{res} (cerebellar vermis) though in other regions an intermediate mobility was observed (parietal cortex and anterior thalamus) (figure 39). In the posterior thalamus of this case a higher molecular mass pattern was observed (described as type 7 by Hill, 1998) (figure 39). This was the only case to show three different mobility types and there were even some regions (entorhinal cortex, amygdala and hippocampus) that may of displayed a type 2 mobility but were hard to distinguish from an intermediate mobility. The MV case RU#92/070 that died at the age of 61 displayed what appeared to be both types 1 and 2 (comparison of subfrontal and parietal cortices in figure 40A). The glycoform ratios did show some variation, primarily in the MV case, which had a greater degree of diglycosylation in cerebellar and deep grey matter regions. These regions overlapped with vCJD but not sCJD. The ratios in the MM case were different to both sCJD and vCJD in most cases with a tendency to fall on the X:Y axis reflecting the equivalent levels of diglycosylated and monoglycosylated PrP^{res}. The cases were subtly distinct from the sCJD VV 2A subgroup in that they either contained greater levels of diglycosylated PrP^{res} or to some degree in all cases less nonglycosylated PrP^{res}. Greater levels of monoglycosylated PrP^{res} placed them above the vCJD cases on the scattergraph. Greater levels of diglycosylated PrP^{res} resulted in a position further over to the right of the scattergraph while less nonglycosylated PrP^{res} placed them further away from the origin. The misdiagnosis of fCJD as vCJD based purely on the banding pattern is thus possible.

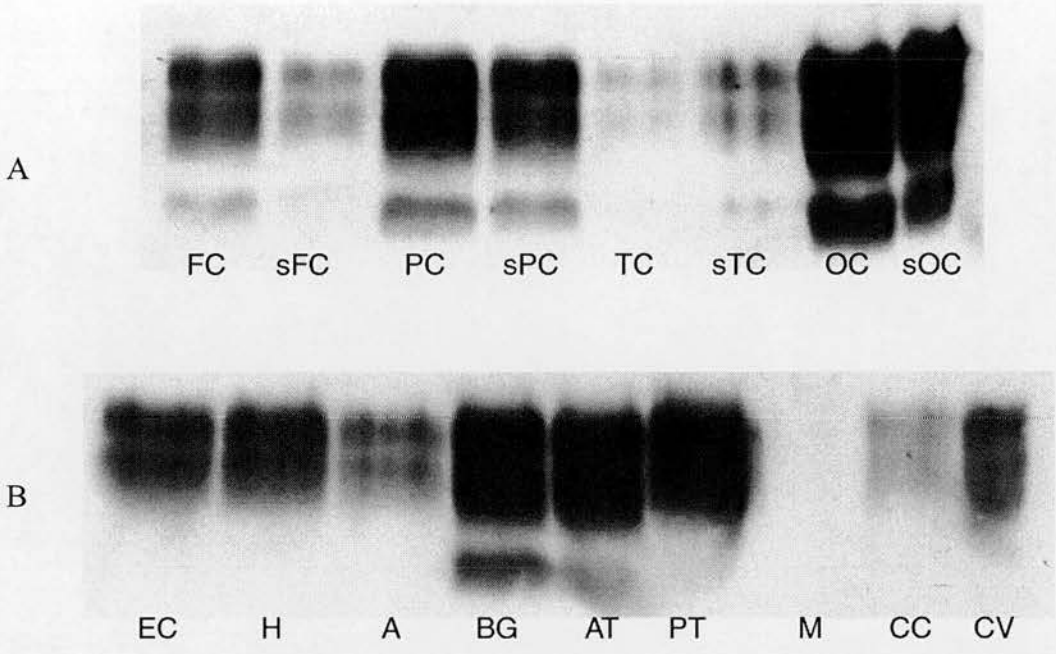

Figure 38. Brain regions of fCJD E200K MM case RU#94/097. **A;** Lane 1 to 8, frontal cortex to suboccipital cortex. **B;** Lane 1 to 9, entorhinal cortex to cerebellar vermis.

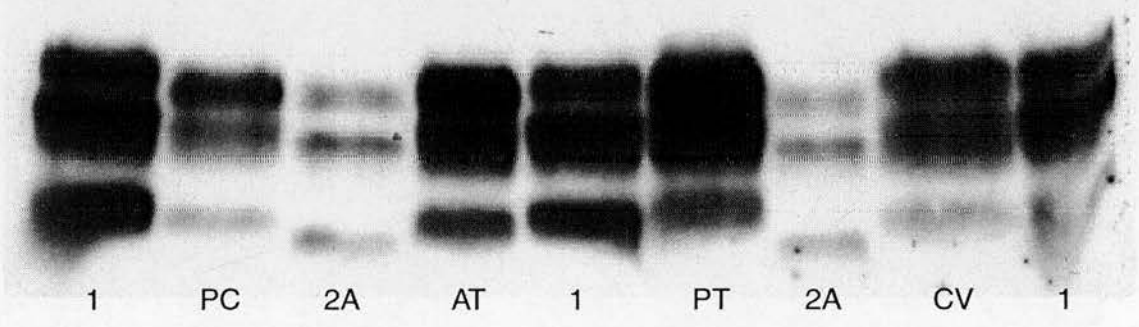

Figure 39. Comparison of brain regions in fCJD E200K MM case RU#94/097 with sCJD standards. Lane 1, sCJD MM 1 standard, lane 2, parietal cortex, type INT, lane 3, sCJD VV 2A standard, lane 4, anterior thalamus, type INT, lane 5, sCJD MM 1 standard, lane 6, posterior thalamus, type 1+, lane 7, sCJD VV 2A standard, lane 8, cerebellar vermis, type 1.

A

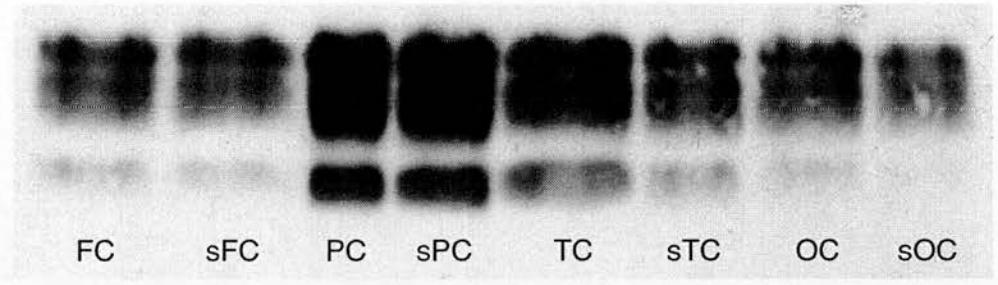

B

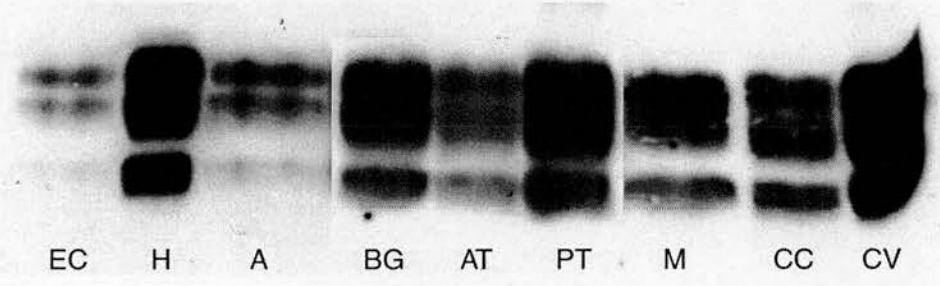

Figure 40. Brain regions in fCJD E200K MV case RU#92/070. **A;** Lane 1 to 8, frontal cortex to suboccipital cortex. **B;** Composite image from 12% SDS-PAGE western blots analysed with 3F4 at different exposure periods to equalise appearance of PrP^{res}. Lane 1 to 3 and lane 7 to 9, entorhinal cortex to amygdala and mesencephalon to cerebellar vermis, 3minute exposure, lane 4 to 6, basal ganglia to posterior thalamus, 15 second exposure.

Summary

- Biopsy and autopsy analysis can yield different PrP^{res} isotypes.
- Multiple isotypes were deteced in sCJD, iCJD and fCJD cases.
- Glycoform ratio variation was seen in sCJD, iCJD and fCJD cases.
- Variant CJD cases were consistent in isotype and glycoform ratio throughout the brain.
- PrP^{res} of type 1 and type 2 can occur in the same brain and even in the same brain region. The amounts of each type making up the total PrP^{res} can vary.
- The PrP^{res} glycoform ratio can vary according to specific anatomical regions.
- Cerebellum derived PrP^{res} displays a more pronounced lower monoglycosylated band.

The PrP^{res} isotype is not consistent throughout the CNS in individual cases. The presence of different isotypes in different brain regions and at autopsy as opposed to biopsy undermines the assumption that the PrP^{res} isotype identified from limited sampling is representative of the individual as a whole. The presence of multiple isotypes in the same brain region may complicate the determination of the isotype and lead to misclassification. In contrast vCJD cases were strikingly consistent in isotype and due to the novel nature of vCJD may be a feature of the strain of agent. A correlation between the PrP^{res} conformation and the neuropathology could not be clearly established but suggests that diffuse staining of PrP or focal and PrP plaques may relate to type 1 or type 2 PrP^{res} respectively. The relative levels of type 1 or type 2 PrP^{res} suggests that the isotype is a feature of PrP accumulation. Thus the classification of cases may be more accurate as predominantly type 1 or 2. More comprehensive analysis of cases may lead to reclassification of some cases and provide a better differentiation of the sCJD subgroups. Spongiform change may correlate to increased glycosylation of PrP^{res} but the two are not mutually exclusive. The anatomical specificity of the glycoforms is a contributing factor, but the lack of difference in vCJD and some sCJD cases indicates the disease process is dominant. The consistency of the monoglycosylated PrP^{res} prominence in the cerebellum suggests that there is a strong pressure influencing PrP glycosylation in the cerebellum.

CHAPTER 6: Divalent cation chelation studies.

6.1 Metal ion status of isotype standards

PrP^{res} was extracted in a native form from patients, using an EDTA free buffer. The concentrations of EDTA and the pH in commonly used lysis or homogenisation buffers are not sufficient to significantly chelate ions from PrP. The concentration of copper or zinc required to maintain PrP^{res} conformation is similar to physiological levels (25 μM). During this study it was reported that removal of bound metal ions from PrP^{res} with divalent metal ion chelators or washing in buffer and subsequent proteinase K treatment, led to an increase in relative mobility of samples. This increased mobility was termed 2^- and was observed in types 1 and 2 of sCJD according to the nomenclature of Collinge *et al* (Wadsworth *et al*, 1999a). Treatment of samples primarily with the broad specificity chelator $EDTA^{-4}$ (ethylene-diamine-tetraacetic acid), but also more specific chelators EGTA and triethylenetetramine (Cu^{2+} specific), dipicolinic acid and 1,10 phenanthroline (Zn^{2+} specific) or washing in *N*-ethylmorpholine buffer alone, demonstrated the possibility of PrP^{sc} with either bound copper or zinc, to be responsible for PrP^{res} conformation. This was proposed to account for some of the variability in typing classification between groups.

It was thus decided to assess whether our isotyping classification could be reconciled with other reported classifications by treating our standards with metal ion chelators. Are differences in PrP^{res} isotype due to differential metal ion binding? Treatment of our isotype standard samples with EDTA, to obtain PrP^{res} in a metal ion unbound form, and comparison with the relative mobility of untreated standards was the first priority. Further to this, cases with the anomalous intermediate mobility and multiple isotypes were also investigated after EDTA treatment to investigate whether they were experimentally induced artifacts. In addition iCJD and GSS cases were investigated to assess whether the phenomenon was restricted to sCJD or was aetiologically determined.

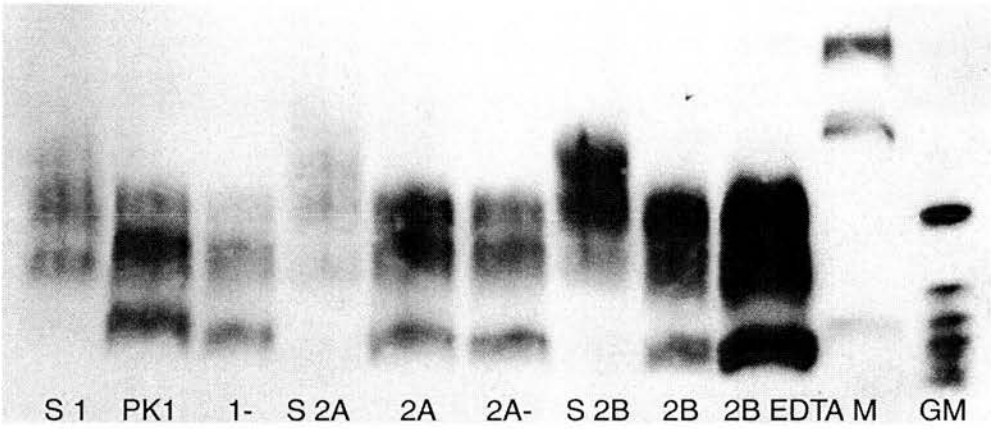

Figure 41. The effect of chelation on PrP^{res} mobility. EDTA treatment of standards. Criterion precast 8-16% gradient gel, analysed with 3F4. Lane 1, postnuclear supernatant from sCJD MM 1, lane 2, PK treated sCJD MM 1, lane 3, EDTA and PK treated sCJD MM 1 (1-), lane 4, postnuclear supernatant from sCJD VV 2A, lane 5, PK treated sCJD VV 2A, lane 6, EDTA and PK treated sCJD VV 2A (2A-), lane 7, postnuclear supernatant from vCJD MM 2B, lane 8, PK treated vCJD MM 2B, lane 9, EDTA and PK treated vCJD MM 2B (2B), lane 10, ECL markers (from top 46 kDa, 31 kDa, 20 kDa), lane 11, BFAV markers (second from top 21 kDa, 20 kDa, 19 kDa, 16 kDa).

EDTA is a divalent cation chelating agent that removes co-factor ions such as copper or zinc. The use of different homogenisation buffers may account for some of the variety in the results observed between research groups, such as the level of EDTA incorporated. In order to determine whether bound divalent cations contribute to the M_r of samples EDTA (500 mM) was added to the standard sCJD types 1 and 2A and vCJD standard 2B samples prior to PK treatment.

A small but clear increase in the mobility of the type 1 nonglycosylated fragment occurs in PrP^{res} PK treated without bound metal ion (figures 41 and 42). This results in an intermediate mobility that co-migrates with samples classified as intermediate mobility (figure 42). The type 2 standards also display a slight increase in M_r though less noticeable. The vCJD type 2B samples showed no such difference in M_r and indicates possibly the lack of bound metal ions in vCJD derived PrP^{res} or the presence of the most open native conformation to PK cleavage. The lack of change in the type 2B mobility in comparison to the type 2A may indicate a very minor difference in conformation between the two PrP^{res} types. However, due to the small differences in molecular weights of the order of 0.5 to 1 kDa, SDS-PAGE lacks the resolution required to provide uneqivocal determination of conformational differences and an alternative technique is desirable. The changes in mobility

between metal ion bound and unbound forms of PrP^{res} are slight and do not appear to account for the differences in mobility between type 1 and 2. The difference in codon 129 of the standards (VV type 1 and MM type 2) does not appear to influence the metal ion bound PrP^{res} conformation.

6.2 Intermediates and EDTA

Intermediate type PrP^{res} is extracted in a cation bound form, shown by an increase in relative mobility (figure 42). Type 1 and intermediate mobility cases have a more prominent M_r shift, possibly due to having a conformation when bound to cations more protective to PK NH_3-terminal cleavage. The presence of bound cations on the PrP^{res} of intermediate mobility cases rules out the possibility that these samples are a result of experimental artifact related to isolation in homogenisation buffers causing chelation of the metal ions. This does not rule out the possibility that types 2A and 2B contain similar levels of bound cations without this leading to a more protective conformation.

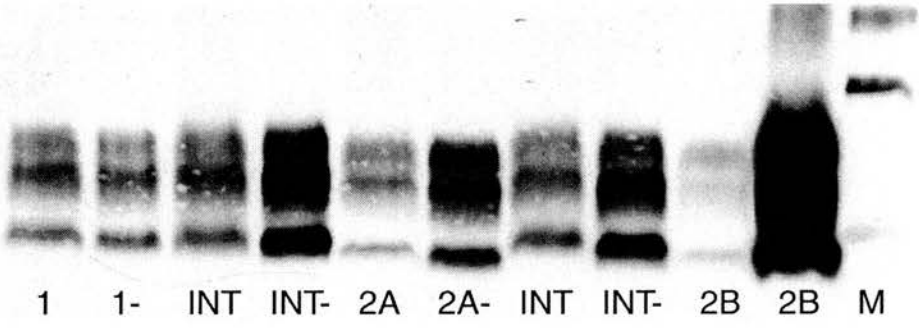

Figure 42. Comparison of PK digested intermediates with and without EDTA treatment and standards. Criterion precast 8-16% gradient gel analysed with 3F4. Lane 1, sCJD MM 1, lane 2, sCJD MM 1 EDTA (1-), lane 3, sCJD MM INT, lane 4, sCJD MM INT EDTA (INT-), lane 5, sCJD VV 2A, lane 6, sCJD VV 2A EDTA (2A-), lane 7, sCJD MM INT, lane 8, sCJD MM INT EDTA (INT-), lane 9, vCJD MM 2B, lane 10, vCJD MM 2B EDTA (2B), lane 11, ECL markers (from top 46 kDa, 31 kDa, 20 kDa).

The appearance of the glycoform ratios did not appear to differ after EDTA treatment. Glycoform ratio analysis of the effects of EDTA treatment showed no significant effects on the ratios (two tailed paired samples *t* test). This suggests that

there are not differentially metal ion bound proportions of PrP^{res} present within the glycosylated bands that are masked by the relative heterogeneity of these bands.

6.3 Multiple isotypes and EDTA

It is possible that not all PrP^{res} molecules *in vivo* have bound divalent cations. Non-uniform divalent cation loading of PrP^{res} might produce bands resembling the co-occurrence of type 1 and 2 PrP^{res}. Removal of any bound divalent cations with EDTA prior to PK digestion was therefore carried out on two of the cases identified during the neuroanatomical investigations (RU#99/068 and RU#99/014). Both bands remained in samples proteinase K treated in the presence of EDTA and displayed a minor shift in increased M_r (figure 43), consistent with their extraction in a metal ion bound form.

It is also feasible that type 2 PrP^{res} carrying a minor glycan chain, or even two short glycan chains, results in the anomalous banding. Treatment with PNGaseF was unable to resolve two bands within the nonglycosylated region due to the relatively low levels of 1 band in relation to the overall PrP^{res} and high signal.

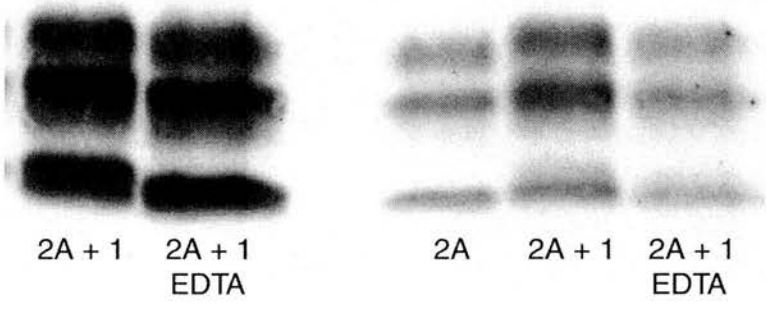

Figure 43. Co-occurrence isotype cases treated with EDTA prior to PK digestion. 12% SDS-PAGE analysed with 3F4. Lane 1, case RU#99/068, lane 2, case RU#99/068 treated with EDTA, lane 3, blank, lane 4, sCJD VV 2A standard, lane 5, case RU#99/014, lane 6, case RU#99/014 treated with EDTA.

6.4 Metal ion binding of iatrogenic and familial prion disease

The influence of PrP primary structure on copper binding has been clearly demonstrated with respect to the octapeptide repeat region, deletion of which or mutation of histidines 68 and 76, can abrogate metal ion binding (Quaglio *et al*, 2001,

Sumudhu *et al*, 2001). The influence of aetiology or pathological mutations in the PrP sequence on metal ion binding and PrP^{res} formation was investigated. For this reason the study was extended to include iCJD due to DM or GHT infection (MV) and GSS cases (MM and MV). In all these cases a similar increase in M_r was observed (figures 44 and 45).

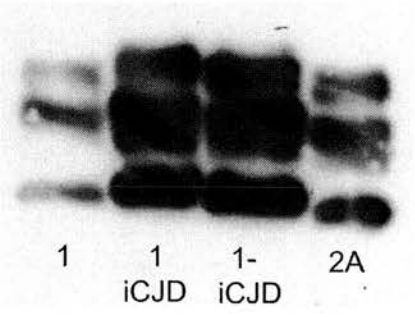

Figure 44. Comparison of iCJD case treated with EDTA to sCJD standards. 12% SDS-PAGE analysed with 3F4. Lane 1, sCJD MM 1 standard, lane 2, iCJD DM MM type 1 case, lane 3, iCJD DM MM case treated with EDTA, lane 4, sCJD VV 2A standard.

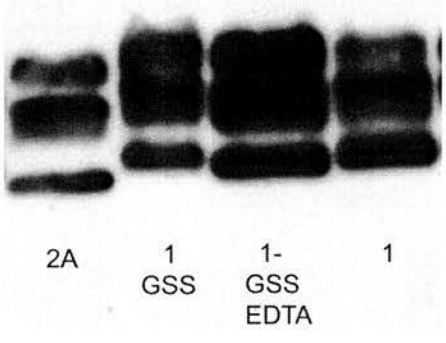

Figure 45. Comparison of GSS case treated with EDTA to sCJD standards. 12% SDS-PAGE analysed with 3F4. Lane 1, sCJD VV 2A standard, lane 2, GSS type 1 case, lane 3, GSS case treated with EDTA, lane 4, sCJD MM 1 standard.

Summary

- PrP^{res} from type 1 and INT cases are more susceptible to NH_3-terminal PK cleavage following EDTA treatment than samples from type 2 cases.
- PrP^{res} from vCJD cases does not display a noticeable change in M_r when treated with EDTA and PK. This indicates that either the PrP^{res} is in an 'open' conformation or does not have bound cations, which may be significant in the disease process.
- In mixed isotype samples, the difference in M_r is not due to differential cation binding.
- The presence of cation bound PrP^{res} in GSS suggests that prevention of metal ion binding to PrP is not responsible for the disease process.

The differences in M_r between isotypes is not due to metal ion binding. PrP^{res} accumulates in a metal ion bound form. The resolution of Western blotting is limited in its' ability to determine minor differences in PrP^{res} conformation arising from metal ion binding. Variant CJD may bind metal ions forming a conformation that is as susceptible to PK as the sCJD type 2 conformation i.e metal ion binding in the octapeptide repeat region may not necessarily confer additional protection to PK cleavage of the NH_3-terminal.

CHAPTER 7: Mouse Transmissions

7.1 Murine molecular strain typing

Is the PrP^{res} isotype a marker of prion strain, is it reproduced upon transmission and can it be used to distinguish the BSE strain? Do animal TSEs have comparable PrP^{res} isotypes to humans? To investigate the application of the human typing classification system to non-human samples and determine the retention of the strain type upon transmission, murine transmissions of CJD were investigated. Brain tissue from three vCJD cases was used to transmit the disease to three strains of mice (VM, RIII and C57 black) in conjunction with mock inoculations. Brain tissue from euthanased mice following onset of prion disease or old age was subjected to the same treatment protocol as human tissue and analysed by Western blotting. The samples were analysed blind to the inoculum and strain of mouse, therefore initially identification of PrP^{res} positive samples was important to identify the inoculated and control samples. The majority of murine samples contained PrP^{res}, with many in similar quantities to that found in human CNS tissue. Five samples clearly did not appear to contain PrP^{res}, despite 20-fold concentration. One sample displayed slight non-specific staining in the region of the diglycosylated band when concentrated and was most likely due to cross reactivity to PK. Some of the samples required 20-fold concentration to detect PrP^{res} and observe all three bands. The samples were all of the type B glycoform (predominantly diglycosylated) with very low amounts and in some cases undetectable levels of nonglycosylated PrP^{res}. The typing classification relies on an observable level of nonglycosylated PrP^{res}, for this reason many of the samples were treated with PNGaseF to remove the glycan chains and produce a distinct nonglycosylated band.

The majority of PrP^{res} positive cases had an intermediate mobility (12 cases), in stark contrast to human samples, which are predominantly type 1 or 2. Five cases were classified as type 2B, the same classification applied to vCJD cases (table 13). One case was type 1 mobility (case 15), yet appeared to have a subtly different glycoform ratio to fCJD cases, more commonly classified as type 1B, and resembled vCJD glycoform more closely. One case displayed a broad nonglycosylated band making classification difficult and suggesting a preponderance of ragged NH_3-terminal ends (case 21). Of note in all the cases was the lower position/ greater mobility of the monoglycosylated band (figure 46) and in a few also the

diglycosylated band, irrespective of the position of the nonglycosylated band. This feature is quite unusual and distinctive for the mouse samples.

Case	Inoculation / Mouse strain	Typing
1	**C / VM**	**Nil**
2	**V1 / RIII**	**2B**
3	**C / C57BL**	**Nil**
4	**V2 / RIII**	**2B**
5	**V3 / RIII**	**INTB**
6	**V2 / C57BL**	**INTB**
7	**V2 / RIII**	**INTB**
8	**V3 / RIII**	**INTB**
9	**C / RIII**	**Nil**
10	**V2 / C57BL**	**2B**
11	**V3 / VM**	**INTB**
12	**C / RIII**	**Nil**
13	**V3 / VM**	**2B**
14	**V3 / C57BL**	**2B**
15	**V1 / C57BL**	**1B**
16	**V2 / VM**	**INTB**
17	**C / VM**	**Nil**
18	**V1 / VM**	**INTB**
19	**V1 / RIII**	**INTB**
20	**V3 / C57BL**	**INTB**
21	**V1 / C57BL**	**INT/2B**
22	**V2 / VM**	**2B**
23	**V1 / VM**	**INTB**
24	**C / C57BL**	**Nil**

Table 13. Murine transmissions.

Original inoculating case (C = control, V = vCJD),

murine strain, resultant mouse isotype.

The M_r of case 21 could not be clearly defined and is discussed in the text.

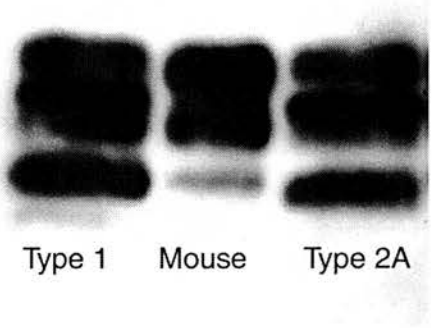

Figure 46. Mouse sample example displaying type 1 vCJD transmission and lower monoglycosylated band. Lane 1, sCJD MM standard type 1, Murine vCJD transmission type 1B, sCJD VV standard type 2A.

After unmasking of the results it was indicated that only vCJD samples had been inoculated, along with controls to three strains of mice (VM, RIII, C57 black). None of the controls yielded PrP^{res} and all the samples from mice inoculated with vCJD did. The isotype of the samples was variable and did in fact represent a large proportion of samples with an intermediate mobility. All of the samples fell within the type B glycoform ratio nomenclature. The glycoform ratios were not within the linear range of X-ray film for many of the samples and chemiluminescence scans along with standards were analysed with the STORM 860 phosphoimager. Generally less than 10% of the PrP^{res} is composed of nonglycosylated PrP^{res} and over 50% is diglycosylated (figure 47). Unexpectedly the vCJD patient or strain of mouse alone did not influence the isotype and no correlation could be found between isoform and inoculating PrP^{res} or host PrP^{c}. Similarly there was no correlation between the presence of a monoglycosylated band with greater M_r and the strain of mouse as reported previously (Somerville, 1999).

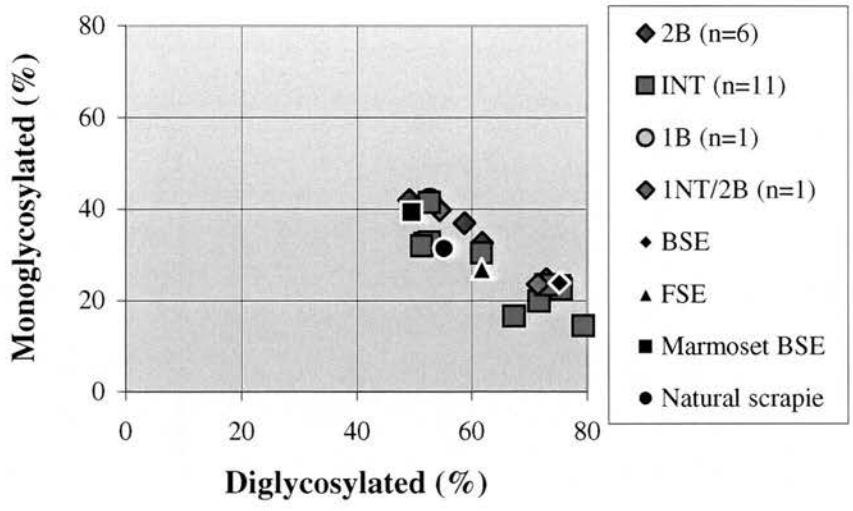

Figure 47. Scattergraph of mean glycoform ratios of PrP^{res} from murine transmissions, natural and experimental animal TSEs. The range of standard deviations among the murine PrP^{res} samples; diglycosylated 0.7-21.5, monoglycosylated 0.3-18.8.

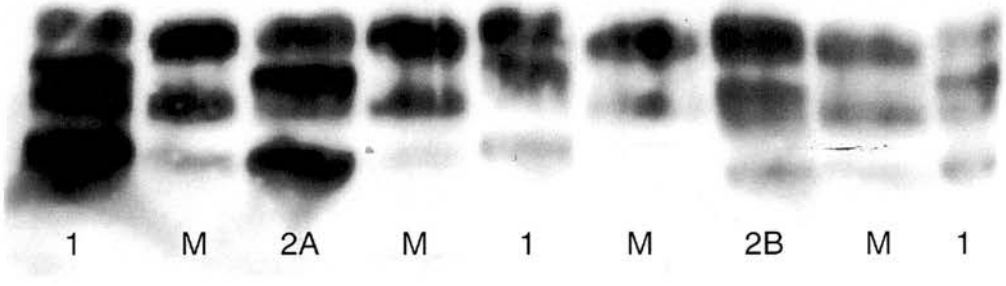

Figure 48. Mouse samples with low monoglycosylated band. Lane 1, sCJD MM type 1, lane 2, murine sample, lane 3, sCJD VV 2A, lane 4, murine sample, lane 5, fCJD type 1B, lane 6, murine sample, lane 7, vCJD type 2B, lane 8, murine sample, lane 9, sCJD MM type 1.

Both C57BL and RIII mice display shorter incubation periods and are designated as *Sinc*^{s7} or *Prn-p*^{a} genotype that translates to leucine at mouse codon 108 (109 human methionine) and threonine at codon 189 (190 human threonine). VM displays a longer incubation period and is designated *Sinc*^{p7} or *Prn-p*^{b} genotype that translates to phenylalanine and valine at the respective codons 108 and 189 (Carlson *et al*, 1986, Westaway *et al*, 1987, Bruce *et al*, 1997). The strains of mouse utilised in this study carry methionine at the equivalent of human codon 129. The resultant

PrP^{res} detected in these mice will reflect the *Prn-p* sequence of the host and yet there was no correlation between the mouse strain and isotype or glycoform ratio. Codon 108 resides at the position of the 3F4 epitope and thus a different antibody that detects mouse PrP was employed (6H4). Glycoform ratio differences between 6H4 and 3F4 were not observed in human samples. The valine at 189 in VM mice is situated between the two glycosylation sites yet no correlation with an influence on the glycoform ratio could be identified. Glycoform ratios from at least three separate runs were analysed. The range of values was roughly 50-80% diglycosylated, 20-40% monoglycosylated and 2-16% nonglycosylated, however, due to the large levels of diglycosylated PrP^{res} there was often less than 5% measurable nonglycosylated PrP^{res}. The large proportional differences between the bands complicated quantitation. The diglycosylated band frequently measured AUC levels above the linear range while the nonglycosylated band levels were below the linear range (examples can be seen in lanes 4 and 6 of figure 48). Comparison with X-ray densitometry results indicated that the greater linear range of the STORM analysis served to increase the relative proportion of diglycosylated and decrease that of the monoglycosylated and nonglycosylated bands. X-ray densitometry may therefore be exerting an artificial upper limit on the proportion of diglycosylated that can be measured within the linear range.

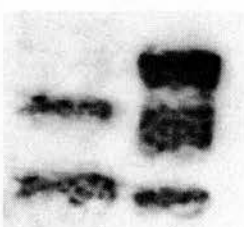

fCJD vCJD

Figure 49. Banding pattern of fCJD V180I coupled to M. Lane 1, fCJD, lane 2, vCJD type 2B frontal cortex.

To help elucidate the mechanism responsible for the phenomenon of different monoglycosylated PrP^{res} mobility in human cerebellar and murine tissue, a case of fCJD that carries a mutation at codon 180 preventing addition of glycan chains to the 181 site was investigated (Nixon *et al*, 2000). The mutated allele is in conjunction with a methionine at codon 129. This case was reported to lack the diglycosylated band after PK treatment, indicating sole conversion of the mutated allele to PrP^{res}, but not the wt allele. The conversion of codon 180 from valine to isoleucing replaces one

hydrophobic (non-polar) amino acid with another and does not directly alter the consensus sequence for N-linked glycosylation, indicating a conformational change that prevents addition of the glycan chain to the second alpha helix. There were low levels of PrP^{res} detected, however 20 fold concentration was able to resolve two bands, representing monoglycosylated PrP^{res} occupied at codon 197 and an nonglycosylated band. This case lacked the diglycosylated band as would be expected if disruption of the N-linked glycosylation occurred and had a nonglycosylated band of type 1 mobility. The upper band was well resolved and in line with the upper portion of the monoglycosylated band present in vCJD frontal cortex (figure 49). This suggests that the 181 site is more occupied in the cerebellar and murine samples. However, the type 1 mobility and low PrP^{res} levels may account for the lack of a lower monoglycosylated band..

7.2 Animal TSEs

Samples from four cases of animal TSE were investigated. One naturally acquired, one acquired presumably through infected Meat and Bone Meal (MBM), one acquired presumably through infected pet food and finally one experimentally infected. Brain tissue from a sheep with naturally acquired scrapie, a terminal BSE infected Fresian cow, a UK case of feline spongiform encephalopathy (FSE) and cerebral tissue from a marmoset with experimentally transmitted BSE were available.

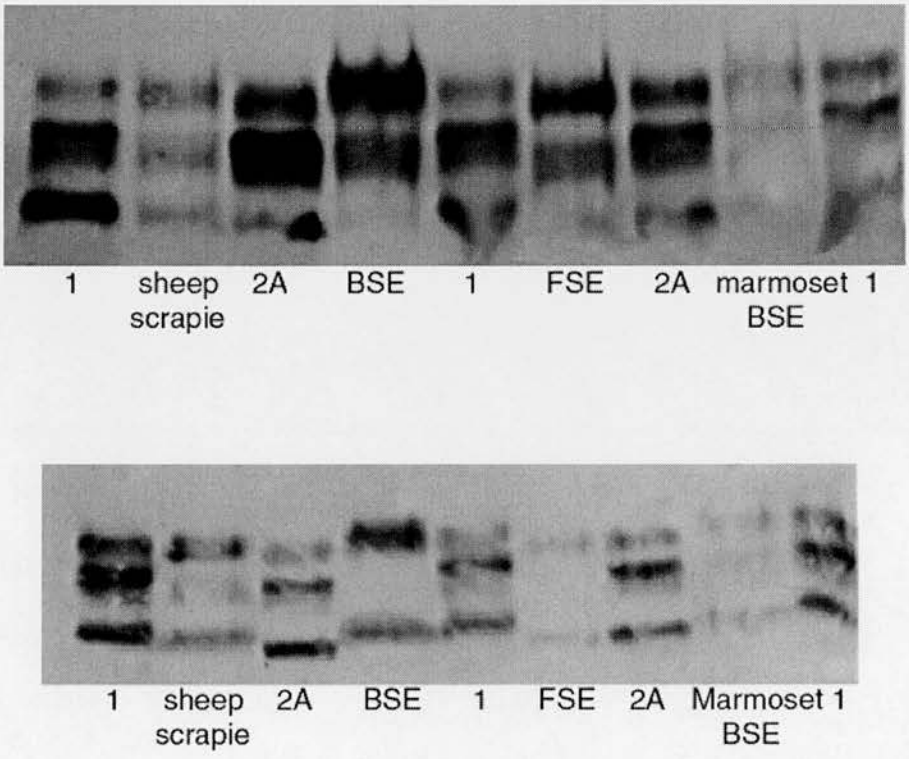

Figure 50. Animal samples. **A:** PK treated samples. Lane 1, sCJD MM type 1 standard, lane 2, sheep scrapie, lane 3, sCJD VV type 2A standard, lane 4, BSE, lane 5, sCJD MM type 1 standard, lane 6, FSE, lane 7, sCJD VV type 2A standard, lane 8, BSE infected marmoset, lane 9, sCJD MM type 1 standard. **B:** PK and PNGaseF treated samples. Lane 1, sCJD MM type 1 standard, lane 2, sheep scrapie, lane 3, sCJD VV type 2A standard, lane 4, BSE, lane 5, sCJD MM type 1 standard, lane 6, FSE, lane 7, sCJD VV type 2A standard, lane 8, BSE infected marmoset, lane 9, sCJD MM type 1 standard.

Host sample (infection)	Isotype	Di (%)	Mono (%)	Non (%)
Sheep brain (natural scrapie)	**1B**	55.2	31.3	13.4
Cow brain (BSE)	**1B**	75.2	23.9	1
Cat brain (BSE)	**2B**	61.8	27	10.6
Marmoset (experimental BSE)	**2B**	49.6	39.4	11.1

Table 14. Results of animal isotyping.

The typing of the animal samples, as with some of the fCJD regional samples and the murine vCJD transmissions displayed a high proportion of diglycosylated PrP^{res} (figure 50A). Even after PNGaseF treatment some diglycosylated PrP^{res} remained (figure 50B). Repeated attempts to deglycosylate all the PrP^{res}, were unsuccessful but were most likely achievable on longer incubations with PNGaseF. Despite the retention of some diglycosylated PrP^{res}, the deglycosylated band mobility was accurately typed repeatedly and showed the same mobility. All the glycan chains are removed intact by PNGaseF ruling out the potential for partial removal of glycan chains accounting for the mobility of the samples. Previous studies have shown scrapie isolates and mouse passaged scrapie strains to have a highly diglycosylated PrP^{res}. The mobility of scrapie cases has been reported in relation to molecular weight with numerous different results (Hill *et al*, 1998, Kuczius and Groschup, 1999, Madec *et al*, 2000a, Moudjou *et al*, 2001). In terms of the mobility relative to human isotyping nomenclature there is very little data available on animal isolates and inferences sometimes have to be made from published Western blots. The scrapie samples typically shown appear to have type 1 mobility, as found here. The glycoform ratio was type B (diglycosylated 55.2% ± 4.5: monoglycosylated 31.3 % ± 1.4: nonglycosylated 13.4% ± 3.4) as seen in all scrapie cases, natural and transmitted and had a glycoform ratio similar to that of vCJD. However, the glycoform ratio was significantly different ($p<0.001$ for di, mono and nonglycosylated bands, one sample two tailed *t* test) from the vCJD cases.

The type 1B finding in relation to the BSE sample was unexpected and goes against numerous other studies that have repeatedly shown a type 2B pattern as seen in vCJD, natural BSE infections and transmission studies. The glycoform ratio was observed to be quite pronounced (diglycosylated 75.2% ± 4: monoglycosylated 23.9%

± 3.8: nonglycosylated 1% ± 0.3) making quantitation of nonglycosylated PrP^{res} and classification of isotype difficult. The glycoform ratio is significantly different from that seen in vCJD ($p<0.001$ for di, mono and nonglycosylated bands, one sample *t* test). Cattle carry a methionine at codon 129 as do all the vCJD cases diagnosed so far ruling out the likelihood of a polymorphic effect. However, being an isolated case, further conjecture on the implications of a type 1B isotype is unsubstantiated and is most likely an anomaly and does not dispute the retention of molecular typing in BSE and vCJD.

The case of FSE had a 2B isotype (diglycosylated 61.8% ± 4.7: monoglycosylated 26.9% ± 4.3: nonglycosylated 10.6% ± 2) comparison with the vCJD cases found a significantly different glycoform ratio ($p<0.001$ for di, mono and nonglycosylated bands, one sample *t* test). The marmoset sample was hard to resolve in terms of mobility, which may be due to low PrP^{res} levels, but was classified as type 2B. The glycoform ratio was similar to that in vCJD (diglycosylated 49.6% ± 0.6: monoglycosylated 39.4% ± 0.1: nonglycosylated 11.1% ± 0.5). However, the glycoform ratio differed significantly from that of the vCJD cases ($p=0.0027$ diglycosylated, $p<0.001$ monoglycosylated and nonglycosylated bands, one sample *t* test). The differences in glycoform ratio between the animal samples and vCJD cases was most likely due to the analysis of single cases and a larger number of cases is required to confirm these findings. The glycoform ratio values of the marmoset experimentally infected with BSE appeared similar to vCJD and was found in the same area of the scattergraph plot as vCJD cases (figure 47). Analysing human and animal samples together aimed to standardise the classifications. There were certain differences that distinguished the animal samples from human PrP^{res} samples; A: increased M_r of monoglycosylated PrP^{res} in murine samples, B: consistently high levels of diglycosylated PrP^{res}. Despite this the samples could still be incorporated to some degree into the human classification system.

Summary

- Transmission of vCJD to mice does not result in retention of the 2B isotype in all cases. An intermediate mobility was seen in the majority of cases.
- Neither the mouse strain, *prn-p* genotype or individual vCJD source correlated with the resulting PrP^{res} pattern.
- The glycoform ratios of the murine PrP^{res} featured a greater proportion of diglycosylated PrP^{res} than vCJD cases.
- Murine PrP^{res} has a prominent lower region in the monoglycosylated band.
- Sole conversion and accumulation of the mutant allele was observed in fCJD V180I, indicating that the mutant allele does not convert the wild type allele to PrP^{res}. This may be due to the lack of diglycosylation or indicate that the presence of PrP^{res} is not sufficient to bring about conversion of wild type PrP^{c}.
- Scrapie and BSE derived infections all resulted in predominantly diglycosylated PrP^{res}. FSE and experimental BSE displayed type 2 PrP^{res} while scrapie and BSE displayed type 1.
- The glycoform ratios of all the animal derived PrP^{res} were significantly different from vCJD.

The PrP^{res} isotype is not consistently retained upon transmission. The maintenance of the isotype upon repeated transmission within an inbred line of mice does not apply to transmission from vCJD cases to mice. The PrP^{res} pattern is therefore not a strain marker and would not distinguish cases arising due to the BSE strain. Classification of animal TSEs can be accomodated in the human typing scheme, suggesting similar PrP^{res} conformations.

Discussion

CHAPTER 8

8.1 Isotyping

8.1.1 Sporadic CJD

The initial investigation focused on single cortical samples and confirmed the presence of two predominant PrP^{res} mobilities. The majority of sCJD cases were type 1 (21 kDa), the rest were type 2 (19 kDa) with the exception of 3 cases with a relative mobility intermediate between these two types. Comparison of molecular weights and relative mobilities of the samples investigated with samples analysed by Collinge *et al*, could not provide a consensus as to the mobilities.

The number of mobility types and their prevalence in the sCJD codon 129 subgroups differs greatly between Collinge *et al*, and the findings of Parchi *et al*, and this study. Collinge *et al*, found 22% of MM cases to be type 1, and 78% to be type 2 and none of type 3, Parchi *et al*, found 93% type 1 and 7% type 2, but in this study 84% of MM cases were type 1 and 16% type 2. In the Collinge study all MV and VV cases were type 2, but Parchi *et al*, found that in MV cases 42% were type 1 and 58% type 2, similar to this study 44% type 1 and 56% type 2. The VV cases analysed by Parchi *et al*, were 17% type 1 and 83% type 2 and in this study the prevalence identical in this subgroup was identical. It was thus decided to adopt the classification system of Parchi *et al*. Type 1 or type 2 PrP^{res} was detected in the majority of sCJD cases and showed that these two PrP isotypes occur in combination with each of the three possible *PRNP* codon 129 genotypes as previously shown (Parchi *et al*, 1999c). The frequencies of isotype / genotype combinations observed in sCJD, do not appear random (Parchi *et al*, 1999c). In contrast to fCJD/FFI D178N, sCJD shows the opposite effect of the polymorphisms. The type 1 mobility is most commonly associated with methionine homozygosity while type 2 is most closely associated with valine homozygosity. The effect of the codon 129 polymorphism is reflected in the conversion of type 1 to type 2 when passaged into transgenic mice $HuPrP^{+/+}$ $Prn\text{-}p^{0/0}$ with a valine at codon 129 of the human PrP gene (Collinge *et al*, 1996, Telling *et al*, 1996b). Homozygote methionine patients made up the majority of sCJD cases, however, when subdivided on the basis of the PrP^{res} type two rather distinct subgroups

are observed. The two subgroups are significantly different when classified according to the PrP^{res} mobility. Likewise, the homozygous valine patients are significantly different in terms of age at onset and disease duration. This suggests that the conformation of the PrP^{res} determines these clinical parameters, or that both PrP^{res} mobility and clinical features are determined by another factor. The age at onset and disease duration of the MM 2A cases would suggest that these patients represent the MM 2 thalamic variant subdivision described by Parchi *et al.* However, examination of autopsy reports from these patients found significant cortical pathology, featuring spongiform encephalopathy, perivacuolar PrP^{sc} deposits in some cases and the cerebellum showed little spongiform change but had focal PrP deposits around areas of spongiform change. The majority of these cases would therefore be described as the cortical subtype, though thalamic involvement was present in some and one featured a prominent thalamic pathology. Further correlation of the clinical phenotype and results of EEG, MRI and cerebrospinal fluid (CSF) findings with Western blotting results would help to define the differences between sCJD subgroups. The extended duration seen in heterozygote sCJD patients would be expected if homodimerisation kinetics between the M and V allele determine the length of clinical symptoms prior to death. However, the MM 2A and VV 1 patients likewise have long durations (possibly due to the young age in the latter). The limited number of heterozygote cases and the possibility of ascertainment bias in favour of long duration cases may also explain the similarity of heterozygote disease duration to vCJD. Classification of sCJD cases by PrP^{res} isotype enables investigation of other factors such as non *PRNP* ORF genotype (Mead *et al*, 2000, Stephenson *et al*, 2000, Jackson *et al*, 2001, Lloyd *et al*, 2001, Mead *et al*, 2001, McCormack *et al*, 2002) in determining susceptibility, phenotype (Hauw *et al*, 2000) or pathological mechanisms. It also enables better identification of the defining features of vCJD in contrast to atypical cases of vCJD.

The correlation between isotype and codon 129 genotype was initially claimed to restrict sCJD to the higher molecular weight isotypes (termed type 1 and 2) with only MM patients forming type 1 PrP^{res} and the lower molecular weight isotype (termed type 3) to iCJD patients (Collinge *et al*, 1996). Further studies by Collinge *et al*, have found sCJD patients displaying all three molecular weight banding patterns, though MM patients have not been identified with the type 3 pattern (Hill, 1998, Wadsworth *et al*, 1999a, Wadsworth *et al*, 1999b, Jackson and Collinge, 2001). The

findings here showed no codon 129 restriction. This may be due to the analysis of a larger cohort and referral of more atypical cases.

Two sCJD cases showed clear intermediate mobility when sampled at different times, other cases (iCJD, GSS, murine transmissions of vCJD) with intermediate mobility were more prevalent in their respective aetiological subgroups. Due to their low frequency in relation to the other two sCJD mobility types, their common MM codon 129 polymorphism and a lack of outstanding phenotypic features, it was concluded that alternative conformations of PrP^{res} can occur without being the cause or effect of pathological or genotypic features of the individual. The presence of bound cations establishes that this difference in conformation is not due to metal ion bound and unbound forms of MM type 1 PrP^{res}. The classification system employed by Collinge *et al*, also described other sCJD banding patterns termed types 6 and 7. They reported one case of sCJD classified as type 6 and one as type 7 (Hill, 1998). Type 6 was observed in a sCJD MV case with a predominantly nonglycosylated PrP^{res} band and mobility of the type 3 group, type 7 was observed in an MM case with higher molecular mass than the type 1 group. In a few cases of sCJD classified as MV 2A and 4 out of 8 MV 2A iCJD cases there was a prominent nonglycosyated PrP^{res} band. The appearance of this pattern is most obvious at shorter X-ray exposures, however, glycoform ratio analysis of linear range PrP^{res} did not identify a greater proportion of the nonglycosylated band in the sCJD cases and it was concluded that this banding pattern is not a true reflection of the PrP^{res} present in sCJD. This emphasises the subjective nature of glycoform ratio typing when applied without careful quantitation. It is therefore important to develop a quantitative and non-subjective classification system. High levels of nonglycosylated PrP^{res} may result from ragged NH_3-terminal cleavage as they often display a broad undefined band, even after PNGaseF treatment, which can hamper mobility classification. This may be due to partial copper bound forms of PrP. The possibility of both type 1 and type 2 nonglycosylated PrP^{res} in samples could also be a factor in high levels of nonglycosylated PrP^{res}. Thus their subgroup classification and any subsequent subgroup comparisons would be fundamentally flawed. Only one sample with a molecular weight similar to type 7 was observed, in the posterior thalamus of the fCJD E200K MM case and suggests this result may represent a rare alternative conformation or possibly an experimental artifact. A higher molecular weight in a fCJD E200K case has been reported previously (Gambetti *et al*, 1995) and also in a sCJD MM case (Aucouturier *et al*, 1999). The conformation of the DY and HY

strains differs in relation to the β-sheet content (Caughey *et al*, 1998) and eight different strains have been differentiated by their conformation (Safar *et al*, 1998). It is more likely that a range of different conformations occur, leading to a wide range of cleavage points in PrP^{res} from codon 74 to 103 (Parchi *et al*, 2000b). These cleavage points are variable even within codon 129/isotype subgroups, however they do confirm the PrP^{res} banding pattern observed and classification system used in this study identify two major PrP^{res} species that correlate with the sites of NH_3-terminal cleavage. It has also been shown that pH influences the mobility of PrP^{res} (Zanusso *et al*, 2001) with low pH conditions generating type 1^+. This may be related to the association of copper with the octapeptide repeat region (Miura *et al*, 1999), but would contradict the suggestion that removal of bound metal ions produces a more susceptible conformation. The 1^+ mobility maybe due to pH induced changes in the β-sheet structure of the carboxyl-terminal as addition of metal ions did not increase the MW of the type 1 samples (Wadsworth *et al*, 1999a). It has also been suggested that nucleic acids or collagen fibres present in brain homogenates affect the molecular weight of PrP^{res} bands (Cardone *et al*, 1999). Thus a range of different variables affect the banding patterns seen and need to be standardised to enable meaningful comparisons of molecular weights and 'strains'.

8.1.2 Variant CJD

Sporadic CJD is the major differential diagnosis for vCJD. This is especially important as sCJD occurs in each polymorphic population (MM, MV, VV), but so far vCJD has only been detected in MM individuals. It may be that only individuals with the MM genotype are susceptible to vCJD or that these individuals are more susceptible and infected individuals in the other genotypes are still in the preclinical phase of the disease. The evidence from iCJD and kuru epidemics suggest that all genotypes are affected, but with differing susceptibility (heterozygotes presenting less frequently and later) and incubation periods (Brown *et al*, 1994a, Huillard *et al*, 1999, Lee *et al*, 2001). As with the occurrence in MM individuals, the 2B isotype has remained constant and is a distinctive marker of the disease aetiology. The young age at onset, prolonged disease duration, psychiatric signs and distinctive neuropathology in differential diagnostic of vCJD has been extensively reported and these features were not examined due to the lack of variability in PrP^{res}. The consistent molecular phenotype of the vCJD cases is in accordance with the hypothesis that it signifies the

BSE 'strain' (Collinge *et al*, 1996, Bruce *et al*, 1997, Hill *et al*, 1997a) and showed no difference in terms of age at onset. Mouse transgenic studies have indicated the effect of human codon 129 variants (*Prnp* null background) for the neuropathological feature, isotype and incubation times after species barrier transmission of bovine MM 2B PrP^{sc} or vCJD MM 2B (Collinge *et al*, 1996, Bruce *et al*, 1997). The 2B isotype was not consistently retained upon transmission to mice encoding methionine at the equivalent codon to human 129. The 2B (type 4) isotype is retained upon transmission to mice carrying human PrP with the methionine polymorphism (Hill, personal communication). The conversion of the isotype on transmission to mice expressing human *PRNP* encoding valine at codon 129 suggests that transmission of BSE to humans with an MV or VV codon 129 genotype may accumulate PrP^{res} with a different relative mobility to MM vCJD cases.

8.1.3 Iatrogenic CJD

A relatively large number of iCJD cases were available, 2 were DM cases while the other 16 were GH. Both the DM cases were MM type 1, while the GH cases were VV, MV or unknown. This in accordance with earlier findings (Brown *et al*, 1994a). Iatrogenic CJD cases provided the opportunity to look for differences in isotyping, in relation to the route of entry. As previously described DM cases were restricted to the type 1 mobility, however, the GHT cases could be either type 1 or 2. Previously only small iCJD cohorts have been investigated and reported with Western blotting, n = 4 (Deslys *et al*, 1994), 5 (Collinge *et al*, 1996), 1 (Antoine *et al*, 1997), 6 (Parchi *et al*, 1997), 1 (Cardone *et al*, 1999) and 5 (Parchi *et al*, 2000b). The first study utilised a scrapie-associated fibrils protocol and did not distinguish between isotypes or the codon 129 polymorphisms (Deslys *et al*, 1994). The other studies identified both type 1 and 2 mobilities (Parchi *et al*, 2000b) and involvement of all three codon 129 genotypes (Windl *et al*, 1996). The correlation of these isotypes to the genotypes seems to correlate to sCJD, with type 1 occurring predominantly in methionine homozygotes and type 2 occurring in MV and VV patients, though overall susceptibility is greater in VV individuals in contrast to sCJD. The analysis of 18 cases allowed a greater sample size and the identification of the rare type 1 VV (1 case) and previously unreported type 1 MV (2 cases) individuals. The differences in classification systems employed make it harder to compare the results, but taking type 1 and 2 of Collinge *et al*, as the type 1 identified in this study and type 3 as the type 2,

it appears that there is little restriction on PrP^{res} isotype formation by either codon 129 or route of entry. There were no type 2 MM cases which may reflect the relative rarity of this mobility in sCJD MM individuals. The lack of donor and recipient strain typing correlations are due to the often undefined source of infection such as pooled pituitary hormone and possibly scrapie infected DM which makes the identification of codon 129 and retained passage variables such as lesion profile and isotype impossible. In one study in which cranial surgery transmitted sCJD from an MM individual to an MV individual, the clinical symptoms and neuropathology were congruent, and interestingly PrP deposits were found in spinal cord and peripheral nerve of the host. The source of the agent may be a greater influencing factor as batches of DM were found to result in cases of iCJD with the MM genotype while different sources have affected VV individuals (Brown *et al*, 1994a). Most cases of iCJD are presumed to have arisen from sCJD cases and it has been seen that sCJD retains molecular phenotype on transmission (Telling *et al*, 1996b). The identification and molecular strain typing of both the donor and resulting iCJD infections should be followed up wherever possible as it provides the only source of information concerning human to human transmission of CJD, which is desperately needed to assist in the identification of iatrogenic transmission of vCJD. The younger age at onset and shorter disease duration in the heterozygote GHT cases supports the contention that interaction of PrP^{sc} and PrP^{c} molecules and subsequent conversion is aided by identical primary sequence. The additional finding that an iCJD case can accumulate two types (conformations) of PrP^{res} can be interpreted in one of three ways; a) a pooled batch of growth hormone was infected by two different sCJD patients, b) one sCJD patient with two PrP^{res} isotypes infected a single batch or c) the different conformations arose in *vivo*. The substantial numbers of donors pooled in growth hormone batches does not rule out the possibility of two sCJD infections, despite the relative rarity of sCJD. If dilution of PrP^{res} from one source leads to individuals receiving different infectious PrP^{res} conformations or two PrP^{res} conformations form *in situ* from one infecting strain, then the assumptions about retention of conformation from donor to host on transmission must be reassessed.

8.1.4 Familial TSEs

The majority of isotyping and glycoform ratio findings in familial TSEs were reported during the course of this study, predominantly with respect to the D178N mutation. Familial forms of prion disease, like the idiopathic form, can display both the type 1 and type 2 mobility with differing glycoform ratios (Cardone *et al*, 1999). Only one case with the D178N mutation, diagnosed as FFI, was analysed and displayed low levels of PrP^{res} in the frontal cortex and basal ganglia. This reflects the findings of previous studies (Brown *et al*, 1995, Parchi *et al*, 1995b, Rossi *et al*, 1998). It was by no means an in depth study of regional distribution, as numerous investigations of this type have been carried out on FFI patients with MM or MV codon 129 polymorphisms and differing disease durations (Parchi *et al*, 1998c, Parchi *et al*, 2000a). Unfortunately no cases of fCJD D178N were available for comparative analysis, though once again many such studies have been performed and the findings would likely contribute little to the well characterised differences in isotype (Monari *et al*, 1994, Gambetti *et al*, 1995, Parchi *et al*, 1998c, Parchi *et al*, 1999b). However, comparison of FFI, fCJD D178N and fCJD E200K have found PrP^{res} of three mobilities and a degree of different prominent diglycosylation, all of which could be classed as the B type (Gambetti *et al*, 1995). Transmission studies of FFI MM and MV or fCJD 178 VV, to TgMHu2M mice displayed retention of isotype and neuropathological features (Telling *et al*, 1996b). If the codon 129 and isotype determine clinical features in preference to the mutation, it may imply that the mutation is a predisposing factor and that strains dominate, making a virus hypothesis more likely.

Cases of fCJD with the E200K mutation co-segregated with methionine are the most common familial prion disease and invariably display type 1 mobility with prominent diglycosylation (Gambetti *et al*, 1995, Cardone *et al*, 1999). Investigation of the three cases here found the same type 1B pattern in both MM and MV individuals. The clinical features are similar to sCJD, primarily featuring dementia and commonly ataxic gait deficiencies (Simon *et al*, 2000). The codon 129 polymorphism of the unmutated allele is usually the same as the mutated allele due to the preponderance of the methionine codon 129 polymorphism. However, the relatively small numbers of cases do not make distinguishing between clinical signs and neuropathology in all the homozygous and heterozygous subgroups easy. Cases of the E200K mutation coupled with valine at codon 129 and type 2 mobility are a

rare subgroup (Hainfellner *et al*, 1999, Puoti *et al*, 2000). These patients also have prominent diglycosylation of PrP^{res}. One patient studied had a long disease duration, but rapidly progressive dementia (Hainfellner *et al*, 1999) which along with *PRNP* sequencing can distinguish these cases from vCJD, that Western blotting alone would not. These patients have phenotypic features in common with sCJD VV 2A cases including ataxia, dementia, plaque-like prion deposits in the cerebellum and the Western blotting pattern (Kovacs *et al*, 2000) suggesting a strong codon 129-isotype correlation with disease phenotype. Studies on cultured fibroblasts isolated from fCJD patients and mice expressing transgenes with the corresponding mutations suggest that, unlike sCJD, mutations at codons 178 or 200 cause aberrant glycosylation due to their proximity to the glycosylation consensus sequences and inhibit transport of the unglycosylated form to the cell surface (Capellari *et al*, 2000) resulting in the prominent diglycosylation of the PrP^{res}. Though other reports have found a lack of glycosylated PrP^{res} in human patients (Gabizon *et al*, 1994) and mutant murine PrP expressing CHO cells (Wong *et al*, 2000b).

The GSS cases investigated displayed different mobilities, dependent upon the codon 129 polymorphism, though the heterozygote case was from a different family and may, be a result of other factors. Typical diglycosylated, monoglycosylated and nonglycosylated bands, and smaller PrP^{res} fragments are detected in GSS (Kitamoto *et al*, 1991, Tagliavini *et al*, 1991, Young *et al*, 1997, Parchi *et al*, 1998a, Piccardo *et al*, 1998, Tagliavini *et al*, 2000). As well as the typical PrP^{res} banding pattern, cases of GSS accumulate 7, 8, and 11 kDa fragments (Tagliavini *et al*, 1991, Parchi *et al*, 1998a). GSS P102L cases display the 1B isotype as well as the low molecular weight bands, however, cases with the F198S or D202N mutation display the 2B isotype. PrP with a P102L mutation expressed in *E.coli* shows decreased α-helical content but not increased protease resistance, suggesting the mutation affects the conformation and hence cleavage site of the PrP^{res} (Cappai *et al*, 1999). In this study the focus was on the three 'typical' bands, as resolved by 12% acrylamide gels in the classical P102L variant of GSS and a 2B isotype was not detected. Most commonly P102L co-segregates with methionine (Young *et al*, 1997) and cases are almost completely restricted to the methionine homozygous population. Heterozygote cases have a more even distribution of PrP plaques (Brown *et al*, 1995) though this is unlikely to account for the difference in isotype identified in this study. The valine allele can co-segregate with the mutation and has been detected as 11 kDa PrP^{res} fragments (Tagliavini *et al*, 1991). The diversity of PrP^{res} fragments seen in GSS cases and

some sCJD cases (Chen *et al*, 1995, Cardone *et al*, 1999) highlights the limitations of strain typing based upon the three typical PrP^{res} bands and comparison with neuropathological features such as PrP plaque formation.

Familial CJD patients with insertional mutations of four or five octapeptide repeats have been studied and display type 1 mobility with MM codon 129 (Parchi *et al*, 2000b). Insertional and even benign deletions of octarepeats do not directly affect the PrP^{res} isotype mobility as they are present in the region of PrP that is cleaved by PK (Lehmann and Harris, 1996). They also do not appear to affect the cleavage point via additional metal ion binding or alteration of the overall conformation of the mtPrP as they co-migrate with sCJD MM 1 cases. Further studies into the effect of metal ion chelators on the banding pattern may help elucidate the role of the additional octapeptide repeats and their metal ion association in the development of the pathology. Transgenic mice featuring deletions of the NH_3-terminal up to codon 93 are phenotypically normal, susceptible to scrapie infection and produce protease-resistant truncated PrP (Shmerling *et al*, 1998). This suggests that this region of PrP^c and metal ion binding are not essential for propagation of prions and that other mechanisms can compensate to retain viability.

The codon 129 polymorphism, as already stated, correlates closely with mobility, glycoform ratio, clinical symptoms and neuropathology of familial TSEs. Similarities in phenotypic presentation between familial and sporadic CJD are all the more important when codon 129 and isotype are the same, implying that these factors have a greater influence than point mutations on the phenotype. The sCJD VV1 subgroup is rather similar to fCJD D178N VV type 1 cases with young age at onset, long disease duration, a lack of PSWCs and cortical pathology featuring ballooned neurons.

8.2 Glycoform ratio findings

8.2.1 Sporadic and variant CJD

Currently the improved classification of CJD phenotypes, in terms of clinical, neuropathological and molecular features is the focus of a considerable amount of research. The use of glycotypes to define molecular 'strains' of TSEs in humans has been most succesfully applied to the differentiation of sCJD and vCJD, to support the contention that vCJD is a result of BSE infection. The suggestion that similar

'strains' can likewise be identified amongst the numerous sCJD phenotypic variants is dependent on greater resolution of the glycoform ratio differences, in addition to the M_r of the PrP^{res}. Comparison of quantitative levels of PrP^{res} glycoforms are hampered by the extensive number of experimental variables and limit the assumptions that can be made about the *in vivo* levels.

Cell specific differences in PrP^c glycosylation have been proposed to account for neuropathological targeting (DeArmond *et al*, 1997b), thus the location and degree of tissue sampling may from the outset influence the levels of PrP^{res} glycoforms detected. The accumulation of one or other PrP^{res} glycoform at less than 10% of the total PrP^{res} level may not be detectable. Despite this low levels of PrP^{CTM} (<10% of total PrP) have been proposed to be capable of causing disease (Hegde *et al*, 1998). The homogenisation procedure may result in different solubilisation of PrP aggregates and the resulting analysis of different pellet or supernatant fractions. Storage conditions may lead to differential sample degradation and some subsequent loss of detectable PrP^{res}. The use of different Western blotting methods can influence the glycoform ratios at a number of steps. Thickness of polyacrylamide gels and subsequent transfer to membranes can influence the relative levels with the lower molecular weights bands transferring more readily to membranes. Use of different antibodies, with preferences for different glycoforms (Zanusso *et al*, 1998a) or detection of different epitopes such as 6H4 and 3F4 influence the different forms of PrP^{res} detected.

These factors should be taken into account when comparing results from different groups and drawing conclusions on the *in vivo* PrP^{res} levels. By analysis of a large cohort of cases utilising the same technique the quantitative analysis could be standardised and variables minimised.

Glycoform analysis of PrP^{res} has use in distinguishing certain forms of human TSE such as vCJD, FFI and fCJD. It can even identify the codon 129 genotype to some extent in sCJD cases (i.e. VV 2A cases) and the codon 129 genotype could often be accurately predicted from the appearance of the PrP^{res} banding. The glycoform ratio findings in the sCJD VV 2A subgroup are similar to those published by one large study (Parchi *et al*, 1999c) though they also reported a similar ratio in the sCJD MM 2A cortical subgroup that was not observed here. Confusingly, the glycoform ratio of the sCJD MM 2A thalamic subgroup (Parchi *et al*, 1999c) and the analogous sFI phenotype (Parchi *et al*, 1999a) featured a very different glycoform ratio to other publications on the sFI phenotype (Mastrianni *et al*, 1999). Another study of six

sCJD patients found a similar increased diglycosylated glycoform ratio in a VV type 1 patient and an MM type 1 patient, but a more typical sCJD glycoform ratio in the VV type 2 patient and a VV patient with an intermediate mobility (Aucouturier *et al*, 1999). The rest of the sCJD codon 129 subgroups were indistinguishable by glycoform analysis alone and the inclusion of this variable in sCJD 'strain typing' does not aid classification. Differentiation of sCJD based on isotype mobility represents the limit of the Western blotting technique. The small degree of glycoform ratio difference seen between cases was most obvious in terms of variable diglycosylated levels, due to higher levels of nonglycosylated PrP^{res} in some cases. This may be due to NH_3-terminal cleavage by PK producing nonglycosylated PrP^{res} with different cleavage sites (Parchi *et al*, 2000b). The greatest amount of glycoform ratio variability was found in the nonglycosylated band of type 2 cases by Parchi et al, (Parchi *et al*, 1996). Full sequencing of the *PRNP* gene is required to detect mutations or rare polymorphisms that can produce glycoform ratios resembling vCJD. In combination this data should, in almost all cases, differentiate between vCJD and other forms of human TSE.

Glycoform ratios are distinct in vCJD and can be easily differentiated from sCJD by eye, providing an important diagnostic marker that does not require quantitation. The highly glycosylated PrP^{res} found in vCJD appears to be a reliable molecular marker for this form of CJD, confirming the original observation made in 10 cases by Collinge *et al* (Collinge *et al*, 1996) and extending it to 50 cases of known genotype. The differentiation of sCJD VV 2A cases from other sCJD cases, due to a more prominent glycosylation, can be seen by eye with experience, though quantitation aides in the distinction. It remains to be seen whether the codon 129 polymorphism will differentiate the glycoform ratio in non-MM vCJD cases (if they occur). It is not possible to predict the isotype in VV vCJD cases. They may have an even more prominent hyperglycosylation based on the findings in sCJD VV cases, if the type 2 mobility is retained. The glycoform ratio may be similar as seen between fCJD E200K MM and VV cases. They may display a lower relative mobility and similar glycoform ratio as seen in transmissions to transgenic mice carrying a valine encoding 129 human transgene, or may display a relative lack of diglycosylation as seen in sCJD VV 1 cases if the relative mobility is different. Thus the current knowledge in this field does not allow for definitive prediction of glycoform ratios in hypothetical genotypic-aetiological situations and rests on the contentious issue of strain or host dominance in TSEs.

Surprisingly a predominantly nonglycosylated pattern was uncommon, as cell culture models have demonstrated that the nonglycosylated band is more prone to conversion to a protease resistant form and lack of glycosylation enhances PrP^{res} formation (Taraboulos *et al*, 1990a, Lehmann and Harris, 1997, Ma and Lindquist, 1999, Korth *et al*, 2000). In fact the blockade of cell mediated glycosylation increases the propensity for PrP^{sc} formation (Caughey, 1999) and the generation of recombinant glycosylated PrP^{sen} inhibits cross species formation of PrP^{res} (Priola and Lawson, 2001). However, it inhibits transport to the cell surface and subsequent internalisation both of which play important roles in PrP conversion (Caughey *et al*, 1989). Studies on the PrP^{c} charge heterogeneity in Syrian hamster brains suggest that glycosylated PrP^{c} is not required for formation of PrP^{res}. However, the common appearance of predominant diglycosylation reflects the relative levels of this glycoform expressed in uninfected brain tissue, thus accumulation of the other glycoforms may be indicative of a specific pathological mechanism (DeArmond, 1999).

8.2.2 Sporadic CJD carrying an uncommon polymorphic deletion

The influence of the codon 129 polymorphism and point mutations on PrP^{res} banding patterns are well documented, the influence of other polymorphisms has not been documented. The other human polymorphisms 171, 219 and deletion of one of the five octarepeats between codons 51 and 91 (Puckett *et al*, 1991) are present in distinct ethnic groups and far smaller proportions of the population. The octapeptide deletion has not been shown to be pathogenic or predisposing to the development of CJD. The presence in only ~1% of caucasians (Bosque *et al*, 1992, Windl *et al*, 1996) and low overall incidence of CJD makes epidemiological comparisons difficult. Due to the proximity of the primers to the *PRNP* start and stop codons and the small but significant presence of this polytmorphism in the general population, it was concluded that the deletion seen in a sCJD MV case was most likely the R34 mutation between the 4^{th} and 5^{th} octapeptide repeats. The distinct glycoform ratio of a sCJD heterozygote case with an octapeptide deletion, type 1 mobility and increased levels of diglycosylated PrP^{res}, suggests that this non-pathogenic polymorphism influences glycosylation of host PrP^{res} either constitutively or in response to TSE infection. This finding may acount for the glycoform ratio findings in the study by Acoutier *et al*, (Aucouturier *et al*, 1999). The effect of this polymorphism on disease phenotype is

dependent upon the assumption that the isotype observed was representative of the patient as a whole, as one sCJD MV case was identified with neuroanatomically varying isotypes and another with variable glycoform ratios, including increased diglycosylation. Unfortunately the tissue available from this anomalous case was not described and tissue for regional analysis of a sCJD MV 1 was not available, precluding determination of regional influences on glycoform ratios in cases diagnosed as sCJD MV type 1. The presumed impairment of metal ion binding in individuals with this polymorphism may also play a role in disease susceptibility or PrP function and responses to the development of pathology. This may manifest itself through an increased disease duration. Increased disease duration in all sCJD subgroups also reduces the sensitivity of EEG and therefore some cases of sCJD with 24 bp deletions may not be identified, reducing their apparent prevalence. The presence of this polymorphism may predispose to sCJD but this conjecture is not supported by the similar prevalence of identified cases of sCJD with this polymorphism and normal individuals with the polymorphism.

8.2.3 Iatrogenic CJD

So far there is little explicit description of the glycoform ratios seen in iCJD cases, though a predominance of the monoglycosylated band has been observed and quantified (Collinge *et al*, 1996, Cardone *et al*, 1999) and one case has been reported with a glycoform ratio resembling vCJD. Type 1 cases have a greater degree of nonglycosylated PrP^{res} than type 2 cases who display equal levels of diglycosylated and nonglycosylated, as seen in cases of kuru, which are also type 2 mobility (Collinge *et al*, 1996). The degree of diglycosylation was less apparent than in some sCJD cases but may still correlate with PrP amyloid plaque formation in these patients.

8.2.4 Familial CJD

The glycoform ratios of the MM and MV cases featuring the E200K mutation investigated were very similar to those previously reported in E200K MM patients (Cardone *et al*, 1999) and to the sCJD VV 2A subgroup. The glycoform ratio in fCJD E200K cases has been shown to differ to FFI and CJD178 (Gambetti *et al*, 1995), in this case an E200K type 1 case was compared, though the codon 129

genotype was not specified. E200K VV patients are reported to display the 2B isotype and a glycoform ratio featuring more pronounced diglycosylation very similar to that of vCJD (Hainfellner *et al*, 1999, Puoti *et al*, 2000). E200K cases co-segregating with methionine at codon 129 analysed by Parchi, P. and Gambetti, P. (1998, unpublished data) have a similar glycoform ratio to the type 2 E200K VV cases according to Hainfellner *et al*, 1999. However, the published values of Hainfellner *et al*, are more prominently diglycosylated than the published data of Gambetti *et al*, 1995 and the findings are more readily interpreted merely as the type B pattern. Therefore, it is of paramount importance in any cases of suspected non-MM vCJD that the whole *PRNP* coding region is checked for mutations. It is also important as the phenotype of fCJD E200K VV cases feature a prolonged disease duration, unsteady gait and a neuropathology similar to sCJD VV 2A cases with plaque-like PrP deposits. Features such as a rapidly progressive dementia, along with diffuse PrP staining, as opposed to florid plaques, in the cerebral cortex, thalamus basal ganglia, brain stem and cerebellum distinguish these cases from vCJD.

The glycoform ratio of the FFI case investigated was outwith the linear range but displayed a high degree of diglycosylated PrP^{res} (~60%), similar to vCJD and previous reports (Monari *et al*, 1994, Gambetti *et al*, 1995, Montagna *et al*, 1998, Parchi *et al*, 1998c, Parchi *et al*, 1999b).

The GSS cases displayed two different glycosylation ratios, the MV case diagnosed as intermediate mobility from the frontal cortex and the MM case classified as 1B from the frontal cortex had glycoform ratios resembling the sCJD VV 2A cases, fCJD E200K cases and previously published reports (Cardone *et al*, 1999). However, the MM case diagnosed as type 1B from thalamic tissue had a more pronounced diglycosylation (like vCJD and FFI) than seen in a previous study (Parchi *et al*, 1998a).

The glycoform ratios of the insertional mutations were similar to sCJD cases and the PrP^{res} banding pattern resembled that seen in another study (Parchi *et al*, 2000b) though values were not stated to allow comparison. Unlike the sCJD case featuring an octapeptide deletion, increased levels of diglycosylated PrP^{res} were not observed.

8.3 Regional findings

Only one hemisphere was available in each study, the neuropathology of the other hemisphere was assessed by immunohistochemistry and H&E staining. This allows comparisons between Western blotting and neuropathological features (generally similar features are seen in each hemisphere). However, inter-hemispheral differences have been noted in sCJD MM cases (MacDonald *et al*, 1996) and it must not be assumed that the pathology seen in one hemisphere is present to the same degree in the other and is thus an indicator of a glycosylation state or isotype conformation found in that corresponding region.

It has been suggested that neuropathological features of TSEs can be correlated to banding patterns. The classical triad of neuropathological features may correlate to the PrP^{res} isotype, such as plaque formation, specific perivacuolar or diffuse staining patterns, correlating to type 1 or 2. Spongiform change or astrocytic gliosis might be an indicator of the degree of glycosylation. The presence or absence of PrP^{res} as detected by Western blotting may not correlate with neuropathological features and this may be related to levels of PrP^{res} required to produce structural lesions, which varies with brain region (Gambetti *et al*, 1995).

Correlation of isotypes with PrP^{res} morphological deposits has been made (Puoti *et al*, 1999) and this would support the nucleation-dependent polymerisation model of prion protein conformational transmittance. Due to the differential spatial distribution of neuropathological features in different patients according to aetiology and genotype it may be possible to identify correlations with neuroanatomically specific PrP^{res}. The types of staining pattern and plaque formation observed differs considerably. Immunocytochemistry enables the identification of different morphological PrP deposition, including plaques. Many polyclonal and monoclonal antibodies have been used as well as different pretreatment protocols, amplification and detection systems and they can influence the sensitivity and specificity of PrP visualisation (Hardt *et al*, 2000). Monoclonal antibodies to PrP are used, such as KG9, which has very noticeable pericellular staining and 3F4 which has slightly better synaptic staining sensitivity, to visualise the PrP deposits. Differences in the staining specificities of monoclonal antibodies to PrP may relate to the accessibility of the epitopes in different types of PrP aggregates, though some antibodies show differences in glycoform specific staining on Western blots (Zanusso *et al*, 1998a). The banding patterns observed suggests a degree of correlation of PrP plaques or

plaque-like structures with increased glycosylation and relative mobility. However, this was not seen in a case displaying regional glycoform ratio and results suggest that the increased glycosylation may correlate with spongiform change, neuronal loss or astrocytosis. The overall levels of PrP^{res} observed on Western blotting did not appear to correlate with the levels of deposits observed on immunocytochemistry. The reasons for this could be interhemispheral differences.

In an isotype-immunostain comparative study both type 1 and 2 isotypes have been observed. In patients with only diffuse PrP staining, only type 1 PrP^{res} was found. In patients with both staining patterns (4 MM, 1 MV), type 1 PrP^{res} was found in areas of diffuse staining and type 2 PrP^{res} was found in areas of focal staining. In the 1 MV patient with both staining patterns there were both PrP^{res} types, in the other 2 MV patients there was only type 2 PrP^{res}. Two VV patients had type 2 PrP^{res} with perineuronal and plaque-like deposits superimposed to diffuse staining (Puoti *et al*, 1999). So far no reports of differing glycosylation related to brain region have been made, so the influence of this variable must be inferred from the different PrP^{res} deposition seen in sCJD, fCJD and FFI cases and their glycoform ratios.

8.3.1 Sporadic CJD

The assumption that single cortical samples display PrP^{res} isotypes representative of an individual as a whole was systematically investigated and found both molecular weight differences and glycoform ratio variability in the PrP^{res} detected. The presence of multiple PrP^{res} conformations within individuals was the most frequent form of variability and a World Health Organisation study designed to establish a consensual typing classification found both type 1 and 2 conformations. This was attributed to the large amounts of tissue sampled and suggests that within most individuals a degree of both isotypes are present. The proportion of sCJD cases previously reported to contain both isotypes (3%) (Parchi *et al*, 1999c) suggested that this was an uncommon occurrence. However a more detailed study found 3 out of 14 (24%) patients to have both isotypes (Puoti *et al*, 1999) and in another study of 32 cases of CJD, 2 were found to have both isotypes (6.3%) (Baron and Biacabe, 2001). In contrast to the cases investigated here, the type 1 nonglycosylated band was more prominent. The findings of 2 out of 6 (33%) sCJD cases with both isotypes in this investigation supports a high prevalence of this phenomenon, though the prevalence upon routine isotyping in sCJD cases was only 4.5%. The multiple isotypes found in

routine analysis were not restricted by the codon 129 polymorphism but based on the findings on small tissue samples in large cohorts of patients it seems likely that there is a predisposition to formation of one isotype by the codon 129 polymorphism, although not to the exclusion of the other isotype. It was reported that 4 MM cases and an MV case featured both isotypes (Puoti *et al*, 1999), though it may be that MM cases are more prone to formation of both isotypes. The results here represent the first report of widespread PrP^{res} glycoform heterogeneity within individual cases of sCJD, iCJD and fCJD. The glycoform ratio findings were limited to a few individuals but suggest the codon 129 polymorphism plays a role, with heterozygosity producing a more varied pattern. The mechanism by which this variability arises may be regional variation in PrP^{c} glycosylation of the host as opposed to differential conversion of the glycoforms. The finding of two very distinct mobilities and glycoform ratios in one case (Head *et al*, 2001) highlighted the potential overlap of sCJD and vCJD 'strain types'. Other regional studies on PrP^{res} levels and banding patterns have been carried out primarily focusing on the FFI phenotype (Parchi *et al*, 1995b, Mastrianni *et al*, 1999). The largest previous study involved sampling from large portions of tissue (3-5 grams) in 8 regions (Brown *et al*, 1995) and focused on establishing the relative levels of PrP^{res}. Differences in the PrP^{res} banding patterns were not identified by Brown *et al*, in this study, though heterozygotic sCJD cases were not analysed. The investigations here involved the sampling of a greater degree of subcortical and deep grey matter regions. Comparison of the relative mobilities and glycoform ratios of these regions with the isotyping classifications, established for a large cohort of sCJD and vCJD cases, identified the potential for misclassification. Cases were chosen based on their codon 129 polymorphism and cortical isotype classsification and included sCJD heterozygotes as well as including the first neuroanatomical investigation of vCJD cases.

Differences in isotype have been correlated with the PrP^{res} deposits seen on immunohistochemistry (Puoti *et al*, 1999). PrP plaques have not been reported in the sCJD MM 1 subgroup (Parchi *et al*, 1996, Tranchant *et al*, 1999). It has been suggested that diffuse staining without the presence of plaques is indicative of type 1 mobility on Western blot (Puoti *et al*, 1999). The lack of any type 2 PrP^{res} in the sCJD MM 1 case investigated may represent the lack of PrP plaques. Overall PrP^{res} quantities in different brain regions were similar, in contrast to the findings of Brown *et al*, who found the greatest levels in the occipital cortex while the cerebellum displayed less and levels in the basal ganglia were barely detectable (Brown *et al*,

1995). A different isolation procedure was adopted and this can lead to loss of PrP^{res} (Parchi *et al*, 2000a). Other ancilliary diagnostic investigations (e.g. CSF, MRI and EEG) do not help to further differentiate cases in the MM 1 subgroup, neither do age at onset or disease duration (Zerr *et al*, 2000) and it seems that this subgroup is fairly homogenous.

The sCJD MM 2A case investigated conformed to the cortical subgroup described by Parchi *et al*, (Parchi *et al*, 1999c) based on clinical and neuropathological features. MM2 cortical cases have pathology resembling that of the MM1 subgroup aside from a lack of cerebellar involvement. This is reflected in their lack of ataxic symptoms (Parchi *et al*, 1999c). The PrP deposits are typically strong coarse or perivacuolar in nature and affect the occipital lobe greatest (Worrall *et al*, 1999) as well as there being thalamic lesions. The lack of PrP plaque-like deposits, yet the presence of type 2 PrP^{res} suggests that other morphological deposits are composed of PrP^{res} of the type 2 conformation.

Parchi *et al*, 1999 carried out a neuroanatomical Western blotting study of a sFI case showing thalamic atrophy, especially the medial dorsal, anterior ventral and inferior olive. A wide range of tissues were quantitatively assessed for PrP^{res}. The amounts and distribution of PrP^{res} was the same as in Familial Insomnia and the type 2 mobility was seen throughout (Parchi *et al*, 1999c). The PrP^{res} levels and distribution are quite different to sCJD. A sCJD MV 1 case was unavailable for comparison with the MV 2A cases, though a previous study found that the glycoform ratios appeared identical in temporal, parietal and occipital cortices of one patient (Tranchant *et al*, 1999).

The two sCJD MV 2A cases investigated had greatly differing disease durations (21 months in the first case and 8 months in the second case). The occipital lobe is relatively spared in short disease duration cases, however, there was relatively less PrP^{res} in the occipital lobe of the long disease duration than the short disease duration case. Sporadic MV 2A cases have pathological lesion involvement of the basal ganglia along with thalamic, focal cortical involvement and presence of kuru-plaques. There is strong synaptic staining that co-localises with spongiform change and plaque-like focal deposits in the cerebral cortex as well as neuronal tract staining (Parchi *et al*, 1999c). These neuropathological features may correlate with the PrP^{res} observed, plaque-like and kuru-plaques resulting in type 2 PrP^{res} deposits and the prominent basal ganglia and thalamic pathology resulting in increased PrP^{c} glycosylation as a protective mechanism prior to PrP^{res} formation. Such a protective

mechanism could operate through stearic hindrance of dimer formation (Zuegg and Gready, 2000). However, in the regional study of a sCJD MV 2A case in which glycoform variation was found, the other hemisphere displayed less PrP amyloid plaques in these regions and a more prominent synaptic deposition. Studies on transgenic mice with mutated PrP glycosylation consensus sequences has indicated that PrP^c location in the thalamus and amyloid-like PrP deposits are dependent on the presence of glycosylated PrP^c (DeArmond *et al*, 1997b). High intensity of the basal ganglia in MRI (T2-weighted) is sensitive in all subgroups of sCJD but most reliable with MV2 patients. Hyper intense signals on T2 and diffusion weighted MRI in the cortex can also be prominent and correlate to spongiform degeneration, astrocytic gliosis and neuronal loss (Samman *et al*, 1999). This may be related to the longer disease duration as hyperintensities have been shown to become more pronounced over time (Zerr *et al*, 2000). Therefore it is also possible that they correlate to increased glycosylation, possibly as a protective response because it is also related to a longer disease duration seen in the long disease duration MV 2A case and the sCJD MV 1 case featuring a 24 bp deletion. A degree of glycoform ratio differentiation has been noted in sCJD type 1 and 2 cases, in a limited number of regions. Type 1 sCJD cases displayed a greater proportion of diglycosylated PrP^{res} in the cingulate gyrus, monoglycosylated PrP^{res} in the mesencephalon and nonglycosylated PrP^{res} in the hippocampus. In the type 2 cases the locus ceruleus displayed a greater proportion of diglycosylated PrP^{res} and the cerebellum displayed prominent nonglycosylated PrP^{res} (Parchi *et al*, 1996). Without codon 129 distinction and the values obtained for all the regions tested it is difficult to compare these results with the differences in glycoform ratio detected in this study. However, the increased diglycosylation in the locus ceruleus was similar to that seen in the basal ganglia and thalamic regions of the first sCJD MV 2A case investigated. The increased nonglycosylated PrP^{res} in the cerebellum may result from the presence of type 1 and 2 nonglycosylated bands that are not clearly separate from each other.

The VV1 subgroup is the rarest and has a distinct clinicopathological phenotype. A sCJD VV case with a young age at onset, long disease duration, presenting with behavioural symptoms and featuring more dementia than cerebellar deterioration, displayed type 1 mobility on biopsy and type 2 at autopsy (Head *et al*, 2001). Biopsy material did not show the presence of plaques but rather diffuse granular "synaptic" staining. The autopsy displayed a similar histological appearance in the cerebral cortex, though the caudate nucleus, putamen, thalamus and brain stem

displayed small numbers of PrP-positive plaque-like structures upon PrP immunocytochemistry. This does not account for the presence of the type 2 PrP^{res} in the frontal cortex at autopsy. The presence of PrP^{res} type 1 throughout the brain of the case neuroanatomically investigated and a lack of PrP plaques on immunocytochemistry, also reported in patients of this subgroup (Parchi *et al*, 1999c, Worrall *et al*, 1999), supports the contention that this correlates with diffuse PrP^{res} morphology. A lack of glycoform ratio differences in the case investigated was also found in another study examining a wide range of tissues (Worrall *et al*, 1999). It was reported that PrP^{res} levels correlated directly with the degree of spongiform degeneration (Worrall *et al*, 1999). In this study there was status spongiosis of the cerebral cortex and spongiform change in the basal ganglia and cerebellum, all of which showed significant PrP^{res} levels.

In a study of 12 valine homozygotes, five of which were identified as type 2A there was a relatively uniform phenotype (Kovacs *et al*, 2000). The frontal and parietal cortices displayed mild to severe spongiform change and PrP deposits of three types (neuronal, diffuse/synaptic and plaque-like deposits). The occipital cortex displayed spongiform change, diffuse PrP staining with a laminar accentuation and plaque-like PrP deposits. The basal ganglia has severe confluent spongiform change as well as diffuse PrP staining, perineuronal and plaque-like deposits. Plaque-like structures and type 2 PrP^{res} supports the hypothesis of Puoti *et al*, that the two are related but the additional presence of diffuse deposits did not result in additional type 1 PrP^{res}. In another study on 3 sCJD VV cases featuring only type 2 PrP^{res}, similar neuropathological features were seen, though only occasionally did the cerebral cortex display PrP plaque-like structures, while punctate nonamyloid PrP and diffuse staining was seen in the substantia nigra and granular cerebellar layer (Tranchant *et al*, 1999).

There may be some correlation between the PrP^{res} glycoform ratios and clinical or neuropathological features in cases such as sCJD VV 2A, MV or vCJD. The presence of spongiform change, PrP plaques, or plaque-like deposits and their neuroanatomical location, high signal MRI findings and lack of characteristic EEG PSWCs, may be related to prolonged disease duration and could result in the increased degree of glycosylation seen in some cases.

The spatial distribution of M and V allele expression in heterozygotes and their conversion into PrP^{res} in different brain regions is currently unknown but would greatly improve the understanding of the pathological mechanisms involved in

conversion of PrP^{c} to PrP^{sc} and neuropathological targeting of prion strains. This could be elucidated with cyanogen bromide cleavage (CNBr) or endoproteinase Lys-C and Edman degradation of SDS-PAGE isolated PrP^{res}. The cleavage sites have been determined by Edman degradation (Parchi *et al*, 2000b), however, codon 129 is too distal to the NH_3-terminal for analysis without further cleavage. Tthe NH_3-terminal PK cleavage sites have been located between codon 78 and 103 in sCJD and Edman degradation can only process up to 30 amino acids. Alternatively allele specific antibodies, could differentiate between codon 129 polymorphic PrP, could be used either on immunocytochemistry or Western blotting, depending on their applicability. Allele specific monoclonal antibodies have been produced to the 219 polymorphism present in the japanese population (Matsunaga *et al*, 2001) and PrP antisera that differentiated between wild type and mutant forms of PrP featuring the E200K mutation have been produced (Gabizon *et al*, 1996).

8.3.2 Variant CJD

The relative consistency of the PrP^{res} banding pattern throughout the CNS in vCJD patients reflects the consistency of the neuropathological profile (Armstrong *et al*, 2002). This suggests dominance of the BSE 'strain' over host PrP^{c}, though the restriction of this aetiology to the methionine homozygous population could also account for the consistency. The banding pattern was not completely consistent and the prominence of the lower portion of the monoglycosylated band in the cerebellum suggested alternative occupancy at codon 181 of the N-linked glycan chains. The banding pattern of a fCJD case carrying a V180I mutation that prevents attachment of oligosaccharide chains to the 181 site, elucidated the nature of this monoglycosylated phenomenon. This case, as expected, lacked a band in the position normally occupied by the diglycosylated band. This confirms that the uppermost PrP^{res} band is in fact diglycosylated. There was also a band present in the upper monoglycosylated region, demonstrating that PrP^{res} glycosylated solely at the 197 site can form PrP^{res} of this M_r. There was no detectable signal in the lower region of the monoglycosylated band. Whether this is due to the low PrP^{res} levels as a whole, or implies that PrP^{res} is not glycosylated at codon 181 and does not form a band in this region, is open to conjecture. Studies comparing transgenic mice with mutations at either the codon 183 or 199 site that prevent glycosylation of PrP^{c} demonstrated that the oligosaccharide chains at the 181 residue are more abundant and variable in structure

in the cerebellum than those at the 191 site (DeArmond *et al*, 1997b). The possibility remains that the lower proportion of the monoglycosylated band represents PrP glycosylated at codon 181. The low levels of PrP^{res} in these patients may explain the lack of transmissibility to mice (Tateishi *et al*, 1996) or may be due to hindrance of homodimeric conversion of monoglycosylated CJD V180I PrP^{res} and murine PrP^{res}. Expression of Syrian hamster PrP^{c} featuring a threonine to alanine mutation at codon 183 preventing glycosylation at the first consensus sequence in transgenic mice null for mouse PrP, prevented transmission of scrapie strains (DeArmond *et al*, 1997b). This was probably due to retention of the mutant PrP in the cell body (DeArmond, 1999). The transmission and molecular of strain typing of E200K and D178N mutation individuals has been investigated however, neither of these mutations is within the consensus sequences for N-linked glycosylation of PrP^{c}. The availability of patients with V180I, T183A or F198S *PRNP* mutations is more restricted, but their potential application to molecular strain typing studies warrants further investigation and may help elucidate the role of glycan chains in protein function. The T183A mutation leads to severe spongiform change in the putamen and PrP^{res} deposition in the putamen and cerebellum (Nitrini *et al*, 1997). This suggests disruption of this glycan attachment site leads to disturbance of PrP^{c} specifically in these areas, possibly due to perturbed cellular processing of the PrP^{c} (Rogers *et al*, 1990, Lehmann and Harris, 1997).

The glycoform ratios of non-CNS tissue have been shown to display differing glycoform ratios. Lymphoreticular tissues (tonsil, spleen and lymph node) feature a more prominent hyperglycosylation designated type 4t (Hill *et al*, 1999b, Wadsworth *et al*, 2001). The same pattern has been detected in tonsil tissues using the same technique applied in this study (Head, personal communication). In contrast, investigation of ocular tissues displayed a less pronounced glycosylation, similar to that seen in sCJD (Head *et al*, 2003). These findings provide additional evidence for tissue specific differences in the glycosylation of PrP^{res} accumulations. Recently a progressive increase in nonglycosylated total PrP has been reported in the retina and optic nerve in scrapie infected mice and hamsters, though the monoglycosylated PrP^{res} band was most abundant (Russelakis-Carneiro *et al*, 2002).

8.3.3 Iatrogenic CJD

The regional analysis of an iCJD case heterozygotic at codon 129 resulting from GHT infection showed a degree of glycoform variation, similar to that seen in a sCJD MV case. This suggests that the codon 129 polymorphism of the individual is more important in determining cell specific glycosylation than the aetiology of the disease.

8.3.4 Familial CJD

The two fCJD E200K patients investigated proved harder to assess in terms of both mobility and glycoform ratio, due to the low levels of nonglycosylated PrP^{res}. The most noticeable feature of this was that in some regions the nonglycosylated band was clearly visible and not in others, suggesting by visual examination that the glycoform ratios were heterogenous. These findings may be related to the overall PrP^{res} levels but differences in the relative mobility and hence conformation of the PrP^{res} were also noted. This is surprising as the primary sequence of the mutated form of the *PRNP* is consistent and the PrP^{res} is presumed to develop *de novo* according to the prion hypothesis. The conclusion therefore is that neuroanatomically specific differences in conformation and glycosylation of host PrP^{c} results in the PrP^{res} pattern observed. There is also a more diffuse monoglycosylated band in the cerebellum of both patients and the MM patient appeared to have some prominence in the lower portion of the band (figure 34 B), that is also seen in MM vCJD cases. During the course of this study a similar pattern was reported in an E200K VV patient (Puoti *et al*, 2000). The focal PrP deposits in the molecular layer of the cerebellum in the VV 2 case may account for the relative mobility of the PrP^{res} (Puoti *et al*, 2000). Another study of an E200K VV type 2 patient for PrP^{res} found no difference between three regions (frontal cortex, striatum and cerebellum) (Hainfellner *et al*, 1999). These findings must be taken with caution as the normal or wild type allele in E200K cases may display some of the features of the mutated PrP^{res} partial insolubility and some PK resistance, but in particular anomalous mobility (Capellari *et al*, 2000). This could be in part due to abnormal glycosylation at the 197 site (Capellari *et al*, 2000).

These studies demonstrate considerable molecular diversity within and between cases of CJD. Both parameters of PrP^{res} analysis (conformation and glycosylation status) can vary within an individual. However, the molecular phenotype as well as the clinical and neuropathological phenotype in vCJD is consistent between cases. Despite the relative differences in neuropathological features seen throughout vCJD brain regions, there appears to be no correlation with the molecular phenotype. The prominent deposition of PrP in the occipital cortex, spongiform change in the basal ganglia or thalamic gliosis do not appear to alter the molecular phenotype and a consistent 2B pattern was observed irrespective of brain region. The consistent increase in monoglycosylated cerebellar PrP^{res} found across aetiological subgroups suggests a degree of host dominance over PrP^{res} formation.

8.4 Divalent cation determination of conformation

The three mobility types described in this study were all subject to increased cleavage of the NH_3-terminal after chelation, most apparently in the type 1 and intermediate type. The initial report by Wadsworth *et al*, 1999a described a minor mobility shift of both types 1 and 2 to a smaller size designated 2⁻. These experiments found the type 1 and intermediate mobilities to remain distinct from each other after EDTA treatment, however EDTA treated type 1 had mobility consistent with intermediate cases. Similarly EDTA treated intermediate cases were consistent with type 2 cases. The type 2A cases (analogous to types 3 and 4) displayed a discernable shift in mobility however changes in type 2B cases could not be identified, though other work suggests a very minor shift in mobility.

The influence of the codon 129 genotype on cation binding was assessed as this has been shown to affect recombinant PrP structure (Wong *et al*, 2000a). The levels of Cu, Zn and Mn binding to PrP^{c} and overall levels in the brain of sCJD patients showed some effect of codon 129 genotype and isotype (Wong *et al*, 2001a). The patients classified as type 1 and 2 by Collinge *et al,* cover all the codon 129 permutations, however, only MM individuals were assessed (Wadsworth *et al*, 1999a). In our studies MM and VV sCJD cases, MM DM and MV GHT iCJD as well as MM and MV GSS cases were assessed and the characteristic increase in M_r was dependent upon the isotype and independent of codon 129 genotype or aetiology. The glycoform ratios of EDTA untreated and treated samples were the same as expected. This suggests that the presence of metal ion bound monoglycosylated PrP^{res} co-

migrating with unbound diglycosylated PrP^{res} does not contribute to glycoform ratio differences. The influence of metal ion binding and mobility in fCJD cases with octapeptide repeat mutations or polymorphisms was not assessed but warrants investigation.

It has been suggested that the presence of EDTA in homogenisation buffers could account for the differences in the molecular weights of the banding patterns observed. The procedure adopted in this study and by Collinge *et al*, did not involve the use of EDTA (Collinge *et al*, 1996). The Parchi *et al*, methodology involves the use of 10 mM EDTA, yet due to the consistency between these findings and theirs it seems unlikely that this is the cause of molecular weight discrepancies. Use of metal ion chelators produces artificial susceptibility to PK cleavage and may standardise the PK cleavage site by opening up the NH_3-terminal conformation to allow the maximimum amount of the NH_3-terminal to be hydrolysed i.e. the type 2 conformation. The 'open' conformation of vCJD PrP^{res} may be not be due to a lack of metal ion binding. However, if there is a lack of bound metal ions this may have significant implications for the pathological mechanism operating in this disease and may even support the highly contentious hypothesis concerning the role of environmental metal ions (Purdey, 2000, 2001). Exclusion of metal ion chelators from homogenisation buffers and retention of the metal ions will assess the *in vivo* conformation of PrP^{res} and will be more relevant to the pathological conformation and determination of conversion susceptibility. Differences in metal ion status *in vivo* may be of relevence to neuropathological targeting in a comparable way to suggested cell specific glycosylation. Neuroanatomical investigation of the metal ion bound status of PrP^{res} may identify such differences and could enable targeting of metal ion homeostasis based therapeutics to maximise their effectiveness. The presence of two isotypes in cases remain distinct on EDTA treatment and eliminate the possibility of metal ion bound status as the cause of the different conformations.

Furthermore it has recently been shown that pH can also affect the isotype generated (Zanusso *et al*, 2001), expanding the mitigating factors in pigeonholing PrP^{res} conformations. The findings in this study complicated the nature of PrP^{res} banding patterns but supported the classification of two predominant isotypes. The codon 129 of cases in these two groups showed consistency with the findings of Parchi *et al*, and the findings presented here, with type 1 containing MM and VV individuals and type 2 containing MM, MV and VV individuals at pH 4-7.4 (Zanusso *et al*, 2001). Type 1 VV cases analysed by Zanusso *et al*, were of increased relative

mobility when homogenised at pH 8 prior to PK digestion, but not all the MM cases were. This suggests that the classification system used by Collinge *et al*, could artifactually separate the MM and VV individuals if minor increases in homogenisation buffer pH occurred. The MM and VV cases susceptible to pH defined PK cleavage were found to retain an intact NH_3-terminus prior to experimental proteolysis and were termed type 1^{FL}. This also allows improved understanding of the nature of the PrP^{res} in relation to the disease phenotype and MM cases in the type 1^{FL} (Zanusso *et al*, 2001). This probably accounts for the large numbers of sCJD MM cases classified as type 2 by Collinge *et al*. The intermediate mobility type (INT) identified in a small number of cases (2 MM, 2 MV, 2VV) may represent this pH dependent full length group, their increased relative mobility may thus be due to anomalies in the pH of homogenisation buffer employed or endogenous proteolytic digestion *in vivo* or *ex vivo* during sample preparation prior to PK treatment. This increases the standardisation requirements between laboratories to ensure consensual typing across the board and undermines the diagnostic significance of any particular isotype in relation to strain of agent. However, it does emphasise the ability of Western blotting to resolve different conformations of PrP^{res} and carefully define the nature of the PrP^{res} present *in vivo* resulting in different banding patterns, in terms of the metal ion binding status and intact NH_3-terminus. This requires clear definition of the *ex vivo* experimental conditions and the employment of antibodies directed at different epitopes (e.g. 5B2). The effects of pH, metal ion binding, codon 129 genotype and octapeptide repeat polymorphisms and mutations on the conformation of PrP^{c} and PrP^{res} should be established to help elucidate the role in the pathogenesis of TSEs. However, the use of 2D electrophoresis or mass spectrometry to investigate this may be better able to determine the differences and would allow comparison of nonglycosylated and glycosylated forms of PrP.

8.5 Animal TSEs and experimental transmissions

8.5.1 Murine transmissions of vCJD

Investigation of vCJD transmission to three mouse strains surprisingly found differing isotypes and a degree of differing glycoform ratios. These differences could not be attributed to different donor patients or the mouse strain that was inoculated. Along with the findings in sCJD, iCJD and fCJD patients, this undermines the

molecular strain hypothesis and contradicting previous investigations. However, repeated passage in mice may lead to stabilisation of the isotype pattern as occurs with incubation periods and neuropathological lesion profiles.

Transmission from BSE, vCJD, domestic cats with FSE, cheetahs, experimental BSE in macaque and sheep, to wt (FVB, C57BL, RIII and VM) or transgenic human and bovine PrP^c expressing mice and the original inocula have all displayed the type 2B isotype (Collinge *et al*, 1996, Hill *et al*, 1997a, Somerville *et al*, 1997, Hill, 1998, Hill *et al*, 1998, Kuczius *et al*, 1998, Baron *et al*, 1999, Demart *et al*, 1999, Kuczius and Groschup, 1999, Schaller *et al*, 1999, Scott *et al*, 1999, Baron *et al*, 2000, Madec *et al*, 2000b, Baron and Biacabe, 2001, Hill and Collinge, 2001, Stack *et al*, 2002). The glycoform ratio of vCJD and BSE have been reported to differ yet both appear very similar upon transmission to FVB mice (Hill and Collinge, 2001). Studies on BSE transmission to cheviot sheep have detected an unglycosylated PrP^{res} band of 22 kDa quite different to the 19 kDa band reported in other studies (Hope *et al*, 1999). The M_r of a BSE case in one paper was of greater molecular weight than the sheep passaged BSE PrP^{res} (Stack *et al*, 2002). Interestingly a case of spongiform encephalopathy in a cheetah, implied to be the result of BSE infection, displayed PrP^{res} with a nonglycosylated molecular weight of 22 kDa (type 1). This case also displayed two very different glycotypes, one featuring a prominent diglycosylated band and the other a prominent nonglycosylated band (Baron *et al*, 1997) though a subsequent report of two cheetahs and their transmission to C57Bl mice indicated the first glycoform ratio pattern to be correct (Baron *et al*, 1999). Co-infection of mice with BSE and scrapie isolates that had type 2 and type 1 mobilities respectively, prevents the differentiation of the mobility of nonglycosylated fragments and glycoform ratios. Mixing of the two separate isolates after denaturation also prevents differentiation and results in an intermediate mobility (Baron and Biacabe, 2001). An intermediate mobility was also seen when the DY and HY strains co-exist (Bartz *et al*, 2000). These findings suggest that the intermediate mobility sCJD cases could be a result of multiple isotypes, however, the mixing of types 1 and 2 carried out in this study found a prominence of type 2 PrP^{res} with a less noticeable type 1 nonglycosylated band.

Comparison of the results in this study with previous studies on molecular strain transmissions suggest that the codon 129 of the host PrP^c does not determine the resulting mobility. The three mice strains investigated all carry the methionine genotype at the equivalent codon 129 position and in some cases formed a higher

molecular weight PrP^{res} than the donor, VM (n=4), RIII (n=4) and C57BL (n=3/4). In transgenic mice carrying human *PRNP* with codon 129 valine that were infected with vCJD a type 5 pattern was described that displayed high proportion of the diglycosylated band and the type 2 mobility according to the nomenclature used in the study (Collinge *et al*, 1996). This was attributed to the codon 129 valine polymorphism and later studies on methionine encoding human *PRNP* transgenic mice were reported to accumulate type 4 PrP^{res} (Hill, personal communication). These differences may be attributable to species specific PrP^{res} differences. Caution should therefore be employed when predicting the potential banding pattern in vCJD cases with a valine at one or both codon 129 alleles.

The presence of the lower portion of monoglycosylated PrP^{res} in all the mice analysed, in contrast to the majority of human tissues, suggests a species-specific feature of PrP^{res} formation that may be dependent upon PrP^{c} glycosylation. This phenomenon is similar to that seen in human PrP^{res} isolated from the cerebellum. The determination of PrP^{res} glycosylation seems to be both species and tissue specific. This is probably as a result of differences in PrP^{c} expression and post-translational modification in diverse contexts. The presence of different truncated species cannot be ruled out as the cause of the lower relative mobility of the monoglycosylated band and may be more significant in murine tissue with the use of 6H4 possibly detecting PK resistant glycosylated PrPII.

8.5.2 BSE, FSE, Marmoset BSE and Scrapie

Analysis of single cases of scrapie, BSE, FSE and transmitted BSE do not allow wide-ranging extrapolations and emphasise species specificity. The scrapie case was clearly distinguishable from vCJD and BSE. The BSE case had a type 1 mobility in comparison with human samples, but the FSE case had type 2 mobility and the marmoset had a INT/2B isotype. The sequence of the host *PRNP* is unlikely to determine the isotype, with 264 amino acids in cattle being longer than the shorter sequences of ovine PrP^{c} (256 amino acids) and marmoset PrP^{c} (252 amino acids) (Baker *et al*, 1993, Wopfner *et al*, 1999). The use of Western blotting in the diagnosis of BSE has been evaluated in Swiss (Schaller *et al*, 1999) and French studies (Madec *et al*, 2000b). In the former study the midbrain and medulla were identified as the most reliable site for tissue sampling. While the latter showed the greatest levels of PrP^{res} in the mesencephalon and cerebellum, and detectable levels in the frontal and occipital cortices. The Western blots in each study displayed the 2B isotype. In the

Swiss study the reliability was high as was the sensitivity and specificity, though the authors added the caveat that the brain region and pretreatment protocol were important (Schaller *et al*, 1999). Samples were taken from the midbrain, cerebellum, rostral medulla and adjacent obex and PrP^{res} was found to be most reliable when positive cattle were sampled from the medulla oblongata adjacent to the obex of the IV ventricle. This is in contrast to sheep scrapie that was most reliable when sampled from the cerebellum and midbrain (Schaller *et al*, 1999). The type 1B finding in this study is likely to be an anomaly and unrepresentative of BSE based on the number of findings that contradict this, however, the results in a few studies suggest that a degree of variability may exist among BSE cases (Baron *et al*, 1997, Hope *et al*, 1999, Stack *et al*, 2002). The assessment of glycoform ratios in BSE consistently finds values of roughly 65 % diglycosylated, 25% monoglycosylated and 10% nonglycosylated (Hill *et al*, 1997a, Kuczius *et al*, 1998, Baron *et al*, 1999, Sweeney *et al*, 2000, Hill and Collinge, 2001, Stack *et al*, 2002). The values obtained in this study featured a more pronounced diglycosylation (75% diglycosylated, 24% monoglycosylated, 1% nonglycosylated) this may be a result of the limitations of the linear range. These values overlap with those of the 87V scrapie strain (Somerville *et al*, 1997) but are disparate to the values quoted by other studies, 50% diglycosylated, 40% monoglycosylated and 10% nonglycosylated (Hope *et al*, 1999) and ~53%:34%:~13% respectively (Kuczius *et al*, 1998).

The type 2B pattern in the FSE case supports previous conclusions that these cases are a result of BSE infection (Pearson *et al*, 1991, Pearson *et al*, 1992, Fraser *et al*, 1994, Wells and Wilesmith, 1997). The reported sequence of feline PrP^{c} only covered 126 amino acids preventing comparison (Wopfner *et al*, 1999). A marmoset experimentally infected with BSE was investigated to determine the PrP^{res} of BSE following passage to a primate in comparison to vCJD transmission to mice. The isotype was similar to that seen in some of the murine transmissions and vCJD cases and supports the contention that BSE is the cause of vCJD. The PrP^{c} of marmosets has been demonstrated to have 96% homology with the human amino acid sequence, they are not polymorphic at codon 129 and encode methionine as do all non-human primates studied (Schatzl *et al*, 1995). Sequence variation from human *PRNP* is not found at the 219 polymorphic codon, in the α-helices, sites of post-translational modification or the signal peptide. Despite this, comparison between human and marmoset BSE infection must take into account codon 112 (human M, marmoset V), present in the proposed dimer interface of helix 1 (and the decreased preference for β-

sheet formation of adjacent heterologous a.a.s) as it is known to influence marmoset susceptibility to human prions (Schatzl *et al*, 1995). Species specific differences in *PRNP* prohibits cross species isotyping from being used as a marker of strains, because unlike CJD deriving from a consistent *PRNP* sequence, the host sequence may influence the mobility type. It also undermines the assumption of the BSE/vCJD type 2B molecular pattern representing a strain of agent imposing conformational and post-translational modifications upon the host that can be equated to a single infectious agent strain.

The detection of a type 2B banding pattern in a single case of scrapie is insignificant in terms of the large number of detailed investigations carried out on natural scrapie isolates and murine passaged scrapie strains, however it does provide evidence of a type 2B pattern in sheep when analysed alongside CJD cases. Scrapie PrP^{res} has previously been described as either type 1 or type 2 (Hill *et al*, 1998, Kuczius and Groschup, 1999). Various tissues in sheep have been reported to display different PrP^{c} (Moudjou *et al*, 2001), PrP^{res} banding patterns (Madec *et al*, 2000a) and glycoform ratios (Sweeney *et al*, 2000). PK cleavage in the presence or absence of copper ions has not detected any change in relative mobilities in scrapie (Sweeney *et al*, 2000). The scrapie glycoform has previously been reported to resemble BSE glycoform ratio in both natural isolates (Madec *et al*, 1997, Madec *et al*, 2000a) an experimental isolate of natural scrapie (Hope *et al*, 1999) and mouse passaged strains 22A, 87V and 263K (Somerville *et al*, 1997). The 87V strain also has the same mobility as BSE and is predominantly present in the brainstem (Kuczius and Groschup, 1999). The scrapie strains 22A (Somerville *et al*, 1997) and CH1641 (Hill *et al*, 1998) have a mobility similar to that of type 1 CJD but show some similarities to BSE. Three different mobilities of the nonglycosylated band have been reported for scrapie isolates (~20 kDa, ~24 kDa and ~22 kDa) (Hope *et al*, 1999). In this study CH1641 (isolated in 1970) was also classified as C (Hope *et al*, 1999). In another study a large number of samples were found to have predominance of the diglycosylated band, with varying degrees; 87V (61% diglycosylated : 27% monoglycosylated : 12% nonglycosylated), 22A, ME7 mouse isolates and hessen 1 (~47% diglycosylated : ~35% monoglycosylated : ~18% nonglycosylated) (Kuczius *et al*, 1998). The mobility was not stated but the glycoforms resemble the range covered from FFI to vCJD tonsil.

No difference in PrP^{res} was observed between cerebrum, cerebellum and brainstem samples taken from mouse passaged BSE and natural sheep isolates

(Kuczius *et al*, 1998). Neuroanatomical analysis of PrP^{res} levels has found varying levels, in the cerebellum (greatest levels), brain stem, mesencephalon and frontal cortex (lowest levels) in cases of scrapie occurring in sheep of the PrP^{VRQ} allele (Madec *et al*, 2000a). The central nervous system samples all displayed the same mobility (type 2 or 19 kDa nonglycosylated position) and prominent diglycosylation, irrespective of brain region. These sheep also displayed PrP^{res} in the spleen, lymph nodes and tonsils, though of reportedly different mobility, the predominance of a band in the lower region of the monoglycosylated band in spleen samples could be seen (Madec *et al*, 2000a), as in E200K VV 2 and vCJD cerebellum. Another regional comparative study has been carried out and found PrP^{res} in the cortex, hippocampus, mesencephalon, paraterminal body, cerebellum, medulla and thalamus with the medulla showing consistently high levels (Manousis *et al*, 2000).

Strains could not be distinguished on the basis of glycoform ratio or mobility in a large study of natural and experimental scrapie cases (n=42) including experimental ovine CH1641, BSE or BSE transmissions, (Baron *et al*, 1999). It seems apparent that PrP^{res} isotyping is not sufficient on its own to establish or rule out cases of BSE derived infection. The importance of differential diagnosis of scrapie and BSE is particularly relevant to the identification of possible cases of BSE in the sheep flock. The identification of a type 2B isoform in a natural sheep suspected of having scrapie or even a mouse transmission of it would not necessarily indicate infection by BSE as some type 2B PrP^{res} has been reported in scrapie (Somerville *et al*, 1997, Hope *et al*, 1999). Furthermore there are numerous polymorphisms in sheep and along with the background genotype (i.e. breed) these can influence the susceptibility to scrapie and the PrP^{res} patterns.

8.6 Role of PrP^{res} in diagnosis and molecular strain typing

The findings of this study present two problems in terms of the diagnostic use of human molecular strain typing. The diagnosis and classification of CJD sub-types with isotype / genotype combinations that define sCJD phenotypic variability (Parchi *et al*, 1999c) is still broadly applicable due to the segregation of codon 129 genotypes with mobility features. However, the co-existence of type 1 and 2 PrP^{res} in sCJD cases, noted here and in other studies (Parchi *et al*, 1999c, Puoti *et al*, 2000, Baron and Biacabe, 2001, Head *et al*, 2001, Kovacs *et al*, 2002), brings the classification system into question. Regional variation in sCJD PrP^{res} isotype is not restricted to

methionine homozygotes but can also occur in heterozygotes and valine homozygotes, thus the classification could be re-interpreted merely as cases displaying 'predominantly' type 1 or 2 PrP^{res}. It should also restrict the further differentiation between subgroups based on mobility. It is possible that small amounts of one isotype, e.g. type 1 in a predominantly type 2 case could represent the less dominant strain. The conformation of PrP^{res} may change upon development of a new strain by passage into a new species, along with the phenotype (Peretz *et al*, 2002). This could account for the distinct nature of the BSE strain in comparison to scrapie. Development of a new strain upon cross-species transmission may thwart molecular strain typing but supports the contention that PrP^{res} conformation is a strain marker and indicator of phenotypic features. Other features of the disease along with the codon 129 polymorphism should be taken into account, as atypical features such as young age at onset, long duration or psychological symptoms may be more pertinent features of the phenotype than PrP^{res} conformation. The presence of different isotypes may be tissue specific due to differences in the PrP^{c} expressed and in mature human and bovine sperm a carboxyl-terminally truncated PrP isoform has been detected (Shaked *et al*, 1999b).

Of particular concern is the finding of regional variation in glycoform ratio in sCJD since this is the sole molecular feature that distinguishes the PrP^{res} found in vCJD (type 2B) from that found in a subset of sCJD cases (type 2A). The overlap of PrP^{res} glycoforms patterns as well as mobility is rare and most likely in either sCJD MV or VV type 2 cases, fCJD or FFI, though careful quantitation of glycoform ratios and experienced diagnosis can eliminate the risk of molecular misclassification. The case of sCJD (RU#98/153) described here in a valine homozygote displaying a 2B isotype suggests that age at onset, duration and PrP^{res} can indicate vCJD. Along with a fCJD E200K heterozygote patient displaying type 2B PrP^{res} and the reported case of fCJD E200K 2B in a valine homozygote (Puoti *et al*, 2000), this argues for a cautious integrated approach to the diagnosis of vCJD. The presence of neuroanatomically differing glycoform ratios also contradicts the assumption that the glycoform ratio represents a strain feature that can be transmitted as murine scrapie strains can be transmitted from various brain regions yet retain their incubation periods and clinical phenotype (Carp *et al*, 1997). Scrapie strains are also not dependent upon glycosylation of host PrP^{c} and can be transmitted in its absence (Korth *et al*, 2000). Differences in glycosylation of PrP^{c} and PrP^{sc} in brain regions have been observed in murine scrapie models (Somerville, 1999) and the glycosylation of host PrP^{c} and

infecting PrP^{sc} have also been identified (Rudd *et al*, 1999). Analysis of small cohorts of CJD by Western blotting does not allow definitive conclusions to be made as to the aetiology of the disease without further epidemiological, clinical and neupathological investigations and some such studies are of little benefit (Deslys *et al*, 1997, Hill *et al*, 1997b, Zanusso *et al*, 1998b, Beaudry *et al*, 2002). The absence of a type 2B pattern would not rule out vCJD, as the phenotype in non-MM individuals is unknown, though the presence of this pattern would warrant further investigations. Interestingly in the study by Zanusso *et al*, the FSE pattern was unlike that in cases attributed to BSE infection and may suggest some cases of FSE are sporadic and thus attributing all cases of FSE in the UK to BSE infection would be unwarranted without strain typing studies. In terms of incorporating molecular features into strain typing criteria along with incubation periods and lesion profiling, differences in neuropathological profiles with similar PrP^{res} banding patterns suggest that the isotype does not represent the neuropathology. Therefore, the PrP^{res} banding pattern does not signify the strain of agent when generated *de novo* in sCJD or fCJD individuals. There is also considerable evidence to suggest the presence of multiple scrapie strains (Dickinson *et al*, 1972, Dickinson *et al*, 1975, Kimberlin and Walker, 1978, Bartz *et al*, 2000).

The second problem is more conceptual and mechanistic in nature: A considerable body of work has amassed to suggest that conformational change is the basis of conversion from PrP^{C} to PrP^{Sc} and that agent strain characteristics can be enciphered in conformation variants of PrP^{Sc}. The occurrence of both type 1 and type 2 PrP^{res} in individual cases of sCJD has three possible explanations; a) regional factors can modify isotype in certain individuals, b) isotypes can spontaneously, though rarely interconvert, or c) multiple different isotypes can arise *de novo* in certain individuals.

The banding patterns of PrP are complex and dependent on a number of factors. PrP^{c} conformation can differ independently of the conformation determined by PK cleavage (Aucouturier *et al*, 1999) and the primary sequence can differ in familial forms including containing inserts or deletions. PrP^{c} is post-translationally modified to produce 3 glycoforms that have a wide range of possible glycan chains (up to 400 different possible combinations) (Endo *et al*, 1989) and the full length wt molecule can be truncated in varying degrees into two proteins PrP-I and PrP-II, differentiated in part by their ability to bind 3F4 and 6H4. Levels of these two endogenous cleavage products have also been found to differ in relative amounts between subgroups (Jimenez-Huete *et al*, 1998). The brain homogenates consist of

full length and truncated forms of the protein (Pan *et al*, 2001, Pan *et al*, 2002) that differentially bind metal ions and are truncated in a pH dependent manner possibly due to the affinity of metal binding (Zanusso *et al*, 2001). The degree of PK resistance is also found to differ depending on the strain of agent. Relative PK resistance assays carried out over a wide pH range (2-11) and incorporating GdnSCN (0.25-3 M) have been used as an alternative measure of strain conformation (Madec *et al*, 1997). Prolonged time taken to process samples can lead to degradation of PrP^{res} into a protease resistant PrPII which is not detected by 3F4 (Jimenez-Huete *et al*, 1998). Thus employing this antibody in a diagnostic method can not distinguish differences in banding pattern ratios due to poor sample processing leading to further truncation of the PrP^{res}. Different antibodies produce different banding patterns and immunohistochemistry staining patterns that may be glycoform specific (Zanusso *et al*, 1998a, Liu *et al*, 2001). In addition to this there are numerous protocols, reviewed in (Groschup *et al*, 2001), classification systems and nomenclature (types 1-7 Collinge *et al*, type 1, 2A and 2B Parchi *et al*, type 1B Cardone *et al*, A, B and C Hope *et al*, PrP-I, PrP-II, Pan *et al*, PrP-21, Hooper *et al*, C-1, C-2, Chen *et al*, FL Zanusso *et al*). Differences in relative PK resistance has been applied to sheep scrapie strains (Kuczius *et al*, 1998, Kuczius and Groschup, 1999, Horiuchi *et al*, 2002) and its application to CJD 'strains' may help to further elucidate the nature of the phenotypic differences. Likewise the application of 2D gel electrophoresis to the analysis of PrP^{res} patterns should be a focus of future investigations (Pan *et al*, 2001, Zanusso *et al*, 2002).

There are a number of host factors, including genotypic and tissue specific that can modulate the presentation of TSE disease. The *PRNP* genotype correlates closely with the PrP^{res} formation and accumulation in individuals, however this is not sufficient to conclude that prions are the causative agent. The retention of the distinctive BSE/vCJD PrP^{res} banding pattern suggests that a dominant strain of agent causes vCJD and BSE, possibly through a prion related mechanism involving conformational and glycosylation modulated conversion of host PrP^{c}.

Conclusions

- Cases diagnosed with aetiologies other than TSEs did not display PK resistant PrP.
- The majority of cases displayed nonglycosylated PrP^{res} bands with molecular weights of either 21 or 19 kDa and were termed type 1 and type 2 respectively.
- Two banding patterns were observed, either predominantly monoglycosylated or predominantly diglycosylated.
- The results confirm the presence of type 1 or type 2 PrP^{res} in the majority of sCJD cases and show that these two PrP isotypes occur in combination with each of the three possible *PRNP* codon 129 genotypes.
- The frequencies of isotype / genotype combinations that we have observed in sCJD do not appear random. A small number of cases displayed a nonglycosylated PrP^{res} band intermediate between types 1 and 2. Neither aetiology, codon 129 or phenotypic features distinguished these cases.
- Type 1 MM sCJD cases were the most prevalent.
- Type 2 sCJD cases were more frequently observed in conjunction with a valine allele at codon 129.
- DM iCJD cases were type 1 but the majority of GHT iCJD cases were type 2.
- Sporadic CJD and iatrogenic CJD cannot be differentiated on the basis of the PrP^{res} banding pattern. Iatrogenic CJD cases did not have significantly different glycoform ratios from sCJD cases. The route of entry or codon 129 did not influence the glycoform ratio.
- The highly glycosylated PrP^{res} found in vCJD appears to be a reliable molecular marker for this form of CJD, confirming the original observation made in 10 cases by Collinge *et al* (1996) and extending it to 50 cases of known genotype.
- The type 2B PrP^{res} banding pattern is consistent amongst all vCJD cases to date.
- The type 2B PrP^{res} banding pattern seen in vCJD cases is not restricted to this aetiology. Some familial cases displayed a 1B isotype and the FFI case displayed an isotype similar to vCJD. Familial CJD cases displayed glycoform ratios in the range of vCJD, however, these two groups are distinguished by their isotype or *PRNP* genotype.
- Sole conversion and accumulation of the mutant allele was observed in fCJD V180I, indicating that the mutant allele does not convert the wild type allele to

PrP^{res}. This may be due to the lack of diglycosylation or indicate that the presence of PrP^{res} is not sufficient to bring about conversion of wild type PrP^{c}.

- All sCJD cases had a predominantly monoglycosylated glycoform ratio. In all but the VV 2A subgroup, the unglycosylated band was found in greater levels than the diglycosylated ban.
- Aside from sCJD VV 2A cases and a few MV 1 cases, sCJD subgroups could not be distinguished by their glycoform ratio.
- None of the sCJD glycoform ratios overlapped with vCJD.
- A sCJD MV 1 case carrying an octapeptide repeat deletion had a different glycoform ratio to the other sCJD MV 1 cases.
- Biopsy and autopsy analysis can yield different PrP^{res} isotypes.
- Multiple isotypes were deteced in sCJD, iCJD and fCJD cases.
- Glycoform ratio variation was seen in sCJD, iCJD and fCJD cases.
- Variant CJD cases were consistent in isotype and glycoform ratio throughout the brain.
- PrP^{res} of type 1 and type 2 can occur in the same brain and even in the same brain region. The amounts of each type making up the total PrP^{res} can vary.
- The PrP^{res} glycoform ratio can vary according to specific anatomical regions.
- Cerebellum derived PrP^{res} displays a more pronounced lower monoglycosylated band.
- PrP^{res} from type 1 and INT cases are more susceptible to NH_3-terminal PK cleavage following EDTA treatment than samples from type 2 cases.
- PrP^{res} from vCJD cases does not display a noticeable change in M_r when treated with EDTA and PK. This indicates that either the PrP^{res} is in an 'open' conformation or does not have bound cations, which may be significant in the disease process.
- In mixed isotype samples, the difference in M_r is not due to differential cation binding.
- The presence of cation bound PrP^{res} in GSS suggests that prevention of metal ion binding to PrP is not responsible for the disease process.
- Transmission of vCJD to mice does not result in retention of the 2B isotype in all cases. An intermediate mobility was seen in the majority of cases.
- Neither the mouse strain, *prn-p* genotype or individual vCJD source correlated with the resulting PrP^{res} pattern.

- The glycoform ratios of the murine PrP^{res} featured a greater proportion of diglycosylated PrP^{res} than vCJD cases.
- Murine PrP^{res} has a prominent lower region in the monoglycosylated band.
- Scrapie and BSE derived infections all resulted in predominantly diglycosylated PrP^{res}. FSE and experimental BSE displayed type 2 PrP^{res} while scrapie and BSE displayed type 1.
- The glycoform ratios of the animal derived PrP^{res} was significantly different from vCJD.
- A large number of discrepancies and caveats prevent the use of PrP^{res} molecular strain typing of TSEs and all available data should be taken into consideration when diagnosing cases of CJD.

The hypothesis that the different PrP^{res} banding patterns observed in TSEs correspond to different PrP^{res} conformations that represent a molecular marker of prion strains is not supported by the results of this study. The definition of a 'strain' of prion disease does not extend to the PrP^{res} isotype.

The hypothesis that this molecular marker can be used reliably and consistently to determine TSE aetiology and differentiate between CJD subgroups has not held. The PrP^{res} banding pattern cannot distinguish between sCJD, iCJD and fCJD, or between fCJD and vCJD. The isotype or glycoform ratio analysis could not clearly distinguish sCJD codon 129 subgroups. The co-occurrence of both isotypes can lead to misclassification of cases and undermines attempts to define 'strains' of sCJD based on phenotypic features.

Furthermore correlates between the PrP^{res} banding pattern and the clinico-pathological phenotype could not be established but indicate that there is a relationship between PrP^{res} and the codon 129 polymorphism as well as PrP accumulations, spongiform change and cell specific glycosylation.

The differentiation of sporadic and variant CJD based on the PrP^{res} banding pattern is reliable but does not allow predictions to be made in non-MM cases of vCJD. The use of the distinctive type 2B banding pattern as a marker of the BSE strain in sheep is not exclusive and would be misleading.

References

Adam, J., Crow, T. J., Duchen, L. W., Scaravilli, F., and Spokes, E., 1982, Familial cerebral amyloidosis and spongiform encephalopathy, *J Neurol Neurosurg Psychiatry*, **45**(1):37-45.

Aguzzi, A., and Brandner, S., 1999, Shrinking prions: new folds to old questions., *Nature Medicine*, **5**(5):486-487.

Aguzzi, A., and Weissmann, C., 1996, Sleepless in Bologna: transmission of fatal familial insomnia., *Trends in Microbiology*, **4**:129-132.

Aguzzi, A., and Weissmann, C., 1997, Prion research: the next frontiers., *Nature*, **389**(6653):795-798.

Akhavan-Tafti, H., 1995, Lumigen® PS: Chemiluminescent detection of horseradish peroxidase by enzymatic generation of acridinium esters., *Clinical Chemistry*, **41**(1368):1369.

Aldhous, P., 1990, BSE: spongiform encephalopathy found in cat., *Nature*, **345**(6272):194.

Allan, B., and Tuft, S., 1997, Transmission of Creutzfeldt-Jakob disease in corneal grafts., *BMJ*, **315**:1553-1554.

Alper, T., Cramp, W. A., Haig, D. A., and Clarke, M. C., 1967, Does the agent of scrapie replicate without nucleic acid?, *Nature*, **214**(90):764-766.

Alperovitch, A., Zerr, I., Pocchiari, M., E, M., JdP, C., Hegyi, I., Collins, S., Kretzschmar, H. A., van Duijn, C., and Will, R. G., 1999, Codon 129 prion protein genotype and sporadic Creutzfeldt-Jakob disease., *The Lancet*, **353**:1673-1674.

Anderson, R. M., Donnelly, C. A., Ferguson, N. M., Woolhouse, M. E., Watt, C. J., Udy, H. J., MaWhinney, S., Dunstan, S. P., Southwood, T. R., Wilesmith, J. W., Ryan, J. B., Hoinville, L. J., Hillerton, J. E., Austin, A. R., and Wells, G. A. H., 1996, Transmission dynamics and epidemiology of BSE in British cattle., *Nature*, **382**(6594):779-788.

Antoine, J. C., Michel, D., Bertholon, P., Mosnier, J. F., Laplanche, J. L., Beaudry, P., Hauw, J. J., and Veyret, C., 1997, Creutzfeldt-Jakob disease after extracranial dura mater embolization for a nasopharyngeal angiofibroma., *Neurology*, **48**(5):1451-1453.

Armstrong, R. A., Cairns, N. J., Ironside, J. W., and Lantos, P. L., 2002, Quantitative variations in the pathology of 11 cases of variant Creutzfeldt-Jakob disease (vCJD), *Pathophysiology*, **8**(4):235-241.

Arnold, J. E., Tipler, C., Laszlo, L., Hope, J., Landon, M., and Mayer, R. J., 1995, The abnormal isoform of the prion protein accumulates in late-endosome-like organelles in scrapie-infected mouse brain., *Journal of Pathology*, **176**(4):403-411.

Aucouturier, P., Kascsak, R. J., Frangione, B., and Wisniewski, T., 1999, Biochemical and conformational variability of human prion strains in sporadic Creutzfeldt-Jakob disease, *Neuroscience Letters*, **274**(1):33-36.

Baker, H. E., Poulter, M., T.J., C., Frith, C. D., Lofthouse, R., and R.M., R., 1991, Amino acid polymorphism in human prion protein and age at death in inherited prion disease., *The Lancet*, **337**(8752):1286.

Baker, H. F., R.M., R., and Wells, G. A. H., 1993, Experimental transmission of BSE and scrapie to the common marmoset., *Veterinary Record*, **132**(16):403-406.

Baker, H. F., Ridley, R. M., and Crow, T. J., 1985, Experimental transmission of an autosomal dominant spongiform encephalopathy: does the infectious agent originate in the human genome?, *Br Med J (Clin Res Ed)*, **291**(6491):299-302.

Barcikowska, M., Liberski, P. P., J.W., B., Brown, P., Gajdusek, D. C., and Budka, H., 1993, Microglia is a component of the prion protein amyloid plaque in the Gerstmann-Sträussler-Scheinker syndrome., *Acta Neuropathologica*, **85**:623-627.

Baron, T., P, B., Madec, J. Y., Moutou, F., Vitaud, C., and Savey, M., 1997, Spongiform encephalopathy in an imported cheetah in France., *Veterinary Record*, **141**(11):270-271.

Baron, T. G., and Biacabe, A. G., 2001, Molecular analysis of the abnormal prion protein during coinfection of mice by bovine spongiform encephalopathy and a scrapie agent., *J Virol*, **75**(1):107-114.

Baron, T. G., Madec, J. Y., and Calavas, D., 1999, Similar signature of the prion protein in natural sheep scrapie and bovine spongiform encephalopathy-linked diseases., *J Clin Microbiol*, **37**(11):3701-3704.

Baron, T. G., Madec, J. Y., Calavas, D., Richard, Y., and Barillet, F., 2000, Comparison of French natural scrapie isolates with bovine spongiform encephalopathy and experimental scrapie infected sheep., *Neuroscience Letters*, **284**(3):175-178.

Bartz, J. C., Bessen, R. A., McKenzie, D., Marsh, R. F., and Aiken, J. M., 2000, Adaptation and selection of prion protein strain conformations following interspecies transmission of transmissible mink encephalopathy, *J Virol*, **74**(12):5542-5547.

Bartz, J. C., Marsh, R. F., McKenzie, D. I., and Aiken, J. M., 1998, The host range of chronic wasting disease is altered on passage in ferrets., *Virology*, **251**(2):297-301.

Bartz, J. C., McKenzie, D. I., Bessen, R. A., Marsh, R. F., and Aiken, J. M., 1994, Transmissible mink encephalopathy species barrier effect between ferret and mink: PrP gene and protein analysis., *J Gen Virol*, **75**(Pt 11):2947-2953.

Baskakov, I., Aagaard, C., Mehlhorn, I., Wille, H., Groth, D., Baldwin, M., Prusiner, S. B., and Cohen, F. E., 2000, Self-Assembly of recombinant prion protein of 106 residues., *Biochemistry*, **39**(10):2792-2804.

Beaudry, P., Parchi, P., Peoc'h, K., Desbordes, P., Dartigues, J. F., Vital, A., Vital, C., Capellari, S., Gambetti, P., Delasnerie-Laupretre, N., Mary, J. Y., and Laplanche, J. L., 2002, A French cluster of Creutzfeldt-Jakob disease: a molecular analysis, *Eur J Neurol*, **9**(5):457-462.

Beekes, M., Baldauf, E., Cassens, S., Diringer, H., Keyes, P., Scott, A. C., Wells, G. A. H., Brown, P., Gibbs, C. J. J., and Gajdusek, D. C., 1995, Western blot mapping of disease-specific amyloid in various animal species and humans with transmissible spongiform encephalopathies using a high-yield purification method., *J Gen Virol*, **76**(Pt 10):2567-2576.

Bell, J. E., and Ironside, J. W., 1993a, How to tackle a possible Creutzfeldt-Jakob disease necropsy., *Journal of Clinical Pathology*, **46**(3):193-197.

Bell, J. E., and Ironside, J. W., 1993b, Neuropathology of spongiform encephalopathies in humans., *British Medical Bulletin*, **49**(4):738-777.

Bell, J. E., and Ironside, J. W., 1997, Principles and practice of 'high risk' brain banking., *Neuropathology and Applied Neurobiology*, **23**(4):281-288.

Bendheim, P. E., Brown, H. R., Rudelli, R. D., Scala, L. J., Goller, N. L., Wen, G. Y., Kascsak, R. J., Cashman, N. R., and Bolton, D. C., 1992, Nearly ubiquitous tissue distribution of the scrapie agent precursor protein., *Neurology*, **42**(1):149-156.

Bessen, R. A., Kocisko, D. A., Raymond, G. J., Nandan, S., Lansbury, P. T., and Caughey, B., 1995, Non-genetic propagation of strain-specific properties of scrapie prion protein., *Nature*, **375**(6533):698-700.

Bessen, R. A., and Marsh, R. F., 1992, Biochemical and physical-properties of the prion protein from 2 strains of the transmissible mink encephalopathy agent., *J Virol*, **66**(4):2096-2101.

Bessen, R. A., and Marsh, R. F., 1994, Distinct prp properties suggest the molecular-basis of strain variation in transmissible mink encephalopathy, *J Virol*, **68**(12):7859-7868.

Betmouni, S., Perry, V. H., and Gordon, J. L., 1996, Evidence for an early inflammatory response in the central nervous system of mice with scrapie., *Neuroscience*, **74**(1):1-5.

Blattler, T., Brandner, S., Raeber, A. J., Klein, M. A., Voigtlander, T., Weissmann, C., and Aguzzi, A., 1997, PrP-expressing tissue required for transfer of scrapie infectivity from spleen to brain., *Nature*, **389**(6646):69-73.

Bockman, J. M., Kingsbury, D. T., McKinley, M. P., Bendheim, P. E., and Prusiner, S. B., 1985, Creutzfeldt-Jakob disease prion proteins in human brains., *N Engl J Med*, **312**(2):73-78.

Bode, L., Pocchiari, M., Gelderblom, H., and Diringer, H., 1985, Characterization of antisera against scrapie-associated fibrils (SAF) from affected hamster and cross-reactivity with SAF from scrapie-affected mice and from patients with Creutzfeldt-Jakob disease, *J Gen Virol*, **66 (Pt 11)**:2471-8.

Bons, N., Mestre-Frances, N., Belli, P., Cathala, F., Gajdusek, D. C., and Brown, P., 1999, Natural and experimental oral infection of nonhuman primates by bovine spongiform encephalopathy agents, *Proceedings of the National Academy of Science USA*, **96**(7):4046-4051.

Borchelt, D. R., Rogers, M., Stahl, N., Telling, G., and Prusiner, S. B., 1993, Release of the cellular prion protein from cultured cells after loss of its glycoinositol phospholipid anchor, *Glycobiology*, **3**(4):319-329.

Borchelt, D. R., Scott, M., Taraboulos, A., Stahl, N., and Prusiner, S. B., 1990, Scrapie and cellular prion proteins differ in their kinetics of synthesis and topology in cultured cells., *Journal of Cell Biology*, **110**(3):743-752.

Borchelt, D. R., Taraboulos, A., and Prusiner, S. B., 1992, Evidence for synthesis of scrapie prion proteins in the endocytic pathway., *J Biol Chem*, **267**(23):16188-16199.

Bosque, P. J., Vnencak-Jones, C. L., Johnson, M. D., Whitlock, J. A., and McLean, M. J., 1992, A PrP gene codon 178 base substitution and a 24-bp interstitial deletion in familial Creutzfeldt-Jakob disease., *Neurology*, **42**(10):1864-1870.

Brandner, S., Isenmann, S., Raeber, A., Fischer, M., Sailer, A., Kobayashi, Y., Marino, S., Weissmann, C., and Aguzzi, A., 1996a, Normal host prion protein necessary for scrapie-induced neurotoxicity., *Nature*, **379**(6563):339-343.

Brandner, S., Raeber, A., Sailer, A., Blattler, T., Fischer, M., Weissmann, C., and Aguzzi, A., 1996b, Normal host prion protein (PrPC) is required for scrapie spread within the central nervous system., *Proceedings of the National Academy of Science USA*, **93**(23:13148-51):13148-13151.

Brown, D. R., 1999, Prion protein peptide neurotoxicity can be mediated by astrocytes., *J Neurochem*, **73**(3):1105-1113.

Brown, D. R., Herms, J. W., Schmidt, B., and Kretzschmar, H. A., 1997a, PrP and beta-amyloid fragments activate different neurotoxic mechanisms in cultured mouse cells., *European Journal of Neuroscience*, **9**(6):1162-1169.

Brown, D. R., Qin, K. F., Herms, J. W., Madlung, A., Manson, J., Strome, R., Fraser, P. E., Kruck, T., vonBohlen, A., Schulz-Schaeffer, W., Giese, A., Westaway, D., and Kretzschmar, H., 1997b, The cellular prion protein binds copper in vivo., *Nature*, **390**:684-687.

Brown, D. R., Schmidt, B., and Kretzschmar, H. A., 1996, Role of microglia and host prion protein in neurotoxicity of a prion protein fragment., *Nature*, **380**(6572):345-347.

Brown, D. R., Schulz-Schaeffer, W. J., Schmidt, B., and Kretzschmar, H. A., 1997c, Prion protein-deficient cells show altered response to oxidative stress due to decreased SOD-1 activity., *Experimental Neurology*, **146**(1):104-112.

Brown, D. R., Wong, B. S., Hafiz, F., Clive, C., Haswell, S. J., and Jones, I. M., 1999a, Normal prion protein has an activity like that of superoxide dismutase., *Biochem J*, **344**:1-5.

Brown, K. L., Stewart, K., Ritchie, D. L., Mabbott, N. A., Williams, A., Fraser, H., Morrison, W. I., and Bruce, M. E., 1999b, Scrapie replication in lymphoid tissues depends on prion protein-expressing follicular dendritic cells., *Nature Medicine*, **5**(11):1308-1312.

Brown, P., 1996, Bovine spongiform encephalopathy and Creutzfeldt-Jakob disease., *BMJ*, **312:**790-791.

Brown, P., Cervenakova, L., Goldfarb, L. G., McCombie, W. R., Rubenstein, R., Will, R. G., Pocchiari, M., Martinez-Lage, J. F., Scalici, C., and Masullo, C., 1994a, Iatrogenic Creutzfeldt-Jakob disease: an example of the interplay between ancient genes and modern medicine., *Neurology*, **44**(2):291-293.

Brown, P., Coker-Vann, M., Pomeroy, K., Franko, M., Asher, D. M., Gibbs, C. J. J., and Gajdusek, D. C., 1986a, Diagnosis of Creutzfeldt-Jakob disease by Western blot identification of marker protein in human brain tissue., *N Engl J Med*, **314**(9):547-551.

Brown, P., Gibbs, C. J., P., R.-J., P., A., M.P., S., A., B., Goldfarb, L. G., and Gajdusek, D. C., 1994b, Human spongiform encephalopathy: The National Institutes of Health series of 300 cases of experimentally transmitted disease., *Ann Neurol*, **35**(5):513-529.

Brown, P., Kenney, K., Little, B., Ironside, J. W., Will, R., Cervenakova, L., Bjork, R. J., San Martin, R., Safar, J., and Roos, R., 1995, Intracerebral distribution of infectious amyloid protein in spongiform encephalopathy., *Ann Neurol*, **38**(2):245-253.

Brown, P., Preece, M., Brandel, J. P., Sato, T., McShane, L., Zerr, I., Fletcher, A., Will, R. G., Pocchiari, M., Cashman, N. R., d'Aignaux, J. H., Cervenakova, L., Fradkin, J., Schonberger, L. B., and Collins, S. J., 2000, Iatrogenic Creutzfeldt-Jakob disease at the millennium., *Neurology*, **55**(8):1075-1081.

Brown, P., Preece, M. A., and Will, R. G., 1992, "Friendly fire" in medicine: hormones, homografts, and Creutzfeldt-Jakob disease., *The Lancet*, **340:**24-27.

Brown, P., Rohwer, R. G., and Gajdusek, D. C., 1986b, Newer data on the inactivation of scrapie virus or Creutzfeldt-Jakob disease virus in brain tissue., *The Journal of Infectious Diseases*, **153:**1145-1148.

Bruce, M., A., C., McConnell, I., Foster, J., G.R., P., and Fraser, H., 1994, Transmission of bovine spongiform encephalopathy and scrapie to mice: strain variation and the species barrier., *Philosophical Transactions of the Royal Society of London*, **343:**405-411.

Bruce, M. E., and Dickinson, A. G., 1987, Biological evidence that scrapie agent has an independent genome., *J Gen Virol*, **68**(Pt 1):79-89.

Bruce, M. E., McBride, P. A., and Farquhar, C. F., 1989, Precise targeting of the pathology of the sialoglycoprotein, PrP, and vacuolar degeneration in mouse scrapie., *Neuroscience Letters*, **102**(1):1-6.

Bruce, M. E., Will, R. G., Ironside, J. W., and Fraser, H., 1999, Comparison of the biological characteristics of BSE and CJD in mice., in: *Alzheimer's Disease*

and Related Disorders (I. K., S. DF, W. B., and H. M. Wisniewski, eds.), John Wiley, London, pp. 553-560.

Bruce, M. E., Will, R. G., Ironside, J. W., McConnell, I., Drummond, D., Suttie, A., McCardle, L., A., C., Hope, J., Birkett, C., Cousens, S., Fraser, H., and Bostock, C. J., 1997, Transmissions to mice indicate that 'new variant' CJD is caused by the BSE agent., *Nature*, **389**(6650):498-501.

Budka, H., Aguzzi, A., Brown, P., Brucher, J. M., Bugiani, O., Gullotta, F., Haltia, M., Hauw, J. J., Ironside, J. W., and Jellinger, K., 1995, Neuropathological diagnostic criteria for Creutzfeldt-Jakob disease (CJD) and other human spongiform encephalopathies (prion diseases). *Brain Pathology*, **5**(4):459-466.

Budka, H., Hainfellner, J. A., Almer, G., BrOcke, T., Windl, O., Kretzschmar, H. A., Hill, A., and Collinge, J., 1997, A new Austrian family with fatal familial insomnia: Brain pathology without detectable PrPres., *Brain Pathology*, **7**:1267.

Bueler, H., Aguzzi, A., Sailer, A., Greiner, R. A., Autenried, P., Aguet, M., and Weissmann, C., 1993, Mice devoid of PrP are resistant to scrapie, *Cell*, **73**(7):1339-1347.

Bueler, H., Fischer, M., Lang, Y., Bluethmann, H., H-P., L., DeArmond, S. J., Prusiner, S. B., M, A., and Weissmann, C., 1992, Normal development and behavious of mice lacking the neuronal cell-surface PrP protein, *Nature*, **356**(577):581.

Buschmann, A., Kuczius, T., Bodemer, W., and Groschup, M. H., 1998, Cellular prion proteins of mammalian species display an intrinsic partial proteinase K resistance, *Biochem Biophys Res Commun*, **253**(3):693-702.

Calzolai, L., Lysek, D., Guntert, P., von Schroetter, C., Riek, R., Zahn, R., and Wuthrich, K., 2000, NMR structures of three single-residue variants of the human prion protein., *Proceedings of the National Academy of Science USA*, **97**(15):8340-8345.

Campbell, T. A., Palmer, M. S., Will, R. G., Gibb, W. R., Luthert, P. J., and Collinge, J., 1996, A prion disease with a novel 96-base pair insertional mutation in the prion protein gene., *Neurology*, **46**(3):761-766.

Capellari, S., Parchi, P., Russo, C. M., Sanford, J., Sy, M. S., Gambetti, P., and Petersen, R. B., 2000, Effect of the E200K mutation on prion protein metabolism. Comparative study of a cell model and human brain., *Am J Pathology*, **157**(2):613-622.

Capellari, S., Vital, C., Parchi, P., Petersen, R. B., Ferrer, X., Jarnier, D., Pegoraro, E., Gambetti, P., and J., J., 1997, Familial prion disease with a novel 144-bp insertion in the prion protein gene in a Basque family., *Neurology*, **49**(1):133-141.

Cappai, R., Stewart, L., Jobling, M. F., Thyer, J. M., White, A. R., Beyreuther, K., Collins, S. J., Masters, C., and Barrow, C. J., 1999, Familial prion disease mutation alters the secondary structure of recombinant mouse prion protein:

implications for the mechanism of prion formation., *Biochemistry*, **38**(11):3280-3284.

Cardone, F., Liu, Q. G., Petraroli, R., Ladogana, A., D'Alessandro, M., Arpino, C., Di Bari, M., Macchi, G., and Pocchiari, M., 1999, Prion protein glycotype analysis in familial and sporadic Creutzfeldt-Jakob disease patients., *Brain Research Bulletin*, **49**(6):429-433.

Carlson, G. A., Kingsbury, D. T., Goodman, P. A., Coleman, S., Marshall, S. T., DeArmond, S., Westaway, D., and Prusiner, S. B., 1986, Linkage of prion protein and scrapie incubation time genes., *Cell*, **46**(4):503-511.

Carp, R. I., Meeker, H., and Sersen, E., 1997, Scrapie strains retain their distinctive characteristics following passages of homogenates from different brain regions and spleen., *J Gen Virol*, **78**(Pt 1):283-290.

Castellani, R., Parchi, P., Stahl, J., Capellari, S., Cohen, M., and Gambetti, P., 1996, Early pathologic and biochemical changes in Creutzfeldt-Jakob disease: study of brain biopsies., *Neurology*, **46**(6):1690-1693.

Castellani, R. J., Parchi, P., Madoff, L., Gambetti, P., and McKeever, P., 1997, Biopsy diagnosis of Creutzfeldt-Jakob disease by western blot: a case report., *Human Pathology*, **28**(5):623-626.

Caughey, B., 1991, In vitro expression and biosynthesis of prion protein, *Curr Top Microbiol Immunol*, **172**:93-107.

Caughey, B., 1999, Formation of Protease-Resistant Prion Protein in cell-Free Systems., in: *Prions. Molecular and Cellular Biology.* (D. A. Harris, ed.), Horizon Scientific Press, pp. 27-44.

Caughey, B., Horiuchi, M., Demaimay, R., and Raymond, G. J., 1999, Assays of protease-resistant prion protein and its formation., *Methods Enzymol*, **309**:122-133.

Caughey, B., Race, R. E., Ernst, D., Buchmeier, M. J., and Chesebro, B., 1989, Prion protein biosynthesis in scrapie-infected and uninfected neuroblastoma cells., *J Virol*, **63**(1):175-181.

Caughey, B., and Raymond, G. J., 1991, The scrapie-associated form of PrP is made from a cell surface precursor that is both protease- and phospholipase-sensitive., *J Biol Chem*, **266**(27):18217-18223.

Caughey, B., Raymond, G. J., and Bessen, R. A., 1998, Strain-dependent differences in beta-sheet conformations of abnormal prion protein., *J Biol Chem*, **273**(48):32230-32235.

Caughey, B., Raymond, G. J., Ernst, D., and Race, R. E., 1991, N-terminal truncation of the scrapie-associated form of PrP by lysosomal protease(s): implications regarding the site of conversion of PrP to the protease-resistant state, *J Virol*, **65**(12):6597-6603.

Cervenakova, L., Goldfarb, L., R, G., Lee, H.-S., Gajdusek, D. C., and Brown, P., 1999, Phenotype-genotype studies in kuru: implications for new variant

Creutzfeldt-Jakob disease, *Proceedings of the National Academy of Science USA*, **95:**13239-13241.

Chazot, G., Broussolle, E., Lapras, C., Blattler, T., Aguzzi, A., and Kopp, N., 1996, New variant of Creutzfeldt-Jakob disease in a 26-year-old French man., *The Lancet*, **347**(9009)**:**1181.

Chen, S. G., Parchi, P., Brown, P., Capellari, S., Zou, W., Cochran, E. J., Vnencak-Jones, C. L., J., J., Vital, C., Mikol, J., Lugaresi, E., Autilio-Gambetti, L., and Gambetti, P., 1997, Allelic origin of the abnormal prion protein isoform in familial prion diseases., *Nature Medicine*, **3**(9)**:**1009-1015.

Chen, S. G., Teplow, D. B., Parchi, P., Teller, J. K., Gambetti, P., and Autilio-Gambetti, L., 1995, Truncated forms of the human prion protein in normal brain and in prion diseases., *J Biol Chem*, **270**(32)**:**19173-19180.

Choi, S. I., Ju, W. K., Choi, E. K., Kim, J., Lea, H. Z., Carp, R. I., Wisniewski, H. M., and Kim, Y. S., 1998, Mitochondrial dysfunction induced by oxidative stress in the brains of hamsters infected with the 263 K scrapie agent., *Acta Neuropathologica*, **96**(3)**:**279-286.

Clinton, J., Forsyth, C., Royston, M. C., and Roberts, G. W., 1993, Synaptic degeneration is the primary neuropathological feature in prion disease - a preliminary-study., *Neuroreport*, **4:**65-68.

Collee, J. G., 1996, A dreadful challenge., *The Lancet*, **347**(9006)**:**917-918.

Collinge, J., Brown, J., Hardy, J., Mullan, M., Rossor, M. N., Baker, H., Crow, T. J., Lofthouse, R., Poulter, M., Ridley, R., and et al., 1992, Inherited prion disease with 144 base pair gene insertion. 2. Clinical and pathological features, *Brain*, **115**((Pt 3))**:**687-710.

Collinge, J., Owen, F., Poulter, M., M., L., T.J., C., Rossor, M. N., J., H., Mullan, M. J., I., J., and Lantos, P. L., 1990, Prion dementia without characteristic pathology., *The Lancet*, **336:**7-22.

Collinge, J., Palmer, M. S., Sidle, K. C., Gowland, I., Medori, R., Ironside, J. W., and Lantos, P., 1995, Transmission of fatal familial insomnia to laboratory animals . *The Lancet*, **346**(8974)**:**569-570.

Collinge, J., Sidle, K. C., Meads, J., Ironside, J. W., and Hill, A. F., 1996, Molecular analysis of prion strain variation and the aetiology of 'new variant' CJD., *Nature*, **383**(6602)**:**685-690.

Collinge, J., Whittington, M. A., Palmer, M. S., Smith, C. J., Clarke, A. R., and Jeffreys, J. J., 1994, Prion protein is necessary for normal synaptic function., *Nature*, **370:**295-297.

Collins, S., A, B., Fletcher, A., Byron, K., Harper, C., McLean, C. A., and Masters, C., 2000, Novel prion protein gene mutation in an octogenarian with Creutzfeldt-Jakob disease., *Arch Neurol*, **57**(7)**:**1058-1063.

DeArmond, S. J., 1999, PrPc Glycoform heterogeneity as a function of brain region: Implications for selective targeting of neurons by prion strains, *Journal of Neuropathology & Experimental Neurology*, **58:**1000-1009.

DeArmond, S. J., Nixon, R., and Qiu, Y., 1997a, Mechanisms of cell dysfunction in prion diseases: PrPSc accumulation in plasma membrane, *Brain Pathology*, **7:**1267.

DeArmond, S. J., Sanchez, H., Yehiely, F., Qiu, Y., Ninchak-Casey, A., Daggett, V., Camerino, A. P., Cayetano, J., Rogers, M., Groth, D., Torchia, M., Tremblay, P., Scott, M. R., Cohen, F. E., and Prusiner, S. B., 1997b, Selective neuronal targeting in prion disease., *Neuron*, **19**(6)**:**1337-1348.

DeArmond, S. J., Yang, S. L., Lee, A., Bowler, R., Taraboulos, A., Groth, D., and Prusiner, S. B., 1993, 3 Scrapie prion isolates exhibit different accumulation patterns of the prion protein scrapie isoform, *Proceedings of the National Academy of Science USA*, **90:**6449-6453.

DebBurman, S. K., Raymond, G. J., Caughey, B., and Lindquist, S., 1997, Chaperone-supervised conversion of prion protein to its protease-resistant form., *Proceedings of the National Academy of Science USA*, **94**(25)**:**13938-13943.

Demart, S., Fournier, J. G., Creminon, C., Frobert, Y., Lamoury, F., Marce, D., Lasmezas, C., Dormont, D., Grassi, J., and Deslys, J. P., 1999, New insight into abnormal prion protein using monoclonal antibodies, *Biochem Biophys Res Commun*, **265**(3)**:**652-657.

Dennis, J. W., Granovsky, M., and Warren, C. E., 1999, Protein glycosylation in development and disease, *Bioessays*, **21**(5)**:**412-21.

Deslys, J. P., Jaegly, A., d'Aignaux, J. H., Mouthon, F., de Villemeur, T., and Dormont, D., 1998, Genotype at codon 129 and susceptibility to Creutzfeldt-Jakob disease., *The Lancet*, **351**(9111)**:**1251.

Deslys, J. P., Lasmezas, C., and Dormont, D., 1994, Selection of specific strains in iatrogenic Creutzfeldt-Jakob disease., *The Lancet*, **343**(8901)**:**848-849.

Deslys, J. P., Lasmezas, C. I., Streichenberger, N., Hill, A., Collinge, J., Dormont, D., and Kopp, N., 1997, New variant Creutzfeldt-Jakob disease in France., *The Lancet*, **349**(9044)**:**30-31.

Dickinson, A. G., Fraser, H., McConnell, I., Outram, G. W., Sales, D. I., and Taylor, D. M., 1975, Extraneural competition between different scrapie agents leading to loss of infectivity, *Nature*, **253**(5492)**:**556.

Dickinson, A. G., Fraser, H., Meikle, V. M., and Outram, G. W., 1972, Competition between different scrapie agents in mice, *Nat New Biol*, **237**(77)**:**244-245.

Dorandeu, A., Wingertsmann, L., Chretien, F., Delisle, M. B., Vital, C., Parchi, P., Montagna, P., Lugaresi, E., Ironside, J. W., Budka, H., Gambetti, P., and Gray, F., 1998, Neuronal apoptosis in fatal familial insomnia., *Brain Pathology*, **8**(3)**:**531-537.

Edenhofer, F., Rieger, R., Famulok, M., Wendler, W., Weiss, S., and Winnacker, E. L., 1996, Prion protein PrPc interacts with molecular chaperones of the Hsp60 family., *J Virol*, **70**(7):4724-4728.

el Hachimi, K., Chaunu, M. P., Cervenakova, L., Brown, P., and Foncin, J. F., 1997, Putative neurosurgical transmission of Creutzfeldt-Jakob disease with analysis of donor and recipient: agent strains., *C R Acad Sci III*, **320**(4):319-328.

Endo, T., Groth, D., Prusiner, S. B., and Kobata, A., 1989, Diversity of oligosaccharide structures linked to asparagines of the scrapie prion protein., *Biochemistry*, **28**:8380-8388.

Farquhar, C. F., Somerville, R. A., and Bruce, M. E., 1998, Straining the prion hypothesis., *Nature*, **391**(6665):345-346.

Fischer, M. B., Roeckl, C., Parizek, P., Schwarz, H. P., and Aguzzi, A., 2000, Binding of disease-associated prion protein to plasminogen., *Nature*, **408**(6811):479-483.

Foster, J. D., Bruce, M., McConnell, I., A., C., and Fraser, H., 1996, Detection of BSE infectivity in brain and spleen of experimentally infected sheep., *Veterinary Record*, **138**(22):546-548.

Foster, J. D., Hope, J., and Fraser, H., 1993, Transmission of bovine spongiform encephalopathy to sheep and goats., *Veterinary Record*, **133**(14):339-341.

Fraser, H., G.R., P., McConnell, I., Bruce, M. E., Wyatt, J. M., and T.J., G.-J., 1994, Transmission of feline spongiform encephalopathy to mice., *Veterinary Record*, **134**(17):449.

Gabizon, R., Halimi, M., and Meiner, Z., 1994, Genetics and biochemistry of Creutzfeldt-Jakob disease in Libyan Jews, *Biomed Pharmacother*, **48**(8-9):385-90.

Gabizon, R., Telling, G., Meiner, Z., Halimi, M., Kahana, I., and Prusiner, S. B., 1996, Insoluble wild-type and protease-resistant mutant prion protein in brains of patients with inherited prion disease., *Nature Medicine*, **2**(1):59-64.

Gajdusek, D. C., 1977, Unconventional viruses and the origin and disappearance of kuru, *Science*, **197**(4307):943-960.

Gambetti, P., Parchi, P., Petersen, R. B., Chen, S. G., and Lugaresi, E., 1995, Fatal familial insomnia and familial Creutzfeldt-Jakob disease: clinical, pathological and molecular features., *Brain Pathology*, **5**(1):43-51.

Ghetti, B., Piccardo, P., Spillantini, M. G., Ichimiya, Y., Porro, M., Perini, F., Kitamoto, T., Tateishi, J., Seiler, C., Frangione, B., Bugiani, O., Giaccone, G., Prelli, F., Goedert, M., Dlouhy, S. R., and Tagliavini, F., 1996, Vascular variant of prion protein cerebral amyloidosis with tau-positive neurofibrillary tangles: the phenotype of the stop codon 145 mutation in PRNP., *Proceedings of the National Academy of Science USA*, **93**(2):744-748.

Gilch, S., Spielhaupter, C., and Schatzl, H. M., 2000, Shortest known prion protein allele in highly BSE-susceptible lemurs., *Biol Chem*, **381**(5-6):521-523.

Gill, A. C., Ritchie, M. A., Hunt, L. G., Steane, S. E., Davies, K. G., Bocking, S. P., Rhie, A. G., Bennett, A. D., and Hope, J., 2000, Post-translational hydroxylation at the N-terminus of the prion protein reveals presence of PPII structure in vivo., *EMBO Journal*, **19**(20):5324-5331.

Goldfarb, L. G., Brown, P., Cervenakova, L., and Gajdusek, D. C., 1994, Molecular genetic studies of Creutzfeldt-Jakob disease., *Mol Neurobiol*, **8**(2-3):89-97.

Goldfarb, L. G., Brown, P., McCombie, W. R., Goldgaber, D., Swergold, G. D., Wills, P. R., Cervenakova, L., Baron, H., Gibbs, C. J. J., and Gajdusek, D. C., 1991, Transmissible familial Creutzfeldt-Jakob disease associated with five, seven, and eight extra octapeptide coding repeats in the PRNP gene., *Proceedings of the National Academy of Science USA*, **88**(23):10926-10930.

Goldmann, W., Chong, A., Foster, J., Hope, J., and N., H., 1998, The shortest known prion protein gene allele occurs in goats, has only three octapeptide repeats and is non-pathogenic., *J Gen Virol*, **79**(Pt 12):3173-3176.

Goodbrand, I. A., Ironside, J. W., Nicolson, D., and Bell, J. E., 1995, Prion protein accumulation in the spinal cords of patients with sporadic and growth hormone associated Creutzfeldt-Jakob disease, *Neuroscience Letters*, **183**(1-2):127-130.

Gray, F., Chretien, F., Adle-Biassette, H., Dorandeu, A., Ereau, T., Delisle, M. B., Kopp, N., Ironside, J. W., and Vital, C., 1999, Neuronal apoptosis in Creutzfeldt-Jakob disease., *Journal of Neuropathology & Experimental Neurology*, **58**(4):321-328.

Griffith, J. S., 1967, Self-replication and scrapie, *Nature*, **215**(105):1043-1044.

Groschup, M. H., Beekes, M., McBride, P. A., Hardt, M., Hainfellner, J. A., and Budka, H., 1999, Deposition of disease-associated prion protein involves the peripheral nervous system in experimental scrapie., *Acta Neuropathol (Berl)*, **98**(5):453-457.

Groschup, M. H., Junghans, F., Eiden, M., and Kuczius, T., 2001, Characterization of Bovine spongiform Encephalopathy and Scrapie Strains/Isolates by Immunochemical Analysis of PrP^{sc}, in: *Molecular Pathology of the Prions* (H. F. Baker, ed.), Humana Press Inc.,, Totowa, NJ, pp. 71-82.

Groschup, M. H., Weiland, F., Straub, O. C., and Pfaff, E., 1996, Detection of scrapie agent in the peripheral nervous system of a diseased sheep, *Neurobiol Dis*, **3**(3):191-195.

Hainfellner, J. A., and Budka, H., 1999, Disease associated prion protein may deposit in the peripheral nervous system in human transmissible spongiform encephalopathies., *Acta Neuropathol (Berl)*, **98**(5):458-460.

Hainfellner, J. A., Liberski, P. P., Guiroy, D. C., Cervenakova, L., Brown, P., Gajdusek, D. C., and Budka, H., 1997, Pathology and immunocytochemistry of a kuru brain., *Brain Pathology*, **7**(1):547-553.

Hainfellner, J. A., Parchi, P., Kitamoto, T., Jarius, C., Gambetti, P., and Budka, H., 1999, A novel phenotype in familial Creutzfeldt-Jakob disease: prion protein

gene E200K mutation coupled with valine at codon 129 and type 2 protease-resistant prion protein., *Ann Neurol*, **45**(6):812-816.

Haraguchi, T., Fisher, S., Olofsson, S., Endo, T., Groth, D., Tarentino, A., Borchelt, D. R., Teplow, D., Hood, L., and Burlingame, A., 1989, Asparagine-linked glycosylation of the scrapie and cellular prion proteins., *Archives of Biochemistry & Biophysics*, **274**(1):1-13.

Hardt, M., Baron, T., and Groschup, M. H., 2000, A comparative study of immunohistochemical methods for detecting abnormal prion protein with monoclonal and polyclonal antibodies., *J Comp Pathology*, **122**(1):43-53.

Hauw, J., Sazdovitch, V., Laplanche, J., Peoc, Kopp, N., Kemeny, J., Privat, N., Delasnerie-Laupretre, N., Brandel, J. P., Deslys, J. P., Dormont, D., and A, A., 2000, Neuropathologic variants of sporadic creutzfeldt-jakob disease and codon 129 of PrP gene., *Neurology*, **54**(8):1641-1646.

Head, M. W., 2001, Molecular aspects of variant Creutzfeldt-Jakob disease., *Review Series Dementia*, **1**(1):1-7.

Head, M. W., Northcott, V., Rennison, K., Ritchie, D., McCardle, L., Bunn, T. J., McLennan, N. F., Ironside, J. W., Tullo, A. B., and Bonshek, R. E., 2003, Prion protein accumulation in eyes of patients with sporadic and variant creutzfeldt-jakob disease, *Invest Ophthalmol Vis Sci*, **44**(1):342-6.

Head, M. W., Tissingh, G., Uitdehaag, B. M. J., Barkhof, F., Bunn, T., Ironside, J. W., and Scheltens, P., 2001, Sporadic Creutzfeldt-Jakob Disease in a Young Dutch Valine Homozygote: Atypical Molecular Phenotype, *Annals of Neurology*, **50**(2):258-261.

Hecker, R., Taraboulos, A., Scott, M., Pan, K. M., Yang, S. L., Torchia, M., Jendroska, K., DeArmond, S. J., and Prusiner, S. B., 1992, Replication of distinct scrapie prion isolates is region specific in brains of transgenic mice and hamsters., *Genes & Development*, **6**(7):1213-1228.

Hegde, R. S., Mastrianni, J. A., Scott, M. R., DeFea, K. A., Tremblay, P., Torchia, M., DeArmond, S. J., Prusiner, S. B., and Lingappa, V. R., 1998, A transmembrane form of the prion protein in neurodegenerative disease., *Science*, **279**(5352):827-834.

Herms, J., Tings, T., Gall, S., Madlung, A., Giese, A., Siebert, H., Schurmann, P., Windl, O., Brose, N., and Kretzschmar, H., 1999, Evidence of presynaptic location and function of the prion protein., *J Neurosci*, **19**(20):8866-8875.

Herms, J. W., Korte, S., Gall, S., Schneider, I., Dunker, S., and Kretzschmar, H. A., 2000, Altered Intracellular Calcium Homeostasis in Cerebellar Granule Cells of Prion Protein-Deficient Mice., *J Neurochem*, **75**(4):1487-1492.

Hill, A., 1998, Molecular studies of human prion proteins, in: *Department of Neurogenetics*, Imperial College, London.

Hill, A. F., Antoniou, M., and Collinge, J., 1999a, Protease-resistant prion protein produced in vitro lacks detectable infectivity., *J Gen Virol*, **80**(Pt 1):11-14.

Hill, A. F., Butterworth, R. J., Joiner, S., Jackson, G., Rossor, M. N., Thomas, D. J., Frosh, A., Tolley, N., Bell, J. E., Spencer, M., King, A., al-Sarraj, S., Ironside, J. W., Lantos, P. L., and Collinge, J., 1999b, Investigation of variant Creutzfeldt-Jakob disease and other human prion diseases with tonsil biopsy samples., *The Lancet*, **353**(9148):183-189.

Hill, A. F., and Collinge, J., 2001, Strain Variations and Species Barriers., in: *Prions. A Challenge for Science.* (H. F. Rabenau, J. Cinatl, and H. W. Doerr, eds.), Medicine and Public Health System. Contrib Microb., pp. 48-57.

Hill, A. F., Desbruslais, M., Joiner, S., Sidle, K. C., Gowland, I., Collinge, J., Doey, L. J., and Lantos, P., 1997a, The same prion strain causes vCJD and BSE., *Nature*, **389**(6650):448-450,526.

Hill, A. F., Joiner, S., Linehan, J., Desbruslais, M., Lantos, P. L., and Collinge, J., 2000, Species-barrier-independent prion replication in apparently resistant species., *Proceedings of the National Academy of Science USA*, **97**(18):10248-10253.

Hill, A. F., Sidle, K. C., Joiner, S., Keyes, P., Martin, T. C., Dawson, M., and Collinge, J., 1998, Molecular screening of sheep for bovine spongiform encephalopathy., *Neuroscience Letters*, **255**(3):159-162.

Hill, A. F., Will, R. G., Ironside, J. W., and Collinge, J., 1997b, Type of prion protein in UK farmers with Creutzfeldt-Jakob disease., *The Lancet*, **350**(9072):188.

Hill, A. F., Zeidler, M., Ironside, J. W., and Collinge, J., 1997c, Diagnosis of new variant Creutzfeldt-Jakob disease by tonsil biopsy., *The Lancet*, **349**(9045):99-100.

Hilton, D. A., Fathers, E., Edwards, P., Ironside, J. W., and Zajicek, J., 1998, Prion immunoreactivity in appendix before clinical onset of variant Creutzfeldt-Jakob disease., *The Lancet*, **352**(9129):703-704.

Hope, J., Morton, L. J., Farquhar, C. F., Multhaup, G., Beyreuther, K., and Kimberlin, R. H., 1986, The major polypeptide of scrapie-associated fibrils (SAF) has the same size, charge distribution and N-terminal protein sequence as predicted for the normal brain protein (PrP), *Embo J*, **5**(10):2591-7.

Hope, J., Wood, S. C., Birkett, C. R., Chong, A., Bruce, M. E., Cairns, D., Goldmann, W., N., H., and Bostock, C. J., 1999, Molecular analysis of ovine prion protein identifies similarities between BSE and an experimental isolate of natural scrapie, CH1641., *J Gen Virol*, **80**(Pt 1):1-4.

Horiuchi, M., Nemoto, T., Ishiguro, N., Furuoka, H., Mohri, S., and Shinagawa, M., 2002, Biological and biochemical characterization of sheep scrapie in Japan, *J Clin Microbiol*, **40**(9):3421-6.

Hornshaw, M. P., McDermott, J. R., Candy, J. M., and Lakey, J. H., 1995, Copper binding to the N-terminal tandem repeat region of mammalian and avian prion protein: structural studies using synthetic peptides., *Biochem Biophys Res Commun*, **214**(3):993-999.

Hsiao, K., Baker, H. F., Crow, T. J., Poulter, M., Owen, F., Terwilliger, J., Westaway, D., Ott, J., and Prusiner, S. B., 1989, Linkage of a prion protein missense variant to Gerstmann-Straussler syndrome., *Nature*, **338**(6213):342-345.

Hsiao, K., and Prusiner, S. B., 1990, Inherited human prion diseases., *Neurology*, **40:**1820-1827.

Hsiao, K. K., Groth, D., Scott, M., Yang, S. L., Serban, H., Rapp, D., Foster, D., Torchia, M., DeArmond, S. J., and Prusiner, S. B., 1994, Serial transmission in rodents of neurodegeneration from transgenic mice expressing mutant prion protein., *Proceedings of the National Academy of Science USA*, **91**(19):9126-9130.

Huillard, Costagliola, D., Maccario, J., Billette de Villemeur, T., Brandel, J. P., Deslys, J. P., Hauw, J. J., Chaussain, J. L., Agid, Y., Dormont, D., and A, A., 1999, Incubation period of Creutzfeldt-Jakob disease in human growth hormone recipients in France., *Neurology*, **53**(6):1197-1201.

Ikeda, T., Horiuchi, M., Ishiguro, N., Muramatsu, Y., Kai-Uwe, G. D., and Shinagawa, M., 1995, Amino acid polymorphisms of PrP with reference to onset of scrapie in Suffolk and Corriedale sheep in Japan., *J Gen Virol*, **76**(Pt 10):2577-2581.

Ilangumaran, S., Robinson, P. J., and Hoessli, D. C., 1996, Transfer of exogenous glycosylphosphatidylinositol(GPI)-linked molecules to plasma membranes., *Trends in Cell Biology*, **6:**163-167.

Imperiali, B., and Rickert, K. W., 1995, Conformational implications of asparagine-linked glycosylation., *Proceedings of the National Academy of Science USA*, **92**(1):97-101.

Ironside, J. W., 1998, Neuropathological findings in new variant CJD and experimental transmission of BSE., *FEMS Immunology & Medical Microbiology*, **21**(2):91-95.

Ironside, J. W., and Bell, J. E., 1997, Florid plaques and new variant Creutzfeldt-Jakob disease., *The Lancet*, **350**(9089):1475.

Ironside, J. W., Bell, J. E., and Hayward, P. A. R., 1992a, Glial and neuronal reactions in Creutzfeldt-Jakob disease., *Clinical Neuropathology*, **ii:**226.

Ironside, J. W., Bell, J. E., and McCardle, L., 1992b, Neuronal and glial reactions in Creutzfeldt-Jakob disease., *Neuropathology and Applied Neurobiology*, **18:**295.

Ironside, J. W., C., B., McCardle, L., and Bell, J. E., 1993a, Microglial cell reactions in human spongiform encephalopathies., *Neuropathology and Applied Neurobiology*, **19**(2):57.

Ironside, J. W., Head, M. W., Bell, J. E., McCardle, L., and Will, R. G., 2000, Laboratory diagnosis of variant Creutzfeldt-Jakob disease., *Histopathology*, **37**(1):1-9.

Ironside, J. W., Knight, R. S., Will, R. G., Smith, P. G., and Cousens, S. N., 1998, New variant Creutzfeldt-Jakob disease is more common in Britain than elsewhere., *BMJ*, **317**(7154):352.

Ironside, J. W., McCardle, L., Hayward, P. A., and Bell, J. E., 1993b, Ubiquitin immunocytochemistry in human spongiform encephalopathies., *Neuropathology and Applied Neurobiology*, **19**(2):134-140.

Ironside, J. W., Sutherland, K., Bell, J. E., McCardle, L., C., B., Estebeiro, K., Zeidler, M., and Will, R. G., 1996, A new variant of Creutzfeldt-Jakob disease: neuropathological and clinical features., *Cold Spring Harbor Symposia on Quantitative Biology*, **61**:523-530.

Jackson, G. S., Beck, J. A., Navarrete, C., Brown, J., Sutton, P. M., Contreras, M., and Collinge, J., 2001, HLA-DQ7 antigen and resistance to variant CJD., *Nature*, **414**:269-270.

Jackson, G. S., and Collinge, J., 2001, The molecular pathology of CJD: old and new variants, *Mol Pathology*, **54**(6):393-399.

Jackson, G. S., Hill, A. F., Joseph, C., Hosszu, L., Power, A., Waltho, J. P., Clarke, A. R., and Collinge, J., 1999a, Multiple folding pathways for heterologously expressed human prion protein., *Biochim Biophys Acta*, **1431**(1):1-13.

Jackson, G. S., Hosszu, L. L., Power, A., Hill, A. F., Kenney, J., Saibil, H., Craven, C. J., Waltho, J. P., Clarke, A. R., and Collinge, J., 1999b, Reversible conversion of monomeric human prion protein between native and fibrilogenic conformations., *Science*, **283**(5409):1935-1937.

Jany, K. D., and Mayer, B., 1985, Proteinase K from Tritirachium album limber. I. Molecular mass and sequence around the active site serine residue, *Biol Chem Hoppe Seyler*, **366**(5):485-92.

Jeffrey, M., Goodbrand, I. A., and Goodsir, C. M., 1995, Pathology of the transmissible spongiform encephalopathies with special emphasis on ultrastructure., *Micron*, **26**(3):277-298.

Jeffrey, M., Goodsir, C. M., Bruce, M., McBride, P. A., Scott, J. R., and Halliday, W. G., 1994, Correlative light and electron-microscopy studies of prp localization in 87v scrapie., *Brain Research*, **656**:329-343.

Jimenez-Huete, A., Lievens, P. M., Vidal, R., Piccardo, P., Ghetti, B., Tagliavini, F., Frangione, B., and Prelli, F., 1998, Endogenous proteolytic cleavage of normal and disease-associated isoforms of the human prion protein in neural and non-neural tissues, *Am J Pathology*, **153**(5):1561-1572.

Kaneko, K., Peretz, D., Pan, K. M., Blochberger, T. C., Wille, H., Gabizon, R., Griffith, O. H., Cohen, F. E., Baldwin, M. A., and Prusiner, S. B., 1995, Prion protein (PrP) synthetic peptides induce cellular PrP to acquire properties of the scrapie isoform., *Proceedings of the National Academy of Science USA*, **92**(24):11160-11164.

Kaneko, K., Wille, H., Mehlhorn, I., Zhang, H., Ball, H., Cohen, F. E., Baldwin, M. A., and Prusiner, S. B., 1997a, Molecular properties of complexes formed between the prion protein and synthetic peptides., *J Mol Biol*, **270**(4):574-586.

Kaneko, K., Zulianello, L., Scott, M., Cooper, C. M., Wallace, A. C., James, T. L., Cohen, F. E., and Prusiner, S. B., 1997b, Evidence for protein X binding to a discontinuous epitope on the cellular prion protein during scrapie prion propagation., *Proceedings of the National Academy of Science USA*, **94**(19):10069-10074.

Kascsak, R. J., Rubenstein, R., Merz, P. A., Tonna-DeMasi, M., Fersko, R., Carp, R. I., Wisniewski, H. M., and Diringer, H., 1987, Mouse polyclonal and monoclonal antibody to scrapie-associated fibril proteins., *J Virol*, **61**(12):3688-3693.

Katamine, S., Nishida, N., Sugimoto, T., Noda, T., Sakaguchi, S., Shigematsu, K., Kataoka, Y., Nakatani, A., Hasegawa, S., Moriuchi, R., and Miyamoto, T., 1998, Impaired motor coordination in mice lacking prion protein, *Cell Mol Neurobiol*, **18**(6):731-742.

Kawahara, M., Kuroda, Y., Arispe, N., and Rojas, E., 2000, Alzheimer's beta - amyloid, human islet amylin, and prion protein fragment evoke intracellular free calcium elevations by a common mechanism in a hypothalamic GnRH neuronal cell line., *J Biol Chem*, **275**(19):14077-14083.

Kawashima, T., Furukawa, H., Doh-ura, K., and Iwaki, T., 1997, Diagnosis of new variant Creutzfeldt-Jakob disease by tonsil biopsy., *The Lancet*, **350**(9070):68-69.

Kelly, J. W., 1998, The environmental dependency of protein folding best explains prion and amyloid diseases., *Proceedings of the National Academy of Science USA*, **95**(3):930-932.

Kenward, N., Landon, M., Laszlo, L., and Mayer, R. J., 1996, Heat shock proteins, molecular chaperones and the prion encephalopathies., *Cell Stress & Chaperones*, **1**(1):18-22.

Kimberlin, R. H., and Walker, C. A., 1978, Evidence that the transmission of one source of scrapie agent to hamsters involves separation of agent strains from a mixture, *J Gen Virol*, **39**(3):487-496.

Kirkwood, J. K., Cunningham, A. A., Wells, G. A. H., Wilesmith, J. W., and Barnett, J. E., 1993, Spongiform encephalopathy in a herd of greater kudu (Tragelaphus strepsiceros): epidemiological observations., *Veterinary Record*, **133**(15):360-364.

Kitamoto, T., Yamaguchi, K., Doh-ura, K., and Tateishi, J., 1991, A prion protein missense variant is integrated in kuru plaque cores in patients with Gerstmann-Straussler syndrome., *Neurology*, **41**:306-310.

Klein, M. A., Frigg, R., Flechsig, E., Raeber, A. J., Kalinke, U., Bluethmann, H., Bootz, F., Suter, M., Zinkernagel, R. M., and Aguzzi, A., 1997, A crucial role for B cells in neuroinvasive scrapie., *Nature*, **390**(6661):687-690.

Kocisko, D. A., Come, J. H., Priola, S. A., Chesebro, B., Raymond, G. J., Lansbury, P. T., and Caughey, B., 1994, Cell-free formation of protease-resistant prion protein., *Nature*, **370**(6489):471-474.

Kocisko, D. A., Priola, S. A., Raymond, G. J., Chesebro, B., Lansbury, P. T., Jr., and Caughey, B., 1995, Species specificity in the cell-free conversion of prion protein to protease-resistant forms: a model for the scrapie species barrier, *Proceedings of the National Academy of Science USA*, **92**(9):3923-3927.

Korth, C., Kaneko, K., and Prusiner, S. B., 2000, Expression of unglycosylated mutated prion protein facilitates PrP^{sc} formation in neuroblastoma cells infected with different prion strains., *J Gen Virol*, **81**(2555):2563.

Korth, C., Stierli, B., Streit, P., Moser, M., Schaller, O., Fischer, R., Schulz-Schaeffer, W., Kretzschmar, H., Raeber, A., Braun, U., Ehrensperger, F., Hornemann, S., Glockshuber, R., Riek, R., Billeter, M., Wuthrich, K., and Oesch, B., 1997, Prion (PrPSc)-specific epitope defined by a monoclonal antibody., *Nature*, **390**(6655):74-77.

Kovacs, G. G., Head, M. W., Bunn, T., Laszlo, L., Will, R. G., and Ironside, J. W., 2000, Clinicopathological phenotype of codon 129 valine homozygote sporadic creutzfeldt-jakob disease., *Neuropathology and Applied Neurobiology*, **26**(5):463-472.

Kovacs, G. G., Head, M. W., Hegyi, I., Bunn, T. J., Flicker, H., Hainfellner, J. A., McCardle, L., Laszlo, L., Jarius, C., and Ironside et, a., 2002, Immunohistochemistry for the prion protein: comparison of different monoclonal antibodies in human prion disease subtypes, *Brain Pathology (Zurich, Switzerland)*, **12**(1):1-11.

Kristensson, K., Feuerstein, B., Taraboulos, A., Hyun, W. C., Prusiner, S. B., and DeArmond, S. J., 1993, Scrapie prions alter receptor-mediated calcium responses in cultured cells, *Neurology*, **43**(11):2335-2341.

Kuczius, T., and Groschup, M. H., 1999, Differences in proteinase K resistance and neuronal deposition of abnormal prion proteins characterize Bovine Spongiform Encephalopathy (BSE) and scrapie strains., *Molecular Medicine*, **5**:406-418.

Kuczius, T., Haist, I., and Groschup, M. H., 1998, Molecular analysis of bovine spongiform encephalopathy and scrapie strain variation., *J Infect Dis*, **178**(3):693-699.

Kuwahara, C., AM, M., Nishimura, T., Haraguchi, K., A, K., Y, M., Saeki, K., Yokoyama, T., S, I., and T, O., 1999, Prions prevent neuronal cell-line death., *Nature*, **400**:225-226.

Laemmli, U. K., 1970, Cleavage of structural proteins during the assembly of the head of bacteriophage T4., *Nature*, **227**(259):680-685.

Lantos, P. L., Bhatia, K., Doey, L. J., al-Sarraj, S., Doshi, R., Beck, J., and Collinge, J., 1997, Is the neuropathology of new variant Creutzfeldt-Jakob disease and kuru similar?, *The Lancet*, **350**(9072):187-188.

Lasmezas, C. I., Deslys, J. P., Demaimay, R., Adjou, K. T., Hauw, J. J., and Dormont, D., 1996a, Strain specific and common pathogenic events in murine models of scrapie and bovine spongiform encephalopathy., *J Gen Virol*, **77**(Pt7):1601-1609.

Lasmezas, C. I., Deslys, J. P., Demalmay, R., Adjou, K. T., Lamoury, F., Dormont, D., O, R., Ironside, J. W., and Hauw, J. J., 1996b, BSE transmission to macaques., *Nature*, **381**(6585):743-744.

Lasmezas, C. I., Deslys, J. P., O, R., Jaegly, A., Beringue, V., Peyrin, J. M., Fournier, J. G., Hauw, J. J., Rossier, J., and Dormont, D., 1997, Transmission of the BSE agent to mice in the absence of detectable abnormal prion protein., *Science*, **275**(5298):402-405.

Lee, H. S., Brown, P., Cervenakova, L., Garruto, R. M., Alpers, M. P., Gajdusek, D. C., and Goldfarb, L. G., 2001, Increased susceptibility to Kuru of carriers of the PRNP 129 methionine/methionine genotype, *J Infect Dis*, **183**(2):192-196.

Lee, H. S., Sambuughin, N., Cervenakova, L., Chapman, J., Pocchiari, M., Litvak, S., Qi, H. Y., Budka, H., del, S. T., Furukawa, H., Brown, P., Gajdusek, D. C., Long, J. C., Korczyn, A. D., and Goldfarb, L. G., 1999, Ancestral Origins and Worldwide Distribution of the PRNP 200K Mutation Causing Familial Creutzfeldt-Jakob Disease., *Am J Hum Genet*, **64**(4):1063-1070.

Lee, I. Y., Westaway, D., Smit, A. F., Wang, K., Seto, J., Chen, L., Acharya, C., Ankener, M., Baskin, D., Cooper, C., Yao, H., Prusiner, S. B., and Hood, L. E., 1998, Complete genomic sequence and analysis of the prion protein gene region from three mammalian species, *Genome Res*, **8**(10):1022-1037.

Leggett, M. M., Dukes, J., and Pirie, H. M., 1990, A spongiform encephalopathy in a cat., *Veterinary Record*, **127**(24):586-588.

Lehmann, S., Daude, N., and Harris, D. A., 1997, A wild-type prion protein does not acquire properties of the scrapie isoform when coexpressed with a mutant prion protein in cultured cells., *Molecular Brain Research*, **52**(1):139-145.

Lehmann, S., and Harris, D. A., 1996, Two mutant prion proteins expressed in cultured cells acquire biochemical properties reminiscent of the scrapie isoform, *Proceedings of the National Academy of Science USA*, **93**(11):5610-5614.

Lehmann, S., and Harris, D. A., 1997, Blockade of glycosylation promotes acquisition of scrapie-like properties by the prion protein in cultured cells [published erratum appears in J Biol Chem 1998 Mar 6;273(10):5988], *J Biol Chem*, **272**(34):21479-21487.

Lemstra, A. W., van Meegen, M., Vreyling, J. P., Meijerink, P. H., Jansen, G. H., Bulk, S., Baas, F., and van Gool, W., 2000, 14-3-3 testing in diagnosing Creutzfeldt-Jakob disease: a prospective study in 112 patients., *Neurology*, **55**(4):514-516.

Levine, R. L., Mosoni, L., Berlett, B. S., and Stadtman, E. R., 1996, Methionine residues as endogenous antioxidants in proteins., *Proceedings of the National Academy of Science USA*, **93**(26):15036-15040.

Liberski, P. P., and Gajdusek, D. C., 1997, Kuru: forty years later, a historical note., *Brain Pathology*, **7**(1):555-560.

Liu, H., Farr-Jones, S., Ulyanov, N. B., Llinas, M., Marqusee, S., Groth, D., Cohen, F. E., Prusiner, S. B., and James, T. L., 1999, Solution structure of Syrian hamster prion protein rPrP(90-231). *Biochemistry*, **38**(17):5362-5377.

Liu, T., Zwingman, T., Li, R., Pan, T., Wong, B. S., Petersen, R. B., Gambetti, P., Herrup, K., and Sy, M. S., 2001, Differential expression of cellular prion protein in mouse brain as detected with multiple anti-PrP monoclonal antibodies, *Brain Research*, **896**(1-2):118-29.

Lloyd, S. E., Onwuazor, O. N., Beck, J. A., Mallinson, G., Farrall, M., Targonski, P., Collinge, J., and Fisher, E. M., 2001, Identification of multiple quantitative trait loci linked to prion disease incubation period in mice., *Proceedings of the National Academy of Science USA*, **98**(11):6279-6283.

Lopez Garcia, F., Zahn, R., Riek, R., and Wuthrich, K., 2000, NMR structure of the bovine prion protein., *Proceedings of the National Academy of Science USA*, **97**(15):8334-8339.

Lowry, O., Rosebrough, N. J., Farr, A. L., and Randall, R. J., 1951, Protein measurement with the Folin phenol reagent, *Journal of Biological Chemistry*, **193**:265-275.

Lu, K., Wang, W., Xie, Z., Wong, B. S., Li, R., Petersen, R. B., Sy, M. S., and Chen, S. G., 2000, Expression and structural characterization of the recombinant human doppel protein, *Biochemistry*, **39**(44):13575-13583.

Ma, J., and Lindquist, S., 1999, De novo generation of a PrPSc-like conformation in living cells., *Nat Cell Biolog*, **1**(6):358-361.

Mabbott, N. A., Brown, K. L., Manson, J., and Bruce, M. E., 1997, T-lymphocyte activation and the cellular form of the prion protein., *Immunology*, **92**(2):161-165.

Madec, J., Groschup, M. H., Calavas, D., Junghans, F., and Baron, T., 2000a, Protease-resistant prion protein in brain and lymphoid organs of sheep within a naturally scrapie-infected flock., *Microb Pathog*, **28**(6):353-362.

Madec, J. Y., P, B., Calavas, D., and Baron, T., 2000b, Efficiency of Western blotting for the specific immunodetection of proteinase K-resistant prion protein in BSE diagnosis in France., *Veterinary Record*, **146**(3):74-76.

Madec, J. Y., Vanier, A., Dorier, A., Bernillon, J., P, B., and Baron, T., 1997, Biochemical properties of protease resistant prion protein PrPsc in natural sheep scrapie., *Arch Virol*, **142**(8):1603-1612.

Manolakou, K., Beaton, J., McConnell, I., Farquar, C., Manson, J., Hastie, N. D., Bruce, M., and Jackson, I. J., 2001, Genetic and environmental factors modify bovine spongiform encephalopathy incubation period in mice., *Proceedings of the National Academy of Science USA*, **98**(13):7402-7407.

Manousis, T., Sachsamanoglou, M., Toumazos, P., Verghese-Nikolakaki, S., Papadopoulos, O., and Sklaviadis, T., 2000, Western blot detection of PrP(Sc) in Cyprus sheep with natural scrapie., *Vet J*, **159**(3):270-273.

Manson, J., West, J. D., Thomson, V., McBride, P., Kaufman, M. H., and Hope, J., 1992, The prion protein gene: a role in mouse embryogenesis?, *Development*, **115**(1):117-122.

Manuelidis, L., Sklaviadis, T., Akowitz, A., and Fritch, W., 1995, Viral particles are required for infection in neurodegenerative Creutzfeldt-Jakob disease., *Proceedings of the National Academy of Science USA*, **92**(11):5124-51288.

Mastrianni, J. A., Nixon, R., Layzer, R., Telling, G. C., Han, D., DeArmond, S. J., and Prusiner, S. B., 1999, Prion protein conformation in a patient with sporadic fatal insomnia., *N Engl J Med*, **340**(21):1630-1638.

Matsunaga, Y., Peretz, D., Williamson, A., Burton, D., Mehlhorn, I., Groth, D., Cohen, F. E., Prusiner, S. B., and Baldwin, M. A., 2001, Cryptic epitopes in N-terminally truncated prion protein are exposed in the full-length molecule: dependence of conformation on pH, *Proteins*, **44**(2):110-8.

McBride, P. A., and Beekes, M., 1999, Pathological PrP is abundant in sympathetic and sensory ganglia of hamsters fed with scrapie., *Neuroscience Letters*, **265**(2):135-138.

McCormack, J. E., Baybutt, H. N., Everington, D., Will, R. G., Ironside, J. W., and Manson, J. C., 2002, PRNP contains both intronic and upstream regulatory regions that may influence susceptibility to Creutzfeldt-Jakob Disease, *Gene*, **288**(1-2):139-46.

McKenzie, D., Bartz, J., Mirwald, J., Olander, D., Marsh, R., and Aiken, J., 1998, Reversibility of scrapie inactivation is enhanced by copper., *J Biol Chem*, **273**(40):25545-25547.

McKinley, M. P., Taraboulos, A., Kenaga, L., Serban, D., Stieber, A., DeArmond, S. J., Prusiner, S. B., and Gonatas, N., 1991, Ultrastructural-localization of scrapie prion proteins in cytoplasmic vesicles of infected cultured-cells., *Laboratory Investigation*, **65**:622-630.

McLean, C. A., Ironside, J. W., Alpers, M. P., Brown, P. W., Cervenakova, L., Anderson, R. M., and Masters, C., 1998, Comparative neuropathology of Kuru with the new variant of Creutzfeldt-Jakob disease: evidence for strain of agent predominating over genotype of host., *Brain Pathology*, **8**(3):429-437.

Mead, S., Beck, J., Dickinson, A., Fisher, E. M., and Collinge, J., 2000, Examination of the human prion protein-like gene doppel for genetic susceptibility to sporadic and variant Creutzfeldt-Jakob disease, *Neuroscience Letters*, **290**(2):117-20.

Mead, S., Mahal, S. P., Beck, J., Campbell, T., Farrall, M., Fisher, E., and Collinge, J., 2001, Sporadic--but not variant--Creutzfeldt-Jakob disease is associated with polymorphisms upstream of PRNP exon 1, *Am J Hum Genet*, **69**(6):1225-35.

Medori, R., Tritschler, H. J., LeBlanc, A., Villare, F., Manetto, V., Chen, H. Y., Xue, R., Leal, S., Montagna, P., and P, C., 1992, Fatal familial insomnia, a prion disease with a mutation at codon 178 of the prion protein gene., *N Engl J Med*, **326**(7):444-449.

Meyer, R. K., McKinley, M. P., K.A., B., Braunfeld, M. B., Barry, R. A., and Prusiner, S. B., 1986, Separation and properties of cellular and scrapie prion proteins., *Proceedings of the National Academy of Science USA*, **83**:2310-2314.

Miura, T., Hori-i, A., Mototani, H., and Takeuchi, H., 1999, Raman spectroscopic study on the copper(II) binding mode of prion octapeptide and its pH dependence, *Biochemistry*, **38**(35):11560-9.

Monari, L., Chen, S. G., Brown, P., Parchi, P., Petersen, R. B., Mikol, J., Gray, F., P, C., Montagna, P., and Ghetti, B., 1994, Fatal familial insomnia and familial Creutzfeldt-Jakob disease: different prion proteins determined by a DNA polymorphism., *Proceedings of the National Academy of Science USA*, **91**(7):2839-2842.

Montagna, P., P, C., P, A., P, T., G, P., R, G., F, P., J., J., Vital, C., Delisle, M.-B., Gambetti, P., and Lugaresi, E., 1998, Clinical features of fatal familial insomnia: phenotypic variability in relation to a polymorphism at codon 129 of the prion protein gene., *Brain Pathology*, **8**:515-520.

Morillas, M., Swietnicki, W., Gambetti, P., and Surewicz, W. K., 1999, Membrane environment alters the conformational structure of the recombinant human prion protein., *J Biol Chem*, **274**(52):36859-36865.

Morrissey, M. P., and Shakhnovich, E. I., 1999, Evidence for the role of PrP(C) helix 1 in the hydrophilic seeding of prion aggregates., *Proceedings of the National Academy of Science USA*, **96**(20):11293-11298.

Moudjou, M., Frobert, Y., Grassi, J., and La Bonnardiere, C., 2001, Cellular prion protein status in sheep: tissue-specific biochemical signatures, *J Gen Virol*, **82**(Pt 8):2017-2024.

Moynagh, J., Schimmel, H., and Kramer, G. N., 1999, The evaluation of tests for the diagnosis of transmissible spongiform encephalopathies in bovines., European commission.

Multhaup, G., Diringer, H., Hilmert, H., Prinz, H., Heukeshoven, J., and Beyreuther, K., 1985, The protein component of scrapie-associated fibrils is a glycosylated low molecular weight protein, *Embo J*, **4**(6):1495-501.

Muramoto, T., DeArmond, S. J., Scott, M., Telling, G. C., Cohen, F. E., and Prusiner, S. B., 1997, Heritable disorder resembling neuronal storage disease in mice expressing prion protein with deletion of an α-helix., *Nature Medicine*, **3**(7):750-755.

Nguyen, J. T., Inouye, H., Baldwin, M. A., Fletterick, R. J., Cohen, F. E., Prusiner, S. B., and Kirschner, D. A., 1995, X-ray diffraction of scrapie prion rods and PrP peptides., *J Mol Biol*, **252**(4):412-422.

Nitrini, R., Rosemberg, S., Passos-Bueno, M. R., daSilva, L., Iughetti, P., Papadopoulos, M., Carrilho, P. M., Caramelli, P., Albrecht, S., Zatz, M., and LeBlanc, A., 1997, Familial spongiform encephalopathy associated with a novel prion protein gene mutation., *Ann Neurol*, **42**(2):138-146.

Nixon, R., Camicioli, R., Jamison, K., Cervenakova, L., and Mastrianni, J. A., 2000, The PRNP-V180I mutation is associated with abnormally glycosylated PrPCJD and intracellular PrP accumulations, *Brain Pathology*, **10**(4):670.

Oesch, B., Doherr, M., Heim, D., Fischer, K., Egli, S., Bolliger, S., Biffiger, K., Schaller, O., Vandevelde, M., and Moser, M., 2000, Application of Prionics Western blotting procedure to screen for BSE in cattle regularly slaughtered at Swiss abattoirs, *Arch Virol Suppl*, (16):189-195.

Oesch, B., Westaway, D., Walchli, M., McKinley, M. P., Kent, S. B., Aebersold, R., Barry, R. A., Tempst, P., Teplow, D. B., and Hood, L. E., 1985, A cellular gene encodes scrapie PrP 27-30 protein., *Cell*, **40**(4):735-746.

Palmer, M. S., Dryden, A. J., Hughes, J. T., and Collinge, J., 1991, Homozygous prion protein genotype predisposes to sporadic creutzfeldt-jakob disease., *Nature*, **352**:340-342.

Pammer, J., Suchy, A., Rendl, M., and Tschachler, E., 1999, Cellular prion protein expressed by bovine squamous epithelia of skin and upper gastrointestinal tract., *The Lancet*, **354**(9191):1702-1703.

Pan, K. M., Baldwin, M., Nguyen, J., Gasset, M., Serban, A., Groth, D., Mehlhorn, I., Huang, Z. W., Fletterick, R. J., Cohen, F. E., and Prusiner, S. B., 1993, Conversion of alpha-helices into beta-sheets features in the formation of the scrapie prion proteins., *Proceedings of the National Academy of Science USA*, **90:**10962-10966.

Pan, T., Colucci, M., Wong, B. S., Li, R., Liu, T., Petersen, R. B., Chen, S., Gambetti, P., and Sy, M. S., 2001, Novel differences between two human prion strains revealed by two-dimensional gel electrophoresis, *J Biol Chem*, **276**(40):37284-37288.

Pan, T., Li, R., Wong, B. S., Liu, T., Gambetti, P., and Sy, M. S., 2002, Heterogeneity of normal prion protein in two- dimensional immunoblot: presence of various glycosylated and truncated forms, *J Neurochem*, **81**(5):1092-1101.

Parchi, P., Capellari, S., Chen, S. G., Petersen, R. B., Gambetti, P., Kopp, N., Brown, P., Kitamoto, T., Tateishi, J., Giese, A., and Kretzschmar, H., 1997, Typing prion isoforms., *Nature*, **386**(6622):232-234.

Parchi, P., Capellari, S., Chin, S., Schwarz, H. B., Schecter, N. P., Butts, J. D., Hudkins, P., Burns, D. K., Powers, J. M., and Gambetti, P., 1999a, A subtype of sporadic prion disease mimicking fatal familial insomnia., *Neurology*, **52**(9):1757-1763.

Parchi, P., Capellari, S., and Gambetti, P., 2000a, Intracerebral distribution of the abnormal isoform of the prion protein in sporadic Creutzfeldt-Jakob disease and fatal insomnia, *Microsc Res Tech*, **50**(1):16-25.

Parchi, P., Capellari, S., Zanusso, G., Singh, N., Gambetti, P., and R.B., P., 1999b, Inherited Prion Diseases: Molecular Pathology and Cell Models., in: *Prions. Molecular and Cellular Biology* (D. A. Harris, ed.), Horizon scientific Press, pp. 67-86.

Parchi, P., Castellani, R., Capellari, S., Ghetti, B., Young, K., Chen, S. G., Farlow, M., Dickson, D. W., Sima, A. A., J.Q., T., Petersen, R. B., and Gambetti, P., 1996, Molecular basis of phenotypic variability in sporadic Creutzfeldt-Jakob disease., *Ann Neurol*, **39**(6):767-778.

Parchi, P., Castellani, R., Capellari, S., Petersen, R., Chen, S. G., Young, K., Farlow, M., J.Q., T., Sima, A., Ghetti, B., and Gambetti, P., 1995a, Protease-resistant prion protein in sporadic Creutzfeldt-Jakob disease (CJD): correlation with clinico-pathological features and PrP genotype., *Journal of Neuropathology & Experimental Neurology*, **54**:416.

Parchi, P., Castellani, R., P, C., Montagna, P., Chen, S. G., Petersen, R. B., Manetto, V., Vnencak-Jones, C. L., McLean, M. J., and Sheller, J. R., 1995b, Regional distribution of protease-resistant prion protein in fatal familial insomnia., *Ann Neurol*, **38**(1):21-29.

Parchi, P., Chen, S. G., Brown, P., Zou, W., Capellari, S., Budka, H., Hainfellner, J., Reyes, P. F., Golden, G. T., Hauw, J. J., Gajdusek, D. C., and Gambetti, P., 1998a, Different patterns of truncated prion protein fragments correlate with distinct phenotypes in P102L Gerstmann-Straussler-Scheinker disease., *Proceedings of the National Academy of Science USA*, **95**(14):8322-8327.

Parchi, P., Giese, A., Capellari, S., and Brown, P., 1998b, The molecular and clinico-pathologic spectrum of phenotypes of sporadic Creutzfeldt-Jakob disease (sCJD). *Neurology*, **50**:A336.

Parchi, P., Giese, A., Capellari, S., Brown, P., Schulz-Schaeffer, W., Windl, O., Zerr, I., Budka, H., Kopp, N., Piccardo, P., Poser, S., Rojiani, A., Streichemberger, N., J., J., Vital, C., Ghetti, B., Gambetti, P., and Kretzschmar, H., 1999c, Classification of sporadic Creutzfeldt-Jakob disease based on molecular and phenotypic analysis of 300 subjects., *Ann Neurol*, **46**(2):224-233.

Parchi, P., Petersen, R. B., Chen, S. G., Autilio-Gambetti, L., Capellari, S., Monari, L., P, C., Montagna, P., Lugaresi, E., and Gambetti, P., 1998c, Molecular pathology of fatal familial insomnia., *Brain Pathology*, **8**(3):539-548.

Parchi, P., Zou, W., Wang, W., Brown, P., Capellari, S., Ghetti, B., Kopp, N., Schulz-Schaeffer, W. J., Kretzschmar, H. A., Head, M. W., Ironside, J. W., Gambetti, P., and Chen, S. G., 2000b, Genetic influence on the structural variations of the abnormal prion protein., *Proceedings of the National Academy of Science USA*, **97**(18):10168-10172.

Pattison, I. H., 1966, The relative susceptibility of sheep, goats and mice to two types of the goat scrapie agent, *Res Vet Sci*, **7**(2):207-12.

Pauly, P. C., and Harris, D. A., 1998, Copper stimulates endocytosis of the prion protein., *J Biol Chem*, **273**(50):33107-33110.

Pearson, G. R., T.J., G.-J., Wyatt, J. M., Hope, J., Chong, A., Scott, A. C., Dawson, M., and Wells, G. A. H., 1991, Feline spongiform encephalopathy., *Veterinary Record*, **128**(22):532.

Pearson, G. R., Wyatt, J. M., T.J., G.-J., Hope, J., Chong, A., Higgins, R. J., Scott, A. C., and Wells, G. A. H., 1992, Feline spongiform encephalopathy: fibril and PrP studies., *Veterinary Record*, **131**(14):307-310.

Peoc, Manivet, P., Beaudry, P., Attane, F., Besson, G., Hannequin, D., Delasnerie-Laupretre, N., and Laplanche, J. L., 2000, Identification of three novel mutations (E196K, V203I, E211Q) in the prion protein gene (PRNP) in inherited prion diseases with Creutzfeldt-Jakob disease phenotype., *Human Mutation*, **15**(5):482.

Peretz, D., Williamson, R. A., Legname, G., Matsunaga, Y., Vergara, J., Burton, D. R., DeArmond, S. J., Prusiner, S. B., and Scott, M. R., 2002, A change in the conformation of prions accompanies the emergence of a new prion strain, *Neuron*, **34**(6):921-932.

Peretz, D., Williamson, R. A., Matsunaga, Y., Serban, H., Pinilla, C., Bastidas, R. B., Rozenshteyn, R., James, T. L., Houghten, R. A., Cohen, F. E., Prusiner, S. B., and Burton, D. R., 1997, A conformational transition at the N terminus of the prion protein features in formation of the scrapie isoform., *J Mol Biol*, **273**(3):614-622.

Perini, F., Frangione, B., and Prelli, F., 1996, Prion protein released by platelets., *The Lancet*, **347**(9015):1635-1636.

Piccardo, P., Dlouhy, S. R., Lievens, P. M., Young, K., Bird, T. D., Nochlin, D., Dickson, D. W., Vinters, H. V., Zimmerman, T. R., Mackenzie, I. R., Kish, S. J., Ang, L. C., DeCarli, C., Pocchiari, M., Brown, P., Gibbs, C. J. J., Gajdusek, D. C., Bugiani, O., Ironside, J. W., Tagliavini, F., and Ghetti, B., 1998, Phenotypic variability of Gerstmann-Straussler-Scheinker disease is associated with prion protein heterogeneity., *Journal of Neuropathology & Experimental Neurology*, **57**(10):979-988.

Pickering-Brown, S. M., Mann, D. M., Owen, F., Ironside, J. W., de Silva, R., Roberts, D. A., Balderson, D. J., and Cooper, P. N., 1995, Allelic variations in apolipoprotein E and prion protein genotype related to plaque formation and age of onset in sporadic Creutzfeldt-Jakob disease., *Neuroscience Letters*, **187**(2):127-129.

Pillot, T., Lins, L., Goethals, M., Vanloo, B., Baert, J., Vandekerckhove, J., Rosseneu, M., and Brasseur, R., 1997, The 118-135 peptide of the human prion protein forms amyloid fibrils and induces liposome fusion., *J Mol Biol*, **274**(3):381-393.

Post, K., Pitschke, M., Schafer, O., Wille, H., Appel, T. R., Kirsch, D., Mehlhorn, I., Serban, H., Prusiner, S. B., and Riesner, D., 1998, Rapid acquisition of beta-sheet structure in the prion protein prior to multimer formation., *Biol Chem*, **379**(11):1307-1317.

Priola, S. A., and Lawson, V. A., 2001, Glycosylation influences cross-species formation of protease-resistant prion protein, *Embo J*, **20**(23):6692-6699.

Prusiner, S. B., 1982, Novel proteinaceous infectious particles cause scrapie., *Science*, **216:**136-144.

Prusiner, S. B., 1991, Molecular-biology of prion diseases., *Science*, **252:**1515-1522.

Prusiner, S. B., 1995, The prion diseases., *Scientific American*, **272**(1)**:**48-51.

Prusiner, S. B., 1997, Prion diseases and the BSE crisis., *Science*, **278**(5336)**:**245-251.

Prusiner, S. B., 1998, The prion diseases., *Brain Pathology*, **8:**499-512.

Prusiner, S. B., Groth, D., Serban, A., Stahl, N., and Gabizon, R., 1993, Attempts to restore scrapie prion infectivity after exposure to protein denaturants., *Proceedings of the National Academy of Science USA*, **90**(7)**:**2793-2797.

Prusiner, S. B., McKinley, M. P., K.A., B., Bolton, D. C., Bendheim, P. E., Groth, D. F., and Glenner, G. G., 1983, Scrapie prions aggregate to form amyloid-like birefringent rods., *Cell*, **35**(Pt 1)**:**349-358.

Prusiner, S. B., Scott, M., Foster, D., Pan, K. M., Groth, D., Mirenda, C., Torchia, M., Yang, S. L., Serban, D., and Carlson, G. A., 1990, Transgenetic studies implicate interactions between homologous PrP isoforms in scrapie prion replication., *Cell*, **63**(4)**:**673-686.

Prusiner, S. B., Scott, M. R., DeArmond, S. J., and Cohen, F. E., 1998, Prion protein biology., *Cell*, **93**(3)**:**337-348.

Puckett, C., Concannon, P., Casey, C., and Hood, L., 1991, Genomic structure of the human prion protein gene, *Am J Hum Genet*, **49**(2)**:**320-329.

Puoti, G., Giaccone, G., Rossi, G., Canciani, B., Bugiani, O., and Tagliavini, F., 1999, Sporadic Creutzfeldt-Jakob disease: co-occurrence of different types of PrP(Sc) in the same brain., *Neurology*, **53**(9)**:**2173-2176.

Puoti, G., Rossi, G., Giaccone, G., Awan, T., Lievens, P. M., Defanti, C. A., Tagliavini, F., and Bugiani, O., 2000, Polymorphism at codon 129 of PRNP affects the phenotypic expression of Creutzfeldt-Jakob disease linked to E200K mutation., *Ann Neurol*, **48**(2)**:**269-270.

Purdey, M., 2000, Ecosystems supporting clusters of sporadic TSEs demonstrate excesses of the radical-generating divalent cation manganese and deficiencies of antioxidant co factors Cu, Se, Fe, Zn. Does a foreign cation substitution at prion protein's Cu domain initiate TSE?, *Med Hypotheses*, **54**(2)**:**278-306.

Purdey, M., 2001, Does an ultra violet photooxidation of the manganese-loaded/copper-depleted prion protein in the retina initiate the pathogenesis of TSE?, *Med Hypotheses*, **57**(1)**:**29-45.

Quaglio, E., Chiesa, R., and Harris, D. A., 2001, Copper converts the cellular prion protein into a protease-resistant species that is distinct from the scrapie isoform, *J Biol Chem*, **276**(14)**:**11432-8.

Raeber, A. J., Borchelt, D. R., Scott, M., and Prusiner, S. B., 1992, Attempts to convert the cellular prion protein into the scrapie isoform in cell-free systems., *J Virol*, **66**(10)**:**6155-6163.

Raymond, G. J., Bossers, A., Raymond, L. D., O'Rourke, K. I., McHolland, L. E., Bryant, I. P., Miller, M. W., Williams, E. S., Smits, M., and Caughey, B., 2000, Evidence of a molecular barrier limiting susceptibility of humans, cattle and sheep to chronic wasting disease., *EMBO Journal*, **19**(17):4425-4430.

Raymond, G. J., Hope, J., Kocisko, D. A., Priola, S. A., Raymond, L. D., Bossers, A., Ironside, J. W., Will, R. G., Chen, S. G., Petersen, R. B., Gambetti, P., Rubenstein, R., Smits, M. A., Lansbury, P. T. J., and Caughey, B., 1997, Molecular assessment of the potential transmissibilities of BSE and scrapie to humans., *Nature*, **388**(6639):285-288.

Ridley, R. M., and Baker, H. F., 1997, The nature of transmission in prion diseases., *Neuropathology and Applied Neurobiology*, **23**:273-280.

Rieger, R., Edenhofer, F., Lasmezas, C. I., and Weiss, S., 1997, The human 37-kDa laminin receptor precursor interacts with the prion protein in eukaryotic cells., *Nature Medicine*, **3**(12):1383-1388.

Riek, R., Hornemann, S., Wider, G., Billeter, M., Glockshuber, R., and Wuthrich, K., 1996, NMR structure of the mouse prion protein domain PrP(121-321). *Nature*, **382**(6587):180-182.

Roels, S., Vanopdenbosch, E., Langeveld, J. P., and Schreuder, B. E., 1999, Immunohistochemical evaluation of tonsillar tissue for preclinical screening of scrapie based on surveillance in Belgium., *Veterinary Record*, **145**(18):524-525.

Rogers, M., Taraboulos, A., Scott, M., Groth, D., and Prusiner, S. B., 1990, Intracellular accumulation of the cellular prion protein after mutagenesis of its Asn-linked glycosylation sites., *Glycobiology*, **1**(1):101-109.

Rosenmann, H., Halimi, M., Kahana, I., Biran, I., and Gabizon, R., 1997, Differential allelic expression of PrP mRNA in carriers of the E200K mutation., *Neurology*, **49**(3):851-856.

Rossi, G., Macchi, G., Porro, M., Giaccone, G., Bugiani, M., Scarpini, E., Scarlato, G., Molini, G. E., Sasanelli, F., Bugiani, O., and Tagliavini, F., 1998, Fatal familial insomnia: genetic, neuropathologic, and biochemical study of a patient from a new Italian kindred., *Neurology*, **50**(3):688-692.

Rudd, P. M., Endo, T., Colominas, C., Groth, D., Wheeler, S. F., Harvey, D. J., Wormald, M. R., Serban, H., Prusiner, S. B., Kobata, A., and Dwek, R. A., 1999, Glycosylation differences between the normal and pathogenic prion protein isoforms., *Proceedings of the National Academy of Science USA*, **96**(23):13044-13049.

Russelakis-Carneiro, M., Saborio, G. P., Anderes, L., and Soto, C., 2002, Changes in the Glycosylation Pattern of Prion Protein in Murine Scrapie., *J Biol Chem*, **277**(39):36872-7.

Ryder, S. J., Hawkins, S. A., Dawson, M., and Wells, G. A. H., 2000, The neuropathology of experimental bovine spongiform encephalopathy in the pig., *J Comp Pathology*, **122**(2-3):131-143.

Rymer, D. L., and Good, T. A., 2000, The role of prion peptide structure and aggregation in toxicity and membrane binding., *J Neurochem*, **75**(6):2536-2545.

Saborio, G. P., Permanne, B., and Soto, C., 2001, Sensitive detection of pathological prion protein by cyclic amplification of protein misfolding., *Nature*, **411**:810-813.

Safar, J., Wille, H., Itrri, V., Groth, D., Serban, H., Torchia, M., Cohen, F. E., and Prusiner, S. B., 1998, Eight prion strains have PrPSc molecules with different conformations., *Nature Medicine*, **4**:1157-1165.

Sakaguchi, S., Katamine, S., Nishida, N., Moriuchi, R., Shigematsu, K., Sugimoto, T., Nakatani, A., Kataoka, Y., Houtani, T., Shirabe, S., Okada, H., Hasegawa, S., Miyamoto, T., and Noda, T., 1996, Loss of cerebellar Purkinje cells in aged mice homozygous for a disrupted PrP gene, *Nature*, **380**(6574):528-531.

Sakaguchi, S., Katamine, S., Shigematsu, K., Nakatani, A., Moriuchi, R., Nishida, N., Kurokawa, K., Nakaoke, R., Sato, H., and Jishage, K., 1995, Accumulation of proteinase K-resistant prion protein (PrP) is restricted by the expression level of normal PrP in mice inoculated with a mouse-adapted strain of the Creutzfeldt-Jakob disease agent., *J Virol*, **69**(12):7586-7592.

Sales, N., Rodolfo, K., Hassig, R., Faucheux, B., Di Giamberardino, L., and Moya, K. L., 1998, Cellular prion protein localization in rodent and primate brain., *European Journal of Neuroscience*, **10**(7):2464-2471.

Samman, I., Schulz-Schaeffer, W. J., Wohrle, J. C., Sommer, A., Kretzschmar, H. A., and Hennerici, M., 1999, Clinical range and MRI in Creutzfeldt-Jakob disease with heterozygosity at codon 129 and prion protein type 2., *J Neurol Neurosurg Psychiatry*, **67**(5):678-681.

Schagger, H., and von Jagow, G., 1987, Tricine-sodium dodecyl sulfate-polyacrylamide gel electrophoresis for the separation of proteins in the range from 1 to 100 kDa, *Anal Biochem*, **166**(2):368-79.

Schaller, O., Fatzer, R., Stack, M., Clark, J., Cooley, W., Biffiger, K., Egli, S., Doherr, M., Vandevelde, M., Heim, D., Oesch, B., and Moser, M., 1999, Validation of a western immunoblotting procedure for bovine PrP(Sc) detection and its use as a rapid surveillance method for the diagnosis of bovine spongiform encephalopathy (BSE). *Acta Neuropathol (Berl)*, **98**(5):437-443.

Schatzl, H. M., DaCosta, M., Taylor, L., Cohen, F. E., and Prusiner, S. B., 1995, Prion protein gene variation among primates [published erratum appears in J Mol Biol 1997 Jan 17;265(2):257]. *J Mol Biol*, **245**(4):362-374.

Scott, M. R., Will, R., Ironside, J. W., Nguyen, H. O., Tremblay, P., DeArmond, S. J., and Prusiner, S. B., 1999, Compelling transgenetic evidence for transmission of bovine spongiform encephalopathy prions to humans., *Proceedings of the National Academy of Science USA*, **96**(26):15137-15142.

Sears, P., and Wong, C. H., 1998, Enzyme action in glycoprotein synthesis, *Cellular & Molecular Life Sciences*, **54**(3):223-252.

Shaked, G. M., Fridlander, G., Meiner, Z., Taraboulos, A., and Gabizon, R., 1999a, Protease-resistant and detergent-insoluble prion protein is not necessarily associated with prion infectivity., *J Biol Chem*, **274**(25):17981-17986.

Shaked, Y., Rosenmann, H., Talmor, G., and Gabizon, R., 1999b, A C-terminal-truncated PrP isoform is present in mature sperm., *J Biol Chem*, **274**(45):32153-32158.

Shibuya, S., Higuchi, J., Shin, R. W., Tateishi, J., and Kitamoto, T., 1998, Protective prion protein polymorphisms against sporadic Creutzfeldt-Jakob disease., *The Lancet*, **351**(9100):419.

Shmerling, D., Hegyi, I., Fischer, M., Blattler, T., Brandner, S., Gotz, J., Rulicke, T., Flechsig, E., Cozzio, A., von Mering, C., Hangartner, C., Aguzzi, A., and Weissmann, C., 1998, Expression of amino-terminally truncated PrP in the mouse leading to ataxia and specific cerebellar lesions., *Cell*, **93**(2):203-214.

Shyng, S. L., Huber, M. T., and Harris, D. A., 1993, A prion protein cycles between the cell surface and an endocytic compartment in cultured neuroblastoma cells., *J Biol Chem*, **268**(21):15922-15928.

Silverman, L., Qin, K., Moore, R. C., Yang, Y., Mastrangelo, P., Tremblay, P., Prusiner, S. B., Cohen, F. E., and Westaway, D., 2000, Doppel is an N-glycosylated GPI-anchored protein: expression in testis and ectopic production in the brains of Prnp{super0/0} mice predisposed to Purkinje cell loss., *J Biol Chem*, **275**(35):26834-26841.

Silvestrini, M. C., Cardone, F., Maras, B., Pucci, P., Barra, D., Brunori, M., and Pocchiari, M., 1997, Identification of the prion protein allotypes which accumulate in the brain of sporadic and familial Creutzfeldt-Jakob disease patients., *Nature Medicine*, **3**(5):521-525.

Simon, E. S., Kahana, E., Chapman, J., Treves, T. A., Gabizon, R., Rosenmann, H., Zilber, N., and Korczyn, A. D., 2000, Creutzfeldt-Jakob disease profile in patients homozygous for the PRNP E200K mutation., *Ann Neurol*, **47**(2):257-260.

Somerville, R. A., 1999, Host and transmissible spongiform encephalopathy agent strain control glycosylation of PrP., *J Gen Virol*, **80**(Pt 7):1865-1872.

Somerville, R. A., Chong, A., Mulqueen, O. U., Birkett, C. R., Wood, S. C., and Hope, J., 1997, Biochemical typing of scrapie strains., *Nature*, **386**(6625):564.

Somerville, R. A., and Ritchie, L. A., 1990, Differential glycosylation of the protein (PrP) forming scrapie-associated fibrils., *J Gen Virol*, **71**(Pt 4):833-839.

Sparkes, R. S., Simon, M., Cohn, V., Fournier, R., Lem, J., Klisak, I., Heinzmann, C., Blatt, C., Lucero, M. M., T, DeArmond, S. J., Westaway, D., Prusiner, S. B., and Weiner, L., 1986, Assignment of the human and mouse prion protein genes to homologous chromosomes., *Proceedings of the National Academy of Science USA*, **83**(7358):7362.

Stack, J., Chaplin, J., and Clark, J., 2002, Differentiation of prion protein glycoforms from naturally occurring sheep scrapie, sheep-passaged scrapie strains

(CH1641 and SSBP1), bovine spongiform encephalopathy (BSE) cases and Romney and Cheviot breed sheep experimentally inoculated with BSE using two monoclonal antibodies, *Acta Neuropathol (Berl)*, **104**(3):279-286.

Stahl, N., Baldwin, M. A., Burlingame, A. L., and Prusiner, S. B., 1990a, Identification of glycoinositol phospholipid linked and truncated forms of the scrapie prion protein., *Biochemistry*, **29**(38):8879-8884.

Stahl, N., Baldwin, M. A., Teplow, D. B., Hood, L., Gibson, B. W., Burlingame, A. L., and Prusiner, S. B., 1993, Structural studies of the scrapie prion protein using mass spectrometry and amino acid sequencing., *Biochemistry*, **32**(8):1991-2002.

Stahl, N., Borchelt, D. R., Hsiao, K., and Prusiner, S. B., 1987, Scrapie prion protein contains a phosphatidylinositol glycolipid., *Cell*, **51**(2):229-240.

Stahl, N., Borchelt, D. R., and Prusiner, S. B., 1990b, Differential release of cellular and scrapie prion proteins from cellular membranes by phosphatidylinositol-specific phospholipase C., *Biochemistry*, **29**(22):5405-5412.

Stephenson, D. A., Chiotti, K., Ebeling, C., Groth, D., DeArmond, S. J., Prusiner, S. B., and Carlson, G. A., 2000, Quantitative trait loci affecting prion incubation time in mice, *Genomics*, **69**(1):47-53.

Stimson, E., Hope, J., Chong, A., and Burlingame, A. L., 1999, Site-specific characterization of the N-linked glycans of murine prion protein by high-performance liquid chromatography/electrospray mass spectrometry and exoglycosidase digestions., *Biochemistry*, **38**(15):4885-4895.

Sumudhu, W., Perera, S., and Hooper, N. M., 2001, Ablation of the metal ion-induced endocytosis of the prion protein by disease-associated mutation of the octarepeat region., *Curr Biol*, **11**(7):519-523.

Supattapone, S., Bosque, P., Muramoto, T., Wille, H., Aagaard, C., Peretz, D., Nguyen, H. O., Heinrich, C., Torchia, M., Safar, J., Cohen, F. E., DeArmond, S. J., Prusiner, S. B., and Scott, M., 1999, Prion protein of 106 residues creates an artifical transmission barrier for prion replication in transgenic mice., *Cell*, **96**(6):869-878.

Sutherland, K., Goodbrand, I. A., Bell, J. E., and Ironside, J. W., 1996, Objective quantification of prion protein in spinal cords of cases of Creutzfeldt-Jakob disease., *Analytical Cellular Pathology*, **10**(1):25-35.

Sweeney, T., Kuczius, T., McElroy, M., Gomez, P. M., Groschup, M. H., and Parada, M. G., 2000, Molecular analysis of Irish sheep scrapie cases [published erratum appears in J Gen Virol 2000 Aug;81 (Pt 8):2121]. *J Gen Virol*, **81**(6):1621-1627.

Swietnicki, W., Petersen, R., Gambetti, P., and Surewicz, W. K., 1997, pH-dependent stability and conformation of the recombinant human prion protein PrP(90-231). *J Biol Chem*, **272**(44):27517-27520.

Swietnicki, W., Petersen, R. B., Gambetti, P., and Surewicz, W. K., 1998, Familial mutations and the thermodynamic stability of the recombinant human prion protein., *J Biol Chem*, **273**(47):31048-31052.

Tagliavini, F., Lievens, P. M., Tranchant, C., JM, W., Mohr, M., Giaccone, G., Perini, F., Rossi, G., Salmona, M., Piccardo, P., Ghetti, B., Beavis, R. C., Bugiani, O., Frangione, B., and Prelli, F., 2000, A 7 kDa prion protein fragment -an integral component of the PrP region required for infectivity- is the major amyloid protein in Gerstmann-Sträussler-Scheinker disease A117V., *J Biol Chem*, **276**(8):6009-6015.

Tagliavini, F., Prelli, F., Ghiso, J., Bugiani, O., Serban, D., Prusiner, S. B., M.R., F., Ghetti, B., and Frangione, B., 1991, Amyloid protein of gerstmann-straussler-scheinker disease (Indiana kindred) Is an 11-kd fragment of prion protein with an n-terminal glycine at codon-58., *EMBO Journal*, **10**:513-519.

Tagliavini, F., Prelli, F., Porro, M., Rossi, G., Giaccone, G., Bird, T. D., Dlouhy, S. R., Young, K., Piccardo, P., Ghett, Bugiani, O., and Frangione, B., 1995, Only mutant prp participates in amyloid formation in gerstmann-Sträussler-scheinker disease with ALA>VAL substitution at codon 117., *Journal of Neuropathology & Experimental Neurology*, **54**:416.

Taraboulos, A., Jendroska, K., Serban, D., Yang, S.-L., and Prusiner, S. B., 1994, Regional mapping of prion proteins in brain., *Proceedings of the National Academy of Science USA*, **89**:7620-7624.

Taraboulos, A., Rogers, M., Borchelt, D. R., McKinley, M. P., Scott, M., Serban, D., and Prusiner, S. B., 1990a, Acquisition of protease resistance by prion proteins in scrapie-infected cells does not require asparagine-linked glycosylation., *Proceedings of the National Academy of Science USA*, **87**(21):8262-8266.

Taraboulos, A., Serban, D., and Prusiner, S. B., 1990b, Scrapie prion proteins accumulate in the cytoplasm of persistently infected cultured cells., *Journal of Cell Biology*, **110**(6):2117-2132.

Tateishi, J., Brown, P., Kitamoto, T., Hoque, Z. M., Roos, R., Wollman, R., Cervenakova, L., and Gajdusek, D. C., 1995, First experimental transmission of fatal familial insomnia., *Nature*, **376**(6539):434-435.

Tateishi, J., Kitamoto, T., Hoque, M. Z., and Furukawa, H., 1996, Experimental transmission of Creutzfeldt-Jakob disease and related diseases to rodents., *Neurology*, **46**(2):532-537.

Telling, G. C., Haga, T., Torchia, M., Tremblay, P., DeArmond, S. J., and Prusiner, S. B., 1996a, Interactions between wild-type and mutant prion proteins modulate neurodegeneration in transgenic mice., *Genes & Development*, **10**(14):1736-1750.

Telling, G. C., Parchi, P., DeArmond, S. J., P, C., Montagna, P., Gabizon, R., Mastrianni, J., Lugaresi, E., Gambetti, P., and Prusiner, S. B., 1996b, Evidence for the conformation of the pathologic isoform of the prion protein enciphering and propagating prion diversity., *Science*, **274**(5295):2079-2082.

Telling, G. C., Scott, M., Hsiao, K. K., Foster, D., Yang, S. L., Torchia, M., Sidle, K. L., Collinge, J., DeArmond, S. J., and Prusiner, S. B., 1994, Transmission of creutzfeldt-jakob-disease from humans to transgenic mice expressing chimeric human-mouse prion protein., *Proceedings of the National Academy of Science USA*, **91**:9936-9940.

Telling, G. C., Scott, M., Mastrianni, J., Gabizon, R., Torchia, M., Cohen, F. E., DeArmond, S. J., and Prusiner, S. B., 1996c, Prion propagation in mice expressing human and chimeric PrP transgenes implicates the interaction of cellular PrP with another protein., *Cell*, **83**(1):79-90.

Tiwana, H., Wilson, C., Pirt, J., Cartmell, W., and Ebringer, A., 1999, Autoantibodies to brain components and antibodies to Acinetobacter calcoaceticus are present in bovine spongiform encephalopathy., *Infection & Immunity*, **67**(12):6591-6595.

Tobler, I., Gaus, S. E., Deboer, T., Achermann, P., Fischer, M., Rulicke, T., Moser, M., Oesch, B., McBride, P. A., and Manson, J. C., 1996, Altered circadian activity rhythms and sleep in mice devoid of prion protein., *Nature*, **380**(6575):639-642.

Towbin, H., Staehelin, T., and Gordon, J., 1979, Electrophoretic transfer of proteins from polyacrylamide gels to nitrocellulose sheets: procedure and some applications, *Proceedings of the National Academy of Sciences U S A*, **76**(9):4350-4.

Tranchant, C., L, G., C, G.-C., Mohr, M., and JM, W., 1999, Basis of phenotypic variability in sporadic Creutzfeldt-Jakob disease., *Neurology*, **52**:1244-1249.

Turner, M. L., and Ironside, J. W., 1998, New-variant Creutzfeldt-Jakob disease: the risk of transmission by blood transfusion., *Blood Reviews*, **12**(4):255-268.

Vey, M., Pilkuhn, S., Wille, H., Nixon, R., DeArmond, S. J., Smart, E. J., Anderson, R. G., Taraboulos, A., and Prusiner, S. B., 1996, Subcellular colocalization of the cellular and scrapie prion proteins in caveolae-like membranous domains., *Proceedings of the National Academy of Science USA*, **93**(25):14945-14949.

Wadsworth, D. F., Hill, A. F., Joiner, S., Jackson, G. S., Clarke, A. R., and Collinge, J., 1999a, Strain-specific prion-protein conformation determined by metal ions., *Cell Biology*, **1**:55-59.

Wadsworth, J. D., Jackson, G. S., Hill, A. F., and Collinge, J., 1999b, Molecular biology of prion propagation., *Curr Opin Genet Dev*, **9**(3):338-345.

Wadsworth, J. D., Joiner, S., Hill, A. F., Campbell, T. A., Desbruslais, M., Luthert, P. J., and Collinge, J., 2001, Tissue distribution of protease resistant prion protein in variant Creutzfeldt-Jakob disease using a highly sensitive immunoblotting assay, *Lancet*, **358**(9277):171-180.

Warwicker, J., 1997, A hypothesis describing a potential link between molecular structure and TSE strains., *Biochem Biophys Res Commun*, **238**(1):185-190.

Weissmann, C., 1994, Molecular biology of prion diseases., *Trends in Cell Biology*, **4**:10-14.

Wells, G. A. H., Scott, A. C., Johnson, C. T., Gunning, R. F., Hancock, R. D., Jeffrey, M., Dawson, M., and Bradley, R., 1987, A novel progressive spongiform encephalopathy in cattle., *Veterinary Record*, **121**(18):419-420.

Wells, G. A. H., and Wilesmith, J. W., 1997, The neuropathological profile and epidemiology of feline spongiform encephalopathy Great Britain., *Brain Pathology*, **7**:1247.

Westaway, D., Goodman, P. A., Mirenda, C. A., McKinley, M. P., Carlson, G. A., and Prusiner, S. B., 1987, Distinct prion proteins in short and long scrapie incubation period mice., *Cell*, **51**(4):651-662.

Wildegger, G., Liemann, S., and Glockshuber, R., 1999, Extremely rapid folding of the C-terminal domain of the prion protein without kinetic intermediates, *Nat Struct Biol*, **6**(6):550-553.

Will, R. G., A, A., Poser, S., Pocchiari, M., Hofman, A., E, M., de Silva, R., D'Alessandro, M., Delasnerie-Laupretre, N., Zerr, I., and van Duijn, C., 1998, Descriptive epidemiology of Creutzfeldt-Jakob disease in six European countries, 1993-1995. EU Collaborative Study Group for CJD., *Ann Neurol*, **43**(6):763-767.

Will, R. G., Ironside, J. W., Zeidler, M., Cousens, S. N., Estibeiro, K., A, A., Poser, S., Pocchiari, M., Hofman, A., and Smith, P. G., 1996, A new variant of Creutzfeldt-Jakob disease in the UK., *The Lancet*, **347**(9006):921-925.

Williams, A. E., Lawson, L. J., Perry, V. H., and Fraser, H., 1994a, Characterization of the microglial response in murine scrapie., *Neuropathology and Applied Neurobiology*, **20**(1):47-55.

Williams, A. E., Vandam, A. M., Manahing, W. H., Berkenbosch, F., Eikelenboom, P., and Fraser, H., 1994b, Cytokines, prostaglandins and lipocortin-1 are present in the brains of scrapie-infected mice., *Brain Research*, **654**:200-206.

Willoughby, K., Kelly, D. F., Lyon, D. G., and Wells, G. A. H., 1992, Spongiform encephalopathy in a captive puma (Felis concolor). *Veterinary Record*, **131**(19):431-434.

Windl, O., Dempster, M., Estibeiro, J. P., Lathe, R., de Silva, R., Esmonde, T., Will, R., Springbett, A., Campbell, T. A., Sidle, K. C., Palmer, M. S., and Collinge, J., 1996, Genetic basis of Creutzfeldt-Jakob disease in the United Kingdom: a systematic analysis of predisposing mutations and allelic variation in the PRNP gene., *Human Genetics*, **98**(3):259-264.

Wong, B. S., Chen, S. G., Colucci, M., Xie, Z., Pan, T., Liu, T., Li, R., Gambetti, P., Sy, M. S., and Brown, D. R., 2001a, Aberrant metal binding by prion protein in human prion disease., *J Neurochem*, **78**(6):1400-1408.

Wong, B. S., Clive, C., Haswell, S. J., Williamson, R. A., Burton, D. R., Gambetti, P., Sy, M. S., Jones, I. M., and Brown, D. R., 2000a, Copper has differential effect on prion protein with polymorphism of position 129 [published erratum appears in Biochem Biophys Res Commun 2000 May 19;271(3):842]. *Biochem Biophys Res Commun*, **269**(3):726-731.

Wong, B. S., Liu, T., Li, R., Pan, T., Petersen, R. B., Smith, M. A., Gambetti, P., Perry, G., Manson, J. C., Brown, D. R., and Sy, M. S., 2001b, Increased levels of oxidative stress markers detected in the brains of mice devoid of prion protein., *J Neurochem*, **76**(2):565-572.

Wong, B. S., Liu, T., Paisley, D., Li, R., Pan, T., Chen, S. G., Perry, G., Petersen, R. B., Smith, M. A., Melton, D. W., Gambetti, P., Brown, D. R., and Sy, M. S., 2001c, Induction of HO-1 and NOS in doppel-expressing mice devoid of PrP: implications for doppel function., *Mol Cell Neurosci*, **17**(4):768-775.

Wong, B. S., Wang, H., Brown, D. R., and Jones, I. M., 1999, Selective oxidation of methionine residues in prion proteins., *Biochem Biophys Res Commun*, **259**(2):352-355.

Wong, K., Qiu, J., VanClef, J., Prusiner, S. B., and DeArmond, S. J., 1995, Scrapie prions cause decreased membrane fluidity in cultured cells., *Journal of Neuropathology & Experimental Neurology*, **54**:416.

Wong, K., Qiu, Y., Hyun, W., Nixon, R., VanCleff, J., Sanchez-Salazar, J., Prusiner, S. B., and DeArmond, S. J., 1996, Decreased receptor-mediated calcium response in prion-infected cells correlates with decreased membrane fluidity and IP3 release., *Neurology*, **47**(3):741-750.

Wong, N. K., Renouf, D. V., Lehmann, S., and Hounsell, E. F., 2000b, Glycosylation of prions and its effects on protein conformation relevant to amino acid mutations, *J Mol Graph Model*, **18**(2):126-134, 163-5.

Wopfner, F., Weidenhofer, G., Schneider, R., von Brunn, A., Gilch, S., Schwarz, T. F., Werner, T., and Schatzl, H. M., 1999, Analysis of 27 mammalian and 9 avian PrPs reveals high conservation of flexible regions of the prion protein., *J Mol Biol*, **289**(5):1163-1178.

Worrall, B. B., Herman, S. T., Capellari, S., Lynch, T., Chin, S., Gambetti, P., and Parchi, P., 1999, Type 1 protease resistant prion protein and valine homozygosity at codon 129 of PRNP identify a subtype of sporadic Creutzfeldt-Jakob disease., *J Neurol Neurosurg Psychiatry*, **67**(5):671-674.

Wyatt, J. M., G.R., P., Smerdon, T. N., T.J., G.-J., and Wells, G. A. H., 1990, Spongiform encephalopathy in a cat., *Veterinary Record*, **126**(20):513.

Wyatt, J. M., G.R., P., Smerdon, T. N., T.J., G.-J., Wells, G. A. H., and Wilesmith, J. W., 1991, Naturally occurring scrapie-like spongiform encephalopathy in five domestic cats., *Veterinary Record*, **129**(11):233-236.

Young, K., Clark, H. B., Piccardo, P., Dlouhy, S. R., and Ghetti, B., 1997, Gerstmann-Straussler-Scheinker disease with the PRNP P102L mutation and valine at codon 129., *Brain Research Mol Brain Research*, **44**(1):147-150.

Zahn, R., Liu, A., Luhrs, t., Riek, R., von Schroetter, C., Lopez Garcia, F., Billeter, M., Calzolai, L., Wider, G., and Wuthrich, K., 2000, NMR solution structure of the human prion protein., *Proceedings of the National Academy of Science USA*, **97**(1):144-150.

Zanusso, G., Farinazzo, A., Fiorini, M., Gelati, M., Castagna, A., Righetti, P. G., Rizzuto, N., and Monaco, S., 2001, pH-dependent prion protein conformation in classical Creutzfeldt-Jakob disease, *J Biol Chem*, **276**(44):40377-40380.

Zanusso, G., Liu, D., Ferrari, S., Hegyi, I., Yin, X., Aguzzi, A., Hornemann, S., Liemann, S., Glockshuber, R., Manson, J. C., Brown, P., Petersen, R. B., Gambetti, P., and Sy, M. S., 1998a, Prion protein expression in different species: analysis with a panel of new mAbs., *Proceedings of the National Academy of Science USA*, **95**(15):8812-8816.

Zanusso, G., Nardelli, E., Rosati, A., Fabrizi, G., Ferrari, S., Carteri, A., DeSimone, F., Rizzuto, N., and Monaco, S., 1998b, Simultaneous occurrence of spongiform encephalopathy in a man and his cat in Italy., *The Lancet*, **352**(9134):1116-1117.

Zanusso, G., Righetti, P. G., Ferrari, S., Terrin, L., Farinazzo, A., Cardone, F., Pocchiari, M., Rizzuto, N., and Monaco, S., 2002, Two-dimensional mapping of three phenotype-associated isoforms of the prion protein in sporadic Creutzfeldt-Jakob disease, *Electrophoresis*, **23**(2):347-355.

Zeidler, M., Johnstone, E. C., Bamber, R. W., Dickens, C. M., Fisher, C. J., Francis, A. F., Goldbeck, R., Higgo, R., Johnson-Sabine, E. C., Lodge, G. J., McGarry, P., Mitchell, S., Tarlo, L., Turner, M., Ryley, P., and Will, R. G., 1997a, New variant Creutzfeldt-Jakob disease: psychiatric features., *The Lancet*, **350**(9082):908-910.

Zeidler, M., Stewart, G., Cousens, S. N., Estibeiro, K., and Will, R. G., 1997b, Codon 129 genotype and new variant CJD., *The Lancet*, **350**(9078):668.

Zerr, I., Schulz-Schaeffer, W. J., Giese, A., Bodemer, M., Schroter, A., Henkel, K., Tschampa, H. J., Windl, O., Pfahlberg, A., Steinhoff, B. J., Gefeller, O., Kretzschmar, H. A., and Poser, S., 2000, Current clinical diagnosis in Creutzfeldt-Jakob disease: identification of uncommon variants., *Ann Neurol*, **48**(3):323-329.

Zimmermann, K., Turecek, P. L., and Schwarz, H. P., 1999, Genotyping of the prion protein gene at codon 129, *Acta Neuropathol (Berl)*, **97**(4):355-8.

Zuegg, J., and Gready, J. E., 2000, Molecular dynamics simulation of human prion protein including both N-linked oligosaccharides and the GPI anchor, *Glycobiology*, **10**(10):959-74.

Appendix

A1 Autopsy protocol for frozen tissue sampling (Zeidler et al., 1999) page 43-44.

A2 Acrylamide gel concentration formula:

$$\%T = [\text{ g Acrylamide + g Bis-Acrylamide/TotalVolume }] \times 100$$

A3 Electrophoresis settings:

$$\text{Voltage} = \text{Current/Conductivity}$$

$$I = U/\text{Power}$$

$$\text{Power (watts)} = \text{Voltage x Current (amps)}$$

Calculating electrophoretic run times is dependent on the concentration of a gel, it's propensity to warm up, its' thickness, the size of the transfer membrane required etc,. First dimension gel electrophoresis, should be run in as short a time as possible without heating the glass plates at either constant current or constant voltage. Semidry transfer run conditions are calculated depending on the size of the membrane/gel with a current density of 2.5 mA/cm^2 i.e. 250mA for a 10cm x 10cm gel. Constant current is employed so that there is no need to make adjustments for the numbers of blotting sheet or gel layers.

A4 Centrifugation speeds

The maximum relative centrifugal force (RCF) which is equivalent to the gravitational force (g) can be calculated from the rotational speed (n) (measured in revolutions per minute (rpm)) and the maximum radius of centrifugation (r) (measured in (cm)) and differing dependent on the type of micro-test tube used.

$$\mathbf{RCF = 1.118 \times 10^{-5} \times r \times n^2}$$

A5 Densitometric analysis

Glycoform analysis was performed using a GS-700 imaging densitometer and Quantity One 4.1 software (Bio-Rad Laboratories) or a Storm 860 (Molecular Dynamics™) phosphoimager and ImageQuant software. A standard protocol was established and applied to all the results. The majority of the data was collected on x-ray film to ensure consistency between experiments and repeated analyses of samples, STORM™ analysis was employed for murine samples and fCJD samples.

Bio-Rad Quantity One Protocol

Image acquisition

In Quantity One the default application is 'X-ray film', 'Gray film', 'Green' filter colour and 'Transmissive' light. A practical level of resolution for X-ray film was chosen (300 dpi) and the blot was cropped to include the relevant bands and minimise the size of the resulting image file.

Image adjustment

Images were 'transformed' to scale the contrast of the image to provide the optimal appearance without altering the densitometric data. Background signal was subtracted by selecting an area of the gel which is representative of the general background media. This automatically subtracts the average pixel density in the selected region, from the whole image. Altering Minor 'noise' (such as 'salt and pepper' type speckling) found uniformly across the X-ray film was filtered using the 'Filter Wizard'.

Band quantification

Lanes were defined manually by lines running down the centre of the lane. Lane background was removed using 'Rolling Disk' calculation. This involves calulation and removal of the baseline staining of the lane by comparison of the AUC values of the bands to take into account signal between bands.

Bands were defined automatically by Quantity One and then adjusted manually by referral to the lane intensity trace to take into account differences in band

width, 2/3rds of the actual lane width is optimal to prevent background and take into account the curvature at the corners of bands. To ensure inclusion of the whole band density. Bands were adjusted to encompass the entire lane to ensure 100% density was measured and border at the lowest density regions or troughs as seen on the density trace. The trace optical density (OD) x mm, provides the densitometric value for the area under the curve (AUC). As determined by dilution series runs of each standard, the linear range was defined as scans in which the 3 bands fell within 0.7-7.0 or 0.8-8.0 relative units. The total lane density was 100% with each of the bands making up a proportion of this.

Storm™ ImageQuant Densitometry Protocol

Image manipulation

Images were edited with ImageQuant Tools 2.2. The image display is adjusted to enhance contrast and brightness, with the view being scaled to reduce background and accentuate the signal. The appearance of the images was adjusted with a brightness contrast autoscale sigmoidal curve to give an appearance akin to X-ray film, however this does not affect the quantitative data of the images.

Area quantitation with peak finder

Quantitation is carried out with ImageQuant 5.2. A line graph of pixel intensities generates a curve from which the area under the curve provides quantitative glycoform data and removes background values. Lanes were defined manually. The width of the lines were adjusted to 2/3rds of the width of the lane (~10pixels). The AUC is automatically measured with the 'Peak Finder' according to noise, sensitivity and kernel settings. Automatic quantification settings are optimised to remove background, detect peaks and calculate area under the curve. The peaks and baseline can then be adjusted for each line individually if required. Band width was estimated at 2/3rds of the width of the lane (~10pixels) as carried out with Quantity One. The linear range of the storm scans was taken as AUC values of between 100,000 and 1000 based on the results of the dilution curve of a mouse transmission sample.

Linearity determination.

Proteinase K treated samples used as positive controls were loaded onto 12% gels following doubling (X-ray film) or linear (STORM) dilutions. X-ray film quantitation utilised human sCJD and vCJD standards, whereas the vCJD standard and a murine transmission sample was used to assess the linear range of the STORM™ phosphoimager system.

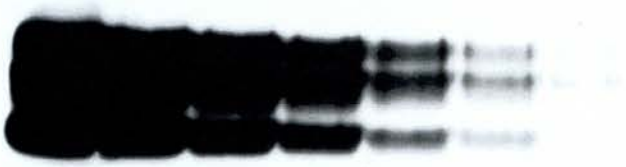

Figure A1. Western blot dilution curve of sCJD MM type 1 standard analysed with 3F4, 4 minute exposure shown.

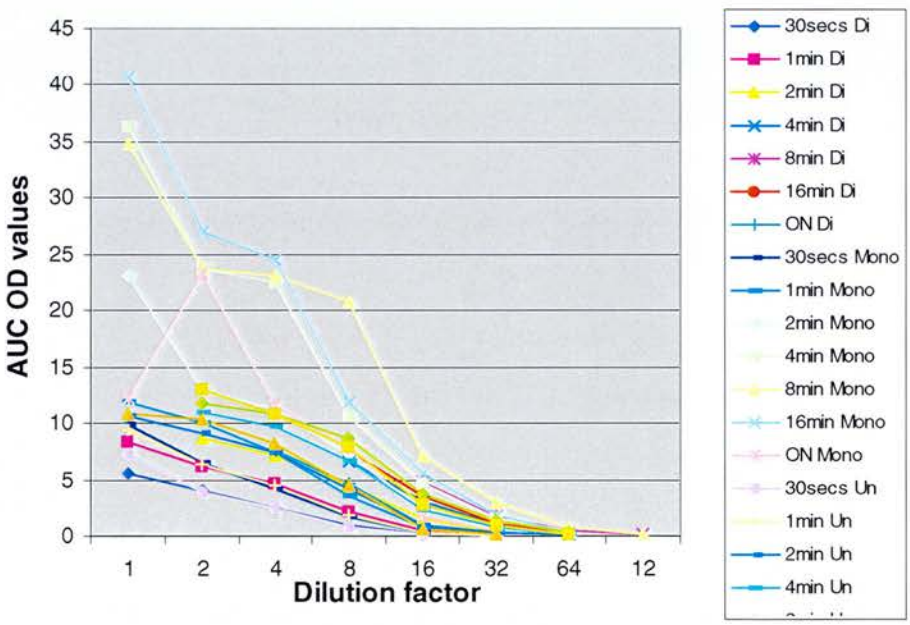

Figure A2. AUC values for sCJD MM type 1 standard shown in figure A1, loaded as a doubling dilution. Each band plotted against the doubling dilutions, at different X-ray film exposure periods.

Figure A3. Western blot dilution curve of sCJD VV type 2A standard analysed with 3F4, 4 minute exposure shown.

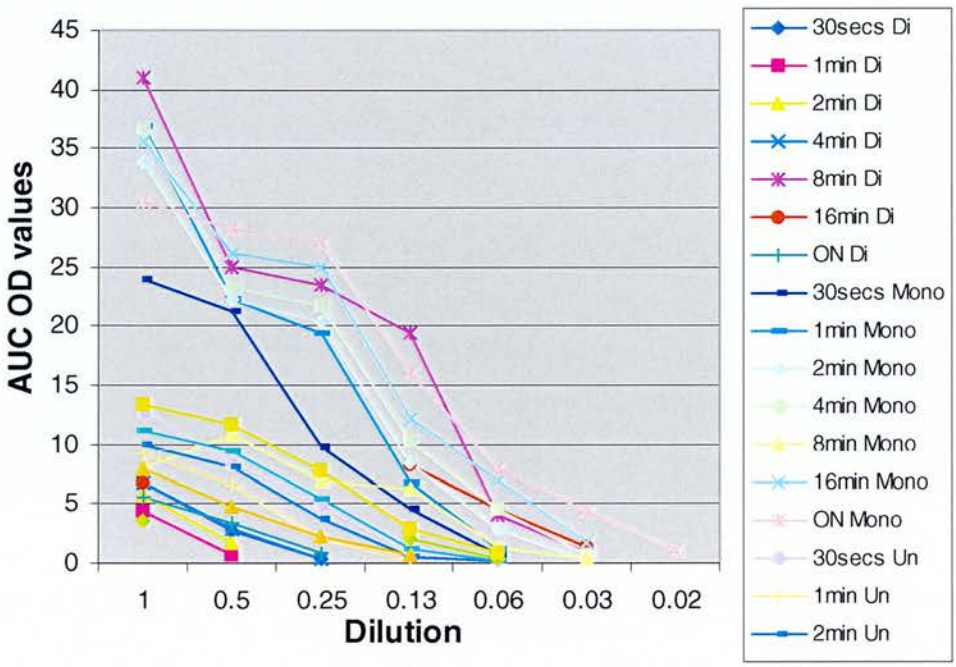

Figure A4. AUC values for sCJD VV type 2A standard shown in figure A3, loaded as a doubling dilution. Each band plotted against the doubling dilutions, at different x-ray film exposure periods.

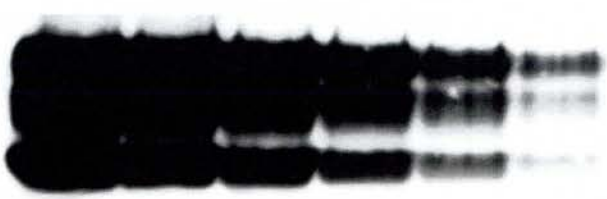

Figure A5. Western blot dilution curve of vCJD MM type 2B standard analysed with 3F4, 8 minute exposure shown.

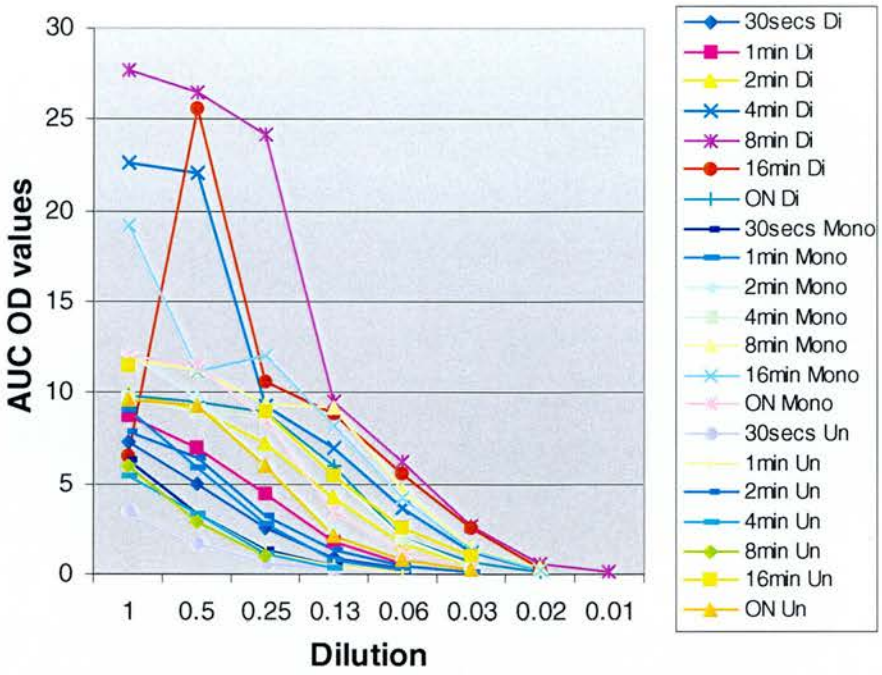

Figure A6. AUC values for vCJD MM type 2B standard shown in figure A5, loaded as a doubling dilution. Each band plotted against the doubling dilutions, at different x-ray film exposure periods.

Dilution curves were carried out for the different isotypes standards (figure A1, sCJD MM 1, figure A3, vCJD MM 2B, figure A5 sCJD VV 2A) with 3F4 primary antibody. First of all the area under the curve (AUC) values for each band, across numerous dilutions at different x-ray film exposure periods were measured. Overlap of linear increases in AUC values demonstrated the possibility of measuring quantitative band ratios from a single lane exposure. To determine the parameters of the quantitative values the AUC values of numerous linear exposures were required. The values from numerous exposures were overlaid to extend the range of density readings (figures A2, A4 and A6). The graph displays a sigmoidal curve, representing saturated levels of signal where all three bands' density ratio values are almost equal, as well as incomplete quantitation, where one band is predominant. The linear range of the bands is represented by the linear increase in density ratio seen in the mid-portion of the graph. The linear values for each exposure time and the corresponding AUC values for each band were compared. The AUC values ranged from a low value of 0.845 to a high value of 7.704 in sCJD MM type 1, a low value of 0.897 and a high value of 12.056 for sCJD VV 2A, low value of 1.101 and a high value of 9.472 for vCJD MM 2B. The high value obtained with the sCJD VV 2A case was due to a

closer relative amount of each band in this subgroup extending the linear range. A conservative approach was adopted to eliminate erroneous readings, provide a range applicable to all subgroups and be in keeping with the linear range of x-ray film of 1 log. It was decided that lanes displaying a band with AUC values above or below, 0.8 to 8 or 0.7 to 7 (i.e all three bands in a lane must fall within one of these two ranges), were either underexposed or saturated respectively, and thus non-linear. Thus readings for the bands in each lane were only reliably representative of the levels of glycoforms in the samples when all three values are within these boundaries.

The STORM linearity was determined in a similar way. The samples were loaded with between 10 and 2µl of a PK treated 10% brain homogenate from a mouse infected with vCJD and a single high density scan performed as opposed to numerous x-ray exposures. The dilution curve of the murine transmission sample (figure A7) was analysed with monoclonal antibody 6H4. The lower range unglycosylated AUC values were difficult to compare on the same scale as the other bands so a log curve of the values were plotted on a separate graph. The high AUC value obtained was 99,067 and the low AUC value 738 (sample well loadings of between 7 and 4µl appeared to be the most linear). The quantitative range of AUC values was thus chosen as between 1000 and 100,000 pixel units representing the 10 log range of linearity.

Figure A7. STORM scan showing dilution curve of murine transmission sample, analysed with 6H4.

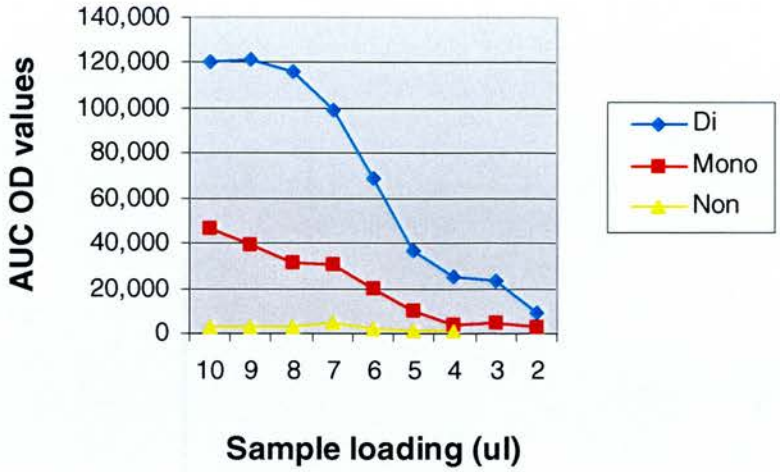

Figure A8. AUC values for murine transmission sample shown in figure A7. Each band plotted against the dilutions.

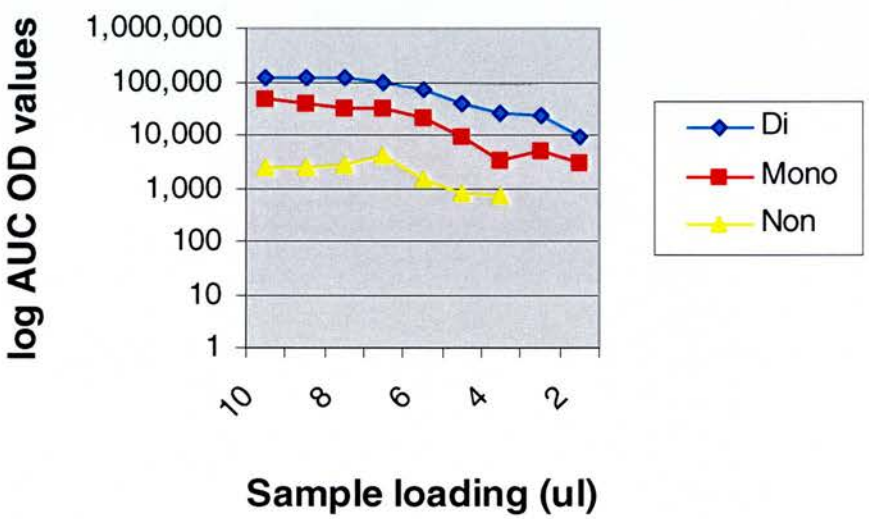

Figure A9. Log AUC values for murine transmission sample shown in figure A7. Each band plotted against the sample loading.

The variance that can arise due to repeated exposure times and repeated sampling of the tissue (intra-assay error) has been quantified.

Comparison of 21 different exposure periods of the sCJD MM 1 standard, within the linear range from the same PVDF Western blot found SDs of 3.1, 2.6 and 1.5 for di, mono and nonglycosylated bands respectively and SEs of 0.6, 0.57, 0.32 for di, mono and nonglycosylated bands respectively. Unpaired two tailed *t* tests comparing the glycoform ratios of the di, mono and nonglycosylated bands measured in sCJD MM 1, sCJD VV 2A and vCJD MM 2B standards following extensive repeated analysis (n = 29, 29 and 24 respectively) by x-ray film exposure was carried out. The SDs and SEs are both low. Sporadic CJD MM 1 SDs (Di 3.3:Mono 4.9: Non 5.8), VV 2A (Di 3.6: Mono 2.6: Non 4.9) and vCJD SDs (Di 5.4: Mono 3.7: Non 5.3) sCJD MM1 SEs (Di 0.73:Mono 1.06: Non 1.27), VV 2A (Di 0.74: Mono 0.53: Non 0.97) and vCJD SEs (Di 1.1: Mono 0.74: Non 1.1). The *t* test showed a highly significant difference between most of the bands for all three cases cases (sCJD MM 1 vs VV 2A $p < 0.000$ for the di and non glycosylated band, $p = 0.06$ for the monoglycosylated band, sCJD MM 1 vs vCJD $p < 0.000$ for all three bands, sCJD VV 2A vs vCJD $p < 0.000$ for the di and monoglycosylated band $p = 0.085$ for the nonglycosylated band). One way ANOVA confirmed that the variation within the groups was less than that between the groups (F test significance = 0.00) with $p < 0.000$ for all the band comparisons aside from sCJD MM 1 vs VV 2A monoglycosylated $p = 0.014$ and sCJD VV 2A vs vCJD nonglycosylated band $p = 0.304$). Analysis of multiple exposures for each experimental analysis as well as multiple experiments of all the samples in this study had SDs calculated and were very similar to the results obtained for the standards here.

Where glycoform ratio data is stated, repeated analysis was possible in the following proportions of cases:

Subgroup	Duplicate analysis (%)	Triplicate analysis (%)	>3 analyses (%)
sCJD MM 1	65.1	52.4	27
sCJD MM 2A	83.3	41.7	33.3
sCJD MV 1	33.3	16.7	16.7
sCJD MV 2A	38.5	30.8	23.1
sCJD VV 1	100	100	75
sCJD VV 2A	66.7	55.6	33.3
vCJD MM 2B	80.1	44.7	14.9
iCJD	80	53.3	40
fCJD	42.9	42.9	42.9

New cases were analysed up until the end of the study period and in some cases limited tissue was available, reducing the number of experimental runs that could be carried out.

A6 Histological findings

Kovacs *et al*, 2000

PrP immunocytochemistry

The results of PrP immunocytochemistry are classified as follows:

Vacuolar

Sparse granular positivity was observed around and between confluent vacuoles. In areas of microcystic spongiform change this pattern was absent.

Diffuse/synaptic

Generalised staining of the neuropil with small dot-like granular deposits of chromagen.

Neuronal

I. Intracellular punctate immunoreactivity.

II. Pericellular punctuate, or granular immunopositivity around unstained neuronal perikarya.

Immunoreactive granular deposits and plaques

Dense positivity in a granular or plaque-like formation not visible in H&E sections, occasionally surrounding a solid centre. Seen as fine granular deposits and unicentric cored plaques. In some cases these were noticed in the perivascular space.

Kovacs *et al*, 2002

PrP IMMUNOSTAINING PATTERNS CHARACTERISTIC OF PRION DISEASE CASES

The following immunostaining patterns were observed: (I) fine deposition (diffuse/synaptic pattern); (II) coarser depositions (these include the granular, the patchy/perivacuolar - including morula type - deposits); (III) plaques (with amyloid characteristics, eg. kuru-type and florid plaques, or without amyloid characteristics, as plaque-like deposits or so called focal deposits); (IV) pericellular deposits as dot-like and/or coarse granular immunoractivity around unstained neuronal perikarya.

Neuropathology and Applied Neurobiology (2000), **26**, 463–472

Clinicopathological phenotype of codon 129 valine homozygote sporadic Creutzfeldt–Jakob disease

G. G. Kovacs*, M. W. Head†, T. Bunn†, L. Laszlo‡, R. G. Will† and J. W. Ironside†

**Department of Neurology, Semmelweis University of Medicine, Budapest, Hungary; †National CJD Surveillance Unit, Departments of Pathology and Clinical Neurosciences, University of Edinburgh, Edinburgh, UK; and ‡Department of General Zoology, Eotvos University of Sciences, Budapest, Hungary*

G. G. Kovacs, M. W. Head, T. Bunn, L. Laszlo, R. G. Will and J. W. Ironside (2000) *Neuropathology and Applied Neurobiology* **26**, 463–472

Clinicopathological phenotype of codon 129 valine homozygote sporadic Creutzfeldt–Jakob disease

The naturally occurring polymorphism at codon 129 of the human prion protein gene (*PRNP*) influences susceptibility to sporadic Creutzfeldt–Jakob Disease (CJD); the majority of the patients are methionine homozygotes at this locus, while valine homozygotes represent only 10% of cases. The aim was to study the clinical and neuropathological phenotype of sporadic CJD in valine homozygotes, to estimate the reliability of current clinical diagnostic criteria, and to identify any consistent and distinct features. Twelve cases of sporadic CJD with a codon 129 valine homozygote genotype were identified at the National CJD Surveillance Unit in Edinburgh. In addition to a retrospective clinical analysis, tissue blocks were stained by conventional techniques and by immunocytochemistry for prion protein. Frozen brain tissue was available from five cases for Western blot analysis of PrP^{RES}, which in all cases showed a type 2 mobility. The cases included four males and eight females, average age 63.6 years, with a mean duration of illness of 6 months. Eleven patients presented with ataxia, and none had the characteristic EEG changes found in sporadic CJD. The neuropathological phenotype comprised spongiform change and prion protein immunopositivity most marked in the subcortical grey matter and cerebellum, prion protein positive plaque-like deposits in all regions, laminar deposition of prion protein in the cerebral cortex, and hippocampal involvement (which is seldom reported in sporadic CJD). In conclusion, these cases exhibited a fairly uniform phenotype, which is relatively distinct from sporadic CJD in methionine homozygotes, and thus diagnosis may be difficult using existing clinical criteria.

Keywords: codon 129, Creutzfeldt–Jakob disease, immunocytochemistry, prion protein, prion gene, valine, Western blot

Introduction

Creutzfeldt–Jakob Disease (CJD) is a rare and invariably fatal neurodegenerative disorder, associated with accumulation in the central nervous system of the abnormal, protease resistant form of the prion protein (PrP), which is encoded on the short arm of the human chromosome 20 [reviewed in 21]. CJD is the most common form of the human transmissible spongiform encephalopathies (TSE): TSEs can be acquired (kuru, iatrogenic and new variant CJD), sporadic (CJD), or inherited (familial CJD, Gerstmann–Straussler–Scheinker disease, fatal familial insomnia) [21].

Clinically, sporadic CJD is characterized by progressive dementia, myoclonus and, in a high proportion of cases, electroencephalogram (EEG) changes consisting of periodic sharp wave complexes (PSWC) with triphasic morphology [9,27]. Neuropathologically, the diagnostic features are spongiform change, astrocytosis,

Correspondence: Professor J. W. Ironside, CJD Surveillance Unit, Western General Hospital, Edinburgh EH4 2XU, United Kingdom. E-mail: j.w.ironside@ed.ac.uk

nerve cell loss, and prion protein amyloid plaques in a minority of cases; accumulation of protease-resistant PrP in the brain is best demonstrated by Western blot analysis [12,14,18]. Clinical diagnostic criteria have been developed for CJD [5,26], but some atypical cases of sporadic CJD may be excluded by these criteria, thus representing a potentially underdiagnosed group. This clinical variability in sporadic CJD is thought to be influenced by host genotype and the agent 'strain' as identified on Western blot analysis of prion protein [18,19,28]. Polymorphisms have been identified at codon 129, 171, and 219 in the human prion protein gene (*PRNP*) [19,23,28]; the methionine/valine polymorphism at codon 129 is the most widely examined amongst sporadic CJD cases. Studies in Europe [26] have shown that 74% of sporadic cases of CJD are methionine homozygotes at codon 129, thus representing a predisposing factor for CJD in the Caucasian population (in contrast to similar studies from Japan) [10,23]. The codon 129 polymorphism also influences susceptibility in some forms of iatrogenic CJD [6].

Diagnostic clinical criteria for CJD which allow classification as definite, probable or possible CJD are largely based on the predominant phenotype in sporadic CJD associated with methionine homozygosity. The aim of this study was to examine the clinicopathological phenotype in the homozygous valine subgroup of sporadic CJD, and to determine whether these cases exhibit atypical features that may compromise the application of current diagnostic criteria.

Materials and methods

Case selection and preparation of tissue

Cases of sporadic CJD of known valine/valine genotype at the *PRNP* codon 129 locus were identified from the brain bank at the National CJD Surveillance Unit in Edinburgh.

After *post-mortem* the brains were fixed by immersion in 15% formalin for a minimum of 3 weeks. Tissue blocks were taken from the frontal, parietal, temporal (including hippocampal formation) and occipital cortex, basal gang-lia, thalamus, pons, cerebellum, hypothalamus and if available, the spinal cord.

Blocks were decontaminated in 96% formic acid for 1 h prior to routine processing into paraffin wax. From each block, 5 μm serial sections were floated on Vectabond-coated slides and stained using haematoxylin and eosin (H&E) and with immunocytochemistry using two anti-PrP antibodies (KG9-monoclonal, 1:200 dilution–Source: Dr C. Birkitt-Compton; 3F4-monoclonal, 1:2000 dilution–Source: R. Kascsak, New York), using a consensus protocol [2]. After counterstaining with haematoxylin, sections were dehydrated, cleared in xylene and mounted in Pertex.

PRNP coding sequence analysis

Genomic DNA was purified from peripheral blood leuco-cytes and the *PRNP* coding region was amplified by the polymerase chain reaction. Known disease specific mutations were excluded by single strand conformational analysis and a direct sequencing protocol was used to identify the codon 129 genotype [28].

Biochemical analysis of PrP

Western blot analysis of protease-resistant prion protein (PrP^{RES}) in samples of frontal cortex was performed by an established method [7]. Briefly, a 10% brain homogenate was made from frozen tissue, cleared by low speed centrifugation and the supernatant digested with 50 μg/ml proteinase K. PrP^{RES} isoforms were separated by SDS-PAGE, transferred to nitrocellulose and detected using the antibody 3F4, a horseradish peroxidase conjugated secondary antibody and enhanced chemiluminescence. The resultant isoform patterns were classified on the basis electrophoretic mobility as type 1 or type 2 [18].

Results

Twelve cases were identified, which will be referred to subsequently as CJD1, CJD2 to CJD12. The clinical features of these cases are summarized in Table 1.

Clinical findings

The age at death ranged from 49 to 80 years, with an average age at death of 64 years. The mean duration of illness was 6 months (range 4–17 months).

Eleven patients had unsteady gait as the presenting symptom, seven had memory disturbance, and two

complained of visual impairment. One patient (CJD9) had itching as a presenting complaint, which has been described recently in CJD [22]. During the clinical course all patients developed dementia, myoclonus (and/or startle response) and developed akinetic mutism before death.

Routine cerebrospinal fluid tests showed no relevant abnormalities; 14-3-3 immunoassays were not performed in any of the cases. Characteristic periodic triphasic complexes were not present in the 11 cases with available EEG findings.

Histological findings

In routine sections the degree of spongiform change was assessed and classified on a five-point scale from – (absent) to +++(severe microcystic and confluent vacuoles); a summary of the neuropathological and prion immunocytochemical findings is shown in Table 2. In general, the grading of the spongiform change also reflected the degree of neuronal loss.

PrP immunocytochemistry

Case CJD 3 showed only slight positivity after repeated immunostaining with anti-PrP antibody KG9. In this case the observations represent results with the 3F4 anti-PrP antibody. The results of PrP immunocytochemistry are classified as follows:

Vacuolar Sparse granular positivity was observed around and between confluent vacuoles. In areas of microcystic spongiform change this pattern was absent.

Diffuse/synaptic Generalized staining of the neuropil with small dot-like granular deposits of chromagen.

Neuronal

1 Pericellular punctuate, or granular immunopositivity around unstained neuronal perikarya.

2 Sparse intracellular punctate immunoreactivity.

Immunoreactive granular deposits and plaque-like deposits Dense positivity in a granular or plaque-like forma-tion not visible in H&E sections, occasionally surrounding a solid centre. These formations resembled those men-tioned by Miyazono *et al.* [16] as fine granular deposits and unicentric cored plaques. In some cases these were noticed in the perivascular space as described by Watanabe *et al.* [25].

Anatomical mapping

The key neuropathological features are summarized in relation to neuroanatomical structures in Figure 1.

Occipital cortex Seven cases showed mild to severe spongiform change and eight had PrP plaques (in CJD1, CJD8 and CJD9, plaques were also present in the subcortical white matter). The diffuse/synaptic PrP immunostaining had a laminar accentuation in CJD1, CJD2, CJD6, CJD7.

Table 1. Clinical findings in the examined cases

Case number	Age *(years)*	*Sex*	*Duration of illness (months)*	*Clinical symptoms (P: presenting T: terminal)*	*EEG**
CJD1	49	Female	11	P: G-V T: D-M-AM-S	–
CJD2	53	Male	6	P: G-MI T: D-M-AM	–
CJD3	54	Male	17	P: MI-G T: D-M-AM	–
CJD4	59	Female	4	P:G-MI T: D-V-M-AM	–
CJD5	59	Female	6	P: G-MI T: D-M-AM	–
CJD6	60	Male	4	P: G-MI-VGP T:D-V-S-AM	–
CJD7	62	Female	7	P: G-MI T: D-M-AM	–
CJD8	64	Female	5	P: G-DI T: D-S-AM	–
CJD9	72	Male	7	P: G-I T: D-M-AM	–
CJD10	75	Female	4	P: G T: D-M-AM	–
CJD11	77	Female	4	P: MI-V T:D-M-AM	**
CJD12	80	Female	6	P: DI-G-UM T: D-M-AM	–

*Characteristic PSWC and triphasic morphology. **Data not available. G, unsteady gait. D, dementia. M, myoclonus. S, startle. AM, akinetic mutism. MI, memory impairment. DI, dizziness. V, visual disturbance. I, itching. UM, unvoluntary movements. VGP, vertical gaze paresis.

Table 2. Prion protein immunostaining pattern and degree of spongiosis in different anatomical regions examined

Case Site	*CJD1*	*CJD2*	*CJD3*	*CJD4*	*CJD5*	*CJD6*	*CJD7*	*CJD8*	*CJD9*	*CJD10*	*CJD11*	*CJD12*
HP												
CA1	DP/+	D/++	D/+	D/+	D/++	DP/++	D/+	D/+	D/+	D/+	0/−+	D/++
CA2	D/−+	D/−+	D/−	D/−	0/−	D/−	0/−	0/−	D/−	0/−	0/−	0/−
CA3	D/−+	D/−+	D/−	D/−	0/−	D/−	0/−	0/−	D/−	0/−	0/−	0/−
CA4	D/+	DP/+	D/−	N/−	DN/−	D/−+	0/−	0/−	D/−	0/−+	0/−	D/−
DG	D/+	DP/++	D/−	D/−+	D/−+	D/++	DP/−+	DP/−	0/−	0/−+	0/−	D/−
SU	D/+	D/+++	D/+	D/+	D/+++	D/+++	DN/++	D/++	DN/++	D/+++	D/++	DNP/++
TE	DNP/++	DNP/−+	D/++	DP/−	0/−	DVP/++	DNP++	0/−	DNP/−	**	DP/+	**
PG	DNP/++	DNP/+++	D/++	DNP/−	N/+	DP/++	DNP/++	DNP/−	DNP/−	N/−	DV/+	DNP/−
CE	DP/+	DP/+++	0/−	DP/++	DP/+++	DP/+++	DP/−	DP/++	DP/+++	DP/+	DP/−+	DP/+
DN	DN/−	DN/−	0/−	**	0/−	0/−	DN/−	0/−	DN/−	**	DN/−+	0/−
PO	DN/−	DN/−	0/−+	DN/−	DN/−	DN/−	**	DN/−+	DN/−	DN/−+	DN/−	DN/+
TH	D/−+	DP/++	D/++	DNP/++	DP/++	DP/+	DP/+++	DP/++	DNP/++	DP/++	P/+	DNP/++
OC	DNP/++	DP/++	D/−	0/−+	0/−+	DNP/++	DPV/−+	P/−	P/−	0/−	P/+	P/−
FR	DNP/++	DP/+++	0/++	DP/+	D/++	DNP/++	DNPV/+++	DNP/+	DN/+	0/−	D/+	DNP/+++
PA	DNP/++	DNP/++	D/++	P/+	D/+	DNP/−+	DNP/++	DNP/+	DNP/+	N/−	D/+	DNP/+
HY	D/−+	DP/++	0/−	DNP/++	DP/++	**	DP/+	**	DP/++	D/+	D/+	0/−
BG	DNP/+++	DNP/+++	DN/+++	DNP/+++	DP/+++	DP/+++	DNP/+++	DNP/+++	DNP/++	DNP/+++	DP/+++	DNP/+++
SC	**	DP/−	**	**	**	**	**	**	DP/−	D/−	**	**

HP, hippocampus proper. DG, dentate gyrus. SU, subiculum. TE, temporal isocortex. PG, parahippocampal gyrus. CE, cerebellum. DN, dentate nucleus. TH, thalamus. OC, occipital. FR, frontal. PA, parietal. HY, hypothalamus. BG, basal ganglia. *Prion immunostaining pattern*: 0 – no positivity; D – diffuse/synaptic; N – neuronal; P – plaque; V – vacuolar. *Spongiosis*: – focal/none, −+ mild, + medium, ++ severe microcystic, +++ severe microcystic and confluent.

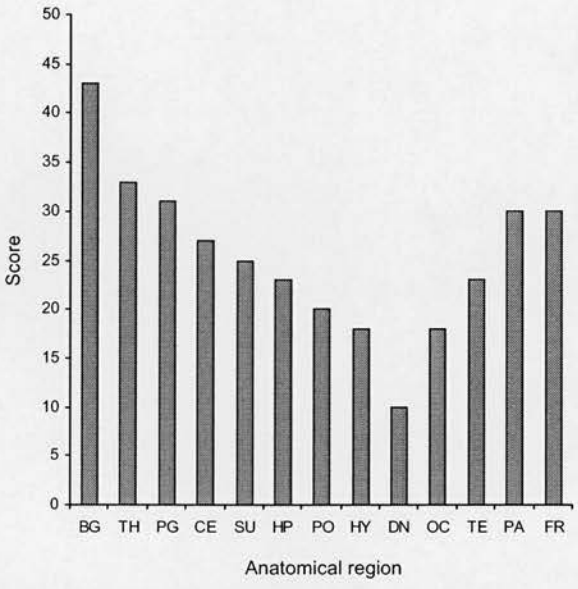

Figure 1. Summary of the neuropathological features in the anatomical regions examined. The presence of severe spongiform change, diffuse/synaptic, neuronal and plaque-like prion immunopositivity was scored semiquantitatively (0–4) in each anatomical region for every case. This allows a relative 'score' for each region to be calculated that reflects the relative severity of pathological involvement (the maximum score for any given region would be 48 (12×4), if each case contained severe spongiosis and the three different prion immunostaining patterns in that anatomical region). BG, basal ganglia. TH, thalamus. PG, parahippocampal gyrus (entorhinal cortex). CE, cerebellum. SU, subicular cortex. HP, hippocampus (including CA regions and dentate gyrus). PO, pons. HY, hypothalamus. DN, dentate nucleus. OC, occipital cortex. TE, inferior temporal cortex. PA, parietal cortex. FR, frontal cortex.

Frontal cortex Moderate to severe confluent spongiform change (Figure 2**a**) was seen in all cases except CJD10, plaque-like deposits were visible in seven (in three cases in the subcortical white matter also). The synaptic/diffuse PrP immunostaining in 10 cases and neuronal (Figure 2**c**,**d**) in six cases showed laminar accentuation (layer V–VI).

Parietal/parasagittal cortex Mild to severe spongiform change was seen in all except CJD10. Plaque-like deposits were visible in eight cases (in three cases in the subcortical white matter also). Diffuse/synaptic PrP deposition was present in 10 cases, perineuronal deposition was identified in eight cases and laminar accentuation in six.

Basal ganglia (caudate nucleus, putamen, globus pallidus) Every case showed severe, confluent spongiform change and diffuse/synaptic PrP immunostaining. Perineuronal positivity was noticed in nine cases, and plaque-like deposits were present in all cases except CJD3. Plaques were also seen in the adjacent white matter in five cases (Figure 2**e**).

Hippocampal formation In Ammon's horn, spongiform change affected the CA1 region in all cases (Figure 2**b**), predominantly in the pyramidal layer, whilst CA 2,3,4 were relatively spared. The usual PrP immunostaining pattern was diffuse/synaptic and occasionally perineuronal, mainly in the CA1 and CA4 region. Scanty plaque-like deposits were noticed in three cases.

In the dentate gyrus, the molecular layer showed microcystic spongiform change from mild to severe degree in seven cases with diffuse/synaptic PrP immunopositivity in nine cases, whereas small plaque-like deposits were visible in the granular layer in three cases.

The adjacent subiculum was affected by spongiform change from a level of moderate to severe, confluent with diffuse/synaptic PrP immunostaining in all cases and perineuronal deposition in three cases. Plaque-like deposits were noticed only in CJD12.

Inferior temporal cortex and parahippocampal gyrus (entorhinal cortex) In two cases the inferior temporal cortex was not available. In the remaining cases spongiform change was found in the temporal cortex in six cases and in the parahippocampal gyrus in seven cases. PrP immunostaining of the inferior temporal cortex showed diffuse/synaptic positivity in eight cases, perineuronal deposition in four and perivacuolar deposition in one. The immunostaining pattern had a laminar accentuation (deeper lamina: V–VI) in four cases. Plaque-like deposits were visible in seven cases, of which five had plaques in the subcortical white matter also. In the parahippocampal gyrus, 10 cases showed diffuse/synaptic PrP staining, nine perineuronal staining, one vacuolar staining, with laminar dominance in seven cases, and plaque-like deposits in eight (five of which also showed plaque-like deposits in the subcortical white matter).

Pons (mid level) Mild spongiform change in the pontine nuclei was seen in four cases, while diffuse/synaptic and intraneuronal PrP immunoreactivity was noticed in 10 cases, but plaque-like deposits were not visible.

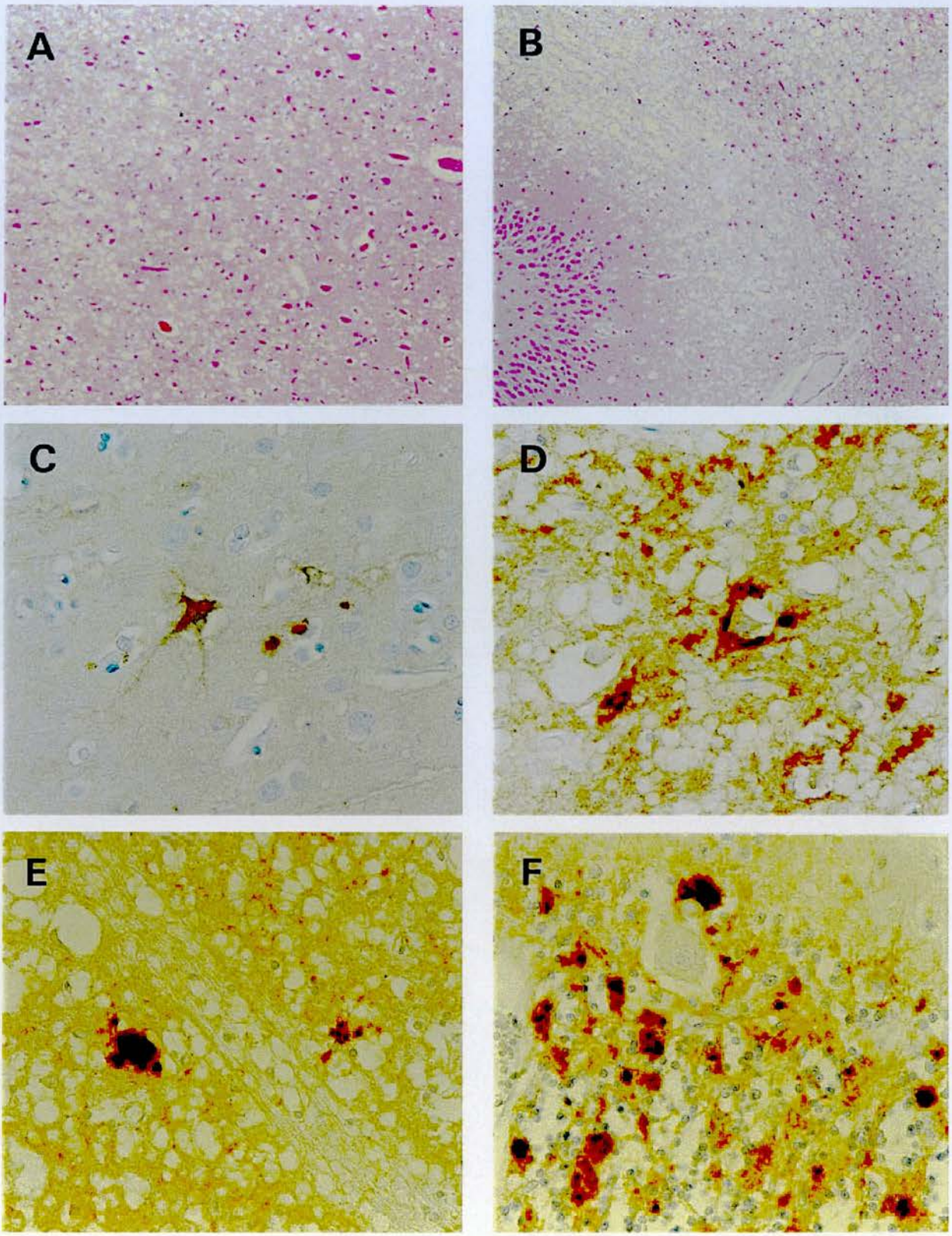
A
B
C
D
E
F

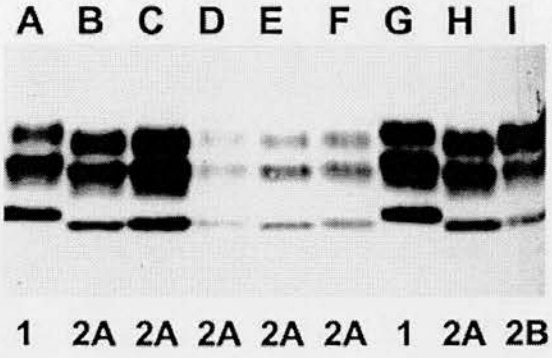

Figure 3. Western blot analysis of PrP^{RES} in homogenates of frontal cortex from sporadic CJD case 2 (lane B) case 4 (lane C), case 7 (lane D), case 10 (lane E), and case 12 (lane F). PrP^{RES} isotype standards are shown in lanes A and G (M/M type 1), lane H (V/V type 2A, case 2), and lane I (M/M type 2B, new variant CJD). Lanes are identified by letter (top) and the PrP^{RES} isotype (bottom).

Cerebellum Spongiform change affected the molecular layer (10 cases) to a mild to severe (confluent) degree. Purkinje cells were relatively spared but the number of granular cells was variably reduced. Plaque-like deposits plaques were visible in the granular layer in all cases except CJD3, in the molecular layer in seven cases, and in eight cases in the white matter. The main immunostaining pattern was diffuse punctuate with granular deposits (Figure 2f). In the 10 cases where the dentate nucleus was visible, five showed prion immunoreactivity without obvious pathological changes.

Thalamus Spongiform change affected all three nuclei (anterior, dorsomedial, ventrolateral) in a mild to severe degree. The predominant immunostaining pattern was diffuse/synaptic (11 cases) with neuronal pericellular and occasionally intracellular reactivity in three cases. Plaque-like deposits were observed in 10 cases, both in the neuropil and the perivascular space.

Hypothalamus Ten cases were examined. Eight cases showed mild to severe spongiform change and diffuse/synaptic immunostaining, while plaque-like deposits were visible in five cases.

Spinal cord Sections of the spinal cord were available in only three cases (CJD2, CJD9, CJD10). Spongiform change was not present in any case, but plaque-like deposits were visible in two cases with diffuse/synaptic PrP immunostaining most intense in the substantia gelatinosa in all three cases.

PrP Typing

Frozen material was available in 5/12 cases examined (CJD2, CJD4, CJD7, CJD10, and CJD12). Western blot analysis on the frontal cortex (Figure 2) showed that in each of these cases the PrP^{RES} had a type 2 mobility. The glycoform ratios were typical of sporadic CJD (type 2A) and distinct from that associated with new variant CJD (type 2B) (Figure 3).

Discussion

The present study has identified the clinical and neuropathological features of 12 codon 129 valine homozygote sporadic CJD cases in the archives of the CJD Surveillance Unit in Edinburgh, UK. The polymorphism at this codon is thought to influence disease susceptibility in sporadic and iatrogenic CJD, with homozygosity as a predisposing factor [6,19]. Valine homozygote cases are rare, and their disease phenotype may lead to difficulties in clinical diagnosis and in the application of current diagnostic criteria for CJD.

Clinical data was available in all 12 valine homozygote cases of sporadic CJD. The average age at death in this series was 64 years, in keeping with many series of unselected sporadic CJD cases, but a recent multicentre study of sporadic CJD has demonstrated an excess of valine homozygotes in patients aged less than 50 years [1]. Unsteadiness of gait was a presenting symptom in the majority of cases (11/12), in comparison to 20–30% of cases with initial ataxia in sporadic CJD [4,27]. Similar cases have been classified as the 'ataxic variant' of CJD, and the results of lesion profiling of spongiform change in such cases in one recent large study are similar to our descriptive findings [19]. Early impairment of memory

Figure 2. (a) Spongiform change in the frontal neocortex (haematoxylin and eosin (H&E)) (left side of the picture represents the deeper cortical layers). (b) Severe spongiform change in Ammon's horn (H&E) (dentate gyrus on the left, CA1 region on the right). (c) Intraneuronal prion immunopositivity in the frontal neocortex. (d) Perineuronal prion immunostaining in the frontal neocortex. (e) Diffuse/synaptic and plaque-like prion positivity in the putamen, with widespread spongiform change. (f) Plaque and diffuse-granular prion immunopositivity in the cerebellum.

was common (7/12) as in sporadic CJD. During the clinical course dementia, myoclonus (often with a startle response) and akinetic mutism were the dominant features. All these features are characteristic of sporadic CJD. In contrast the 'typical' EEG abnormalities found in sporadic CJD were absent in all 11 cases in which EEG data was available. The average age at death was similar to that in larger series [4,9,26].

Current diagnostic criteria for CJD allow diagnostic classification as 'definite', 'probable' or 'possible' CJD [5]. None of the valine homozygote cases in this report would have been categorized clinically as 'probable' CJD and, although all the cases would have fulfilled criteria for 'possible' CJD, these cases would not have been included in analysis (or official statistics) in many studies without neuropathological verification. There is a need for further information on diagnostic tests such as CSF 14-3-3, CSF immunoassay and magnetic resonance brain imaging in valine homozygote cases of sporadic CJD in order to try and improve clinical diagnosis.

Important neuropathological (immunocytochemical) findings in these valine homozygote cases are involvement of the hippocampal formation, the presence of PrP-positive plaques, the laminar accentuation of PrP immunostaining, and a significant trend to more severe changes in the subcortical grey matter and cerebellum (Table 3). Previous neuropathological reviews have emphasized that the hippocampus is typically spared in sporadic CJD [12,14]. Misuzawa *et al.* [17] described the involvement of the hippocampus in CJD, concluding that the molecular-lacunosum layer was the area most frequently affected, as in some descriptions of kuru. In the present cases, the stratum pyramidale (predominantly in CA1) was also affected and examination of this region using prion immunocytochemistry revealed the presence of abnormal prion protein. This feature, along with the affection of subicular cortex, parahippocampal gyrus and temporal isocortex resembled the distribution of pathology in Alzheimer's disease [3]; it is of note that the cases in the present series developed significant early memory impairment.

Widespread loss of parvalbumin-positive neurones is thought to be a distinctive feature of CJD [11]. Guentchev *et al.* [11] demonstrated that loss of parvalbumin-positive neurones in the hippocampus is most commonly the only pathological change in the hippocampus, suggesting, that this could be an early event followed later by spongiform change. Although parvalbumin immunostaining was not used, the present results show that the codon 129 valine homozygote cases have visible neuropathological changes in the hippocampus, either because of the longer duration of illness, or because of different neuronal targeting, perhaps related to a distinct form of disease-associated prion protein. The severe pathology of the basal ganglia and cerebellum is also distinct from previous studies of sporadic CJD (which presumably included mainly methionine homozygote cases) [12,14]; movement disorders and specifically gait disorder occurred early in the clinical course in the present cases. The thalamic pathology in the present cases also differs from sporadic CJD in methionine homozygotes and fatal familial insomnia, and shows severe spongiform change and widespread prion protein immunoreactivity [19]. The occurrence of severe pathological changes in these subcortical structures was unrelated to the duration of illness.

Western blotting studies showed that type 2 PrP^{RES} was present in all cases studied; the relative uniformity of the clinical and pathological phenotype in this series indicates that probably all the cases would have a type 2 PrP^{RES}. Overall, the features of the 12 cases in this study correspond to those of the VV2 subgroup reported in the small series of Tranchant *et al.* [24] and the large multicentre series of Parchi *et al.* [19]. However, it has not been possible to assess the clinical features in relation to current diagnostic criteria and record the neuropathological features (particularly the hippocampal pathology) in much greater detail.

The significance of prion protein subtype in terms of differential neuroanatomical targeting requires further investigation; different prion immunostaining patterns might indicate different stages of prion propogation in susceptible neurones, thus influencing cell survival. The significance of the laminar appearance of neuropathological features in the neocortical deeper layers is not clear, although it may reflect distinct characteristics in subgroups of cortical neurones, perhaps relating to differences in PrP^{C} expression [8]. PrP-positive plaques were found in every case examined except CJD3. This case had a significantly longer duration of illness than the other cases. It is of interest that it has previously been suggested that plaque formation is predominantly associated with prolonged illness duration [15], although not in all series [20,25]. The plaques identified on PrP immunocytochemistry were morphologically distinct from kuru plaques and may represent an immature

form of amyloid plaque, as described in murine scrapie models [13]. The presence of a valine-associated isoform of the abnormal prion protein appears to favour plaque formation in sporadic CJD; kuru-type plaques (visible on routinely stained sections) are associated with codon 129 heterozygosity and type 2 PrP^{RES} in sporadic CJD [19].

In summary, cases of sporadic CJD with a valine homozygous genotype at codon 129 in *PRNP* have a clinicopathological phenotype that is relatively distinct from the typical phenotype of sporadic CJD associated with methionine homozygosity. Valine homozygote cases may have a more prolonged duration of illness, do not exhibit the 'typical' EEG, and often present with ataxia. Neuropathologically, the characteristic features are plaque-like deposits on PrP immunocytochemistry, laminar perineuronal/synaptic deposition of PrP in the cerebral cortex, spongiform change most marked in subcortical grey matter structures, and involvement of the hippocampus. These results, which include a detailed neuropathological survey, support the findings of Parchi *et al.* [19] suggesting that VV2 sporadic CJD is a distinct entity. There is a clear need for further study of determinants of phenotypic variability in sporadic CJD, reinforcing the importance of neuropathological and biochemical examination in this disorder [14,18].

Acknowledgements

Gábor G. Kovács was supported by a project grant (T-10 422/1996) of the Hungarian Ministry of Health. The CJD Surveillance Unit is funded by the Department of Health and the Scottish Executive. The authors are indebted to Professor J. E. Bell, Dr L. Bridges, Dr D. Hilton, Dr J. Mclaughlin, Dr M. Mirakhur, Dr T. Moss, Dr J. Neal, Dr C. O'Brien, Dr F. Scaratt, Professor R. O. Weller and Dr J. Xuereb for referring cases to the Unit, and to Mrs K. Estebeiro for genetic analysis. The authors gratefully acknowledge the technical work of Mrs Linda McCardle.

References

1 Alperovitch A, Zerr I, Pocchiari M *et al.* Codon 129 prion protein genotype and sporadic Creutzfeldt–Jakob disease. *Lancet* 1999; **353**: 1673–4
2 Bell JE, Gentleman S, Ironside JW *et al.* Prion protein immunocytochemistry – UK five centre consensus report. *Neuropathol Appl Neurobiol* 1997; **23**: 26–36
3 Braak H, Braak E. Evolution of the neuropathology of Alzheimer's disease. *Acta Neurol Scand Suppl* 1996; **165**: 3–12
4 Brown P, Cathala F, Sadowsky D, Gajdusek DC. Creutzfeldt–Jakob disease in France. II Clinical characteristics of 124 consecutive verified cases during the decade 1968–1977. *Ann Neurol* 1979; **6**: 430–7
5 Budka H, Aguzzi A, Brown P *et al.* Tissue handling in suspected Creutzfeldt–Jakob Disease and other human spongiform encephalopathies (prion diseases). *Brain Pathol* 1995; **5**: 319–22
6 Collinge J, Palmer MS, Dryden AJ. Genetic predisposition to iatrogenic Creutzfeldt–Jakob disease. *Lancet* 1991; **337**: 1441–2
7 Collinge J, Sidle KCL, Meads J, Ironside JW, Hill AF. Molecular analysis of prion strain variation and the aetiology of 'new variant' CJD. *Nature* 1996; **383**: 685–90
8 DeArmond SJ, Qiu Y, Sanchez H *et al.* PrP^{C} glycoform heterogeneity as function of brain region: implications for selective targeting of neurons by prion strains. *J Neuropathol Exp Neurol* 1999; **58**: 1000–9
9 deSilva R. Human spongiform encephalopathy clinical presentation and diagnostic tests. In *Methods in Molecular Medicine: Prion Diseases* Eds. H Baker, RM Ridley. Totowa, New Jersey: Humana Press, 1996: 59–85
10 Doh-Ura K, Kitamoto T, Sakaki Y, Tateishi J. CJD discrepancy. *Nature* 1991; **353**: 801–2
11 Guentchev M, Hainfellner JA, Trabattoni GR, Budka H. Distribution of parvalbumin-immunoreactive neurons correlates with hippocampal and temporal cortical pathology in Creutzfeldt–Jakob disease. *J Neuropath Exp Neurol* 1997; **56**: 1119–24
12 Ironside JW. Review: Creutzfeldt–Jakob disease. *Brain Pathol* 1996; **6**: 379–88
13 Jeffrey M, Goodsir CM, Bruce ME *et al.* Morphogenesis of amyloid plaques in 87V murine scrapie. *Neuropath Appl Neurobiol* 1994; **20**: 535–42
14 Kretzschmar HA, Ironside JW, DeArmond Tateishi J. Diagnostic criteria for sporadic Creutzfeldt–Jakob disease. *Arch Neurol* 1996; **53**: 913–20
15 Masters CL, Gajdusek DC, Gibbs CJ Jr. Creutzfeldt–Jakob disease virus isolations from the Gerstmann–Straussler syndrome with an analysis of the various forms of amyloid plaque deposition in the virus-induced spongiform encephalopathies. *Brain* 1981; **104**: 559–88
16 Miyazono M, Iwaki T, Kitamoto T, Kaneko Y, Doh-ura K, Tateishi J. A comparative immunohistochemical study of kuru and senile plaques with special reference to glial reactions at various stages of amyloid plaque formation. *Am J Pathol* 1991; **139**: 589–98
17 Misuzawa H, Hirano A, Llena JF. Involvement of hippocampus in Creutzfeldt–Jakob disease. *J Neurol Sci* 1987; **82**: 13–26
18 Parchi P, Castellani R, Capellari S *et al.* Molecular basis of phenotypic variability in sporadic Creutzfeldt–Jakob disease. *Ann Neurol* 1996; **39**: 767–78

19 Parchi P, Giese A, Capellari S *et al.* Classification of sporadic Creutzfeldt–Jakob disease based on molecular and phenotypic analysis of 300 subjects. *Ann Neurol* 1999; **46**: 224–33
20 Pickering-Brown SM, Mann DMA, Owen F *et al.* Allelic variations in apolipoprotein E and prion protein genotype related to plaque formation and age of onset in sporadic Creutzfeldt–Jakob disease. *Neurosci Lett* 1995; **187**: 127–9
21 Prusiner SB. Prion diseases and the BSE crisis. *Science* 1997; **278**: 245–51
22 Shabtai H, Nisipeanu P, Chapman J, Korczyn AD. Pruritus in Creuztfeldt–Jakob disease. *Neurology* 1996; **46**: 940–1
23 Shibuya S, Higuchi J, Shin R-W, Tateishi J, Kitamoto T. Protective prion protein polymorphism against sporadic Creutzfeldt–Jakob disease. *Lancet* 1998; **351**: 419
24 Tranchant C, Geranton L, Guiraud-Chaumeil C, Mohr M, Warter JM. Basis of phenotypic variability in sporadic Creutzfeldt–Jakob disease. *Neurology* 1999; **52**: 1244–9
25 Watanabe R, Duchen LW. Cerebral amyloid in human prion disease. *Neuropath Appl Neurobiol* 1993; **19**: 253–60
26 Will RG, Alperovitch A, Poser S *et al.* Descriptive epidemiology of Creutzfeldt–Jakob disease in six European countries, 1993–1995. *Ann Neurol* 1998; **43**: 763–7
27 Will RG, Matthews WB. A retrospective study of Creutzfeldt–Jakob disease in England and Wales 1970–1979 I. Clinical features. *J Neurol Neurosurg Psychiatry* 1984; **47**: 134–40
28 Windl O, Dempster M, Estibeiro JP *et al.* Genetic basis of Creutzfeldt–Jakob disease in the United Kingdom: a systematic analysis of predisposing mutations and allelic variation in the *PRNP* gene. *Hum Genet* 1996; **98**: 259–64

Received 18 January 2000
Accepted after revision 18 July 2000

Sporadic Creutzfeldt-Jakob Disease in a Young Dutch Valine Homozygote: Atypical Molecular Phenotype

Mark W. Head, PhD,[1] Gerrit Tissingh, MD,[2]
Bernard M. J. Uitdehaag, MD, PhD,[2]
Frederik Barkhof, MD, PhD,[3] Tristan J. R. Bunn, MSc,[1]
James W. Ironside, FRCP,[1]
Wouter Kamphorst, MD, PhD,[4] and
Philip Scheltens, MD, PhD[2]

A case of sporadic Creutzfeldt-Jakob disease (sCJD) is described in a young Dutch protein prion gene *(PRNP)* codon 129 valine homozygote. Certain clinical and molecular features of this case overlap those of variant CJD. The case highlights possible difficulties in the differential diagnosis of vCJD and the more rare sCJD subtypes based on molecular features alone.

Ann Neurol 2001;50:258–261

Creutzfeldt-Jakob disease (CJD) is a rare, rapidly progressive, and invariably fatal neurodegenerative condition characterised clinically by dementia and ataxia and pathologically by neuronal loss, gliosis, and spongiform change in the brain. It can be inherited (familial CJD), acquired (iatrogenic CJD), or idiopathic (sporadic CJD, sCJD). Irrespective of aetiology, CJD is characterised by the accumulation of an altered form (PrP^{Sc}) of a host-encoded glycoprotein (PrP^{C}). Mutations in the gene encoding PrP, termed *PRNP,* are closely associated with the inherited forms of the disease, whereas medical histories that include procedures such as human growth hormone treatment or dura mater grafting are strongly indicative of iatrogenic CJD. Susceptibility and disease phenotype can be substantially modified by the common methionine/valine polymorphism at codon 129 of *PRNP.*

In 1996, a new form of the disease, variant CJD (vCJD), was described in the United Kingdom,[1] which appears to result from infection with the bovine spongiform encephalopathy (BSE) agent.[2,3] vCJD patients are younger than sCJD patients and usually present with psychiatric symptoms, followed by ataxia, movement disorders, and dementia during a protracted disease course. The eventual size of the current epidemic of vCJD is uncertain, but accurate long-term predictions necessitate ongoing surveillance and accurate diagnosis. The phenotype described in the first 10 cases has proved consistent, allowing formulation of clinical diagnostic criteria for probable vCJD in living patients with strong predictive value.[4] The recent inclusion of a postthalamic high magnetic resonance imaging (MRI) signal (the pulvinar sign) has further strengthened the criteria.[4,5] Nevertheless, a definite diagnosis of vCJD requires neuropathological examination of the brain.[6] Another consistent finding in vCJD has been the presence in the brain of a predominantly diglycosylated form of the protease-resistant prion protein (PrP^{res}).[6–8] A further accentuation of this "glycosylation signature" in PrP^{res} was found in vCJD tonsil.[9] Thus far, all patients with a definite diagnosis of vCJD who have been tested have been methionine homozygotes at codon 129 of *PRNP.* This has prompted speculation concerning the possibility and potentially novel phenotype(s) of BSE infection in humans with valine at codon 129.[3,10]

In practice, sCJD is the major differential diagnosis of vCJD.[4] However, sCJD has a remarkably diverse clinicopathological phenotype. A recent study of 300 sCJD cases identified six distinct subtypes.[11] Each subtype correlated with a particular combination of PrP^{res} isotype, defined by the molecular size of the nonglycosylated, protease-resistant core fragment (type 1, 21 kDa, or type 2, 19 kDa) and *PRNP* codon 129 genotype (methionine homozygosity, MM; heterozygosity, MV; or valine homozygosity, VV). Two of the least frequent subtypes of sCJD require particular attention in relation to vCJD. First, the PrP^{res} in methionine homozygous type 2 (MM2) cases differ only in glycosylation site occupancy from the PrP^{res} found in vCJD. Second, the valine homozygous type 1 (VV1) sCJD subtype has a young age at onset and, in common with MM2 cases, a prolonged disease course. These clinical features alone may prompt neurologists to consider, perhaps inappropriately, a diagnosis of vCJD.

This report describes a case of sCJD in a valine homozygote, which brings several issues surrounding the differential diagnoses of vCJD and sCJD into sharp focus.

Case Presentation

A previously healthy 42-year-old woman was referred to the outpatient memory clinic of the Vrije University Medical Centre suffering from progressive memory

From the [1]National Creutzfeldt-Jakob Disease Surveillance Unit and Department of Pathology, University of Edinburgh, Western General Hospital, Edinburgh, UK; [2]Department of Neurology, [3]Department of Radiology, and [4]Department of Pathology, Vrije Universiteit Medical Center, Amsterdam, the Netherlands.

Received Dec 6, 2000, and in revised form May 9, 2001. Accepted for publication May 9, 2001.

Address correspondence to Dr Head, National CJD Surveillance Unit, Western General Hospital, Edinburgh, EH4 2XU, UK.
E-mail: m.w.head@ed.ac.uk

loss, spatial disorientation, depression, and headache over the previous 8-month period. Sensory and psychiatric features were not evident. The patient had no family history of dementia and no obvious iatrogenic exposure to prions and had been continuously resident in the Netherlands. On admission, neurological examination revealed global memory impairment, visual agnosia, visuospatial disturbances, mild cerebellar ataxia, and minor involuntary movements, best described as "fidgety." Clinical tests showed 14-3-3 positive cerebrospinal fluid and an absence of periodic sharp wave complexes on electroencephalography (EEG). MRI showed signal increase in the grey matter on diffusion-weighted images. No mutations were found in *PRNP,* but the patient was homozygous for valine at codon 129. Given the early age at onset and the already protracted disease course, a brain biopsy (right frontal cortex) was performed 2 months after admission, to confirm the provisional diagnosis of CJD and discount a diagnosis of vCJD. Neuropathological examination of this material showed transcortical microvacuolar spongiform change, variable neuronal loss, and gliosis (Fig 1A). No amyloid plaques were visible using Congo red or periodic acid-Schiff stains. PrP immunohistochemistry showed a diffuse granular "synaptic" pattern, with no plaques visible (Fig 1B). Western blot analysis showed easily detectable levels of PrP^{res}, with a 21 kDa nonglycosylated band (type 1) and an unremarkable glycoform ratio (Fig 2). Immunohistochemical and Western blotting studies were carried out exactly as described previously.[6] Taken together, these findings support a diagnosis of sCJD, the atypical clinical features of the case being consistent with the rare VV1 sCJD subtype.

Over the following months, the patient became akinetic and mute, with persistent mild ataxia (she was still able to walk 14 months after the first symptoms) and myoclonic jerks towards the end of the disease course. She died 18 months after the onset of symptoms. Permission for post-mortem examination was restricted to the brain. Histopathological examination of the left cerebral hemisphere, cerebellum, and brain stem showed pathology similar to that seen at biopsy: cerebral cortical spongiform change, more severe neuronal loss, and gliosis (Fig 1C), as well as a synaptic PrP immunostaining pattern and absence of plaques (Fig 1D). This histological appearance was typical of all cortical regions examined, with no laminar pattern of PrP deposition. Spongiform change was also present in the hippocampus. The caudate nucleus and putamen exhibited severe spongiform change, but this feature was less marked in the thalamus and brain stem. PrP immunocytochemistry showed granular synaptic staining in all of these regions, along with small numbers of PrP-positive plaque-like structures (which were not evident on routine microscopy). Patchy spongiform change was present in the cerebellar molecular layer, accompanied by Purkinje cell loss and gliosis. PrP deposition occurred in a granular synaptic pattern, with occasional small plaque-like structures in the molecular layer and around the dentate nucleus.

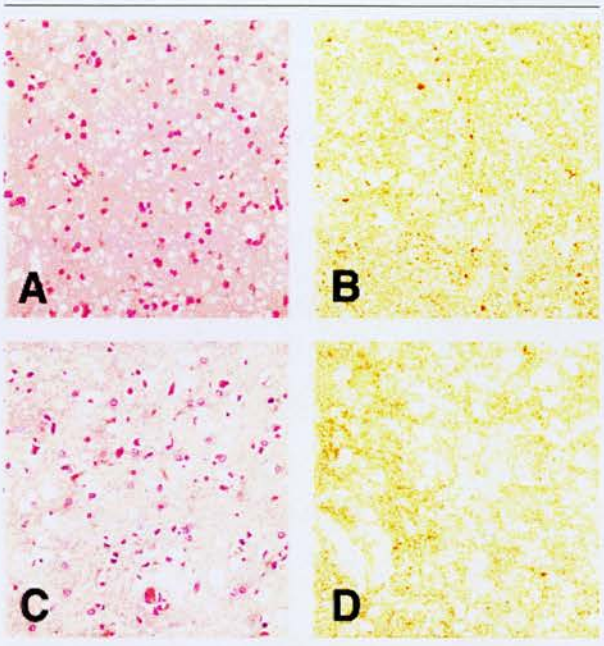

Fig. 1. (A) The frontal cortex in the brain biopsy specimen shows widespread microvacuolar spongiform change, with occasional areas of confluent vacuolation. No plaques are present. Haematoxylin and eosin. (B) Immunocytochemistry for prion protein shows widespread positivity in a reticular (synaptic) pattern in the frontal cortex from the biopsy specimen. No plaques are present. KG9 monoclonal antibody/haematoxylin counterstain following proteinase K digestion. (C) The frontal cortex in the autopsy specimen shows spongiform change, with a coarse pattern of vacuolation. Neuronal loss and astrocytosis are more evident than in the biopsy. Haematoxylin and eosin. (D) Immunocytochemistry for PrP in the frontal cortex in the autopsy specimen shows a widespread synaptic pattern of deposition. No plaques are visible, and there is no evidence of a laminar or perineuronal pattern of PrP accumulation. KG9 monoclonal antibody/haematoxylin counterstain following proteinase K digestion. (A–D) Original magnification ×175.

Western blot analysis of a frozen autopsy sample of the left frontal cortex (the only frozen tissue available) contrasted starkly with that seen at biopsy. The nonglycosylated PrP^{res} was clearly of type 2 mobility (19 kDa); moreover, the glycoform ratio was not characteristic of sCJD and resembled that seen in vCJD (Fig 2). Multiple sampling and analysis from different regions of the available autopsy and biopsy frontal cortex samples (n = 4 and 6, respectively) showed a reproducible difference in the glycoform ratio between these 2 samples (Fig 3).

Discussion

All vCJD cases thus far described have been homozygous for methionine at codon 129 of the *PRNP* gene,[4] although this genotype represents a minority of the normal Caucasian population.[11] Comparison with the only other peripherally acquired forms of CJD currently known (iatrogenic CJD and Kuru) suggests that all three codon 129 genotypes might be susceptible to vCJD but that the incubation times could differ.[10,12] Although the codon 129 *PRNP* polymorphism has a major influence in the neuropathology of sCJD, the neuropathological changes in Kuru are modified only to a minor degree by *PRNP* codon 129 polymorphisms.[10,13] Modelling of vCJD in human valine homozygotes using "humanized" mice has suggested that the "glycoform signature" of vCJD will be conserved on a valine background.[9]

The fundamental question posed by this case in the first instance was whether it might represent vCJD in a valine homozygote. These fears were raised by the early onset, long duration, and behavioural symptoms early in the illness without neurological signs. Brain biopsy confirmed the clinical diagnosis of CJD and indicated that the patient had a rare PrP^{res} isotype/codon 129 genotype combination.[11] The clinical features of this case (early onset, long duration, progressive dementia) and clinical test results (normal EEG, cortical abnormalities on MRI) bear a strong resemblance to the four VV1 cases reported.[11,14] The histological features in the brain biopsy are similar to the VV1 cases of sCJD,[11,14] but in the autopsy material there is a closer resemblance to the neuropathology in VV2 cases of sCJD,[11] although no laminar pattern of PrP deposition was identified in any region of the cerebral cortex.

Fig. 2. Western blot analysis of protease-resistant prion protein (PrP^{res}) in frontal cortex from this case at biopsy (b, lane B) and at autopsy (a, lane E). For comparison, the following PrP^{res} types are shown: type 1 from an MM1 case of sporadic Creutzfeldt-Jakob disease (sCJD, lanes A and C), type 2A from a VV2 case of sCJD (lane D), and type 2B from an MM2 case of variant CJD (lane F). Markers are shown (lane G) and their approximate molecular weights indicated in kilodaltons.

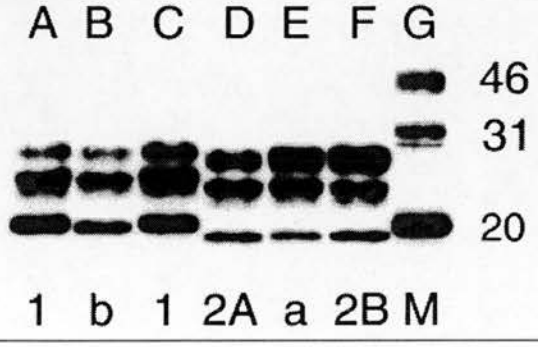

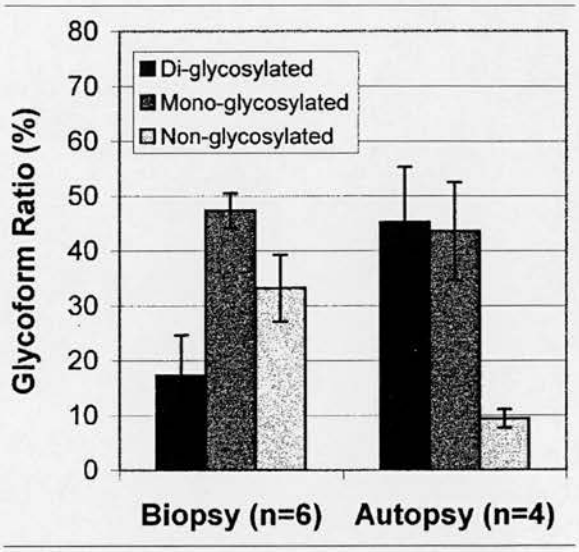

Fig. 3. Histogram showing mean glycoform ratios (%) from multiple samplings and analysis of biopsy (n = 6) and autopsy (n = 4) frontal cortex. Error bars show the standard deviation of the mean.

We therefore believe this case to be sporadic in nature and not related to exposure to BSE. However, the autopsy finding of a PrP^{res} isotype (type 2) and glycoform ratio distinct from that seen in the biopsy is difficult to interpret. Two potential explanations present themselves: (1) disease progression may involve changes in PrP isotype, the single other biopsy/autopsy pair available to us, from a case of vCJD, showing no such difference (data not shown); (2) we may have inadvertently sampled 2 different areas of this brain, which displayed regional variation in PrP^{res} isotype throughout the disease course. Parchi et al.[11] commented that around 3% of sCJD cases contain both type 1 and type 2 PrP^{res} in the cortex. Other estimates are considerably higher (5/14), and it has been further contended that histological heterogeneity correlates with PrP^{res} isotypic heterogeneity.[15] Our own experience indicates that both regional variation in PrP^{res} isotype (1 or 2) and glycoform ratio can occur in sCJD cases.

It is undoubtedly true that the cortical PrP^{res} glycoform ratio can distinguish between sCJD and vCJD in the vast majority of cases.[7,8] However, glycoform ratios resembling those seen in vCJD have been reported previously in fatal familial insomnia,[16] P102L Gerstmann-Sträussler-Scheinker disease,[17] and E200K familial CJD.[18,19] The finding of such a glycoform ratio in this case of sCJD suggests that caution is required in the diagnosis of vCJD on the basis of glycoform ratio in the absence of any other confirmatory evidence.

The UK Department of Health and the Scottish Executive fund the National CJD Surveillance Unit (NCJDSU).

The work of Ms Linda McCardle and her histopathology staff at the NCJDSU is gratefully acknowledged. We also thank Dr W. A. van Gool for performing the 14-3-3 analysis and sequencing the *PRNP* gene, Dr J. Driessen for initial diagnostic workup and referral, Ms T. Koene for the neuropsychological examination, Dr J. Ploegmakers for the brain biopsy and Dr E. Jonkman for the EEG analyses.

References

1. Will RG, Ironside JW, Zeidler M, et al. A new variant of Creutzfeldt-Jakob disease in the UK. Lancet 1996;347:921–925.
2. Bruce ME, Will RG, Ironside JW, et al. Transmission to mice indicate that "new variant" CJD is caused by the BSE agent. Nature 1997;389:498–501.
3. Hill A, Desbruslais M, Joiner S, et al. The same prion strain causes vCJD and BSE. Nature 1997;389:448–450.
4. Will RG, Zeidler M, Stewart GE, et al. Diagnosis of new variant Creutzfeldt-Jakob disease. Ann Neurol 2000;47:575–582.
5. Zeidler M, Sellar RJ, Collie DA. The pulvinar sign on magnetic resonance imaging in variant Creutzfeldt-Jakob disease. Lancet 2000;355:1412–1418.
6. Ironside JW, Head MW, Bell JE, et al. Laboratory diagnosis of variant Creutzfeldt-Jakob disease. Histopathology 2000;7:1–9.
7. Collinge J, Sidle KCL, Meads J, et al. Molecular analysis of prion strain variation and the aetiology of "new variant" CJD. Nature 1996;383:685–690.
8. Parchi P, Capellari S, Chen SG, et al. Typing prion isoforms. Nature 1997;386:232–233.
9. Hill AF, Butterworth RJ, Joiner S, et al. Investigation of variant Creutzfeldt-Jakob disease and other human prion diseases with tonsil biopsy samples. Lancet 1999;353:183–189.
10. Cervenakova L, Goldfarb LV, Garruto R, et al. Phenotypic-genotypic studies in Kuru: implications for new variant Creutzfeldt-Jakob disease. Proc Natl Acad Sci USA 1999;95:13239–13241.
11. Parchi P, Giese A, Capellari S, et al. Classification of sporadic Creutzfeldt-Jakob disease based on molecular and phenotypic analysis of 300 subjects. Ann Neurol 1999;46:224–233.
12. Huillard d'Aignaux J, Costagliola D, Maccario J, et al. Incubation period of Creutzfeldt-Jakob disease in growth hormone recipients in France. Neurology 1999;53:1197–1201.
13. McLean CA, Ironside JW, Alpers MP, et al. Comparative neuropathology of Kuru with the new variant of Creutzfeldt-Jakob disease: evidence for strain of agent predominating over genotype of host. Brain Pathol 1998;8:429–437.
14. Worrall B, Herman ST, Capellari S, et al. Type 1 protease resistant prion protein and valine homozygosity at codon 129 of PRNP identify a subtype of sporadic Creutzfeldt-Jakob disease. J Neurol Neurosurg Psychiatry 1999;67:671–674.
15. Puoti G, Giaccone G, Rossi G, et al. Sporadic Creutzfeldt-Jakob disease: co-occurrence of different types of PrPSc in the same brain. Neurology 1999;53:2173–2176.
16. Telling GC, Parchi P, DeArmond SJ, et al. Evidence for the conformation of the pathologic isoform of the prion protein enciphering and propagating prion diversity. Science 1996;274:2079–2082.
17. Parchi P, Chen SG, Brown P, et al. Different patterns of truncated prion protein fragments correlate with distinct phenotypes in P102L Gerstmann-Straussler-Scheinker disease. Proc Natl Acad Sci USA 1998;95:8322–8327.
18. Hainfeller JA, Parchi P, Kitamoto T, et al. A novel phenotype in familial Creutzfeldt-Jakob disease: prion protein gene E200K coupled with valine at codon 129 and type 2 protease-resistant prion protein. Ann Neurol 1999;45:812–816.
19. Puoti G, Rossi G, Giaccone G, et al. Polymorphism at codon 129 of PRNP affects phenotypic expression of Creutzfeldt-Jakob disease linked to E200K mutation. Ann Neurol 2000;48:269–270.

Frameshift Mutation in the Collagen VI Gene Causes Ullrich's Disease

Itsuro Higuchi, MD,[1] Tadafumi Shiraishi, MD,[1] Teruto Hashiguchi, MD,[2] Masahito Suehara, MD,[3] Takahito Niiyama, MD,[1] Masanori Nakagawa, MD,[1] Kimiyoshi Arimura, MD,[1] Ikuro Maruyama, MD,[1] and Mitsuhiro Osame, MD[1]

Patients with Ullrich's disease have generalized muscle weakness, multiple contractures of the proximal joints, and hyperextensibility of the distal joints. Recently, we found a deficiency of collagen VI protein in two patients with Ullrich's disease. In this study, we detected a homozygous 26 bp deletion in exon 14 of the collagen VI alpha 2 gene (COL6A2) in one patient. This mutation causes a frameshift and a premature termination codon, and results in a truncated collagen VI alpha 2 chain. Our data suggest that at least some cases of Ullrich's disease result from recessive mutations in COL6A2.

Ann Neurol 2001;50:261–265

Ullrich's disease is a unique congenital disorder described as congenital hypotonic-sclerotic muscular dystrophy by Ullrich in 1930.[1] The major clinical findings include generalized muscle weakness and wasting, striking contractures of the proximal joints, hyperflexibility of the distal joints from an early infantile stage, and a progressive course. Muscle biopsies have revealed unequivocal pathological changes of muscular dystrophy.[2,3] Although the gene locus has not been mapped yet, this disease is considered to be a distinct entity of multisystemic involvement inherited as an autosomal recessive trait.[4,5] Recently, we found a complete deficiency of collagen VI in two patients with Ullrich's disease.[6] Our present molecular genetic study confirmed the disease entity of Ullrich's disease, which was called "a forgotten muscular dystrophy" in a previous report.[7]

From the [1]Third Department of Internal Medicine and [2]Department of Laboratory and Molecular Medicine, Faculty of Medicine, Kagoshima University, Kagoshima; and [3]National Okinawa Hospital, Okinawa, Japan.

Received Feb 5, 2001, and in revised form May 7, 2001. Accepted for publication May 9, 2001.

Address correspondence to Dr Higuchi, Third Department of Internal Medicine, Faculty of Medicine, Kagoshima University, 8-35-1 Sakuragaoka, Kagoshima 890-8520, Japan.
E-mail: ihiguchi@med6.kufm.kagoshima-u.ac.jp

Brain Pathology 12: 1-11(2002)

RESEARCH ARTICLE

Immunohistochemistry for the prion protein: comparison of different monoclonal antibodies in human prion disease subtypes

Gábor G. Kovács M.D.[1,2*], Mark W. Head Ph.D.[3*], Ivan Hegyi M.D.[4], Tristan J. Bunn[3], Helga Flicker[1], Johannes A. Hainfellner M.D.[1], Linda McCardle[3], Lajos László Ph.D.[5], Christa Jarius M.D.[1], James W. Ironside M.D. FRCPath[3], and Herbert Budka M.D.[1]

[1] Institute of Neurology, University of Vienna, and Austrian Reference Centre for Human Prion Diseases, Vienna, Austria;
[2] Department of Neurology, Semmelweis University, Budapest, Hungary[§];
[3] National CJD Surveillance Unit and Department of Pathology, University of Edinburgh, Western General Hospital, Edinburgh, UK;
[4] Institute of Neuropathology[§], Department of Pathology, Zurich, Switzerland;
[5] Department of General Zoology, Eötvös University of Sciences, Budapest, Hungary.

[§] Previous address
[*] Contributed equally

Demonstration of the abnormal form of the prion protein (PrP) in the brain confirms the diagnosis of human prion disease (PrD). Using immunohistochemistry, we have compared ten monoclonal antibodies in PrD subtypes including sporadic and variant Creutzfeldt-Jakob disease (CJD), fatal familial insomnia, Alzheimer's disease (AD), and control brains. CJD subgroups were determined using Western blot analysis for the protease-resistant PrP type in combination with sequencing to determine the genotype at the methionine/valine polymorphism at codon 129 of the prion protein gene. None of the antibodies labeled given subgroups exclusively, but the intensity of immunoreactivity varied among morphologically distinct types of deposit. Fine granular or synaptic PrP deposits stained weakly or not at all with antibodies against the N-terminus of PrP, and were visible in one case only with 12F10 and SAF54. Coarser and plaque type deposits were immunolabeled with all antibodies. The immunostaining patterns appear characteristic for the disease subgroups. Labeling of certain neurons in all cases irrespective of disease, and staining at the periphery and/or throughout the senile plaques of AD patients were also noted. Antibodies such as 6H4 and 12F10 failed to give this type of labeling and are therefore less likely to recognise non-pathological PrP material in immunohistochemistry.

Introduction

A common feature of sporadic, acquired, and inherited prion diseases is the accumulation of an abnormal conformer of the host encoded prion protein (PrP^{Sc}) in the brain (20). Visualisation of PrP by immunohistochemistry in formalin fixed tissue serves to confirm the diagnosis; specific pretreatment of paraffin sections is necessary to abolish or diminish the immunoreactivity of the normal cellular PrP (PrP^{C}) (4). Detection of protease resistant prion protein (PrP^{Res}) by Western blotting has proven to be a useful additional test.

New monoclonal antibodies, including one specific for the abnormal form of PrP have been developed (3, 12), and several antigen retrieval procedures have been used, and new ones suggested (2, 19, 25). In a recent ring trial including seven neuropathological centers (Edinburgh, Fukuoka, Helsinki, Milan, Paris, Vienna, and Zurich), formic acid, hydrated or hydrolytic autoclaving, guanidine thiocyanate, and combined protocols with different monoclonal and polyclonal antibodies were compared (9). This study has shown that the quality of staining depends both on the primary antibody and the tissue pretreatment. Using brain tissue of Alzheimer's disease (AD) and control cases with non-dementing illness, it was also demonstrated that nonspecific labeling can occur in the absence of prion disease (9). Although the post mortem diagnostic possibilities constantly widen (7, 23), there is still a need for a highly reliable neuropathological method demonstrating PrP in the most readily available formalin fixed, paraffin embedded material. This need is further reinforced by the discovery of variant Creutzfeldt-Jakob disease (vCJD), related to bovine spongiform encephalopathy (24, 27).

In addition to point mutations and insertions within the prion protein gene (*PRNP*), polymorphisms, such as

Corresponding author:
Professor Herbert Budka, Institute of Neurology, AKH 4J, Währinger Gürtel 18-20, POB 48, A-1097 Vienna, Austria; Tel.: +43-1-40400-5500, -5573; Fax: +43-1-40400-5511, -5573; E-mail: H.Budka@akh-wien.ac.at

Antibody	Epitope	Isotype	Supplier	Dilution	Immunogen
FH11	23-85	IgG2b	TSE Resource Centre, Birkett CR, Compton, U.K.	1:1000	Sheep recPrP
BG4	23-85	IgG2b	TSE Resource Centre, Birkett CR, Compton, U.K.	1:1000	Cow recPrP
8G8	95-110	IgG2a	CEA, Service de Pharmacologie et d'Immunologie, Saclay, France	1:500	Human recPrP
3F4	109-112	IgG2a	SENETEK, Maryland Heights, MO, USA	1:300	Hamster SAF
6H4	144-152	IgG1	Prionics, Zürich, Switzerland	1:500	Cow recPrP
12F10	142-160	IgG2a	CEA, Service de Pharmacologie et d'Immunologie, Saclay, France	1:1000	Human recPrP
SAF54	142-160	IgG2b	CEA, Service de Pharmacologie et d'Immunologie, Saclay, France	1:1000	Hamster SAF
L42	141-159	IgG1	FRC for Virus Diseases of Animals, Dr. M.H. Groschup, Tübingen, Germany	1:300	Sheep recPrP
KG9	140-180	IgG1	TSE Resource Centre, Birkett CR, Compton, U.K.	1:1000	Cow recPrP
DF7	140-180	IgG2b	TSE Resource Centre, Birkett CR, Compton, U.K.	1:2000	Cow recPrP

(rec: recombinant)

Table 1. Characteristics of the ten monoclonal antibodies used in this study.

that at codon 129 (methionine/valine; MV), influence the clinicopathological presentation of the disease (20). Recently a molecular classification of sporadic Creutzfeldt-Jakob disease (sCJD) suggested two major types of protease-resistant PrP (PrP^{Res}), type-1 and type-2 (15, 16), although others report additional types seen on Western blots (5). Some prion disease subtypes are extremely difficult to confirm by PrP immunohistochemistry (*e.g.* fatal familial insomnia, FFI; sCJD codon 129 VV homozygote, type-1 prion protein). In this study, our aim was to compare different monoclonal antibodies in relation to human prion disease subtypes, including FFI, and to assess the reliability of their application in respect of definitive diagnosis.

Materials and methods

Twenty cases of human prion disease, five cases of neuropathologically verified (CERAD criteria) Alzheimer's disease (staged according to Braak and Braak), and three cases of control brains with no neurodegenerative disorder were selected from the tissue banks of the Institute of Neurology, University of Vienna, Austria, and the National CJD Surveillance Unit, Edinburgh, UK. Fourteen cases were sporadic, and three were variant CJD. Three were from the Austrian FFI family, reported previously (1). Formalin fixed, paraffin-embedded tissue blocks from cortex (frontal and/or temporal) and cerebellum were obtained. In the FFI cases, thalamus was also included. Blocks from thirteen CJD cases were pretreated with formic acid for one hour prior to processing to paraffin wax, while four sCJD cases (sCJD1, 2, 5 and 8; see following text), the FFI cases, the AD and control cases were not.

PrP immunohistochemistry. In accordance with the ring trial, we employed an extensively used 3 tiered tissue pretreatment protocol, including 10 minutes hydrated autoclaving at 121°C, 5 minutes 96% formic acid, and 2 hours 4M guanidine thiocyanate at 4°C prior to anti-PrP antibody incubation (2, 9), referred to as protocol A. In each subtype, we selected one case for comparison using the recently suggested pretreatment protocol (25), which includes 10 mM citric acid 121°C autoclave 10 min, 88% Formic acid for 5 minutes and 4 M Guanidine thyocyanate 2 hours at 4°C, referred to as protocol B. In selected sections, we also compared our results using 30 minutes hydrated autoclaving at 121°C, and 5 minutes 96% formic acid without further treatments, referred to as protocol C.

The characteristics of the ten monoclonal antibodies used are summarized in Table 1. Applying the pretreatments of protocol A prior to performing the study, we tested different dilutions of the antibodies using two different blocks showing patchy/perivacuolar and diffuse/synaptic PrP immunoreactivity. The dilution of antibodies used in our study reflect the best results in respect of background and specific immunolabeling. Negative controls were included with the primary antibodies being substituted with irrelevant, isotype-matched control antibodies.

The immunolabeling of sections was visualised using the avidin-biotin-complex method (Amersham Life Science, UK and SIGMA, Germany) and diaminobenzidine (DAB, Fluka Chemie AG, Switzerland) in an automated immunostaining machine (Shandon, SequenzaT™; Astmoor, Runcorn, Cheshire, England, UK). The intensity of labeling was evaluated by a scoring system: W = weak specific immunolabeling; M = distinct, moderately strong specific immunolabeling, clearly distinguishable from background; S = strong specific immunolabeling.

Case	PrP type*		Age at death (years)	Duration (months)	Sex	Remark
	Cortex	Cerebellum				
sCJD1	1	1	45	12	M	129 codon Met/Met
sCJD2	NA	1	65	2	M	129 codon Met/Met
sCJD3	1	1	61	3	F	129 codon Met/Met
sCJD4	1	1	78	8	M	129 codon Met/Val
sCJD5	2A	Neg	72	8	F	129 codon Met/Met
sCJD6	2A (+1)	1	72	8	M	129 codon Met/Met
sCJD7	2A (+1)	2A (+1)	62	11	M	129 codon Met/Met
sCJD8	2A	2A	58	7	M	129 codon Val/Val
sCJD9	2A	2A	72	2	F	129 codon Val/Val
sCJD10	2A	2A	65	6	F	129 codon Val/Val
sCJD11	1	1	42	11	M	129 codon Val/Val
sCJD12	2A	NA	70	10	F	129 codon Met/Val
sCJD13	2A	2A	64	21	F	129 codon Met/Val
sCJD14	2A	NA	62	8	F	129 codon Met/Val
vCJD15	2B	2B	33	18	M	129 codon Met/Met
vCJD16	2B	2B	25	14	M	129 codon Met/Met
vCJD17	NA	NA	28	16	F	129 codon Met/Met
FFI 1	2B	NA	25	13	M	129 codon Met/Met
FFI 2	NA	NA	58	8	F	129 codon Met/Met
FFI 3	NA	NA	37	11	M	129 codon Met/Met
AD1	Neg	NA	80	-	M	Braak V
AD2	Neg	NA	79	-	M	Braak V
AD3	Neg	NA	77	-	F	Braak IV
AD4	NA	NA	78	-	F	Braak IV
AD5	NA	NA	80	-	F	Braak V
CO1	Neg	NA	67	-	M	COPD; Pneumonia
CO2	Neg	NA	66	-	M	Myocardial infarct
CO3	Neg	NA	55	-	F	Pulmonary embolism

Table 2. Patient data on the 28 cases in this study; the CJD and FFI cases include PrP type and *PRNP* codon 129 genotype, the Alzheimer cases include Braak staging, and the cause of death is included for the control cases. NA: Not available; Neg: negative; sCJD: sporadic, vCJD: variant Creutzfeldt-Jakob disease; FFI: fatal familial insomnia; AD: Alzheimer's disease; CO: control; M: male; F: female; COPD: chronic obstructive pulmonary disease. *According to Western blotting.

Pattern	Case numbers							
	sCJD 1-3	sCJD 4	sCJD 5-7	sCJD 8-10	sCJD 11	sCJD 12-14	vCJD 15-17	FFI 1-3
Cerebral cortex								
Diffuse/synaptic	3/3-D	0/1	1/3-F	3/3-F	1/1-F	2/3-D	0/3	1/3-F
Patchy/perivacuolar	1/3-F	1/1-F	3/3-D	0/3	0/1	1/3-D	3/3-F	0/3
Plaque-like or plaque	1/3-F	1/1-F	0/3	3/3-F	0/1	2/3-D	3/3-D	0/3
Pericellular	1/3-F	0/1	0/3	3/3-D	0/1	2/3-D	3/3-D	0/3
Cerebellar cortex								
Fine deposit	3/3-D	0/1	1/3-F	2/3-D	1/1-F	3/3-F	0/3	1/3-F
Coarse deposit	3/3-D	1/1-D	1/3-F	3/3-D	0/1	3/3-D	3/3-D	0/3
Plaque-like or plaque	1/3-F	1/1-D	3/3-F	3/3-D	0/1	3/3-D	3/3-D	0/3
Pericellular	0/3	0/3	0/3	0/3	0/1	0/3	3/3-D	0/3

Table 3. Number of cases showing a particular PrP immunostaining pattern and distribution of immunoreactivity (F-focal or D-diffuse, widespread) in the cerebral and cerebellar cortex in different prion disease case groups. (sCJD: sporadic, vCJD: variant Creutzfeldt-Jakob disease; FFI: fatal familial insomnia).

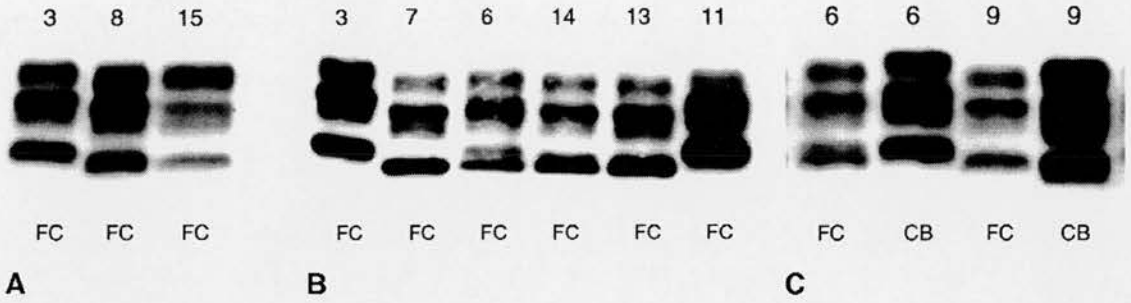

Figure 1. A. Western blot analysis of proteinase K treated samples of frontal cortex (FC), from cases sCJD3 (3), sCJD8 (8), and vCJD15 (15). sCJD3 shows type-1 (21 kDa nonglycosylated, lowest band), and sCJD8 and vCJD15 show type-2 PrP^{Res} (19 kDa nonglycosylated, lowest band). Type-2 PrP^{Res} can be further subclassified as those samples where the monoglycosylated, middle band predominates, termed type 2A (sCJD8), or those where the diglycosylated, top band predominates, termed type 2B (vCJD15). **B**. Western blot analysis of proteinase K treated samples from frontal cortex (FC) from cases sCJD3, 7, 6, 14, 13, and 11. sCJD3 and CJD11 show type-1 PrP^{Res} whereas sCJD7, 14, and 13 show type-2 PrP^{Res}. sCJD6 shows a mixture of predominantly type-2 with a minority type-1 visible in the non-glycosylated lowest band. **C**. Western blot analysis of proteinase K treated samples from frontal cortex (FC) and cerebellum (CB) of cases sCJD6, and sCJD9. The frontal cortex of sCJD6 shows a mixture of type-1 and –2 nonglycosylated, lowest bands whereas the corresponding cerebellum sample appears to contain type-1 only. sCJD9 frontal cortex and cerebellum contains only type-2 PrP^{Res} nonglycosylated bands.

Prion protein gene analysis. Genomic DNA was prepared from peripheral blood leukocytes and the *PRNP* coding region was amplified by the polymerase chain reaction. Known disease specific mutations were excluded by single strand conformational analysis, and a direct sequencing protocol was used to identify the codon 129 genotype (28).

Biochemical analysis of PrP. Western blot analysis of PrP^{Res} in samples of frontal and/or temporal cortex and/or cerebellar cortex was performed. Briefly, a 10% brain homogenate was made from frozen tissue, cleared by low speed centrifugation, and the supernatant digested with 50 μg/ml proteinase K. Protease resistant PRP (PrP*Res*) isoforms were separated by SDS-PAGE, transferred to nitrocellulose or PVDF membranes, and detected using the antibody 3F4, a horseradish peroxidase conjugated secondary antibody and enhanced chemiluminescence system (10).

Results

Data of age at death, sex, duration of illness, PrP^{Res} isotype, and codon 129 polymorphism of the investigated prion disease, Alzheimer's disease and control cases are summarized in Table 2.

Western Blotting banding patterns and isotyping. *Different PrP isotypes can co-exist.* The Western blot isoform patterns were classified on the basis of electrophoretic mobility as type-1 (non-glycosylated PrP^{Res}, 21 kDa) and type-2 (non-glycosylated PrP^{Res}, 19 kDa) (Figure 1A). Further differences in glycoform ratio were observed between type-2 cases of sCJD (type-2A) and vCJD (type-2B) (Figure 1A). According to this classification system, we selected three cases each of sCJD MM type-1, MM type-2A, VV type-2A, MV type-2A, and vCJD (MM type-2B), and one case each of sCJD VV type-1 and MV type-1, in addition to the three FFI cases (MM type-2B). In sCJD5, the sample of the cerebellum contained no detectable PrP^{Res} by Western blot. Further Western blot analysis confirmed the original PrP^{Res} isotype classifications in the majority of cases; however, re-examination of sCJD6 and sCJD7 provided clear demonstration of the existence of both type-1 and type-2 PrP^{Res} in both of these two cases. In sCJD6, the cortex showed both type-1 and type-2A PrP^{Res} in the

Figure 2. (Opposing page) Average intensity of PrP immunoreactivity (S: strong; M: moderate; W: weak) in the cerebral (**A-F**) and cerebellar (**G-J**) cortex in different prion disease case groups. The applied monoclonal antibodies are labeled with different colours and the amino acid number of the recognized epitope on the prion protein is indicated below in the map. (sCJD: sporadic, vCJD: variant Creutzfeldt-Jakob disease; FFI: fatal familial insomnia). **A**: Diffuse/synaptic (picture taken from sCJD1); **B**: Patchy/perivacuolar (sCJD5); **C** (sCJD1) and **D** (vCJD16): Plaque-like deposit and plaque; **E** (sCJD8) and **F** (vCJD16): Pericellular. **G**: Fine granular deposits (sCJD1); **H**: Coarse deposits (sCJD8); **I**: Plaque-like deposit and plaque (sCJD12); **J**: Pericellular (vCJD16); (all with 3F4 antibody, all ×450, except I: ×600).

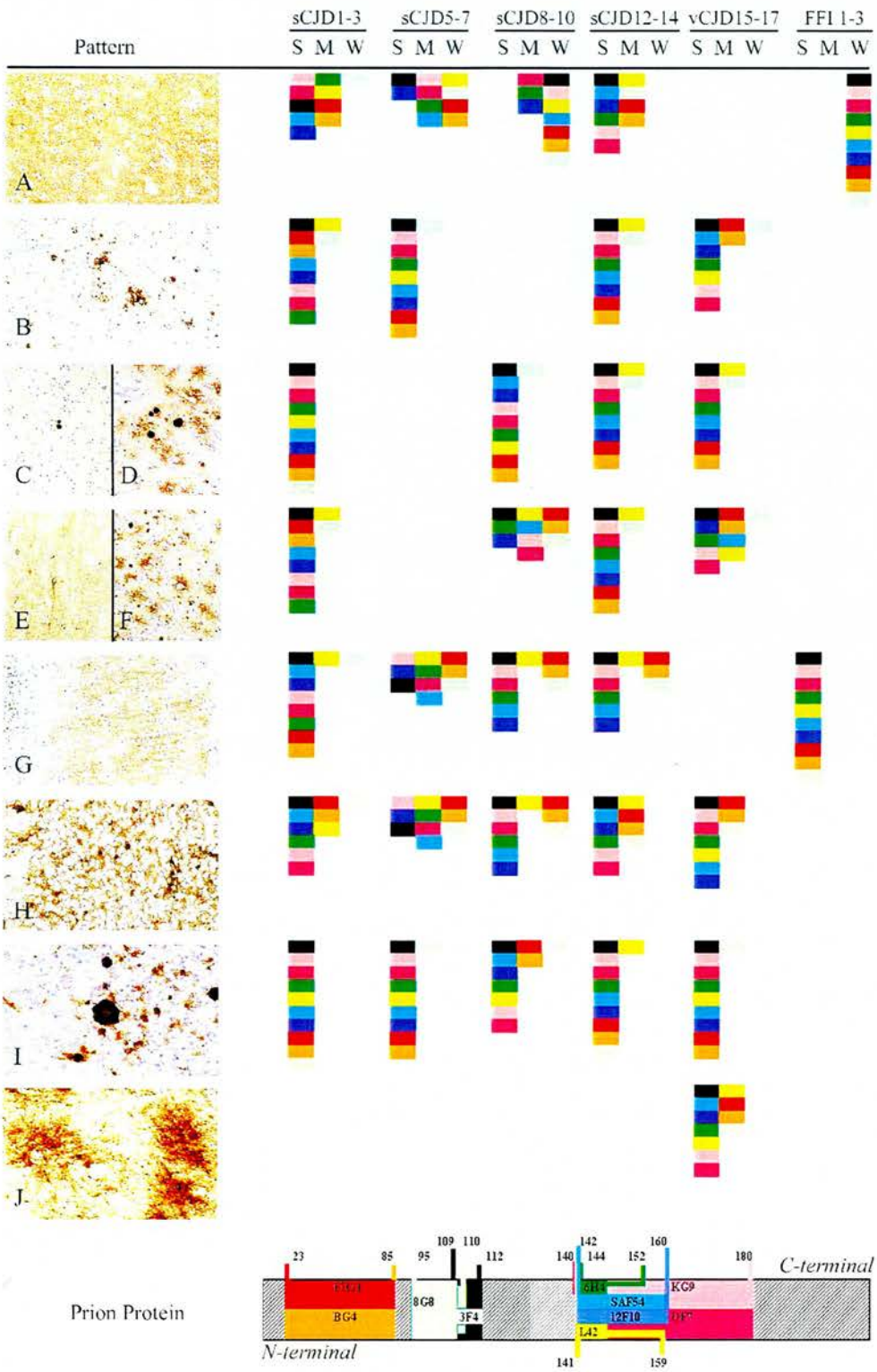
Pattern
sCJD1-3
sCJD5-7
sCJD8-10
sCJD12-14
vCJD15-17
FFI 1-3
S M W
A
B
C
D
E
F
G
H
I
J
Prion Protein
N-terminal
C-terminal
23
85
95
109
110
112
140
142
144
152
160
180
141
159
BG4
8G8
3F4
KG9
SAF84
12F10
L42

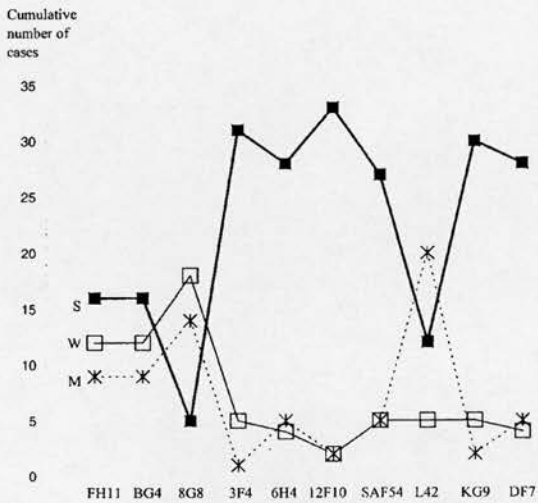

Figure 3. Cumulative number of cases with strong (S), moderate (M) and weak (W) PrP immunoreactivity of each antibody. The result for each case was entered both for cerebral and cerebellar cortices as well as for the four major patterns of immunohistochemistry according to Figures 2. Thus, more than one result could enter the number of cases on the y-axis.

same sample (Figure 1B), whereas only type-1 was detectable in the corresponding cerebellar sample (Figure 1C). Similarly, both types-1 and –2 were seen in sCJD7 cortex and were also detectable in the cerebellum. Multiple sampling of the cerebellum from this case showed type-2 was present in each area sampled, but the co-occurrence of type-1 was variable, as was the amount of PrP^{Res} *in toto* (data not shown). No frozen tissue was available for vCJD17 and Western blot analysis was not performed. The diagnosis of vCJD in this case was made according to the established clinical and neuropathological criteria only.

Immunostaining patterns and differences between antibodies. *PrP immunostaining patterns characteristic of prion disease cases.* The following immunostaining patterns were observed: (I) fine deposition (diffuse/synaptic pattern); (II) coarser depositions (these include the granular, the patchy/perivacuolar - including morula-type deposits); (III) plaques (with amyloid characteristic, *e.g.* kuru-type and florid plaques, or without amyloid characteristic, as plaque-like deposits or so called focal deposits); and (IV) pericellular deposits as dot-like and/or coarse granular immunoreactivity around unstained neuronal perikarya. Average scoring of the signal (weak; moderate; strong) using different antibodies in distinct disease subtypes is shown in Figure 2; the occurrence of different PrP immunostaining patterns in each case group is summarized in Table 3.

Strong immunoreactivity was observed in the majority of patterns and subtypes with antibodies to the mid region of the prion protein (3F4, 6H4, 12F10, SAF54, KG9, DF7), while those against the N-terminus or adjacent region (FH11, BG4, 8G8) rarely showed this. In spite of having an epitope in the mid portion, immunoreactivity with L42 was somewhat weaker although still clearly distinguishable (Figure 3). Fine depositions were particularly weak or unlabeled with FH11, BG4, 8G8 antibodies (Figure 4A and B). In sCJD VV type-1, the faint diffuse/synaptic staining of the cerebral cortex was only visible with 12F10 and SAF54. The coarser and plaque type deposits of both cerebral and cerebellar cortex were clearly immunolabeled with all antibodies.

In the cerebral cortex of sCJD subtypes, diffuse/synaptic PrP immunoreactivity was noted predominantly in MM type-1 and MV type-2A cases and focally in others, including the VV type-1 case. Patchy/perivacuolar deposits were observed in all MM type-2A cases, while only one MM type-1 and MV type-2A, and the MV type-1 case exhibited this staining pattern. Amyloid plaques were abundant in MV type-2A and vCJD, while plaque-like deposits were observed in all VV type-2A cases, and scantily in one MM type-1 case. Pericellular PrP immunoreactivity characterized VV type-2A and vCJD, but only rarely was it observed in MV type 2A and focally in one MM type-1 case. In the latter, this was coarse and the majority of antibodies strongly immunolabeled it, in contrast to the more wide-

Figure 4. (Opposing page) **A**. Strongly immunolabeled fine deposits in the molecular, coarser deposits in the granular layer and plaques in both layers of the cerebellum (sCJD13; 12F10 antibody; ×600). **B**. Weakly immunoreactive fine deposits, strongly immunolabeled coarse deposits and plaques in the corresponding region as figure 4A of the cerebellum (sCJD13; 8G8 antibody; ×600). **C**. Coarse immunoreactivity forming focal aggregates in the molecular layer of the cerebellum (sCJD6; 3F4 antibody; ×750) **D**. Neuronal immunopositivity in the frontal cortex of a control case (CO2; DF7 antibody; ×600) **E**. Senile plaques show immunoreactivity using antibodies against the N-terminus of the PrP in Alzheimer's disease (AD4; FH11 antibody; ×600) **F**. Senile plaques (arrows) show no immunopositivity using 6H4 antibody (AD4, corresponding region as figure 4E; ×600) **G**. Immunohistochemistry for PrP using pretreatments of protocol A (see text) in the frontal cortex: pericellular immunoreactivity in the deeper layers (to the right) (sCJD8; 3F4 antibody; ×300). **H**. Immunohistochemistry for PrP using pretreatments of protocol B (see text) in the frontal cortex: pericellular immunoreactivity, neuronal immunolabeling and stronger background (sCJD8, corresponding region as in Figure 4G; 3F4 antibody; ×300).

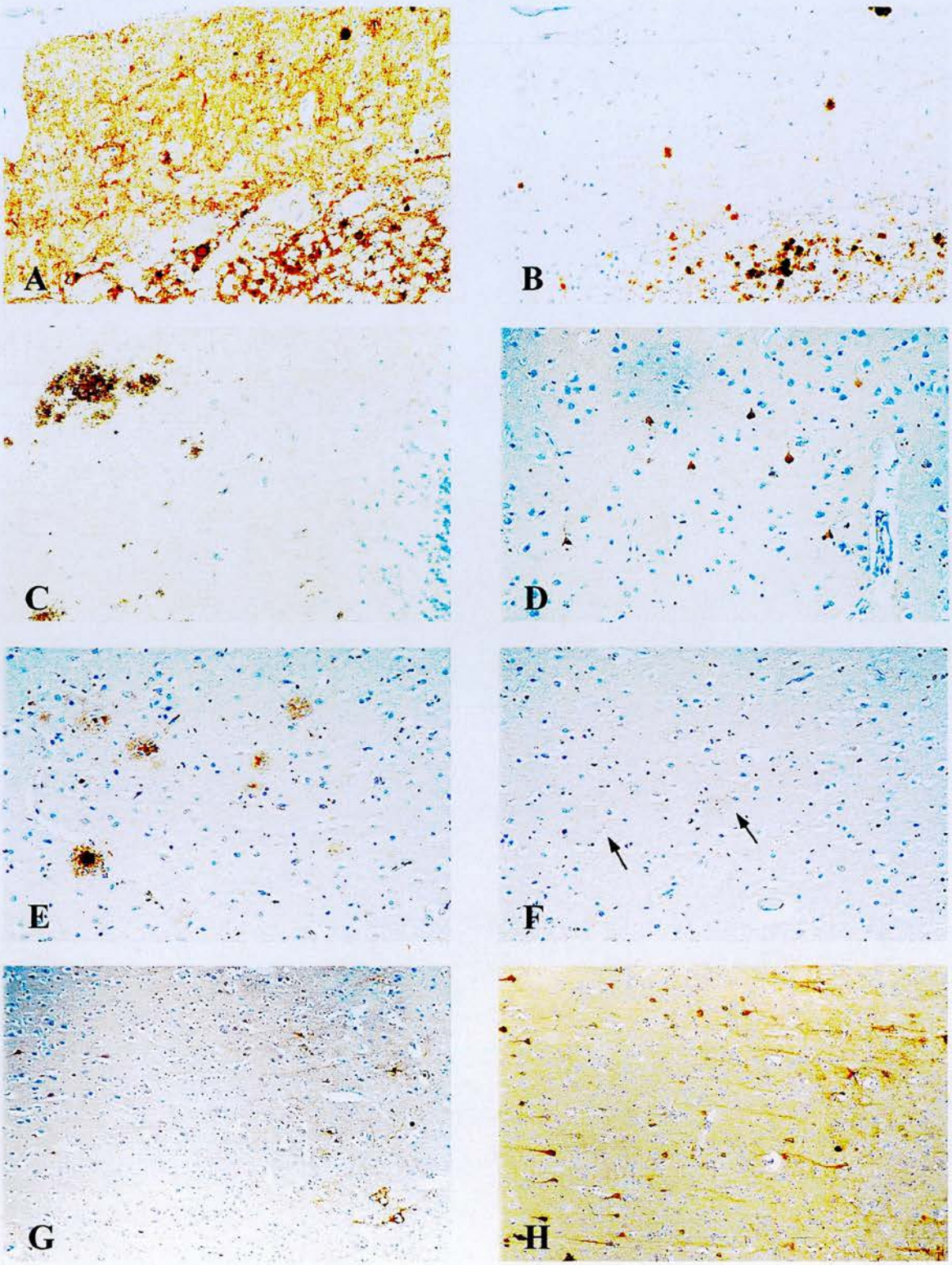
A
B
C
D
E
F
G
H

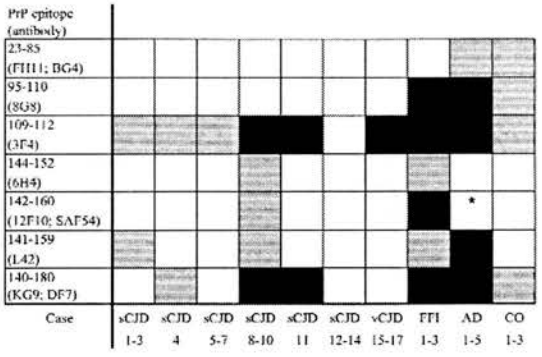

Figure 5. Presence of intraneuronal immunoreactivity (cerebral and/or cerebellar neurons) for the prion protein. The black represents many, while grey indicates few immunoreactive cells. Blank fields indicate no labeling. *Observed only with SAF54 antibody.

spread but finer pericellular deposits of all sCJD VV type-2A cases which were less prominently immunolabeled with antibodies against the N-terminus of PrP.

In the cerebellum, fine granular deposits in the molecular and somewhat coarser deposits in the granular layer were seen in nearly all subtypes. Amyloid plaques and/or plaque-like deposits were abundant in the vCJD, MV type-2A, VV type-2A cases, and the MV type-1 case, while only one MM type-1 case exhibited sparse plaque-like deposits in the cerebellar white matter. All three MM cases that exhibited type-2A PrP^{Res} in at least one of the investigated samples (sCJD5,6,7) displayed peculiar coarse PrP immunoreactivity forming focal plaque-like aggregates in the molecular layer (Figure 4C). This was also noted in sCJD5, where Western blot failed to detect PrP^{Res}. Interestingly, sCJD6 and 7 showed both fine and coarse PrP deposits; this was clearly and spatially distinguishable in the cerebellum. Pericellular immunolabeling was observed only in vCJD, this was surrounding molecular layer neurons.

In FFI, the cortex exhibited weak diffuse/synaptic deposits in one case only; the cerebellum contained a coarser deposition in the molecular layer. In spite of severe gliosis and loss of neurons, the thalamus lacked PrP immunoreactivity.

The KG9 antibody proved to be especially strong in vCJD cases. Otherwise, we did not observe any correlation between the presence of immunoreactivity, the immunogen and/or the isotype of the antibody applied.

In Alzheimer's disease and control cases, no staining patterns similar to the above were seen.

PrP immunostaining patterns common to prion disease and control cases. (I) Intraneuronal punctuate and diffuse type of PrP immunoreactivity was observed predominantly in the cortex of VV type-2A and FFI cases. Notable was the lack or only occasional presence of intraneuronal immunoreactivity in MM-1, MV-1, MV-2A, MM-2A and MM-2A+1 (in the latter predominantly in Purkinje cells) and vCJD cases. This type of immunoreactivity was not observed with antibodies against the N-terminus. In FFI, neurons of the cerebral cortex and Purkinje cells were immunopositive, while none were in the thalamus, except for some rare neurons labeled with the 3F4 antibody. Interestingly, immunopositivity was not seen in Purkinje cells of the only FFI case with marked PrP deposition in the molecular layer. In Alzheimer's disease and control cases, all antibodies except 6H4 and 12F10 (and L42 in controls) immunostained cortical neurons to some degree (Figure 4D); the immunolabeling with N-terminal antibodies was less prominent than with others (summarized in Figure 5). Intraneuronal PrP immunoreactivity was less pronounced in controls than in Alzheimer's and prion disease brains.

(II) Glial and (III) vessel wall immunolabeling was variable, but seen in at least one of every type with each antibody. (IV) Neurofibrillary tangles of Alzheimer's disease were free of PrP immunoreactivity, but PrP colocalization with senile plaques and dystrophic neurites was evident. The latter were labeled with all antibodies, though to a different degree. Antibodies against the N-terminus of PrP labeled most consistently and strongly the core of senile plaques, while other antibodies showed only occasional and weak immunostaining of the core of the plaques; 6H4 and 12F10 stained the fewest plaques (Figure 4E and F).

Comparison of pretreatment protocols. Protocol B resulted in a high background in nearly all of the cases (Figure 4G and H). Intraneuronal, glial, and senile plaque-associated deposits were stronger, or appeared also in cases and/or with antibodies not immunopositive using protocol A and C. In contrast, the diffuse/synaptic immunoreactivity was more intense in MM type-1, VV type-1, and in FFI applying protocol B. In our hands, protocols A and C did not exhibit significant difference, nor could we demonstrate any difference between cases with formic acid pretreated blocks and those left untreated.

Discussion

Detection of the abnormal form of PrP in tissue is the gold standard for the definitive diagnosis of human prion diseases (4). The abundance of available antibod-

ies and pretreatment protocols requires urgent harmonization of anti-PrP immunohistochemistry. With one exception (L42; for description see ref. 26), using commercially available monoclonal antibodies, we have compared the immunostaining patterns in different subtypes of human prion disease and evaluated Alzheimer's disease and control cases.

Our results confirm that prion disease subtypes as defined by *PRNP* codon 129 genotype exhibit characteristic PrP deposition patterns; this is most distinctive in the cerebellum (22). The extension of such subclassification to include PrP^{Res} isotype is subject to a number of complications. A recent study suggested that individual brains might contain different PrP^{Res} types (21), and that the regional PrP immunostaining pattern correlates with the particular PrP^{Res} type found in that region. This study confirms the former observation by detecting the presence of type-1 PrP^{Res} as a minor component along with type-2A PrP^{Res} in a frontal cortex sample from a case of sporadic CJD in a methionine homozygote (sCJD6) previously classified as having type-2A PrP^{Res}. Interestingly, the corresponding cerebellar sample showed type-1 PrP^{Res} in the absence of detectable type-2A. Another MM case with both type-1 and –2 in the cortex (sCJD7) also showed variable overall levels and a mixture of both types of PrP^{Res} in the cerebellum. The cerebellum in this case also showed spatially and morphologically distinct patterns of PrP immunoreactivity. Furthermore, this particular pattern of coarse aggregated deposits (Figure 4C) was noted in all MM homozygote cases that had detectable type-2A PrP^{Res} in at least one sample. These observations are consistant with an association between the presence of mixed PrP^{Res} isotypes, as determined by Western blotting, and the mixed morphological appearance of PrP aggregates, as determined by immunohistochemistry. However, in order to establish the exact nature of this correlation, fine mapping of affected areas by immunohistochemistry and Western blot will be required.

Antibodies directed against N-terminal epitopes react differently with both fine extra- and intracellular deposits and senile plaques, when compared to antibodies directed to other regions. The NMR solution structure of the human prion protein contains a flexibly extended N-terminal tail, a globular domain, and a short flexible chain end of residues 229-230 (29). According to differential proteinase K cleavage sites, type-1 and 2 PrP^{Res} fragments differ in the extent of the truncated N-terminal region (17). In our hands, the fine deposits were not consistently immunolabeled with the N-terminal antibodies, while the coarser deposits and plaques were clearly immunoreactive. This might reflect a higher accessibility of the flexible N-terminal end in the amyloid and preamyloid states (*e.g.* patchy/perivacuolar or plaque-like deposits) (14).

We confirm previous studies showing that PrP immunoreactivity localized to neurons is frequently observed also in non-prion disease cases (6, 18). Western blot analysis confirms the absence of PrP^{Res} in the brains of the investigated control and AD cases, further supporting the proposition that these deposits represent the cellular form of PrP. In control and AD cases all antibodies, except 6H4 and 12F10, gave this pattern of staining.

The amount of intraneuronal staining was clearly different between sCJD subtypes, with VV type-2A cases containing the most. This is in accordance with our observation that areas containing fewer PrP deposits exhibit more intraneuronal staining. It should be noted that 6H4 and 12F10 immunolabeled intraneuronal deposits only in sCJD VV type-2A. This might mean that this form of immunoreactivity in this sCJD subtype (which showed similarity with FFI) reflects a different stage of prion protein processing that might be relevant to the pathogenesis of VV type-2A cases (13).

Formic acid treatment enhances amyloid antigenicity, presumably by limited proteolysis or denaturation of amyloid protein aggregates (11). Application of lower concentrations of formic acid and the addition of citrate buffer in the pretreatment protocol labeled more intraneuronal (also with antibodies not labeling immunoreactivity in the original pretreatment) and fine (diffuse/synaptic) deposits, thus buried epitopes became uncovered. This also suggests, that at least some of the intraneuronal PrP immunoreactivity might reflect a different conformational stage of the prion protein in prion diseases versus controls. Accordingly, though it might be useful to apply protocol B in diagnosing prion disease cases with weak or no staining of fine deposits (*e.g.* sCJD VV type-1 or FFI), care must be taken using this protocol because of the frequent occurrence of nonspecific labeling and higher levels of background staining.
PrP accumulates mainly at the periphery but also throughout the β A4 plaques of Alzheimer's disease patients (6, 8). This is most clearly seen with the use of N-terminal antibodies. We could not demonstrate PrP^{Res} in the Western blots of AD patients, and the substitution of the primary PrP antibodies by nonspecific, isotype-matched antibodies did not show similar labeling to that observed with PrP immunostaining. Furthermore, antibodies against different epitopes of PrP exhibited immunoreactivity in the same manner. As a result, we

think that this immunoreactivity is specific and might reflect co-aggregation of the non-pathological form of PrP.

Conclusions

None of the tested antibodies proved to be specific for any prion disease group, but the intensity of labeling is related to the morphological type of PrP deposits present. Fine granular or synaptic PrP deposits stained weakly or not at all with antibodies against the N-terminus of PrP, and were visible in one case only with 12F10 and SAF54. Coarser and plaque type deposits were immunolabeled with all antibodies. The PrP deposition patterns are characteristic for the subtypes, especially those found in the cerebellum. Immunolabeling of certain neurons in all brains examined presumably results from the detection of remaining or aggregated, non-pathological form of PrP, and its detection is influenced by the pretreatments used. Some antibodies exhibit immunoreactivity restricted to cases of prion disease (6H4, 12F10) and thus are more reliable tools for the specific immunolabeling of the abnormal form of PrP . However, it is important to emphasize that any positive signal in immunohistochemistry for disease-associated PrP needs to be interpreted with caution and experience. Finally, in at least some cases, the same brain and the same anatomical region contain a mixture of PrP^{Res} types; this may correlate with the morphology of PrP accumulation.

Acknowledgements

We are grateful to Professor Pierluigi Gambetti and Dr. Piero Parchi (Institute of Pathology, Case Western Reserve University, Cleveland, USA, and Department of Neurological Sciences, University of Bologna, Italy), for providing the PrP Western blot results of cases CJD1, 2, 5, and 8. This study was supported by EU funded projects "European Centralised Facility for Human TSEs (TSECFAC)" and "Human TSEs: the neuropathology network (PRIONET)" (project leader: H.Budka).

References

1. Almer G, Hainfellner JA, Brucke T, Jellinger K, Kleinert R, Bayer G, Windl O, Kretzschmar HA, Hill A, Sidle K, Collinge J, Budka H (1999) Fatal familial insomnia: a new Austrian family. *Brain* 122: 5-16
2. Bell JE, Gentleman SM, Ironside JW, McCardle L, Lantos PL, Doey L, Lowe J, Fergusson J, Luthert P, McQuaid S, Allen IV (1997) Prion protein immunocytochemistry--UK five centre consensus report. *Neuropathol Appl Neurobiol* 23(1): 26-35
3. Bodemer W (1999) The use of monoclonal antibodies in human prion disease. *Naturwissenschaften* 86(5): 212-220
4. Budka H, Aguzzi A, Brown P, Brucher JM, Bugiani O, Collinge J, Diringer H, Gullotta F, Haltia M, Hauw JJ, Ironside JW, Kretzschmar HA, Lantos PL, Masullo C, Schlote W, Tateishi J, Weller RO (1995) Neuropathological Diagnostic Criteria for Creutzfeldt-Jakob Disease (CJD) and Other Human Spongiform Encephalopathies (Prion Diseases). *Brain Pathol* 5(4): 459-466
5. Collinge J, Sidle KC, Meads J, Ironside J, Hill AF (1996) Molecular analysis of prion strain variation and the aetiology of 'new variant' CJD. *Nature* 383(6602): 685-690
6. Esiri MM, Carter J, Ironside JW (2000) Prion protein immunoreactivity in brain samples from an unselected autopsy population: findings in 200 consecutive cases. *Neuropathol Appl Neurobiol* 26(3): 273-284
7. Giaccone G, Canciani B, Puoti G, Rossi G, Goffredo D, Iussich S, Fociani P, Tagliavini F, Bugiani O. (2000) Creutzfeldt-Jakob disease: Carnoy's fixative improves the immunohistochemistry of the proteinase K-resistant prion protein. *Brain Pathol* 10(1): 31-37
8. Hainfellner JA, Wanschitz J, Jellinger K, Liberski PP, Gullotta F, Budka H (1998) Coexistence of Alzheimer-type neuropathology in Creutzfeldt-Jakob disease. *Acta Neuropathol* 96(2): 116-122
9. Hegyi I, Hainfellner JA, Flicker H, Ironside JW, Hauw JJ, Tateishi J, Haltia M, Bugiani O, Aguzzi A, Budka H (1997) Prion protein immunocytochemistry: reliable staining protocol, immunomorphology, and diagnostic pitfalls. *Clin Neuropathol* 16: 262-263
10. Ironside JW, Head MW, Bell JE, Will RG (2000) Laboratory diagnosis of variant Creutzfeldt-Jakob disease. *Histopathology* 37: 1-9
11. Kitamoto T, Ogomori K, Tateishi J, Prusiner SB (1987) Formic acid pretreatment enhances immunostaining of cerebral and systemic amyloids. *Lab Invest* 57(2): 230-236
12. Korth C, Stierli B, Streit P, Moser M, Schaller O, Fischer R, Schulz-Schaeffer W, Kretzschmar H, Raeber A, Braun U, Ehrensperger F, Hornemann S, Glockshuber R, Riek R, Billeter M, Wüthrich K, Oesch B (1997) Prion (PrPSc)-specific epitope defined by a monoclonal antibody. *Nature* 390(6655): 74-77
13. Kovács GG, Head MW, Bunn T, László L, Will RG, Ironside JW (2000) Clinicopathological phenotype of codon 129 valine homozygote sporadic Creutzfeldt-Jakob disease. *Neuropathol Appl Neurobiol* 26(5): 463-472
14. Nakamura S, Ono F, Hamano M, Odagiri K, Kubo M, Komatsuzaki K, Terao K, Shinagawa M, Takahashi K, Yoshikawa Y (2000) Immunohistochemical detection of apolipoprotein E within prion-associated lesions in squirrel monkey brains. *Acta Neuropathol* 100(4): 365-370
15. Parchi P, Castellani R, Capellari S, Ghetti B, Young K, Chen SG, Farlow M, Dickson DW, Sima AA, Trojanowski JQ, Petersen RB, Gambetti P (1996) Molecular basis of phenotypic variability in sporadic Creutzfeldt-Jakob disease. *Ann Neurol* 39(6): 767-778

16. Parchi P, Giese A, Capellari S, Brown P, Schulz-Schaeffer W, Windl O, Zerr I, Budka H, Kopp N, Piccardo P, Poser S, Rojiani A, Streichemberger N, Julien J, Vital C, Ghetti B, Gambetti P, Kretzschmar H (1999) Classification of sporadic Creutzfeldt-Jakob disease based on molecular and phenotypic analysis of 300 subjects. *Ann Neurol* 46(2): 224-233
17. Parchi P, Zou W, Wang W, Brown P, Capellari S, Ghetti B, Kopp N, Schulz-Schaeffer WJ, Kretzschmar HA, Head MW, Ironside JW, Gambetti P, Chen SG (2000) Genetic influence on the structural variations of the abnormal prion protein. *Proc Natl Acad Sci USA* 97(18): 10168-10172
18. Piccardo P, Safar J, Ceroni M, Gajdusek DC, Gibbs CJ Jr (1990) Immunohistochemical localization of prion protein in spongiform encephalopathies and normal brain tissue. *Neurology* 40: 518-522
19. Privat N, Sazdovitch V, Seilhean D, LaPlanche JL, Hauw JJ (2000) PrP immunohistochemistry: different protocols, including a procedure for long formalin fixation, and a proposed schematic classification for deposits in sporadic Creutzfeldt-Jakob disease. *Microsc Res Tech* 50(1): 26-31
20. Prusiner S (1997) Prion diseases and the BSE crisis. *Science* 278: 245-251
21. Puoti G, Giaccone G, Rossi G, Canciani B, Bugiani O, Tagliavini F (1999) Sporadic Creutzfeldt-Jakob disease: co-occurrence of different types of PrP(Sc) in the same brain. *Neurology* 53(9): 2173-2176
22. Schulz-Schaeffer WJ, Giese A, Windl O, Kretzschmar HA (1996) Polymorphism at codon 129 of the prion protein gene determines cerebellar pathology in Creutzfeldt-Jakob disease. *Clin Neuropathol* 15(6): 353-357
23. Schulz-Schaeffer WJ, Tschoke S, Kranefuss N, Drose W, Hause-Reitner D, Giese A, Groschup MH, Kretzschmar HA (2000) The paraffin-embedded tissue blot detects PrP(Sc) early in the incubation time in prion diseases. *Am J Pathol* 156(1): 51-56
24. Scott MR, Will R, Ironside J, Nguyen HO, Tremblay P, DeArmond SJ, Prusiner SB (1999) Compelling transgenetic evidence for transmission of bovine spongiform encephalopathy prions to humans. *Proc Natl Acad Sci USA* 96(26): 15137-15142
25. Van Everbroeck B, Pals P, Martin JJ, Cras P (1999) Antigen retrieval in prion protein immunohistochemistry. *J Histochem Cytochem* 47(11): 1465-1470
26. Vorberg I, Buschmann A, Harmeyer S, Saalmuller A, Pfaff E, Groschup MH (1999) A novel epitope for the specific detection of exogenous prion proteins in transgenic mice and transfected murine cell lines. *Virology* 255(1): 26-31
27. Will RG, Ironside JW, Zeidler M, Cousens SN, Estibeiro K, Alperovitch A, Poser S, Pocchiari M, Hofman A, Smith PG (1996) A new variant of Creutzfeldt-Jakob disease in the UK. *Lancet* 347(9006): 921-925
28. Windl O, Dempster M, Estibeiro JP, Lathe R, de Silva R, Esmonde T, Will R, Springbett A, Campbell TA, Sidle KC, Palmer MS, Collinge J (1996) Genetic basis of Creutzfeldt-Jakob disease in the United Kingdom: a systematic analysis of predisposing mutations and allelic variation in the PRNP gene. *Hum Genet* 98(3): 259-264
29. Zahn R, Liu A, Luhrs T, Riek R, von Schroetter C, Lopez Garcia F, Billeter M, Calzolai L, Wider G, Wüthrich K (2000) NMR solution structure of the human prion protein. *Proc Natl Acad Sci USA* 97(1): 145-150

Prion Protein Accumulation in Eyes of Patients with Sporadic and Variant Creutzfeldt-Jakob Disease

Mark W. Head,[1] Victoria Northcott,[1] Kathleen Rennison,[1] Diane Ritchie,[1] Linda McCardle,[1] Tristan J. R. Bunn,[1] Neil F. McLennan,[1] James W. Ironside,[1] Andrew B. Tullo,[2] and Richard E. Bonshek[2]

Purpose. Creutzfeldt-Jakob disease (CJD) primarily affects the brain. This study was conducted to assess the possible involvement of the eye in sporadic and variant CJD by testing for the presence of the disease-associated, protease-resistant isoform of the prion protein (PrP^{Sc}) in ocular tissue.

Methods. Human eyes from donors with CJD and non-prion neurodegenerative disease control eyes were studied. In situ hybridization and Western blot analysis were used to determine the normal pattern of cellular prion protein (PrP^{C}) expression. Western blot analysis and immunohistochemistry were then used to determine the localization, abundance, and isotype of PrP^{Sc} in eyes in CJD.

Results. PrP^{C} was expressed in the nuclear layers of the retina. In both the sporadic and variant forms of CJD, PrP^{Sc} accumulated throughout the synaptic layers of the retina. The levels of PrP^{Sc} found in the retina were comparable with those found in the brain. Lower levels of PrP^{Sc} could be found in the optic nerve, but no PrP^{Sc} was detectable in other ocular tissues. The glycoform ratio of PrP^{Sc} in the retina did not correspond to that found in the brain.

Conclusions. Presumptive centrifugal spread of PrP^{Sc} from the brain through the optic nerve occurs in two major types of CJD. PrP^{Sc} is a marker of CJD infectivity. Given that routine decontamination may not remove PrP^{Sc} from surgical instruments, a careful risk assessment should be made of possible iatrogenic spread of sporadic and variant CJD after surgery to the retina or optic nerve. (*Invest Ophthalmol Vis Sci.* 2003;44: 342–346) DOI:10.1167/iovs.01-1273

Creutzfeldt-Jakob disease (CJD) is a rare fatal neurodegeneration characterized by neuronal loss, gliosis, and spongiform change in the brain. According to the prion hypothesis, the agent responsible for CJD is an altered form (PrP^{Sc}) of a host-encoded glycoprotein (PrP^{C}) which is highly aggregated and partially resistant to proteolysis.[1] CJD occurs in idiopathic, familial, and acquired forms. The most common of these is the idiopathic form, sporadic Creutzfeldt-Jakob disease (sCJD) which occurs worldwide at a rate of one per million persons per annum and primarily affects the elderly.[1] The acquired forms include Kuru and iatrogenic Creutzfeldt-Jakob disease (iCJD). Most cases of iCJD result from medical exposure to either growth hormone extracted from human cadaveric pituitary glands or from human dura mater grafting during neurosurgical operations.[2] Nevertheless, one definite and two probable cases of iCJD have been attributed to corneal grafting, including the first ever reported case of iCJD.[3–5] Iatrogenic exposure can result in very long incubation periods, measured in years in growth hormone recipients, although the incubation periods after exposure through corneal grafting were short in two cases.[2] These data imply that CJD infectivity resides in ocular tissue and that transplantation of infected ocular tissue offers a direct route for entry of the agent into the brain. Direct confirmation of the former comes from the transmission to primates of disease from pooled CJD eye tissue.[6]

The appearance of a new variant of Creutzfeldt-Jakob disease (vCJD) in the United Kingdom[7] has refocused clinical interest in CJD. vCJD differs from sCJD in a number of important respects, including earlier age at onset, longer disease duration, and presence of peripheral disease and infectivity in elements of the lymphoreticular system.[8–10] This has necessitated a reappraisal of the potential for iatrogenic spread of CJD, including those risks posed by the transplantation of ocular tissues.[11–13] Unfortunately, there is a dearth of primary investigative studies of ocular disease in CJD, even though neuro-ophthalmic features are common[14] and retinal degeneration has been described in an animal model of CJD.[15]

We have taken advantage of a rare opportunity to examine histologically and biochemically eyes of patients with variant and sporadic CJD for the accumulation of the disease-associated form of PrP to better understand the pathogenesis of CJD and provide data for risk assessment of iatrogenic transmission.

Materials and Methods

Pairs of eyes from three autopsy-proven cases of CJD, one sCJD (S) and two vCJD, were examined (V1 and V2). Two pairs of eyes from neurologic control cases were also analyzed. One was an autopsy-proven case of Alzheimer disease (C1) and the other a case of corticobasal ganglionic degeneration (C2). Full permission was obtained for research, and the study protocol conformed with the provisions of the Declaration of Helsinki. In all five cases, frozen and fixed eye and frozen cerebral cortex (CC) was available for study. After enucleation, the left eye of each pair was dissected into the following components; cornea, lens, vitreous body, neural retina, choroid and retinal pigmented epithelium, sclera, and optic nerve. Due to the nature of the eye after death, complete separation was not possible. This was particularly true for the posterior segment tissues, and it is certain that cross contamination occurred between neural retina and the overlying vitreous body and the underlying pigmented epithelium. The right eye of each pair was fixed whole. Two additional control eyes, which had not been decontaminated with formic acid, were used for the in situ hybridization analysis. Both were enucleations, one due to a recurrence of melanoma of the iris (C3) and the other due to optic pain resulting from rubeotic glaucoma (C4).

From the [1]National Creutzfeldt-Jakob Disease Surveillance Unit and Department of Pathology of the University of Edinburgh, Scotland, United Kingdom; and the [2]Academic Department of Ophthalmology, Manchester Royal Eye Hospital, Manchester, United Kingdom.

Supported by The National Creutzfeldt-Jakob Disease Surveillance Unit, which is funded by the UK Department of Health and the Scottish Executive; by Grant G9627376 from the Medical Research Council of the United Kingdom; and by Grant Ec Biotech 4-98-6064 from the European Union.

Submitted for publication December 26, 2001; revised June 3, 2002; accepted July 19, 2002.

Commercial relationships policy: N.

The publication costs of this article were defrayed in part by page charge payment. This article must therefore be marked "*advertisement*" in accordance with 18 U.S.C. §1734 solely to indicate this fact.

Corresponding author: Richard E. Bonshek, Academic Department of Ophthalmology, Royal Eye Hospital, Oxford Road, Manchester, M13 9WH, UK; richard.bonshek@man.ac.uk.

In situ hybridization to localize PrP mRNA was performed with digoxigenin-labeled, PCR-generated, single-stranded sense and antisense RNA probes, visualized with alkaline phosphatase and an nitroblue tetrazolium/5-bromo-4-chloro-3-indoyl phosphate (NBT/BCIP) chromogen as previously described.[16]

The protease-resistant core fragment (PrP^{res}) of disease-associated PrP^{Sc} was detected by Western blot analysis with the monoclonal antibody 3F4, as previously described.[9] Initially, all eye samples were prepared and analyzed as protease-treated 10% (wt/vol) tissue homogenates. In samples in which PrP^{res} was initially found to be low or undetectable, it was concentrated (×20) by centrifugation at 21,000*g* for 1 hour at 4°C and redissolved in SDS-PAGE loading buffer for analysis. Glycoform analysis was performed with a scanning densitometer (model GS700, with Quantity One software; Bio-Rad Laboratories, Herts, UK). The normal cellular protease-sensitive prion protein PrP^{scns} was detected in non-CJD tissues by use of the same Western blot protocol with the omission of the proteinase K digestion and concentration steps.

PrP was localized in sections of formalin-fixed, formic acid–treated eye tissue by immunohistochemistry. The anti PrP monoclonal antibodies KG9, 3F4, and 6H4 were used with a protocol that distinguishes PrP^{Sc} from the normal cellular form of PrP, as previously described.[9] Before immunolabeling, sections were taken to water and formalin pigment removed with saturated picric acid. Sections were washed and then autoclaved at 121°C in distilled water for 10 minutes before immersing in 96% formic acid for 5 minutes at room temperature. Sections were then immunolabeled by overnight incubation in the primary anti-PrP antibodies KG9 diluted 1/250 (Institute for Animal Health, Compton, UK), 6H4 diluted 1/2000 (Prionics AG, Zurich, Switzerland), and 3F4 diluted 1/50 (Dako, High Wycombe, UK), in combination with an avidin-biotin (ABC) kit (Vectastain Elite; Vector Laboratories, Burlingame, CA). Labeling was visualized with diaminobenzidine (DAB), and sections were lightly counterstained with hematoxylin. Selected sections were double immunolabeled for PrP and astrocytes. PrP immunolabeling was performed with the anti PrP antibody KG9, as outlined earlier. After visualization with DAB, sections were thoroughly washed and blocked in normal goat serum (1:5) for 20 minutes. Sections were then incubated with glial fibrillary acidic protein (GFAP) antibody (Dako), washed, and then incubated with a diluted biotinylated secondary antibody. An alkaline phosphatase ABC kit (Dako) was used to complete the immunolabeling with red stain (Vector red; Vector Laboratories) used to visualize the astrocytes. The sections were counterstained with hematoxylin.

Results

In situ hybridization of the non-CJD control eyes (C3 and C4) with the antisense probe showed labeling of the retina around the entire retinal curvature and labeling of nonneural structures, such as cornea and sclera. The labeling of sclera and cornea were particularly intense, but labeling was also seen with the control sense probe, indicating that it resulted from nonspecific binding. The control sense probe showed only background labeling of the retina, confirming the specificity of the signal with the antisense probe and therefore the presence of PrP mRNA in the retina. Specific labeling of cells was seen within the ganglion cell layer (GCL), inner nuclear layer (INL), and outer nuclear layer (ONL; Figs. 1B, 1D). Labeling in the ONL was not uniform and included an intense band of labeling at its outer limit. The corresponding sense probe is shown for comparison (Fig. 1C). The labeling of the nerve fiber layer (NFL) or inner limiting membrane (ILM) appeared to be specific, in that it was absent with the sense probe. However, because of the resolution provided by this technique we could not determine whether it represents specific labeling of ganglion cell axons or artifactual binding to basement membrane structures, as we have reported previously.[16] The poor morphology of the lens in all preparations precluded determination of the level of labeling (data not shown).

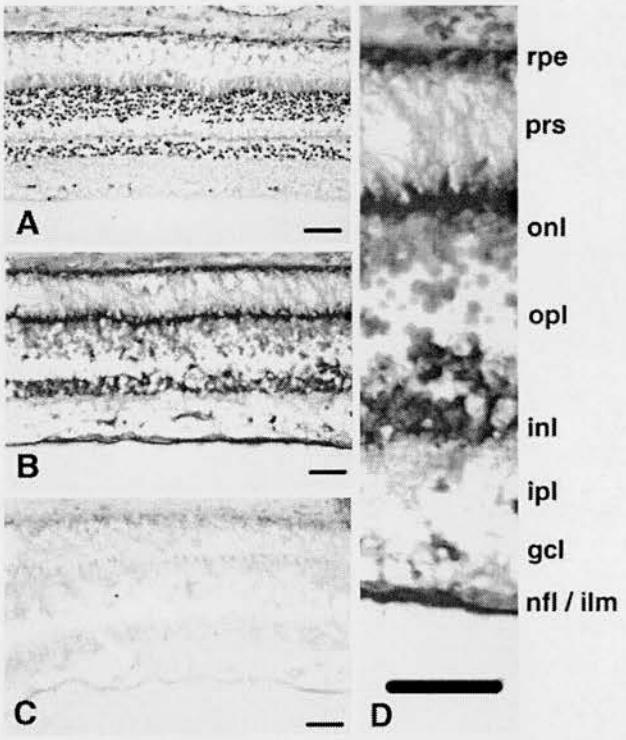

Figure 1. In situ hybridization for PrP RNA in the retina of the non-CJD eye. Antisense (**B**) and sense (**C**) probes are shown hybridized to sections of eyes from case C3. The sections were not counterstained, and positive labeling was seen in all nuclear layers (**B**). A hematoxylin and eosin–stained section is shown (**A**) for orientation with the retinal pigmented epithelium at the *top* and the vitreal surface at the *bottom*. A region of (**B**) is shown at higher magnification in (**D**), and the retinal layers are indicated. rpe, retinal pigmented epithelium; prs, photoreceptor segments; onl, outer nuclear layer; opl, outer plexiform layer; inl, inner nuclear layer; ipl, inner plexiform layer; gcl, ganglion cell layer; nfl/ilm, nerve fiber layer/inner limiting membrane. Scale bar, 50 μm.

Western blot analysis of non-CJD control eyes (C1 and C2) shows the presence of PrP in the neural retina (Fig. 2). The PrP detected in the neural retina was of a mobility similar to that seen in the corresponding brain sample (Fig. 2A). Signals were also seen in lens samples but these were of lower molecular weight. We noted that the concentration of soluble protein in the vertebrate lens far exceeded that in any other organ, including the brain, and that most of these lens proteins are the crystallins, which cluster in the 16- to 30-kDa mass range. Given that our Western blot analyses were loaded with an equal tissue weight equivalent, it seems likely that 3F4 binds to extremely abundant crystallins in the lens lanes. The signals in retina and brain were lost entirely by treatment of the samples with proteinase K, indicating that the PrP detected in the retina, similar to that of the brain, was the protease-sensitive normal cellular form of the protein PrP^{C} (see Fig. 5).

Immunohistochemical staining for PrP by a protocol optimized for PrP^{Sc} detection did not produce a positive reaction in the control non-CJD eye (Fig. 3A). In contrast, immunostaining of the sCJD and vCJD eyes all showed strong positive staining for PrP^{Sc} (Figs. 3B–E). The staining in each case was largely restricted to the inner plexiform layer (IPL) and outer plexiform layer (OPL), in a uniform distribution around the retina. The staining in the OPL was of a coarse granular pattern, whereas the INL staining tended to be of a finer "synaptic" type (Fig. 3C). No positive staining was seen in the photoreceptor cells (PRS) or other neuronal cell bodies. Doubling labeling for

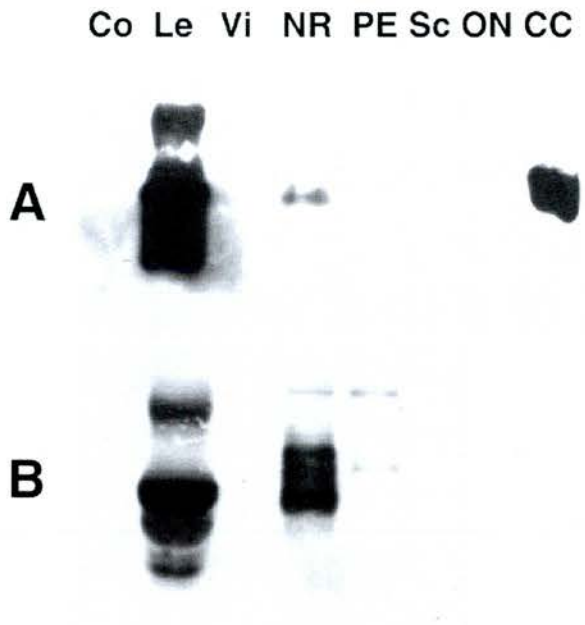

FIGURE 2. Western blot analysis of PrP in cornea (Co), lens (Le), vitreous body (Vi), neural retina (NR), retinal pigmented epithelium and choroid (PE), sclera (Sc), and optic nerve (ON) in the non-CJD eye. (**B**) Case C1; (**A**) case C2. Cerebral cortex (CC) from case C2 was included as a positive control for PrP (**A**). Because of the abundance of PrP in the cerebral cortex, one fifth of this sample was analyzed, compared with the eye sample. Optic nerve was not available for C1.

GFAP and PrP^{Sc} showed GFAP-positive astrocytic end feet in the vCJD retina (Fig. 3D). The cornea, iris, lens, ciliary body, choroid, sclera, and optic nerve sheath all showed a negative reaction. Positive staining was seen in sections of the optic nerve of donors with sCJD and vCJD (Fig. 3F) and in one of the vCJD donor eyes was in an obvious quadrantic distribution. The positive staining seemed to be associated with astrocytic cell bodies, as confirmed by immunocytochemistry for GFAP in the areas where axon loss and secondary myelin loss was accompanied by astrocytosis (data not shown). No evidence of spongiform change or formation of amyloid plaque was observed in the retina or optic nerve on routine stains or on immunohistochemistry for PrP. However, individual neuronal processes showed vacuolation. The retina in sCJD and vCJD showed variable loss of ganglion cells and photoreceptors, some of which may be age-related in the donor with sCJD. No other specific morphologic features were identified in the retina or in the optic nerve.

Western blot analysis for PrP^{res} confirmed the results of the immunohistochemical analysis. PrP^{res} was detectable in the retina from the case of sCJD and in both cases of vCJD. The level of PrP^{res} in the vCJD retina was similar to that seen in the corresponding sample of brain, with lower levels present in optic nerve (Fig 4A). Longer exposure of the Western blot showed all three glycoforms (di-, mono-, and non-glycosylated PrP^{res}) present in the brain, neural retina, and optic nerve (Fig. 4B). Low molecular weight, presumptive crystallin, and degradation products were seen in the lens sample. Weak reactions to a protein of approximately the same mobility as diglycosylated PrP^{res} were also seen in otherwise negative lanes. We observed this band in all heavily exposed Western blot analyses of proteinase K–treated samples and when proteinase K (molecular weight, ~29 kDa) was analyzed in the absence of tissue extracts. Our working assumption is that this band represents weak cross-reactivity between the primary or secondary antibody and proteinase K.

Concentration of any PrP^{Sc} in the samples by a factor of 20 with centrifugation confirmed the positive signal from the

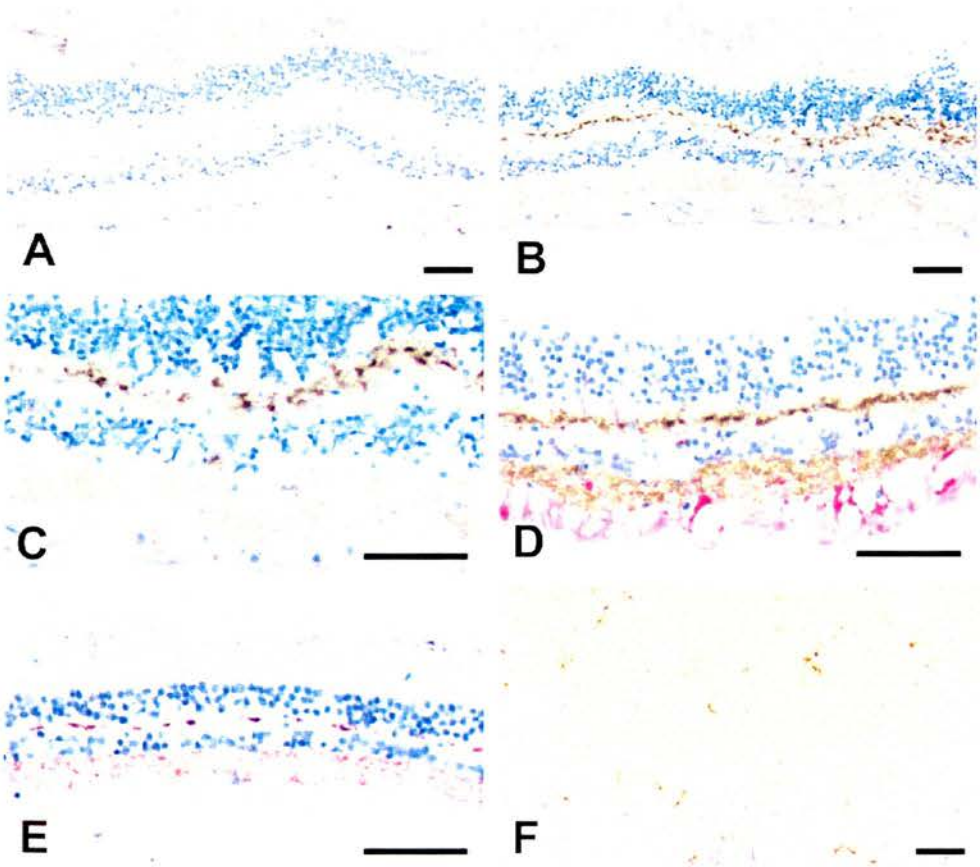

FIGURE 3. Immunohistochemical localization of PrP^{Sc} in retina (**A**–**E**) and optic nerve (**F**) from control, C1 (**A**); sCJD (**B**, **C**); and vCJD, V1 (**D**) and V2 (**E**, **F**). Sections were immunostained for PrP with monoclonal antibody KG9 and diaminobenzidine (*brown*) and counterstained with hematoxylin (*blue*). Double labeling for GFAP with red stain is shown for the retina of V1 (**D**). Scale bars, 50 μm.

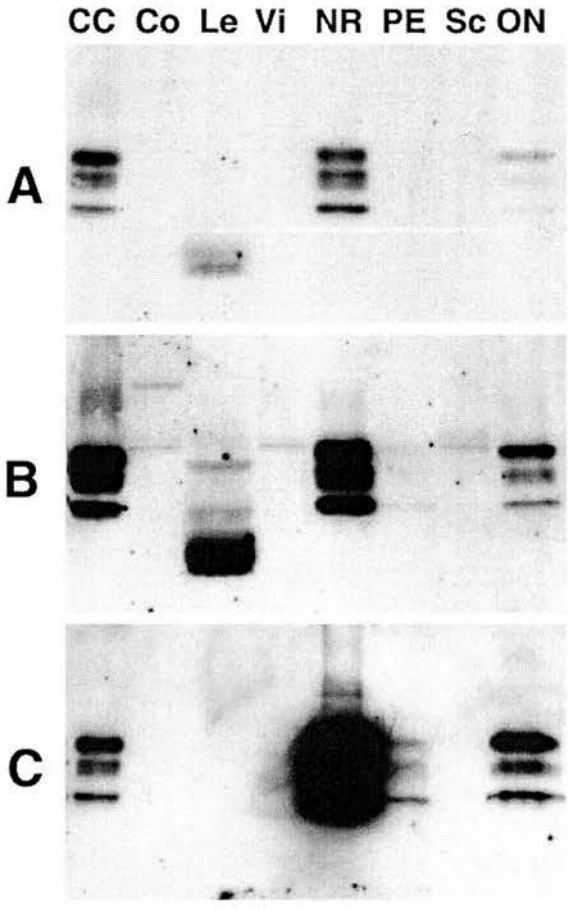

FIGURE 4. Western blot analysis of PrP^{res} in cornea (Co), lens (Le), vitreous body (Vi), neural retina (NR), retinal pigmented epithelium and choroid (PE), sclera (Sc), and optic nerve (ON) in the vCJD eye (V2). An equivalent amount of sample from the cerebral cortex (CC) of the same case is shown as a positive control for the presence of PrP^{res}. Results of a (**A**) short and a (**B**) long exposure of the same Western blot are shown. The same ocular samples were also concentrated by centrifugation before Western blot analysis (**C**). Positive signals from aggregated and protease-resistant PrP were present only in the neural retina, pigmented epithelium, and optic nerve eye samples (**C**).

neural retina and optic nerve, but a weaker signal also became evident in retinal pigmented epithelium (RPE; Fig. 4C). The centrifugal concentration step clearly indicates the dramatic difference in the level of PrP^{res} between positive tissues (retina and optic nerve) and negative tissues (cornea, lens, vitreous body, and sclera). It also serves to confirm that the positive signals in retina and optic nerve are in fact PrP^{Sc}, in that they are insoluble in nondenaturing buffers in addition to being protease resistant, reacting with the antibody 3F4, and having the expected molecular weight of di-, mono-, and non-glycosylated PrP^{res}. The tissue distribution of PrP^{res} in the sCJD eye resembled that found in the vCJD eyes (i.e., restricted to the retina), although frozen optic nerve was not available for study in this case. The level of PrP^{res} in the retina in the case of sCJD was similarly high and exceeded that found in the corresponding brain sample (Fig. 5). Analysis of control (C1) brain and retina in parallel shows that the abundant PrP in these tissues was completely sensitive to proteolytic degradation (PrP^{scns}), and therefore it corresponds to the normal cellular form PrP^{C} (Fig 5). Glycoform ratios of PrP^{res} in the sCJD and vCJD eyes were not identical with those in the corresponding brain samples. Instead, each exhibited a strong shift toward increased abundance of the monoglycosylated form in retina. This was

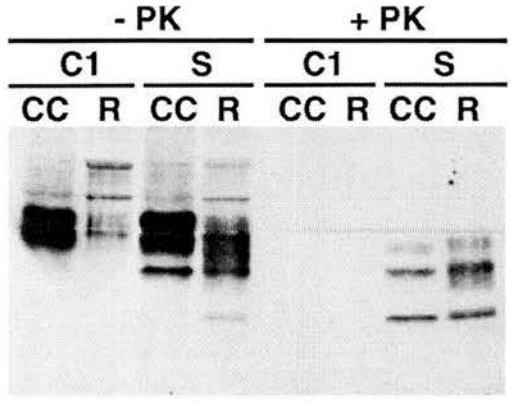

FIGURE 5. Western blot analysis of PrP in the cerebral cortex (CC) and retina (R) from control (C1) and sCJD (S) eyes. The samples are shown with (+PK) and without (−PK) proteinase K digestion before analysis. Similar amounts of PrP^{res} were seen in retina and cerebral cortex in sCJD, but PrP^{res} was absent from the same tissues of the Alzheimer disease control (C1).

particularly noticeable in the cases of vCJD in which the retinal glycoform ratio was no longer typical of vCJD, but more closely resembled that usually associated with sCJD (Fig. 6).

DISCUSSION

The presence of PrP^{Sc} remains the sole, although possibly a surrogate, marker of CJD infectivity currently available. Although this study was not designed to directly address questions of relative infectivity in CJD eye tissues, the finding of PrP^{res} in the eyes of three individuals who died of CJD, though not unexpected, is clearly a cause for concern. Transmission of CJD by intracerebral inoculation of nonhuman primates with CJD eye tissue has been shown previously,[6] but the material used was pooled, and it was therefore not possible to say which ocular components harbored the infectivity. Our results using both immunohistochemistry and Western blot analysis clearly implicate the retina. Although CJD has been transmitted inadvertently by corneal transplantation,[2] PrP^{Sc} was not detectable in the cornea in any of the eyes examined in this study. It is well known that bioassay, even across a species barrier has a greater sensitivity than any currently available assay for PrP^{Sc}. From this we infer that our inability to detect PrP^{res} in the cornea, sclera, and lens cannot be taken as evidence for the

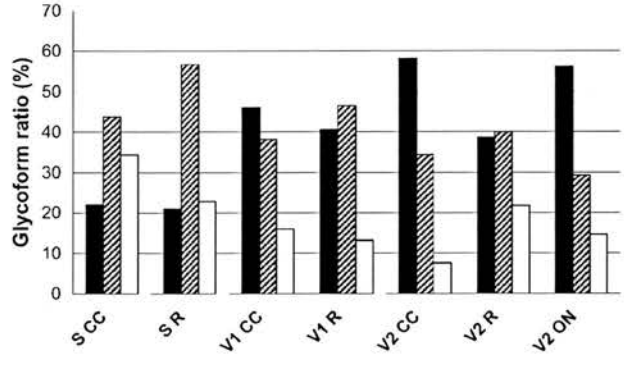

FIGURE 6. Histogram showing the relative abundance of diglycosylated (■), monoglycosylated (▨), and nonglycosylated (□) PrP^{res} in samples of cerebral cortex (CC), retina (R), and optic nerve (ON) from cases of sCJD (S) and vCJD (V1 and V2). All samples of retina showed an increased relative abundance of the monoglycosylated form compared with their respective cerebral cortex samples.

absence of infectivity in these tissues. Although the level of infectivity found in the retina is very much greater than that found in the cornea in a rodent model of scrapie,[17] corneal transplantation failed to transmit disease in monkeys.[18] The issues surrounding the relative levels of CJD infectivity and how this relates to the relative levels of PrP^{Sc} in human ocular tissues can be resolved only by transmission studies using primary human diseased eye tissue.

The agent(s) that cause CJD and related transmissible spongiform encephalopathies are notoriously difficult to decontaminate.[19] Therefore the presence of readily detectable levels of PrP^{Sc} in the retina is clearly pertinent to the current debate over the reuse of surgical instruments in high-risk procedures. The detection of PrP^{res} in the retina at levels equivalent to those found in the brain suggest that retinal surgery may present the same risk and therefore necessitates the same precautions as are taken in neurosurgery. The finding of PrP^{Sc} in the sCJD eye, however, indicates that this risk is not new and predates the appearance of vCJD. To date, there is no evidence that any form of CJD has been transmitted by intraocular surgery, although surgical manipulation of the retina has been undertaken in a significant number of cases only in the past 25 years.

Our data are in agreement in many respects with a recent publication reporting use of Western blot analysis to detect PrP^{res} in the retina and optic nerve of single case of vCJD.[20] This brings the total number of reported cases of vCJD in which retinal positivity has been demonstrated to three, and we would anticipate this to be a general phenomenon. Our estimations of the relative levels of PrP^{res} in retina and optic nerve are different from the report that the optic nerve contains 10 times more PrP^{res} than in retina.[20] The two cases of vCJD reported in this study were investigated by Western blot analysis and immunohistochemistry, are internally consistent and show a greater presence of PrP^{res} in the retina than in the optic nerve, where staining was less intense and less consistent. A further discrepancy is the absence of PrP^{res} from any eye tissue in the case of sCJD analyzed[20] and the abundant PrP^{res} detected in the case of sCJD in this report. Given that our methods appear to be of equivalent sensitivity, it may be that sCJD is heterogeneous in retinal involvement. It may be premature to speculate on the basis of two cases, but there is convincing evidence that the scrapie agent strain and mouse host genotype are known to determine whether ocular involvement occurs in experimental rodent models of scrapie.[21] In this light, it is of interest to note that the sCJD case reported[20] and the sCJD case we report herein differ in both *PRNP* codon 129 genotype and PrP^{res} isotype.

The finding that PrP^{Sc} can be detected in the CJD optic nerve and accumulates in the retina in both sCJD and vCJD is consistent with centrifugal spread from the brain, presumably through the optic nerve. Although other factors may be involved, the accumulation of PrP^{Sc} in the plexiform layers is consistent with the pattern of expression of PrP^{C} in the neural retina (this report) and the known synaptic location of PrP^{C} in neurons.[22]

Lastly, glycosylation site occupancy has been proposed as a marker of the vCJD agent strain, and this appears to be a consistent feature in the vCJD brain.[23] However, PrP^{res} glycosylation occupancy is consistently higher in vCJD lymphoreticular tissues than in brain.[24] In this study, we report the first examples of vCJD PrP^{res} glycoform ratios (found in the retina of both cases of vCJD) that resemble the PrP^{res} glycotype that characterizes sCJD rather than vCJD. The tendency toward monoglycosylation was also evident in the retina from the case of sCJD. This indicates that tissue differentiation, even within the central nervous system can dominate over agent strain in specifying the PrP^{res} glycotype.

Acknowledgments

The authors thank Margaret Le Grice, Suzanne Lowrie, and Mary Nicol for excellent technical assistance, and Helen Reid, consultant neuropathologist at the Hope Hospital (Manchester, United Kingdom), for performing the autopsy in two of the cases presented in this report.

References

1. Prusiner SB. Prions. *Proc Natl Acad Sci USA.* 1998;95:13363–13383.
2. Brown P, Preece M, Brandel J-P, et al. Iatrogenic Creutzfeldt-Jakob disease at the millennium. *Neurology.* 2000;55:1075–1081.
3. Duffy P, Wolf J, Collins G, DeVoe AG, Streeten B, Cowen D. Possible person to person transmission of Creutzfeldt-Jakob disease. *N Engl J Med.* 1974;290:692–693.
4. Uchiyama S, Ishida C, Yago S, Kurumaya H, Kitamoto T. An autopsy case of Creutzfeldt-Jakob disease associated with corneal transplantation. *Dementia.* 1994;8:466–473.
5. Heckmann JG, Lang CJG, Petruch F, et al. Transmission of Creutzfeldt-Jakob disease via a corneal transplant. *J Neurol Neurosurg Psychiatry.* 1997;63:388–390.
6. Brown P, Gibbs CJ, Rodgers-John P, et al. Human spongiform encephalopathy: The National Institutes of Health series of 300 cases of experimentally transmitted disease. *Ann Neurol.* 1994;35:513–529.
7. Will RG, Ironside JW, Zeidler M, et al. A new variant of Creutzfeldt-Jakob disease in the UK. *Lancet.* 1996;347:921–925.
8. Will RG, Zeidler M, Stewart GE, et al. Diagnosis of new variant Creutzfeldt-Jakob disease. *Ann Neurol.* 2000;47:575–582.
9. Ironside JW, Head MW, Bell JE, McCardle L, Will RG. Laboratory diagnosis of variant Creutzfeldt-Jakob disease. *Histopathology.* 2000;37:1–9.
10. Bruce ME, McConnell I, Will RG, Ironside JW. Detection of variant Creutzfeldt-Jakob disease infectivity in extraneural tissues. *Lancet.* 2001;358:208–209.
11. Hogan RN, Brown P, Heck E, Cavanagh HD. Risk of prion disease transmission from ocular donor tissue transplantation. *Cornea.* 1999;18:2–11.
12. Lueck CJ, McIlwaine GG, Zeidler M. Creutzfeldt-Jakob disease and the eye. I. Background and patient management. *Eye.* 2000;14:263–290.
13. Kennedy RH, Hogan RN, Brown P, et al. Eye banking and screening for Creutzfeldt-Jakob disease. *Arch Ophthalmol.* 2001;119:721–726.
14. Lueck CJ, McIlwaine GG, Zeidler M. Creutzfeldt-Jakob disease and the eye. II. Ophthalmic and neuro-ophthalmic features. *Eye* 2000;14:291–301.
15. Hogan RN, Kingsbury DT, Baringer JR, Prusiner SB. Retinal degeneration in experimental Creutzfeldt-Jakob disease. *Lab Invest.* 1983;49:708–715.
16. McLennan NF, Rennison KA, Bell JE, Ironside JW. *In situ* hybridization analysis of PrP mRNA in human CNS tissues. *Neuropathol Appl Neurobiol.* 2001;27:373–383.
17. Hogan RN, Bowman KA, Baringer JR, Prusiner SB. Replication of scrapie prions in hamster eyes precedes retinal degeneration. *Ophthalmic Res.* 1986;18:230–235.
18. Hogan RN, Cavanagh HD. Transplantation of corneal tissue from donors with disease of the central nervous system. *Cornea* 1995;14:547–553.
19. Taylor DM. Inactivation of transmissible degenerative encephalopathy agents: a review. *Vet J.* 2000;159:10–17.
20. Wadsworth JDF, Joiner S, Hill AF, et al. Tissue distribution of protease resistant prion protein in variant Creutzfeldt-Jakob disease using a highly sensitive immunoblot analysis assay. *Lancet.* 2001;358:171–180.
21. Foster JD, Fraser H, Bruce ME. Retinopathy in mice with experimental scrapie. *Neuropathol Appl Neurobiol.* 1986;12:185–196.
22. Herms J, Tings T, Gall S, et al. Evidence of presynaptic location and function of the prion protein. *J Neurosci.* 1999;19:8866–8875.
23. Collinge J, Sidle KC, Meads J, Ironside J, Hill AF. Molecular analysis of prion strain variation and the aetiology of "new variant" CJD. *Nature.* 1996;383:685–690.
24. Hill AF, Butterworth RJ, Joiner S, et al. Investigation of variant Creutzfeldt-Jakob disease and other human prion diseases with tonsil biopsy samples. *Lancet.* 1999;353:183–189.